AN NMR STUDY OF BIOLOGICAL PHOSPHATE INTERACTIONS

by

HENRY R. WILSON

A thesis submitted in partial fulfilment of the requirements

for the Degree of Doctor of Philosophy

in the University of Oxford

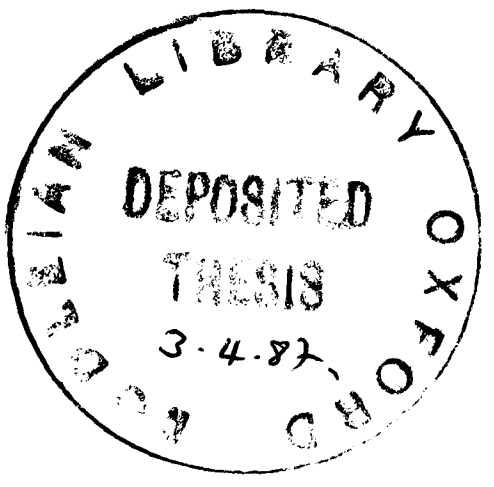

Wolfson College

Oxford

Michaelmas Term

1986

Abstract

An nmr study of biological phosphate interactions

by

Henry R. Wilson

Michaelmas Term, 1986 Wolfson College

An investigation is made of the interactions between a variety of small molecule phosphates and amines, and in particular of triethylenetetramine with hexametaphosphate, pyrophosphate, tripolyphosphate, ADP and ATP and of cyclic triethylenetriamine with hexametaphosphate. For each phosphate/amine pair, observed changes in the pH dependence of ^{1}H and ^{31}P nmr chemical shift are used to calculate the effect of interaction on the pK_a of the two species present and an association constant is evaluated at one particular pH value. These data are then combined to evaluate association constants for a variety of protonation states of the phosphate and amine. Strength of association is interpreted in terms of electrostatic charge and its spatial distribution, comparison is made with Mg^{2+} and Ca^{2+} complexes and biological relevance is discussed.

The interaction of yeast PGK with its substrates is investigated by using the (500MHz and 300MHz) ^{1}H nmr spectrum of the enzyme and (250MHz) ^{31}P nmr spectra of its substrates. On the basis of pH dependence, comparison with the spectrum of horse PGK and T_2 relaxation data, ^{1}H nmr resonances are assigned to surface residues. In particular, resonances are assigned to the three active site histidines (nos. 62,167 and 170), and to the exposed histidine and methionine residues. A series of comparatively well-resolved upfield shifted aromatic peaks, including a relatively exposed tyrosine peak is tentatively assigned to the inter-domain hinge region of the protein.

The effects of MgADP, MgATP and the non-reacting nucleotide analogue MgAMPPNP on the yeast PGK spectrum are characterised. The line-broadening reagent Gd^{3+} is used to distinguish between direct influence and conformational effects. The triose phosphate substrate 3-PG is added to the enzyme as are the anionic probes $[Co(CN)_6]^{3-}$, $[Cr(CN)_6]^{3-}$ and $[Fe(CN)_6]^{3-}$, and the nature of anion binding in the active groove of the protein and elsewhere on its surface is investigated. Movement of the two PGK domains is investigated in three models of the ternary complex: (i) with MgAMPPNP and 3-PG, (ii) with the elongated nucleotide A4P, and (iii) with a mutant form of the enzyme (his388 -gln388). The PGK/substrate interaction is interpreted in terms of the phosphate/amine model.

Acknowledgements

I thank Professor R.J.P. Williams, F.R.S., for the constant supervision of this work and for his unflagging commitment and enthusiasm.

I thank Dr. H.C. Watson and the members of his group, particularly Steve Gamblin, Jenny Littlechild and Brian Cooper, for supplying the enzyme PGK, for unlimited access to the crystallographic model, and for many stimulating discussions.
I am grateful for the support of all my friends and colleagues and in particular of Mark Wormald, Marcus Scott, Barry Levine, Mark Lawrence and David Concar.

Finally, I thank Susie Compton, Julie Edwards and my sister Janet for their help in the production of this thesis.

To my parents

Contents

CHAPTER 1.

INTRODUCTION TO PHOSPHATE/AMINE INTERACTION

Chapter 1 Contents

1.1 INTRODUCTION

This thesis concerns the interaction of phosphate molecules with polyamines and with the protein, yeast phosphoglycerate kinase (PGK). The aim was to understand the binding of anions to cations in both cases. Two approaches are made. The first is based on considerations of the binding constants of the partners, and equilibrium constants will be determined and interpreted in terms of electrostatic interactions after appropriate corrections for salt effects. The method used will be nuclear magnetic resonance (nmr). This method gives the second approach to binding, since through chemical shift information it reveals the nature of the binding as well as its strength.

1.1.1 Ion pair binding in aqueous solutions - Theory

Phosphate molecules bind to amines largely through ion-pair formation. The basis of calculation of the electrostatic attraction is Coulomb's Law for point charges, which states that the electrostatic energy is proportional to the charge product and inversely proportional to distance of separation of the charges. Various unsuccessful attempts were made to incorporate this into a theory of interionic attraction of electrolytes in solution until the work of Debye and Hückel (1923). They derived a general expression for the interaction of an ion with its environment in terms of a mean ionic activity coefficient, f,

$$\lg f = - \frac{A|z_1 z_2| I^{\frac{1}{2}}}{1 + Bg\ I^{\frac{1}{2}}}$$

where A,B are empirically determined constants,

z_1, z_2 are the ionic charges,

I is the ionic strength, and

g is the mean ionic diameter.

In effect the activity coefficient reduces the absolute concentration of an ion in any mass action equation. This equation was found to hold for solutions of 1:1 and 1:2 electrolytes at low concentrations. Guggenheim (1935) established the following form of the equation for 1:1 electrolytes up to I=0.1M.

$$\lg f = A|z_1 z_2|\{I^{\frac{1}{2}}/(1+I^{\frac{1}{2}}) - Q\ I\}$$

where Q is also empirically determined.

More specifically, for aqueous solutions at 25°C, up to I=0.1M, and for 1:1 and 1:2 electrolytes, Davies (1938) found the following to be satisfactory.

$$\lg f = -0.50|z_1 z_2|\{I^{\frac{1}{2}}/(1+I^{\frac{1}{2}}) - 0.2I\}.$$

In the light of further activity coefficient data, Davies (1962) modified this expression to produce

$$\lg f = -0.5|z_1 z_2|\{I^{\frac{1}{2}}/(1+I^{\frac{1}{2}}) - 0.3I\}.$$

The application of these equations is limited to relatively dilute solutions of electrolytes. This equation will be used in the present work to correct concentration terms for ionic strength in the measurement of ion-pair equilibrium constants.

Bjerrum (1926) observed that activity coefficients determined by the above method were different for different pairs of cations and anions and, therefore, that a general treatment was inadequate. His treatment of ion pairs took into account the association of oppositely charged ions lying within a certain distance of each other.

$$K_b = \frac{4\pi N}{1{,}000} \int_a^d \exp\{|z_1 z_2| e^2 (DrkT)^{-1}\} r^2 dr$$

where N is the Avogado number

$(1000)^{-1}$ is the correction from m^3 to dm^3,

e is the electronic charge,

D is the dielectric constant,

r is the interionic distance,

T is the temperature,

a is the closest distance of ionic approach,

and d is the maximum separation over which association is still considered to occur.

The presence of the term "a" means that any application of this equation relates to a particular pair of ions.

The expression is conveniently written

$$K_b = \frac{4\pi N s^3}{1{,}000} \int_{s/d}^{s/a} e^x x^{-4} dx \qquad (1)$$

where $s = |z_1 z_2| e^2/DkT$ and $x = s/r$.

Bjerrum considered that ions whose electrostatic interaction energy exceeds 2kT, are close enough to be considered associated, thus

$$d = |z_1 z_2| e^2/2kDT.$$

At this distance, the "Bjerrum critical distance", the distribution function of ions located around a central ion of opposite charges goes through a minimum. Equation (1) now simplifies to

$$K_f = \frac{4\pi N s^3}{1{,}000} \int_2^{s/a} e^x x^{-4} dx.$$

The definition of the boundary of ion pair association is not clearly defined, however, and later modifications were suggested by Denison, Ramsey and Fuoss (Denison and Ramsey, 1955; and Fuoss, 1958). Moreover, it is stressed that Bjerrum's theory applies to spherical ions. Simply, what Bjerrum's treatment does is to state that there will be selective ion pairs formed within the context of ion atmospheres (general salt effects) which will be selectively dependent on ion charges and sizes. This allows the comparison of present data on phosphate/amine ion pairs (corrected for general salt effects) with a basic theory of ion-pair equilibria.

An investigation of electrostatic interaction between non-spherical organic ions of anisotropic charge distribution

was carried out by Tam and Williams (1984). They began their study by collecting available data for the stability constants of inorganic ion pairs (at 25°C), corrected to zero ionic strength. The values were plotted against charge product and compared with theoretical curves generated from the Bjerrum equation using values of 0.5 and 0.7nm for the distance of closest approach. The comparison is shown in figure 1.1. At a charge product of about 12, the experimental results begin to exceed the theoretical predictions, but in general the data are found to fit well with Bjerrum's description of ionic behaviour.

The study proceeded to consider the association constants of a series of organic carboxylate anions with inorganic cations and with organic cations. The organic ions were of various charge separation, rigidity and shape. The following observations were made.

(i) Variations in strengths of association were too great to be accounted for by Bjerrum's predictions. The model of spherical ions associating in a medium of uniform dielectric strength needs to be replaced by a more realistic electrostatic field model that takes into account anisotropic charge distribution and solvent molecular-hydration effects.

(ii) There is a significant size-matching effect. In other words, the cations that bind most tightly are those best able to fill a gap between two carboxylate groups. With the flexible dicarboxylates, the size of the gap may be adjusted to accommodate a particular cation, with a corresponding loss of entropy.

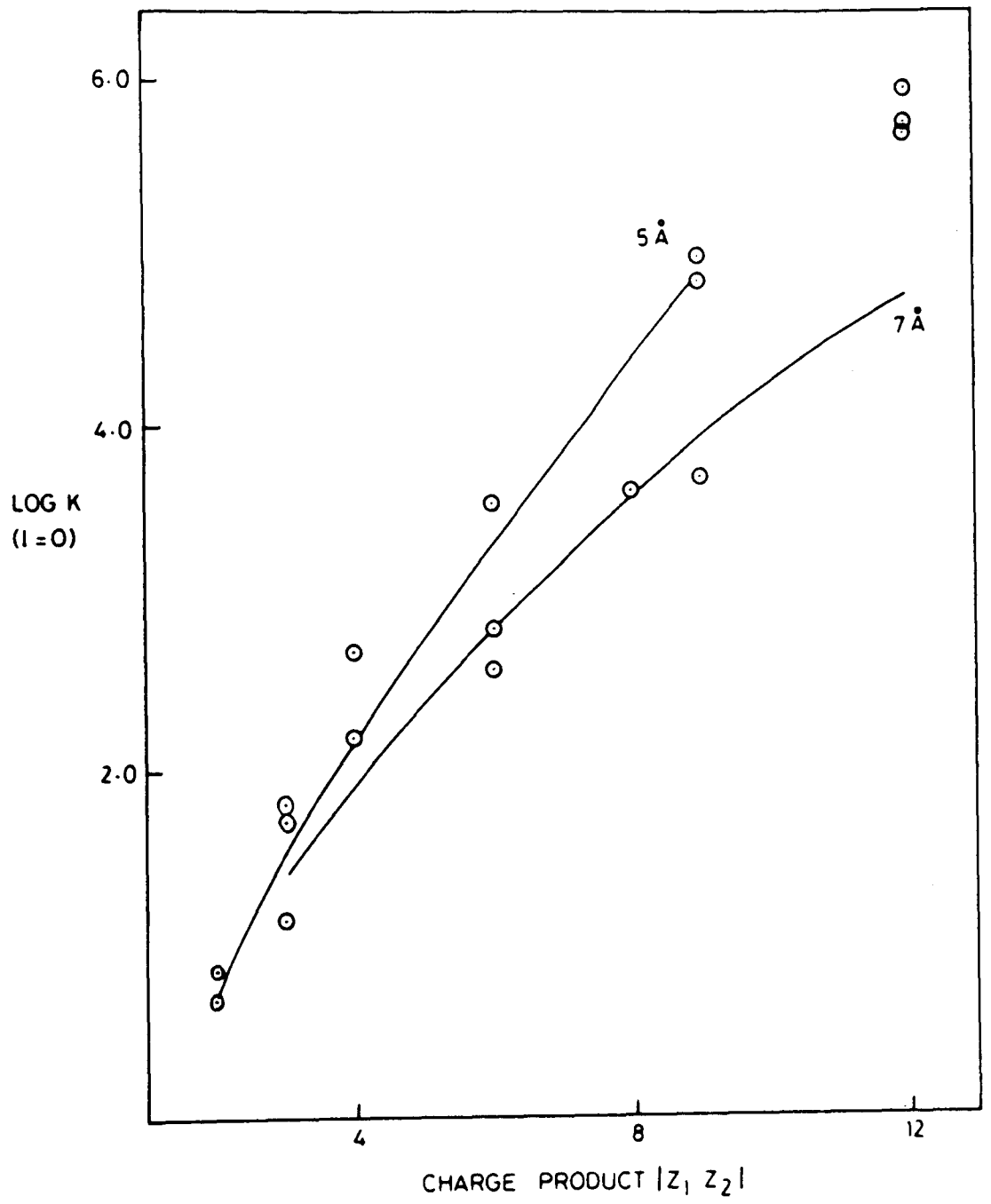

Figure 1.1 Variation of association constants (lgK) with charge product ($|z_1 z_2|$) as $I \rightarrow 0$, for several inorganic ion pairs (Tam and Williams, 1984). Also shown are curves generated from the Bjerrum equation, for 0.5 and 0.7nm, values for the distance of closest approach.

(iii) Charge-matching may help to explain the great selectivity found in biological electrostatic binding.

The concept of charge-matching had previously been suggested by Dietrich et al (1979), in an investigation of the binding of phosphate anions to polyguanidinium salts. The selectivity of such reactions was noted and comparison was made with the interaction between phosphate groups of nucleic acids and polycationic protamines and histones. This interaction will be dealt with in greater detail in this thesis.

Further work by Tam and Williams (1985) reviewed electrostatic interactions in a biological context. They concluded that while there is little interaction between simple small biological anions and cations, the arrangement of charges on a macromolecular framework can result in powerful and selective electrostatic interaction. It was remarked that the arrangement of carboxylate groups in a loop region of calcium-binding proteins gives a highly selective Ca^{2+} site. This is to be compared with the present work which concerns the binding of phosphate groups to clusters of positively charged amine groups found in polyamines and protein.

Methods of Measurement

Measurement of conductivity was the technique used by Tam and Williams (1984) to study strengths of ionic association. Whereas their work involved carboxylate anions, of low pK_a values and fully deprotonated at neutral pH, the present study concerns polyamine cations and phosphate anions

which tend to undergo a deprotonation equilibrium at just such a pH value. State of protonation is, of course, further affected by interaction with counter ions and by ionic strength. Thus, the systems are too complicated to be adequately described by conductivity measurement, and so it was decided to use nuclear magnetic resonance to monitor the effect of ion pairing on the component species. Strength of association and the effect of interaction on protonation state can easily be monitored for the amines by proton nmr, and for the phosphates by phosphorus-31 nmr. The use of the technique can be extended to the investigation of phosphate/protein interaction found in the second part of the current work, and thus the phosphate/protein results can be compared directly with the phosphate/polyamine data.

The first part of the thesis is as follows. Chapter two is a preliminary survey of interactions between small phosphate and polyamine compounds, while six selected interactions are examined in detail in chapter three. Proton and phosphorus-31 nmr chemical shift data are used to investigate the nature of the interactions and strength of association is calculated for a variety of charge states. Variations are interpreted in terms of electrostatic charge and its spatial distribution. Comparison is made with complexes of spherical inorganic ions and with Ca^{2+} and Mg^{2+} complexes found in vivo.

The remainder of the thesis concerns the interaction of yeast phosphoglycerate kinase with its phosphate substrates.

1.1.2 Protein/phosphate interaction

The glycolytic enzyme, yeast phosphoglycerate kinase (PGK) was the protein chosen to extend the phosphate/amine study to phosphate/protein interaction. It has a molecular weight of 45,000a.m.u. which makes it rather large by nmr standards, but its crystal structure is fully determined (Watson et al., 1982), it is readily available and it is comparatively soluble. Earlier studies had shown that nmr analysis of the protein was feasible (Tanswell et al., 1976). The unconfirmed proposal that the domains of PGK move about a hinge region make the enzyme of great interest in its own right and as an example of a protein hinge mechanism.

PGK catalyzes the transfer of a phosphate group from the triose phosphate, 1,3-diphosphoglycerate, to the nucleotide, MgADP, in the first MgATP producing step of the glycolytic pathway. The triose phosphate product is 3-phosphoglycerate, 3-PG. The structure of the enzyme is shown in figure 1.2. It is seen to consist of two equally-sized domains linked by a small hinge region.

The nucleotide binding site has been located by X-ray crystallographic studies (Watson et al., 1982). Binding is principally through hydrophobic interactions between the protein and the adenine ring moiety (Krietsch and Bücher, 1970; Roustan et al., 1973) but in addition the two hydroxyl groups of the ribose moiety form hydrogen bonds with a glutamic acid residue and phosphate/amine interactions occur between the β and γ phosphate residues and two lysine residues.

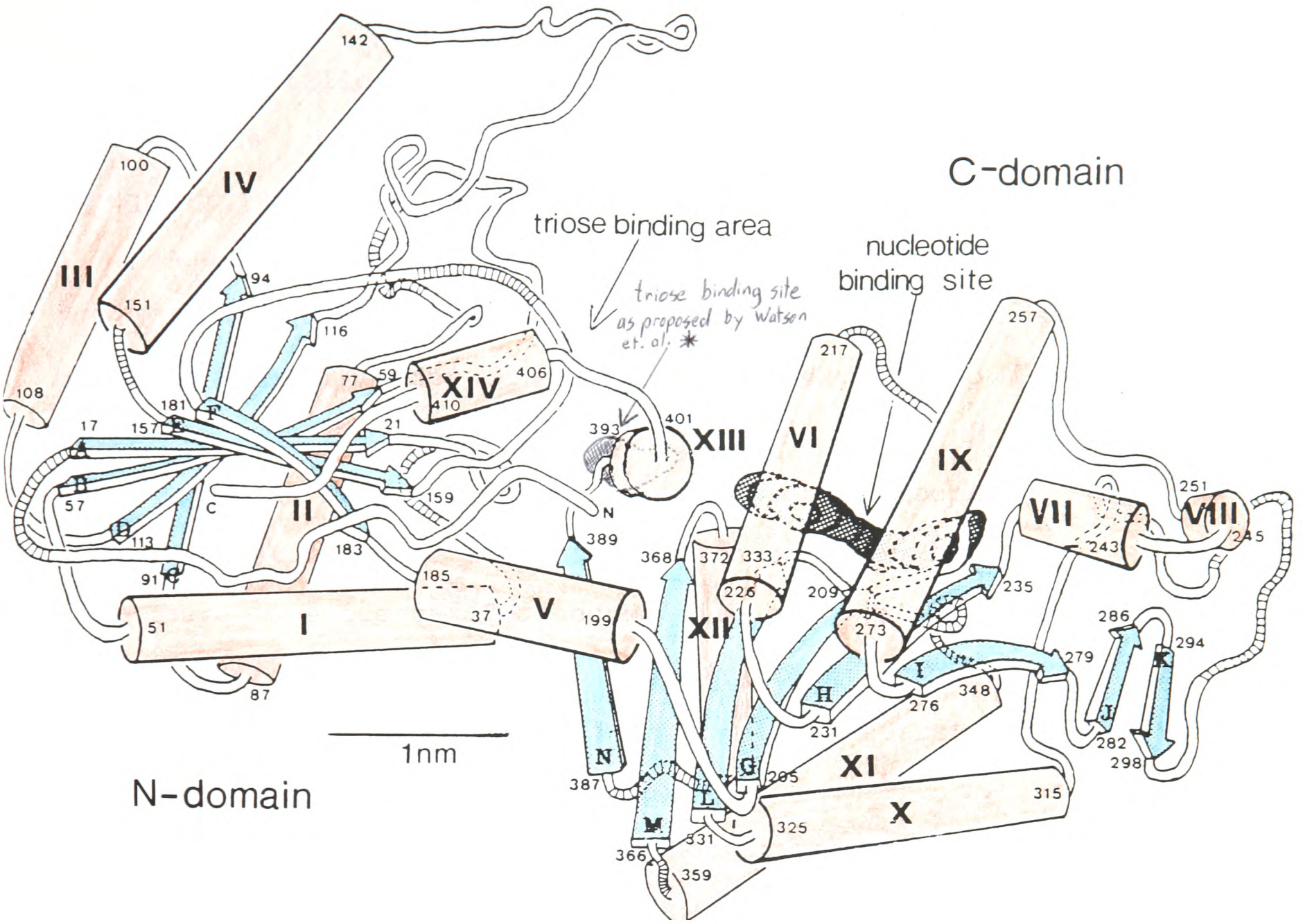

Figure 1.2 The crystal structure of yeast PGK. The N-terminal domain is on the left, α-helices are denoted by red cylinders, β-sheets by blue arrows. (After Watson et al., 1982).

It is noted that the location of the triose binding site shown here is at variance with that suggested by Watson et al.*

Non-crystallographic work showed that 3-PG binds to PGK through its phosphate group, in an interaction that is thought to be predominantly electrostatic (Orr and Knowles, 1974; Adams et al., 1985). A recent study with pig muscle PGK (Tompa et al., 1986) showed that while the phosphate group is necessary for binding, the carboxyl group is also involved. The substrate 1,3-P_2G binds extremely tightly to PGK (Scopes, 1978b) and thus both phosphate groups of this phosphate ester appear to interact with the protein.

There is evidence of a second aion binding site in yeast PGK (Wrobel and Stinson, 1978; Scopes 1978; Schierbeck and Larsson-Raźnikiewicz, 1979). This binding appears to have a regulatory function, either by being adjacent to the active site or else by causing some conformational change in the protein.

The site of triose phosphate binding has not been clearly established by crystallographic studies. Given the electrostatic nature of the interaction, the most obvious location is the positively charged patch on the inner face of the N-terminal domain. Comparison of sequences of PGK from a wide variety of sources (Osinga et al., 1985; Littlechild et al., 1986) showed the basic residues of this region to be largely conserved. Moreover, three proton nmr histidine resonances that have been assigned to this region seen to be strongly affected by triose phosphate binding (Tanswell et al., 1976). It is, however, noted that, in the crystallographic structure of the protein this site lies at a distance of 1.2nm from the γ-phosphate of bound MgATP. The implication is that as well as the "open" form of the

structure, defined by the crystallogrpahic studies, the two domains can swivel around the hinge region to produce a catalytically active "closed form" (see figure 1.3), and that this form contributes to the "nmr-view" of the molecule.

Closure of the two domains of PGK around the hinge region was immediately proposed by Banks et al. (1979) on their determination of the complete sequence and structure of the horse muscle enzyme. In a small angle X-ray scattering study of yeast PGK, Pickover et al. (also 1979) independently showed that the radius of gyration of the enzyme decreased on the binding of substrate. This was consistent with domain movement around the hinge and was compared with the cleft closure found in yeast hexokinase. Further work by Roustan et al. (1980) and by Rice and Blake (1984) produced more evidence of enzyme closure. Moreover, in the light of the knowledge of the crystal structure of yeast PGK, the results of Tanswell et al. (1976), indicated that the metal ion of bound MgATP, located at a distance of 1.2nm from the triose phosphate binding surface in the open crystal structure, approaches within 0.6nm of the histidine residues of the inner face of the N-domain, in the dynamic, active form of the enzyme found in solution.

Comparison of the amino acid sequences of PGK from a variety of sources (Osinga et al., 1985; Littlechild et al., 1986) has shown the hinge region to be very highly conserved, which strongly suggests that it has a vital role in the activity of the enzyme.

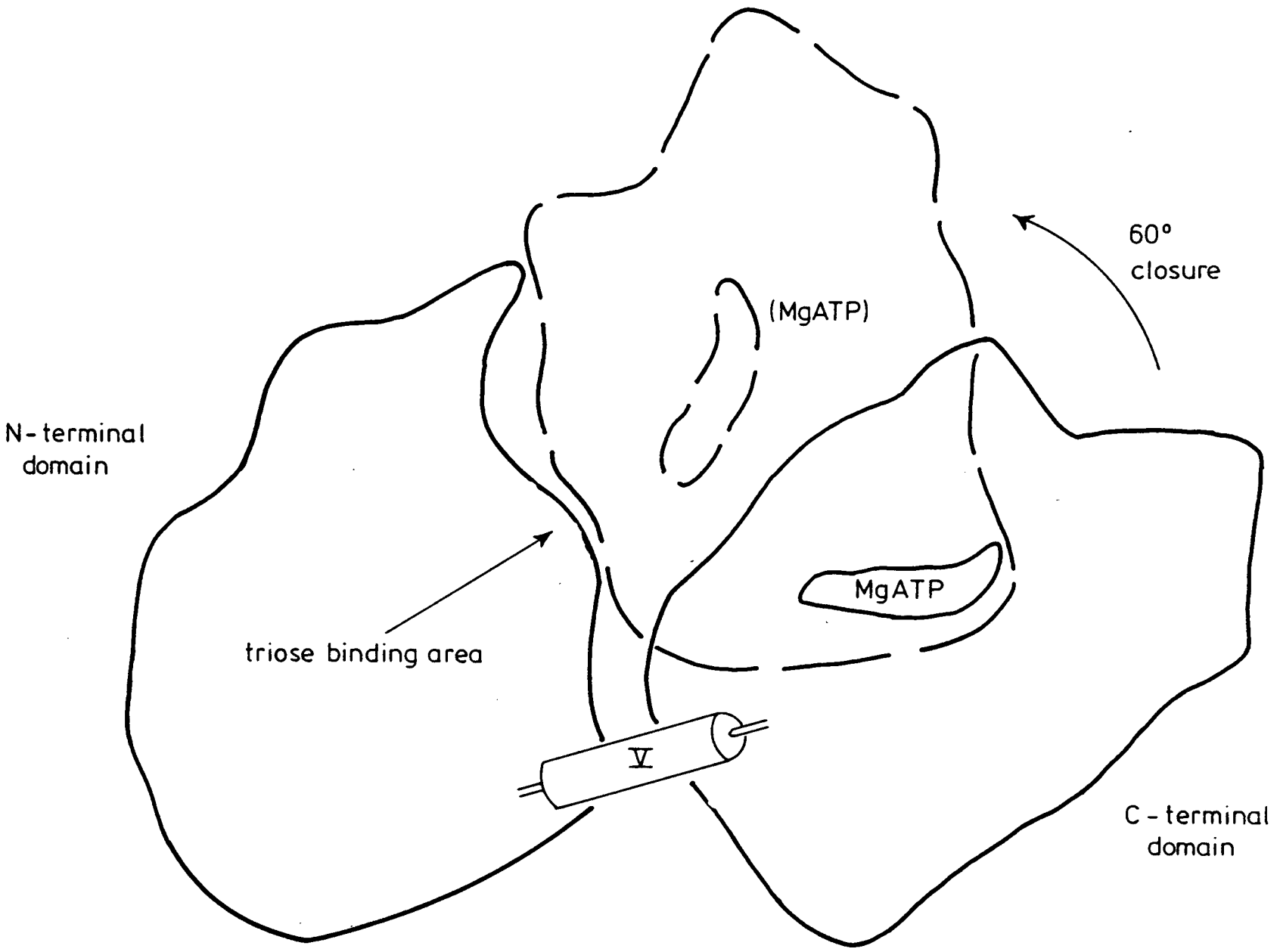

Figure 1.3 Outline of the yeast PGK molecule showing the open crystallographic form and a proposed closed form (broken line). Helix V of the "hinge region", the position of bound nucleotide and the triose binding area are indicated. (After Watson and Gamblin, 1985).

1.1.3 The present work

Proton nmr is the most powerful currently available technique for the study of protein conformation in solution and it is the main method used here to study the interaction of PGK with its substrates. It was used by Tanswell et al., (1976) and even without knowledge of the sequence, and independently from the crystallographic studies, the position of the bound metal ion in the MgATP/PGK complex was determined and three histidine resonances were assigned to the active site of triose phosphate binding.

In the current work, proton nmr chemical shift data, T_2 relaxation studies and comparison with the spectrum of horse PGK, are all used to assign individual peaks and to identify areas of the proton nmr spectrum with regions of the protein. Most of the spectrum, and especially the aromatic peaks are found to represent surface residues of the protein, which includes a lot of the hinge region. These preliminary investigations form the introduction to the present yeast PGK studies and are reported in chapter four of this thesis.

Chapters 5 and 6 concern the location of nucleotide and triose phosphate on yeast PGK and the effect of the binding of these substrates on the conformation of the protein. The line broadening reagent Gd^{3+} is used to locate certain protein residues in relation to the metal ion of the enzyme nucleotide-metal enzyme. Various metal hexacyanide probes, $[M(CN)_6]^{3-}$, are used in a paramagnetic study which distinguishes between the direct effects of anion binding

and the longer range conformational effects. The binding of anions to yeast PGK can be compared directly with the model studies in the first part of the thesis.

In chapter seven, the effect of the presence of both triose phosphate substrate and a nucleotide substrate analogue on the conformation of the protein is examined in an investigation of the ternary complex of yeast PGK. A long chain nucleotide, adenosine 5'-tetraphosphate is used in an attempt to bridge the gap between the C-domain and N-domain active sites. A mutant form of yeast PGK has been prepared (Wilson et al., 1984) with a fully conserved histidine residue of the hinge region replaced by a neutral glutamine residue. This form of the protein is thought to favour the closed conformation and its nmr spectrum is examined here for the first time. It is compared with the spectrum of the ternary complex.

In the last chapter of the thesis, the effect of the phosphate/protein interaction on the phosphorus-31 nmr chemical shift of substrate anions is investigated. The effect of Gd^{3+} on the nmr linewidths of the resonances of substrate phosphate groups is used to gauge substrate/enzyme and substrate/substrate interaction. Finally, the effect of phosphate/protein interaction on nmr chemical shift values of both enzyme and substrate, and the effect on pK_a vslues, are compared with the effects seen for the model phosphate/polyamine interactions.

Chapter 1 References

Adams, B., Burgess, R.J. and Pain, R.H. (1985) Eur.J.Biochem., 152, 715-720.

Banks, R.D. Blake, C.C.F., Evans, P.R., Haser, R., Rice, D.W., Hardy, G.W., Merrett, M. and Phillips, A.W. (1979) Nature 279, 773-777.

Bjerrum, N. (1926) Danske Vidensk.Selsk.Mat.-fys.Medd., 9, 7.

Davies, C.W. (1938) J.Chem.Soc., 2093.

Davies, C.W. (1962) "Ion Association" Butterworths, London.

Debye, P. and Huckel, E. (1923) Physik.Z., 24, 185 and 305.

Denison, J.T. and Ramsey, J.B. (1955) J.Am.Chem.Soc., 77, 2615.

Dietrich, B., Fyles, D.L., Fyles, T.M. and Lehn, J-M. (1979) Helv.Chim.Acta., 62, 2763-2781.

Fuoss, R.M. (1958) J.Am.Chem.Soc., 80, 5059.

Guggenheim, E.A. (1935) Phil.Mag., 19, 588.

Krietsch, W.K.G. and Bucher, T. (1970) Eur.J.Biochem., 17, 568-580.

Littlechild J., Rohl, J. and Watson, H.C. (1986) Personal communication, University of Bristol.

Orr, G.A. and Knowles, J.R. (1974) Biochem.J., 141, 721-723.

Osinga, K.A. Swinkels, B.W., Gibson, W.C., Borst, P., Veeneman, G.H., Van Boom, J.H., Michels, P.A.M. and Oppardoes, F.R. (1985) EMBO J., 4, 13B, 3811-3817.

Pickover, C.A., McKay, D.B., Engelman, D.M. and Steitz, T.A. (1979) J.Biol.Chem., 254, 22, 11323-11329.

Rice, D.W. and Blake, C.C.F. (1984) J.Mol.Biol., 175, 219-223.

Roustan, C., Brevet, A., Pradel, L-A. and van Thoai, N. (1973) Eur.J.Biochem., 37, 248-255.

Roustan, C., Fattoum, A., Jeanneau, R. and Pradel, L-A. (1980) Biochemistry, 19, 5168-5175.

Schierbeck, B. and Larsson-Raznikiewicz, M. (1979) Biochim.Biophys.Acta, 568, 195-204.

Scopes, R.K. (1978a) Eur.J.Biochem., 85, 503-516.

Scopes, R.K. (1978b) Eur.J.Biochem., 91, 119-129.

Tam, S-C. and Williams, R.J.P. (1985) Structure and Bonding, 63, 103-151.

Tam, S-C. and Williams, R.J.P. (1984) J.Chem.Soc.Faraday Trans. 1, 80, 2255-2267.

Tompa, P., Hong, P.T. and Vas, M. (1986) Eur.J.Biochem., 154, 643-649.

Tanswell, P., Westhead, E.W. and Williams, R.J.P. (1976) Eur.J.Biochem., 63, 249-262.

Watson, H.C., Walker, N.P.C., Shaw, P.J., Bryant, T.N., Wendell, P.L., Fothergill, L.A., Perkins, R.E., Conroy, S.C., Dobson, M.J., Tuite, M.F., Kingsman, A.J. and Kingsman, S.M. (1982) EMBO J., 1, 12, 1635-1640.

Watson, H.C. and Gamblin, S.J. (1985) Proc.Int.Symp. Biomol.Struct.Interactions, Suppl. J. Biosci., 8, 499-506.

Wilson, C.A.B., Tuite, M.F., Dobson, M.J., Kingsman, S.M., Kingsman, A.J., Glover, L.A., Hardman, N., Watson, H.C. and Fothergill, L.A. (1984) Biochem. Soc. Trans., Vol.12, 278-279.

Wrobel, J.A. and Stinson, R.A. (1978) Eur.J.Biochem., 85, 345-350.

CHAPTER 2.

A PRELIMINARY SURVEY OF PHOSPHATE/AMINE INTERACTIONS

Chapter 2 Contents

2.1 INTRODUCTION

2.1.1 The present series of studies

A previous study (Tam and Williams, 1984) examined the interaction between several rigid and flexible organic dicarboxylate anions of varying length with simple metal cations and compared the strength of this binding with that of the interaction between the same dicarboxylate anions and several rigid and flexible amines, also of varying length. It was found that, although simple application of Bjerrum's theory of ion-pair formation in determining the strength of interaction was successful for some ion-pairs, consideration had to be made of molecular shape, flexibility and anisotropic charge distribution. It was shown that, generally, as the length of the dicarboxylate anion increased, the strength of cation binding decreased except where a cation of similar spatial charge distribution was involved. In other words, the better the "fit", the better the binding. Loss of entropy on the tight binding of a long flexible molecule, and the molecular nature of the solvent are other factors that have to be taken into consideration.

The present work concerns the interactions between a variety of phosphate-containing anions and a series of cations similar to that studied before. As well as continuing the previous work, the present investigation creates a model for the interaction of phosphate-containing compounds with proteins, assuming that the major interaction is between the phosphate and protein amine groups.

In the previous work the main method used for the analysis of complex ion formation was the conductivity of solutions. This method is not easily employed when the molecules under study have a series of acid dissociation constants, pK_a values, over the region of pH in which association is studied. For this reason, in the analysis of the binding of phosphates to polyamines, use has been made of nmr monitoring of both proton and phosphorus atoms. The difficulty with this method is that relatively high concentrations of species have to be used and therefore extrapolation of the binding constants to zero ionic strength is not likely to be very accurate. The situation is improved by the wide span of charge types studied here, which range from a negative charge of six to a positive charge of four. This means that the association constants can vary over ten orders of magnitude.

2.1.2 Nucleotide studies

Protonation and metal ion complexation of ADP and ATP have been extensively studied by both ^{1}H and ^{31}P nmr (Cohn and Hughes, 1960 and 1962) and signals have been clearly assigned to individual protons and phosphate groups. For ATP, the α and γ phosphates are represented by ^{31}P nmr doublets, because of splitting by the β phosphate, while the effect of the former on the latter causes the β phosphate to be seen as a triplet. Divalent metal ions, when present at equimolar levels, are seen to interact with the β and γ phosphates of ATP and the α and β phosphates of ADP. A later

^{1}H nmr study (Tanswell et al., 1975) confirmed that the metal binds to the terminal pair of phosphates and suggested likely conformations for the metal-nucleotide complexes.

Further ^{31}P nmr work (Ramirez and Marecek, 1980) indicated that the effects of Mg^{2+} and Ca^{2+} on the ^{31}P nmr shifts of ADP and ATP are due to changes in conformation of the polyphosphate chain and that in MgATP, the metal ion interacts with all three phosphate groups. More recently still (Vasavada et al., 1984), changes in the lineshape of the β-phosphate signal have been used to determine exchange rates of diamagnetic cations in their ATP complexes. More generally, it has been found (Gorenstein, 1984) that ^{31}P nmr chemical shift of phosphates is governed largely by σ-bond angles as well as by electronegativity and by π-bond overlap.

2.1.3 Polyamine studies

The metabolism and function of biological polyamines has been extensively reviewed (Pegg and McCann, 1982; Pegg, 1986, and Tabor and Tabor, 1985). Of particular relevance to the present work, their protonation behaviour has been widely studied by nmr. Sudmeier and Reilley (1964) examined the pH dependence of ^{1}H nmr chemical shift for several polyamines, including triethylenetetramine, and assigned resonances to individual methylene groups. Thus they were able to explain microscopic acid-base equilibria in terms of electrostatic and inductive effects. Aikens et al. (1983), used a potentiometric titration technique to determine the macroscopic protonation constants of spermine and spermidine and of four homologous compounds. Subsequent work

by Onasch et al., (1984) used ^{1}H nmr chemical shift to establish the pH dependence of the protonation state of individual nitrogen atoms of spermidine.

2.1.4 Polyamine-nucleotide interaction

Extensive study has been made of the biologically interesting interaction between polyamines and nucleotides. Nakai and Glinsmann (1977) used an anion-exchange resin method to evaluate the strength of the interactions firstly, between three polyamines, putriescine, spermidine and spermine, and the three adenine nucleotides, AMP, ADP and ATP, and secondly, between the same polyamines and several diphosphate nucleotides. Their results are represented in table 2.1 and their conclusions are as follows.

(i) The phosphate moiety of the nucleotide is the significant determinant of polyamine affinity.

(ii) Strength of association depends on structural features of the polyamine ions as well as on charge.

(iii) The polyamines may compete with Mg^{2+} from nucleotides *in vivo*, thus regulating the levels of free and Mg^{2+}-bound nucleotides.

Various phosphate salts of these polyamines were the subject of a structural analysis by Wiewiórowski and Bratek-Wiewiórowska (1984). They characterised both the proton-donating and proton-accepting activities of the amine and phosphate groups and the dependence of the conformation adapted by the polyamine on the geometry, electronic structure and accessibility of the anion.

Table 2.1 Apparent association constants (M^{-1}) for polyamine/nucleotide complexes at pH7.5, 30°C, I=50mM. (Nakai and Glinsmann, 1977). GDP, CDP, TDP and UDP represent guanosine, cytidine, thymidine and uridine diphosphates

	polyamine		
nucleotide	putrescine	spermidine	spermine
AMP	82	230	360
ATP	290	900	9500
ADP	200	330	1300
GDP	170	310	1150
CDP	220	330	1300
TDP	190	310	1350
UDP	200	310	1320

Other studies have used nmr to monitor polyamine-nucleotide interaction. Bunce and Kong (1978) use ^{1}H and ^{13}C nmr to show that, at a concentration of 500mM, the three carbon segment of triprotonated spermidine binds to the phosphate group of AMP and that the four carbon segment binds to the N-7 group of the adenine moiety. At a concentration of 6mM, they found no evidence of binding thus showing that this interaction is, in fact, quite weak.

Weser et al., (1974) used ^{13}C and ^{31}P nmr and circular-dichroism to examine the three-way interaction Cu^{2+}, spermine and AMP. At a concentration of 0.5mmol, neither ^{13}C nmr nor ^{31}P nmr showed any evidence of interaction between polyamine and mononucleotide. Trace amounts of Cu^{2+} were seen to interact both with the polyamine and with the N-7 group and the phosphate group of the nucleotide. The circular-dichroism measurements showed very little change in the Cotton effect of AMP on the addition of polyamine or of Cu^{2+} on their own, but a significant change when they were added together. This was taken as proof of a ternary polyamine-Cu^{2+}-AMP complex. It is noted that there was no evidence of direct amine-phosphate association.

Suzuki et al., (1973) studied the polyamine-catalysed hydrolysis of ATP. Working at concentrations of 1mM they discovered the following.

(i) Longer polyamines such as pentaethylhexamine and pentaethylenetetramine form more stable complexes with ATP than smaller ones such as ethylenediamine.

(ii) As well as the number of amino groups, the spacing affects strength of binding.

(iii) The hydrolysis products are always ADP and P_i.

The spectral evidence suggests that the (sufficiently long) polyamine binds to both the ribose and adenine moieties. The hydrolysis products suggest that the interaction involves the α and β phosphates, but not the γ phosphate.

Kimura et al., (1981) used electrophoresis and polarography to investigate the interaction between macromonocyclic polyamines and dicarboxylate anions at millimolar concentration and at neutral pH. It was found to be of 1:1 stoichiometry and stereospecific, in that only when the two carboxylate groups are close together, such as in succinate, malate and malonate, does binding occur. It is remarked that this latter criterion is met by most of the tricarboxylate acid cycle intermediates and their analogues and this suggests a sterically-controlled, selective receptor role for the polyamines.

Further work by Kimura et al., (1982) showed that the same macromonocyclic polyamines bind inorganic phosphate and adenosine nucleotides, under similar conditions. The inorganic phosphate is found to bind as strongly as the polycarboxylate anions, while the nucleotides bind more strongly, implying interaction with the adenosine moiety. This adenosine phosphate binding is found to be much stronger than that determined by Nakai and Glinsmann (1977) for the open chain polyamines, spermine and spermidine.

In the same work, the interaction of both cyclic and linear polyamines with AMP and ATP was indicated by changes in chemical shift of the ^1H nmr spectrum of the nucleotide, present at 120mM.

Dietrich et al (1979) measured the strength of complexes formed between a series of polyguanidinium ligands and phosphate and carbonate anions. Comparison was made with similar complexes of polyamine anions. While structural effects are observed, the binding is primarily electrostatic. For a given charge, the polyamine ligands form stronger complexes, but the charge of the polyguanidinium complexes maintain their charges at higher pH and the possibility of the use of these compounds as anion complexones is discussed.

2.1.5 Biological relevance

The ability of polyamines to bind to polyvalent anions, such as phosphates, and their natural occurrence strongly suggests that they interact with nucleic acids *in vivo* (Giorgi, 1970). They are reported to be involved in DNA condensation (Proschke, 1984), in synthesis of RNA (Abraham, 1968) and in the synthesis of polyphenylalanine in a cell-free preparation of Escherichia coli (Takeda, 1969), where the polyamines act by replacing Mg^{2+} ions. A recent review (Pegg, 1986) has emphasised the link of polyamines to cell growth and protein synthesis and has suggested that inhibitors of polyamine synthesis can play a role in cancer chemotherapy.

The ability of polyamines, with their well-spaced, nearly independent, amino groups, to bind to DNA with its charge spread over an extended framework, suggests that the emergence of particular polyamines during evolution has been guided by considerations of the pK_a values of individual amino groups, of divalent metal ion competition and of the strength of polyamine/nucleic acid interaction. The selectivity afforded by the stereospecific, charge distribution-dependent nature of the interaction is of great relevance here.

2.1.6 Outline of the present work

In the present chapter, the interactions between a variety of phosphates and amines are considered and the strength of binding and suitability for further nmr

investigation is gauged. In the next chapter, six interactions are considered in more detail. The strength of binding is determined over a wide pH range and the resulting association constants are compared with the charge product of the species concerned. In conclusion, in an attempt to understand any deviation from predictions of binding constants based simply on charge product, consideration is made of molecular shape and charge distribution.

2.2 MATERIALS AND METHODS

2.2.1 The phosphate compounds

Sodium dihydrogenorthophosphate dihydrate, anhydrous sodium pyrophosphate and sodium tripolyphosphate were supplied by BDH Chemicals Ltd. Sodium trimetaphosphate (97%) and sodium hexametaphosphate flake (pure) were obtained from Koch-Light Laboratories Ltd. Crystalline o-phosphoserine and o-phosphotyrosine were supplied by the Sigma Chemical Company. Phosphoenolpyruvate (mono-cyclohexylamine salt) was obtained from BDH. Glyphosate was kindly donated by Zealot's Hill Laboratory, I.C.I. Fructose 1,6-diphosphate (disodium salt) was supplied by the Aldrich Chemical Company. Adenosine mono-, di- and tri-phosphate (sodium salts, higher grade) were obtained from the Sigma Chemical Company. Finally, phenyl phosphate and 1-naphthyl phosphate (disodium salts) were supplied by Fluka AG.

2.2.2 The polyamine compounds

1,2-diaminoethane (98%), 1,3-diaminopropane, 1,4-diaminobutane (97%) and 1,6-diaminohexane (98.5%) were all obtained from BDH Chemicals Ltd. Triethylenetetramine was supplied by the Aldrich Chemical Company. Spermine tetrahydrochloride (99% pure) and hexamethonium chloride dihydrate (pure) were obtained from Fluka AG. Tris(2-aminoethyl)amine was supplied by Sigma Chemical Company. Cyclic triethylenetriamine was kindly donated by Professor Karl Wieghardt, Ruhr Universitat, Bochum, West Germany.

2.2.3 Miscellaneous materials

99.8% deuterium oxide (D_2O) was obtained from the Aldrich Chemical Company, 35% deuterated hydrochloric acid (DCL) from Merck, Sharp & Dohme Ltd. and 40% deuterated sodium hydroxide (NaOD) from BDH Chemicals Ltd. 3-(trimethylsilyl)-1-propanesulphonic acid, sodium salt hydrate (TMS) was supplied by the Aldrich Chemical Company. The disodium salt of ethylenediamine tetra-acetic acid was obtained from Fisons Scientific Apparatus. Trimethylphosphate (TMP) was bought from BDH Chemicals Ltd. as were pH4.0 and pH9.2 buffer solutions.

2.2.4 Nmr methods

The proton spectra were recorded on a Bruker WH300 spectrometer, using a pulse angle of 60°, a sweep width of 3kHz and a memory size of 8K. 32 accumulations were made for each spectrum. Homonuclear presaturation was used for suppression of the HDO peak, continuous wave decoupling being applied at a power level of 6mW (15L) for 0.25s. Resolution enhancement of the spectra was achieved using Gaussian multiplication, was a Gaussian broadening of 0.10 and a line-broadening of -10Hz.

The ^{31}P spectra were recorded on a Bruker AM-250 spectrometer operating at a frequency of 101MHz. Typical parameters were a 40° pulse angle, together with a relaxation delay of 0.7s; 32 accumulations over a 3kHz sweepwidth; a 4K memory size and a line-broadening of 9Hz. Chemical shifts were measured against an external standard of trimethyl-phosphate (δ=0ppm) and upfield shifts given a negative sign.

2.2.5 Sample procedures

Each sample contained 5mM phosphate in 99.8% D_2O, adjusted to pH8 with NaOD and DCl (100mM). 0.1mM EDTA was present to remove any line-broadening metallic impurities. After accumulation of a spectrum, 50mM amine was added to give a 10:1 excess of amine:phosphate. The pH was adjusted to its original value and another spectrum obtained.

In the more detailed investigation of six selected interactions (reported in the following chapter), both ^{1}H and ^{31}P nmr were used. The ^{1}H nmr samples contained 5mM amine, with 1mM TMS present as an internal reference standard. For an excess of phosphate, a 50mM addition was made. A typical ^{31}P nmr sample contained 5mM phosphate and 0.1mM EDTA, made up in 99.8% D_2O. When present, amine was at a concentration of 50mM. Initially, each sample was taken to pH12 by addition of 1M NaOD. In the course of a titration, the pH was lowered, with 100mM DCl, half a unit at a time, to a value less than zero. At each stage the chemical shift of each peak was noted.

In the titrations to determine strength of association for a particular phosphate/amine complex at a particular pH, incremental addition was made of one component to a 5mM solution of the other. After each addition the pH of the sample was adjusted if necessary to within 0.05pH units of its initial value. The total volume increase did not exceed 2% in the course of a titration and thus dilution effects were negligible.

The pH was measured with a Radiometer pH meter 26 used in conjunction with a Wilmad combination pH electrode. The system was standardised before each experiment with pH4.00 and pH9.20 buffer solutions and was accurate to within ±0.02pH units.

All measurements were carried out at room temperature, the nmr probe being set to 27° C.

2.3 RESULTS AND DISCUSSION

This preliminary survey concerned the interactions between a variety of phosphates and multiamines, illustrated by figures 2.1 and 2.2. The effects of an excess of the various amines on the ^{31}P nmr chemical shift (ppm) of the various phosphates are summarised in table 2.2

The extent of the effects, all measured at pH8, is very dependent on the pK_a values of the phosphate under consideration. This is because changes in the protonation state of the phosphate are a major determinant of changes in chemical shift, and these compounds whose pK_a values are the closest to pH8 are the most likely to be affected by any interaction. With this limitation in mind, the following conclusions are made.

(i) With the sole exception of phenyl phosphate/ spermine, which produces a marginal shift of 0.3ppm, no interaction is detected involving compounds with only one phosphate group, whether or not a carboxyl group is also present. Thus the chemical shifts of phosphoserine, phosphotyrosine, phosphoenolpyravate and glyphosate, as well as of inorganic phosphate, AMP and phenyl phosphate are not significantly altered.

(ii) A comparatively small change in chemical shift of 0.3ppm, is seen in one of the fructose 1,6-diphosphate resonances. While this compound does have two phosphate groups, they are held apart, remote from each other, by the monosaccharide ring.

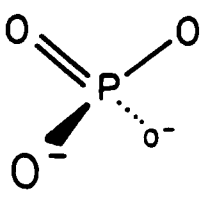

orthophosphate, P_i

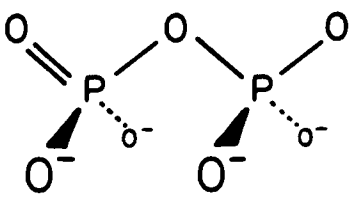

pyrophosphate, PP

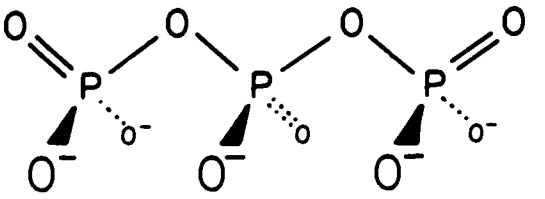

tripolyphosphate, PPP

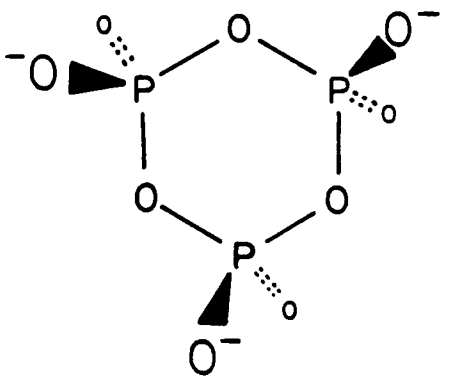

trimetaphosphate

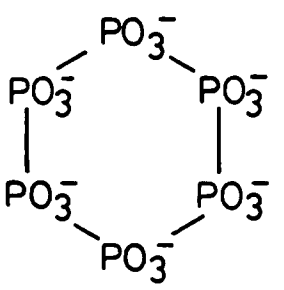

hexametaphosphate

$H_3^+NC(COO^-)(H)CH_2OPO_3^{2-}$

phosphoseine

$H_3^+NC(COO^-)(H)CH_2C_6H_4OPO_3^{2-}$

phosphotyrosine

$CH_2=C(COO^-)OPO_3^{2-}$

phosphoerolypyruvate

$^-O_2CCH_2\overset{+}{N}H_2CH_2PO_3^{2-}$

glyphosate

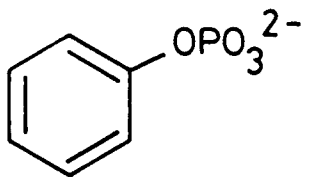

phenyl phosphate

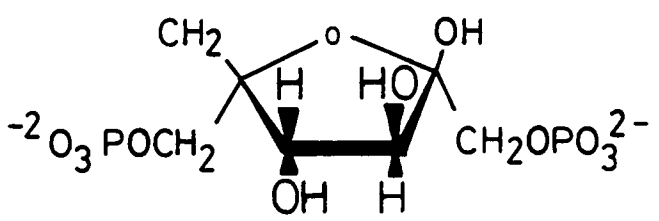

fructose 1,6-diphosphate

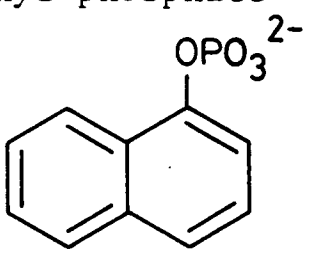

naphthyl phosphate

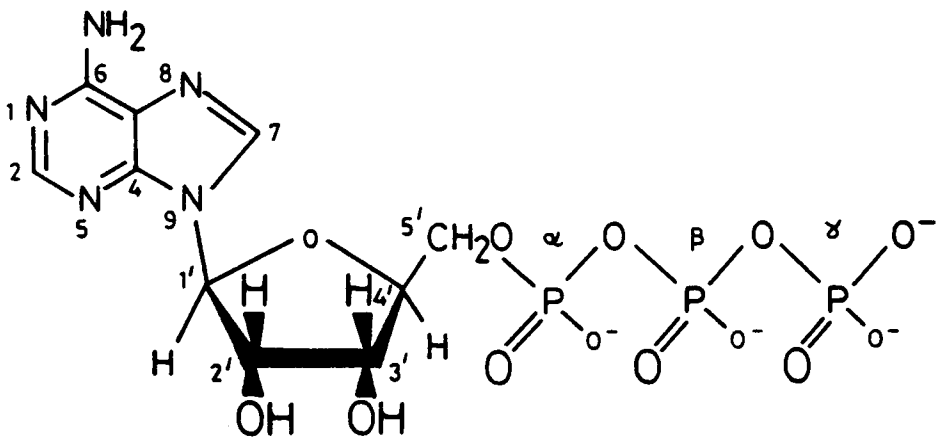

adenosine 5'-triphosphate, ATP

Fig. 2.1 Schematic representation and structural formulae of the phosphate anions used in this study.

$H_3\overset{+}{N}CH_2CH_2\overset{+}{N}H_3$

1,2-diaminoethane

$H_3\overset{+}{N}CH_2CH_2CH_2\overset{+}{N}H_3$

1,3-diaminopropane

$H_3\overset{+}{N}(CH_2)_4\overset{+}{N}H_3$

1,4-diaminobutane

(putrescine)

$H_3\overset{+}{N}(CH_2)_6\overset{+}{N}H_3$

1,6-diaminohexane

$H_3\overset{+}{N}(CH_2)_2\overset{+}{N}H_2(CH_2)_2\overset{+}{N}H_2(CH_2)_2\overset{+}{N}H_3$

triethylenetetramine (trien)

$H_3\overset{+}{N}(CH_2)_3\overset{+}{N}H_2(CH_2)_4\overset{+}{N}H_2(CH_2)_3\overset{+}{N}H_3$

spermine

$(CH_3)_3\overset{+}{N}(CH_2)_6\overset{+}{N}(CH_3)_3$

hexan-1,6-bis-trimethylammonium, (hexamethonium)

$\overset{+}{N}H(CH_2CH_2\overset{+}{N}H_3)_3$

tris(2-aminoethyl)amine

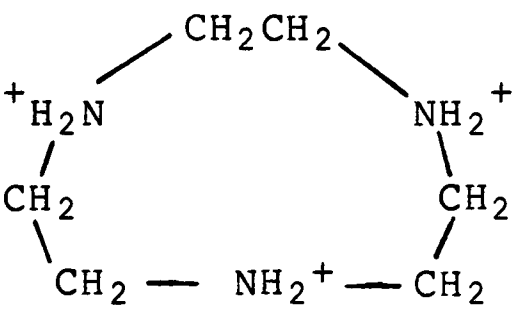

cyclic triethylenetetramine
(nane)

Figure 2.2 Structural representations of the multiamines used in this study, shown in the fully protonated state.

	AMINE								
PHOSPHATE	DIAMINO ETHANE NC_2N	DIAMINO PROPANE NC_3N	DIAMINO BUTANE NC_4N	DIAMINO HEXANE NC_6N	TRIEN NC_2NC_2 NC_2NC_2N	SPERMINE NC_3NC_4 NC_3N	HEXA METHONIUM CHLORIDE $C_3NC_6NC_3$	tris (2-AMINOETHYL) AMINE $N(C_2N)_3$	NANE NC_2N C_2NC_2
Orthophosphate	0.0	0.0	0.0		0.0		0.0	0.0	
Pyrophosphate	+0.7				+0.8		+0.1	+1.0	+0.3
Tripolyphosphate α	+1.0			+1.0	+1.4		+0.1	+1.0	
β	-			+0.5	+1.3		0.0	-	
Trimetaphosphate		+0.1			+0.1		-0.1		
Hexametaphosphate		-0.9			-0.6				
Phosphoserine	0.0	0.0							
Phosphotyrosine			-0.1				0.0		
Phosphoenolpyruvate	0.0								
Glyphosate		+0.1	+0.1		-0.1				
Fructose 1,6-diphosphate (a)					+0.3				
(b)					+0.1				
AMP						0.0			
ADP α					+0.4				
β					+0.3				
ATP α	+0.2		+0.1		+0.2		-0.1	+0.2	
β	+0.9		+0.3		+1.1		0.0	+1.1	
γ	-0.7		+0.6		+0.5		+0.3	+0.7	
Phenylphosphate				0.0		-0.3			
Naphthylphosphate				0.0		0.0			

Table 2.2 The change in ^{31}P nmr chemical shift of a variety of phosphate compounds on interaction with various amines. Schematic formulae are given for the amines. The phosphates were present at concentrations of 5mM and the amines were added in 10:1 excess. pH=8. The structural formulae of most of these compounds are given in figures 2.1 and 2.2.

(iii) No significant effects are seen with trimetaphosphate. This compound bears three negative charges, held apart in a ring structure.

(iv) The other phosphate compounds, pyrophosphate, tripolyphosphate, ADP and ATP, have two or three phosphate groups in a row. The chemical shifts of each change significantly on the various interactions with tris(2-aminoethyl) amine and with the linear polyamines diaminoethane, diaminopropane, diaminobutane, diaminohexane and triethylene-tetramine.

(v) No interaction is seen with hexamethonium chloride. This compound is the same as diaminohexane but with fully methylated amine groups. Thus it appears that interaction with polyphosphate is sterically hindered by the methyl groups.

(vi) The cyclic polyamine nane produces only a small change in the chemical shift of pyrophosphate.

Generally this survey underlines the electrostatic nature of the phosphate/amine interaction by confirming that more highly charged species interact more strongly. The significance of steric factors is remarked.

2.4 CHOICE OF PHOSPHATE AND POLYAMINE COMPOUNDS

On the basis of apparent strength of interaction it was decided to continue the investigation with pyrophosphate, tripolyphosphate, hexametaphosphate and with both ADP and ATP. The nucleotides are, of course, of particular biological relevance and are substrates of the enzyme phosphoglyceratekinase, which is studied later in this work. Hexametaphosphate was included in the investigation because its highest pK_a value is pH1.6 and, therefore, above pH3 it may be regarded as being fully deprotonated. This simplicity makes it ideal for the binding study.

Turning to the choice of polyamine, triethylenetetramine was chosen for the strength of its interaction. Cyclic triethylenetriamine was chosen for reasons of simplicity. Its cyclic nature means that its protons are equivalent and, therefore, that interpretation of its proton nmr spectrum is straightforward.

Chapter 2 References

Abraham, A.J. (1968) Eur.J.Biochem., 5, 143-146.

Aikens, D., Bunce, S., Onasch, F., Parker R., Hurwitz, C. and Clemans, S. (1983) Biophys.Chem., 17, 67-74.

Bunce, S. and Kong, E.S.W. (1978) Biophys.Chem., 8, 357-368.

Cohn, M. and Hughes, T.R. (1962), J.Biol.Chem., 237, 176-181.

Cohn, M. and Hughes, T.R. (1960) J.Biol.Chem., 235, 3250-3253.

Dietrich, B., Fyles, D.L., Fyles, T.M. and Lehn, J-M (1979) Helv.Chim.Acta, 62, 2763-2781.

Giorgi, P.P. (1970) Biochem.J., 120, 643-651.

Gorenstein, D.G. (editor) (1984) "Phosphorus-31 nmr" Academic Press, Incorporated.

Kimura, E., Sakonaka, A., Yatsunami, T. and Kodama, M. (1981) J.Am.Chem.Soc., 103, 3041-3045.

Kimura, E., Kodama, M., and Yatsunami, T. (1982) J.Am.Chem.Soc., 104, 3182-3187.

Nakai, C. and Glinsmann, W. (1977) Biochemistry, 16, 25, 5636-5641.

Onasch, F., Aikens, D., Bunce, S., Schwartz, H., Nairn, D. and Hurwitz, C. (1984) Biophys.Chem., 19, 245-253.

Pegg, A.E. (1986) Biochem.J., 234, 249-262.

Pegg, A.E. and McCann, P.P. (1982) Am.J.Physiol., 243, C212-C221.

Porschke, D. (1984) Biochemistry, 23, 4821-4828.

Ramirez, F. and Marecek, J.F. (1980) Biochim.Biophys.Acta, 589, 21-29.

Sudmeier, J.L. and Reilley, C.N. (1964) Anal.Chem., 36, 1698-1706.

Suzuki, S., Higashiyama, T., and Nakahara, A. (1973) Bioinorganic Chemistry, 2, 145-154.

Tabor, C.W. and Tabor, H. (1985) Microbiol.Rev., 49, 81-99.

Takeda, Y. (1969) J.Biochem., Tokyo, 66, 345-349.

Tam, S-C. and Williams, R.J.P. (1984) J.Chem.Soc., Faraday Trans. 1, 80, 2255-2267.

Tanswell, P., Thornton, J.M., Korda, A.V. and Williams, R.J.P. (1975) Eur.J.Biochem., 57, 135-145.

Vasavada, K.V., Ray, B.D. and Nageswara Rao, B.D. (1984) J.Inorg.Biochem., 21, 323-335.

Weser, U., Strobel, G.J. and Rupp, H. (1974) Eur.J.Biochem., 50, 91-99.

Wiewiórowski, M. and Bratek-Wiewiórowska, M.D. (1984) International Binding Conference, Frontiers Abstracts, 179-180.

CHAPTER 3.

PHOSPHATE/AMINE INTERACTION. SIX INTERACTIONS IN DETAIL

CHAPTER 3 Contents

3.6 ADENOSINE TRIPHOSPHATE WITH TRIEN

3.6.1 pK_a evaluation

3.6.2 lg K_b evaluation

3.6.3 lg K_b at several pH values

3.7 HEXAMETAPHOSPHATE WITH CYCLIC TRIETHYLENETRIAMINE

3.7.1 pK_a evaluation

3.7.2 lg K_b evaluation

3.7.3 lg K_b at several pH values

3.8 SUMMARY AND CONCLUSIONS

3.8.1 Effect of phosphate/amine interaction on chemical shift

3.8.2 Comparative strengths of phosphate/amine complexes

3.1 INTRODUCTION

The results presented in this chapter are in six sections, each of which covers the interaction between a particular phosphate and a particular amine. The methods used for calculation of pK_a values and of strengths of association are described here.

3.1.1 pK_a evaluation

pK_a values are derived from plots of change in proton nmr chemical shift values with pH, by one of the following methods.

Independent pK_a equilibria. When the successive pK_a's are separated by 2 pH units it is possible to treat them individually as independent events. Use is made of the Henderson-Hasselbalch equation as outlined below.

For the protonation equilibrium

$$AH^+ \rightleftharpoons A + H^+$$

the dissociation constant is expressed by

$$K_a = [A][H^+]/[AH^+]$$

$$\rightleftharpoons -\lg K_a = -\lg[H^+] - \lg\{[A]/[AH^+]\}$$

$$\rightleftharpoons pK_a = pH - \lg\{[A]/[AH^+]\}$$

$$\rightleftharpoons \lg\{[A]/[AH^+]\} = pH - pK_a \qquad (1)$$

Change in chemical shift is proportional to degree of protonation:

$$\frac{(\delta-\delta_A)}{(\delta_{AH^+}-\delta)} = \frac{[A]}{[AH^+]}$$

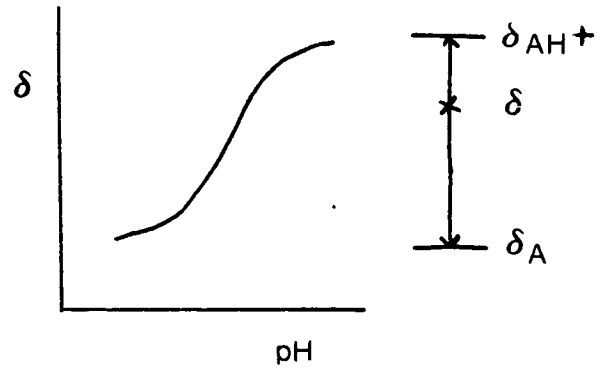

$$\text{now (1)} \rightarrow \lg\left\{\frac{(\delta-\delta_A)}{(\delta_{AH^+}-\delta)}\right\} = pH - pKa$$

Thus, for independent pKa equilibria, a plot of

$$\lg\left\{\frac{(\delta-\delta_A)}{(\delta_{AH^+}-\delta)}\right\} \text{ vs } pH$$

will have a slope of 1 and an x-intercept of pKa.

The method is used for the majority of the pKa values determined here. The graphs were plotted using a Research Machines 380Z microcomputer and a line-fitting programme based on the least squares method. The fit of the various lines to the points was very good, and the error limits are those of pH measurement, ±0.02pH units.

Paired pK_a equilibria. This method was used when two pKa values lie within 2pH units of each other and is fully described under the title of "the projection strip method" in Chapter 4 of "The study of ionic equilibria" by H. Rossotti (1978).

The first step of the calculation is to normalise the chemical shift data so that unprotonated and doubly protonated species are represented by J values of 0 and 2 respectively.

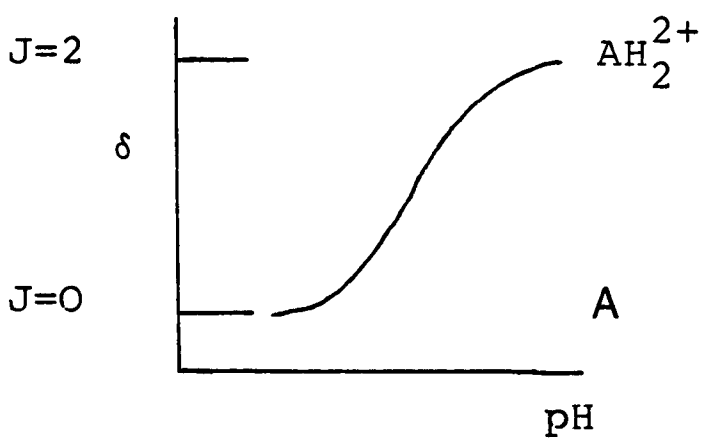

The J values are plotted against pH and, for J values 0.2 to 1.8, a series of corresponding x-values is obtained, as shown below. This series is a projection of the protonation curve along the $lg[H^+]$ axis and is the "projection strip" of the method.

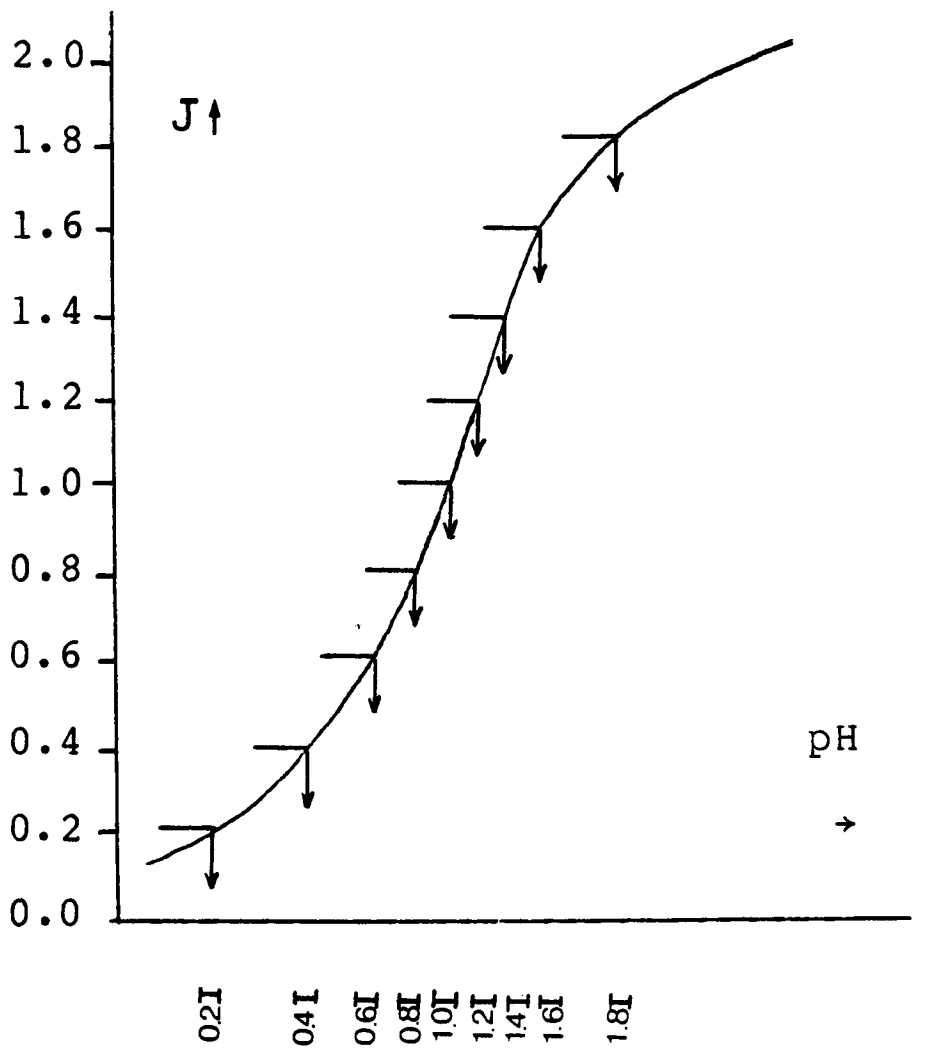

experimental plot

the projection strip

This strip is now superimposed as closely as possible on a series of plots of $lg(K_{a1}/K_{a2})$ against $lg(K_{a2}^{-\frac{1}{2}}[H])$ for the same set of J values, plotted with the same horizontal scale as before.

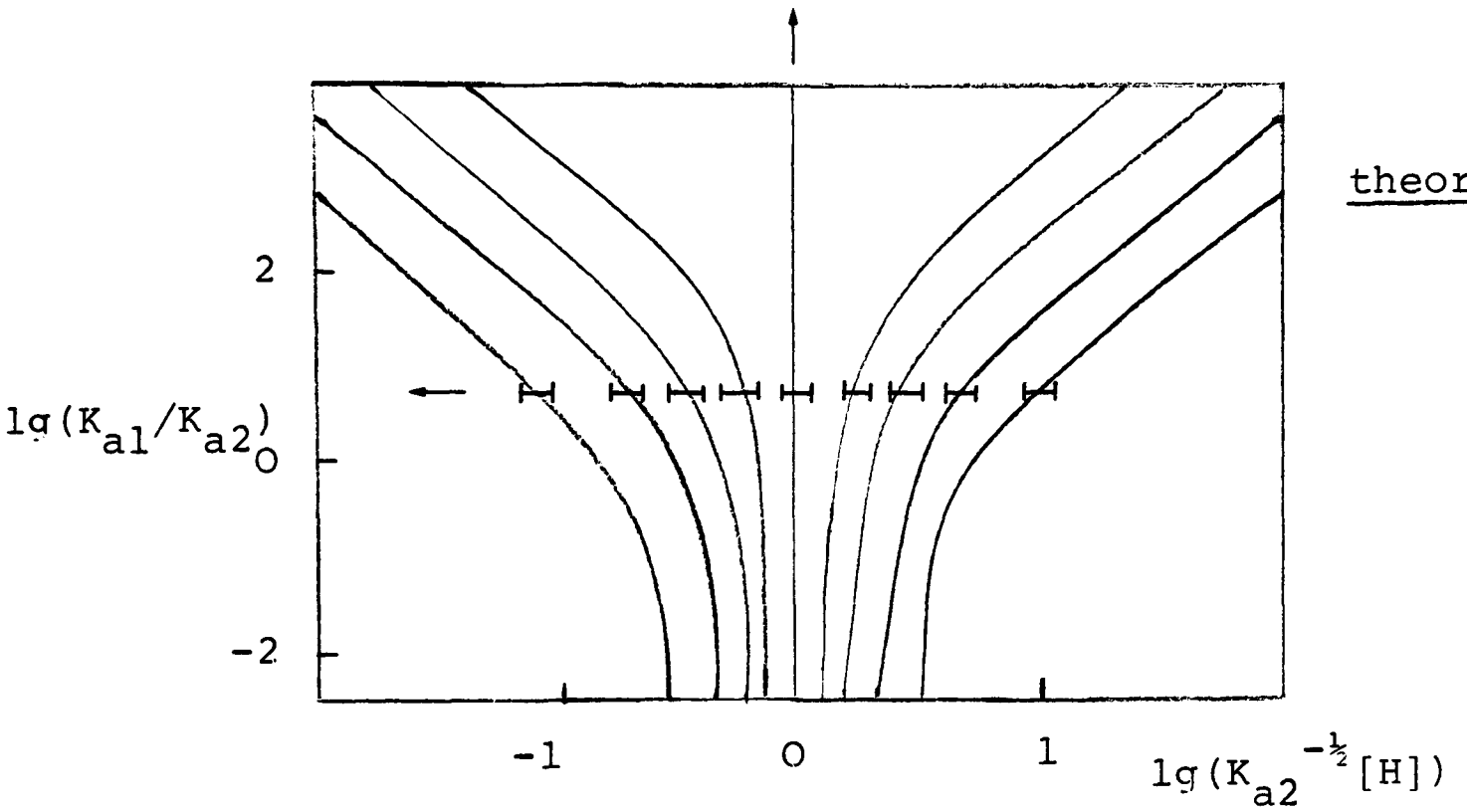

theoretical plot

The difference between pK_{a1} and pK_{a2} is read off from the y-axis and the average of the two values is obtained by tracing the zero line onto the experimental plot and reading off the pH value. An estimate of error is given simply by the minimum width of the bars in the projection strip found to be necessary to give a good fit to the theoretical plot. These estimates are given for each section. This method was used for evaluating pK_a's for

(i) the second two deprotonations of trien;

(ii) the pyrophosphate equilibria; and

(iii) the equilibria of linear tripolyphosphate in the presence of trien.

Acid Dissociation Constants in D_2O

In order to compare the pK_a values of the present work with those of the literature a correction has first to be made to take account of the differences between deuterium and proton behaviour. The glass electrode/pH meter reading procedure used here tends to underestimate the true pD value but this is largely countered by an increase in pKa observed in D_2O solutions. This led Bundi and Wüthrich (1979) to suggest the following relationship for small molecules $pD_{(cal)}$ = pH (meter reading) -0.10. Thus 0.10 pH units are subtracted from the present pK_a values, detrmined in D_2O using a glass electrode, when they are compared with those reported in the literature determined in H_2O. pK_a values in D_2O may well be somewhat different from those in H_2O even after this correction due to specific effects of H-(D-) binding.

Correction to zero ionic strength

All the pK_a values determined here are corrected to conditions of zero ionic strength. Details of the evaluation of the various corrections are found in each section but the general method is as follows.

For the deprotonation

$$\underset{z^2}{AH^{n+}} \rightleftharpoons \underset{(n-1)^2}{A^{(n-1)+}} + \underset{1}{H^+}$$

the difference in charge product is given by

$$\Delta z^2 = \{((n-1)^2 + 1\} - n^2$$

$$\rightleftharpoons \quad \Delta z^2 = -2(n-1)$$

Note: n may have positive or negative values.

The ionic strength of the particular experiment is given by $I = \frac{1}{2}\Sigma cz^2$, where c is the concentration of the various ions present and z is their charge.

The ionic strength correction is given by $F = 0.509\{I^{\frac{1}{2}}/(1+I^{\frac{1}{2}})-0.3I\}$. The correction to zero ionic strength is now given by $c=+F\Delta z$.

It is noted that for a positive Δz^2 value, that is for an increase in charge product on deprotonation, the pK_a rises as the ionic strength falls.

Finally, comparison is made of the pK_a values with those from the literature, (corrected to zero ionic strength), and the validity of the present method of pK_a evaluation is then established.

Establishing protonated and deprotonated chemical shift values

For trien, the chemical shift values for each protonation state are easily identifiable in the case of the free species, but not in the presence of excess phosphate. The $trien^{2+}$ species, in particular, does not have any chemical shift value clearly associated with it when it is bound to phosphate and the value is assumed to be the same as for the free species. This assumption is in fact found to be fully consistent with a detailed comparison of chemical shifts included in the summary at the end of this chapter.

A titration curve of the following type is obtained.

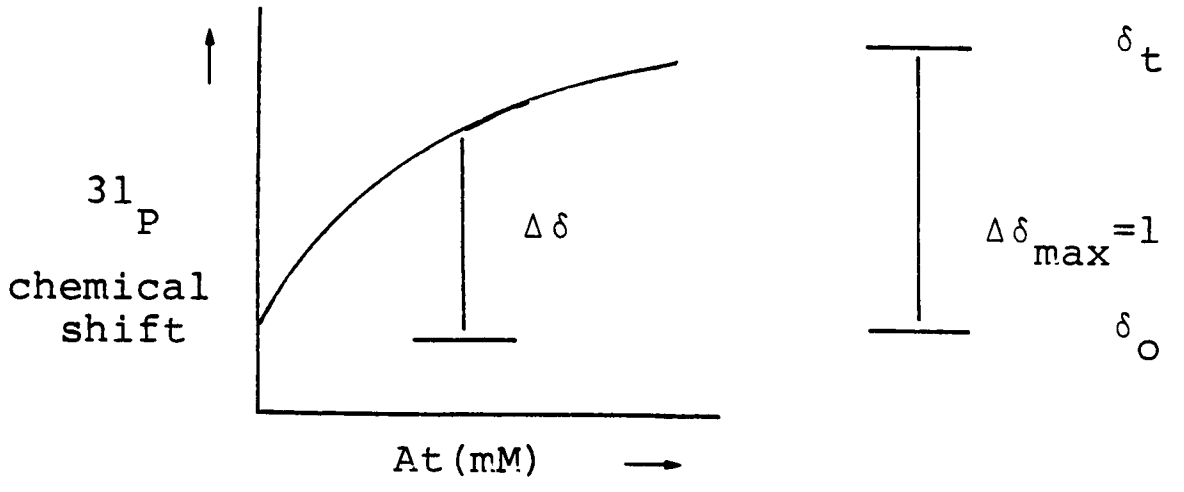

$\Delta\delta$ is directly proportional to fraction of phosphate bound to the amine: $[AP] = \Delta\delta Pt$

$$\text{so (2)} \quad K_b = \frac{\Delta\delta Pt}{(Pt-\Delta\delta Pt)(At-\Delta\delta Pt)}$$

$$\rightleftharpoons \quad K_b = \frac{\Delta\delta}{(1-\Delta\delta)(At-\Delta\delta Pt)}$$

$$\rightleftharpoons \quad K_b = (1-\Delta\delta)^{-1}\ (\frac{At}{\Delta\delta} - Pt)^{-1}$$

Thus for each complex a plot is made of

$$(1-\Delta\delta)^{-1} \quad \text{vs} \quad (\frac{At}{\Delta\delta} - Pt)$$

using a Research Machines 380Z computer and a least squares method that stipulated that the plot pass through the origin. The slope of this line then gives $K_b(mM^{-1})$. The fit of the various lines to data points was good. So the above equations proved sufficient to describe the various systems and it was not necessary to examine the data for complexes of other than 1:1 stoichiometry. The goodness of fit implied that the limits of error for the calculation were those of chemical shift measurement, ±0.01ppm. These limits were used to give minimum and maximum K_b values.

For further calculation K_b is expressed in M^{-1} and $\lg K_b$ evaluated.

For the phosphate titrations, the protonated and deprotonated chemical shift values are generally quite clear and the profiles are analysed independently. The exception is the titration of HMP with excess trien where lack of low pH data makes necessary the assumption that the chemical shift of the protonated species is not significantly altered by phosphate interaction.

3.1.2 Calculation of lgK_b

The theory behind the calculation of lgK_b given in each section is outlined here for the addition of amine A, total concentration A_t(mM), to phosphate P, total concentration P_t(mM), to give the complex AP.

$$A + P \rightleftharpoons AP \qquad K_b = \frac{[AP]}{[A][P]}$$

$$\rightarrow \qquad K_b = \frac{[AP]}{(A_t-[AP])(P_t-[AP])} \qquad (2)$$

Correction for incomplete complex formation

For complexes of the more lowly charged amines, correction has to be made for the fact that not all the amine under observation is phosphate bound. When lgK_b falls below 2.0, binding is less than 80%, and a significant amount of the amine is dissociated from the complex

$$AH^+P = A + P + H^+.$$

On the basis of this equation a more correct value for lgK_b is calculated from the initial value by simple proportion, e.g. if the K_b value represents 20% amine, it is multiplied by a factor of 5, to give a new K_b (and lgK_b) value. This new value, in turn, is used to give a new (higher) value for the percentage of amine that is phosphate bound. This now means that the original estimate of the extent to which K_b was underestimated was too high, and the new percentage figure is now used to determine a more accurate value of K_b. The process is repeated until the difference between successive lgK_b values is less than 0.005 units. It is these final values that are recorded, where indicated, in each section, for complexes of weak association.

The repetitive alogorithm was solved for the various complexes using a Research Machines 380Z microcomputer. Details of the calculation and the microprogram used are given in Appendix I.

Correction to zero ionic strength

For the general case, with m,n and r having positive or negative values,

$$x^{n+} + y^{m+} + rH^{+} \quad C^{(m+n+r)+}$$

$$z^2 \quad n^2 \quad m^2 \quad r \quad (m+n+r)^2$$

$$\Delta z^2 = (m+n+r)^2 - (m^2+n^2+r)$$

$$\rightleftharpoons \quad \Delta z^2 = 2mn + r(2m+2n+r-1).$$

(When no protonation/deprotonation is involved, r=0 and $\Delta z^2=2mn$).

Ionic strength and the correction factor are worked out as before for the pK_a correction. The correction to zero ionic strength is now given by

$$c = -F\Delta z^2$$

This is in contrast to the formula for the ΔpKa correction because for a positive Δz^2 value lgK_b falls as ionic strength falls.

3.1.3 Calculation of association constant at several pH values

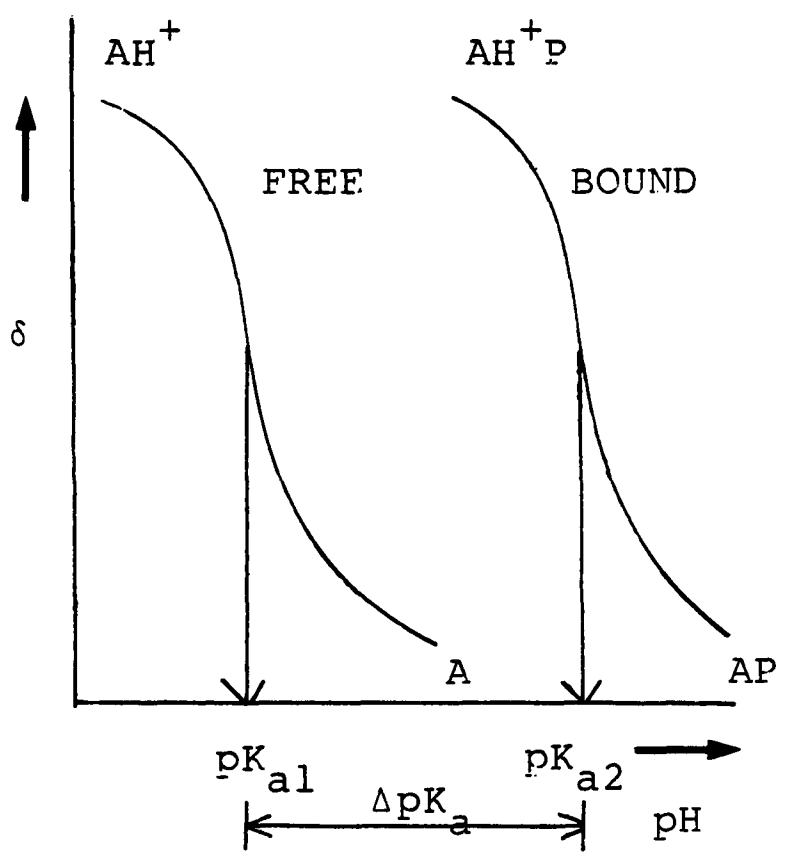

The method is illustrated here by considering the deprotonation of amine AH^+ in the presence and absence of phosphate P. The strength of association has been evaluated (as above) for the complex $AH^+.P$ and together with ΔpK_a it is used to evaluate lgK_b for the deprotonated complex, AP.

pK_a equilibria

free

$$AH^+ \rightleftharpoons A + H^+$$

$$K_{a1} = \frac{[A][H^+]}{[AH^+]}$$

bound

$$AH^+P \rightleftharpoons AP + H^+$$

$$K_{a2} = \frac{[AP][H^+]}{[AH^+P]}$$

$$\Rightarrow \quad \frac{K_{a2}}{K_{a1}} = \frac{[AP][AH^+]}{[AH^+P][A]} \quad \text{——} \quad (3)$$

K_b equilibria

protonated

$$AH^+ + P \rightleftharpoons AH^+P$$

$$K_{b1} = \frac{[AH^+P]}{[AH^+][P]}$$

deprotonated

$$A + P \rightleftharpoons AP$$

$$K_{b2} = \frac{[AP}{[A][P]}$$

$$\Rightarrow \quad \frac{K_{b1}}{K_{b2}} = \frac{[AH^+P][A]}{[AP][AH^+]} \quad \text{——} \quad (4)$$

(3) and (4) $\quad \frac{K_{b1}}{K_{b2}} = \frac{K_{a1}}{K_{a2}}$

$$\lg K_{b1} - \lg K_{b2} = -\lg K_{a2} - (-\lg K_{a1})$$

$$\rightleftharpoons \quad \Delta pK_a = \lg K_{b1} - \lg K_{b2}$$

Quite simply the presence of the phosphate favours the protonated form of the amine and the increase in pK_a so produced is a direct measure of the strength of phosphate/amine association.

Temperatures. All of the present series of experiments were carried out at room temperature and the temperature of the nmr probe was set to 300K. Thus, all the strengths of association are determined here for 27°C.

3.1.4 Outline of the chapter

The methods illustrated above are now applied to the six amine/phosphate interactions.

Whenever possible, the pK_a values obtained for each species are compared with values taken from the literature, thus checking the accuracy of the method.

Strength of association is determined at one particular pH value and then, using the ΔpKa values, strengths are determined for species in their various charge states. These lkK_b values are plotted against charge product and deviations from predicted values are considered.

The final section consists of a summary and comparison of the observed effects of the various phosphate/amine interactions on chemical shift and of the strengths of association and charge products of the various complexes. Apparent anomalies are explained in terms of spatial charge distribution and biological relevance is considered.

3.2 HEXAMETAPHOSPHATE WITH TRIETHYLENETETRAMINE

3.2.1 pK_a evaluation

Free triethylenetetramine

The pH profile of the acid/base titration of free triethylenetetramine is given in figure 3.1. The limiting chemical shift values of each resonance for each equilibrium are indicated as are the average pK_a values. pK_a's 1 and 2 are sufficiently isolated to be analysed singly while pK_a's 3 and 4 are treated as a pair and are subjected to "projection strip" analysis. The maximum error required for the curve fitting of the latter method is found to be ±0.07pH units, compared to ±0.02 pH units for the single pK_a analysis.

A pK_a value for each proton resonance is established and a weighted average is then taken. The weighting favours the proton that is closest to, and the resonance most affected by, the particular amine group that is losing a proton. Thus the pK_a1 and pK_a2 averages favour resonance C over resonance A, while the pK_a3 and pK_a4 averages depend more on resonance A than on resonance C.

The four pK_a values are presented below and are compared with literature values (Högfeldt and Perrin, 1979). Correction to conditions of zero ionic strength are as follows. Evaluations of ionic strength include figures for Na^+ and Cl^- ions which take into account

(i) the 1M NaOD added at the beginning of each experiment, to adjust pH; and

(ii) the 0.1M DCl added during the course of the experiment.

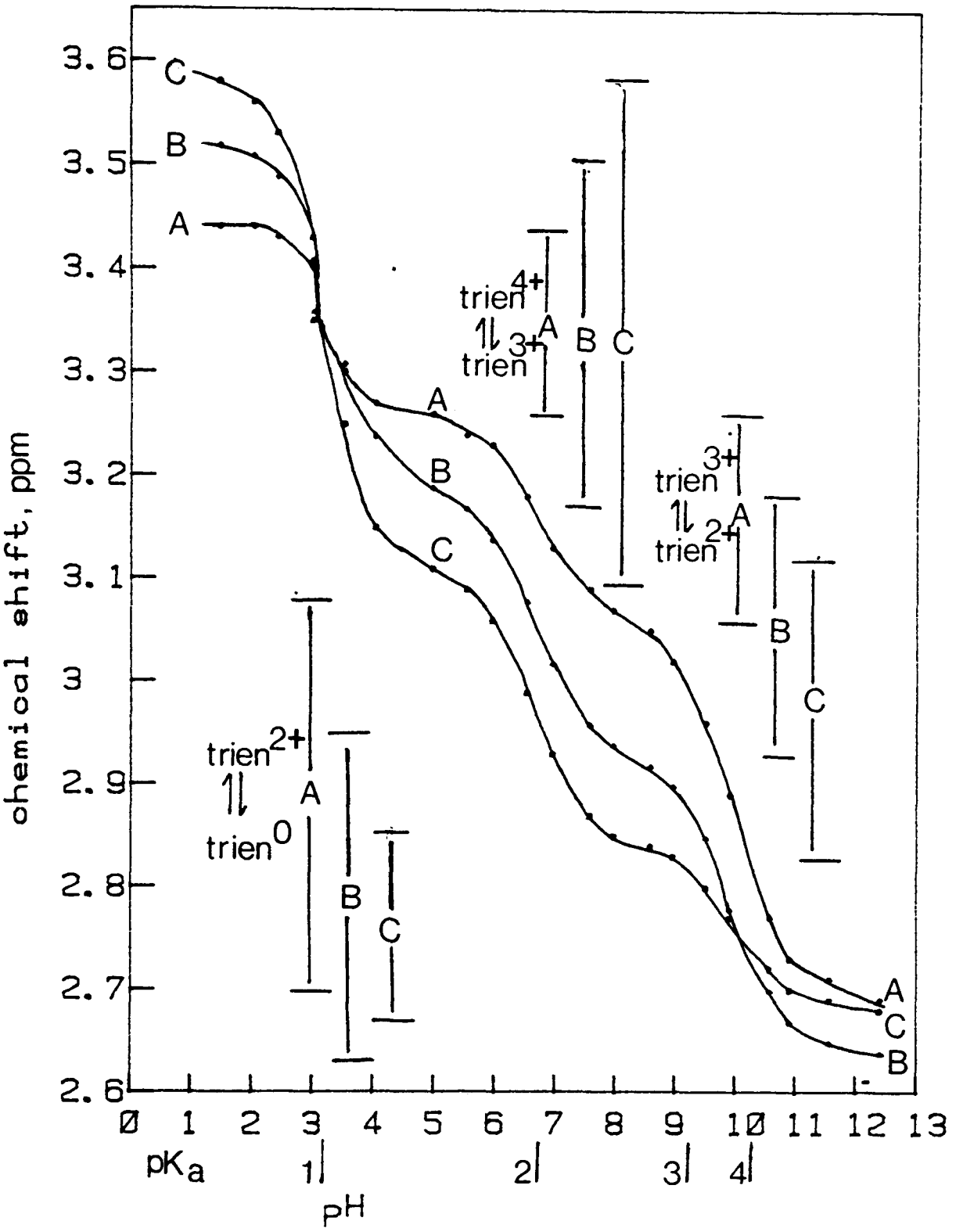

Figure 3.1 ^{1}H nmr pH profile of triethylenetetramine (T=300K). The methylene groups A,B and C are as follows.

$$\overset{+}{H_3N}\ \underset{A}{CH_2}\underset{B}{CH_2}NH\underset{C}{CH_2}\underset{C}{CH_2}NH\underset{B}{CH_2}\underset{A}{CH_2}\overset{+}{NH_3}$$

The limiting δ values for each of the equilibria are shown and the averages of the corresponding pK_a values are indicated along the x-axis.

The calculation is given in detail since the deduced pK_a values are used in several subsequent studies.

Ionic strength corrections, free trien

$trien^{1+}/trien^{\circ}$ n=1, $\Delta z^2 = 2(n-1)$

$\rightleftharpoons$ $\Delta z^2 = 0$

$trien^{2+}/trien^{1+}$

ionic strength	70mM Na^+ 30mM Cl^- 5mM $trien^{2+}/trien^{1+}$	I = 56mM, F = 0.088 $\Delta z^2 = -2$, C = -0.18

$trien^{3+}/trien^{2+}$

ionic strength	70mM Na^+ 50mM Cl^- 5mM $trien^{3+}/trien^{2+}$	I = 76mM, F = 0.098 $\Delta z^2 = -4$, C = -0.39

$trien^{4+}/trien^{3+}$

ionic strength	70mM Na^+ 75mM Cl^- 5mM $trien^{4+}/trien^{3+}$	I =104mM, F = 0.108 $\Delta z^2 = -6$, C = -0.65

The pK_a values are summarised as follows.

equilibrium		pK_a (uncorrected)	pK_a $I \rightarrow 0$
trien	$4^+/3^+$	(3.22)	2.57 (±.02)
	$3^+/2^+$	(6.73)	6.34 (±.02)
	$2^+/1^+$	(9.34)	9.16 (±.07)
	$1^+/0$	(10.34)	10.34 (±.07)

For the literature comparison shown below the present results are corrected for the deuterium isotope effect and compared with results reported by Rorabacher et al. (1971) recorded at 25°C and I = 100mM and corrected here to zero ionic strength.

		pK_a (I → 0)	
		present work, -0.10	literature
trien	$4^+/3^+$	2.47	2.75
	$3^+/2^+$	6.24	6.32
	$2^+/1^+$	9.06	9.10
	$1^+/0$	10.24	10.09

The agreement with the literature is good, given errors in the present method - nmr procedures always require high concentrations. The most substantial difference between present and literature values, 0.28, is found for the $trien^{4+}/trien^{3+}$ deprotonation while the other discrepancies do not exceed 0.15. The present results were reproducible under the experimental conditions used and were, therefore, the values used for all subsequent calculations.

Free hexametaphosphate

The pH profile of free hexametaphosphate is shown in figure 3.3. The single pK_a is evaluated, within an error of ±0.02pH units, and ionic strength correction is as follows.

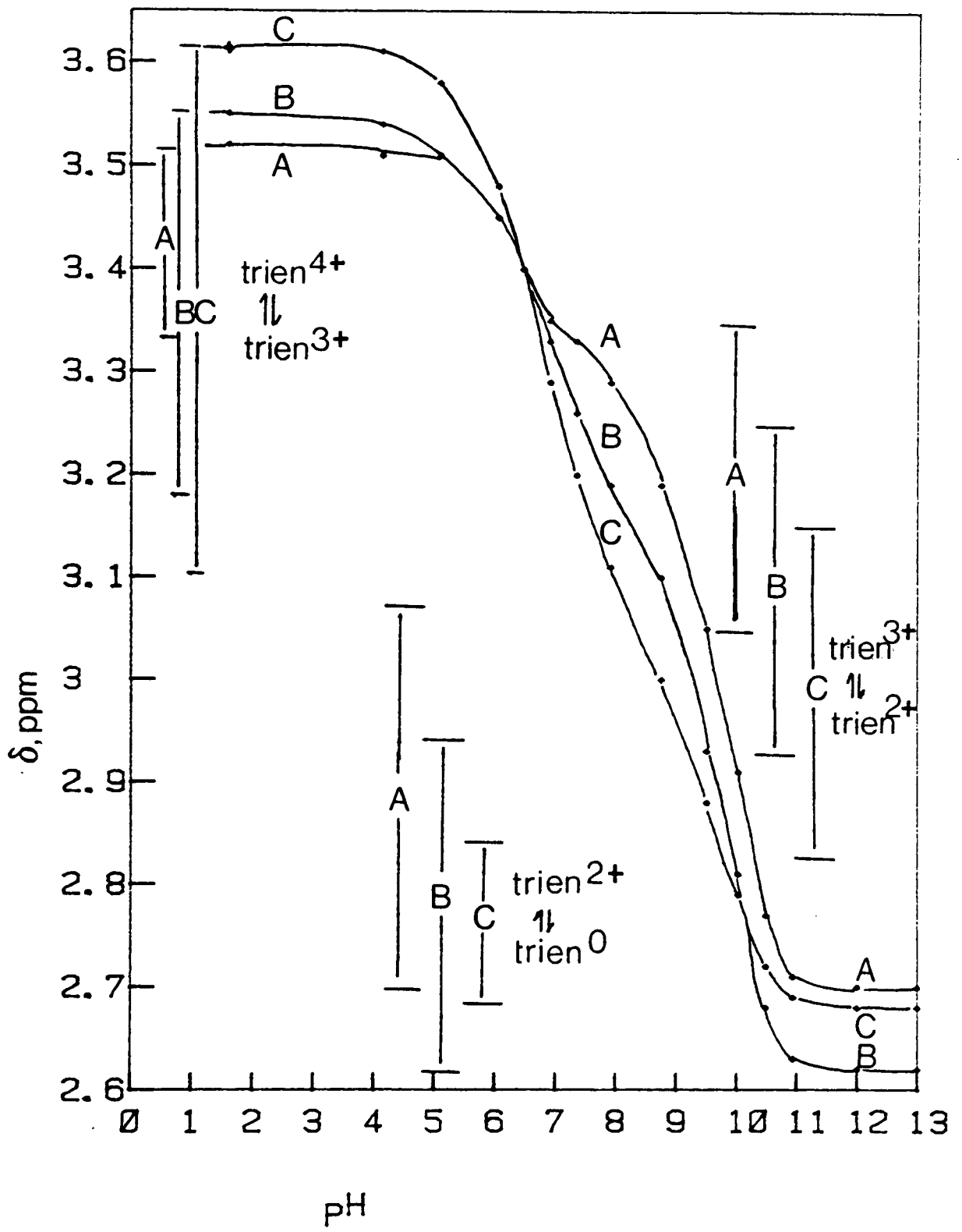

Figure 3.2 ^{1}H nmr pH profile of triethylenetetramine in the presence of excess hexametaphosphate.

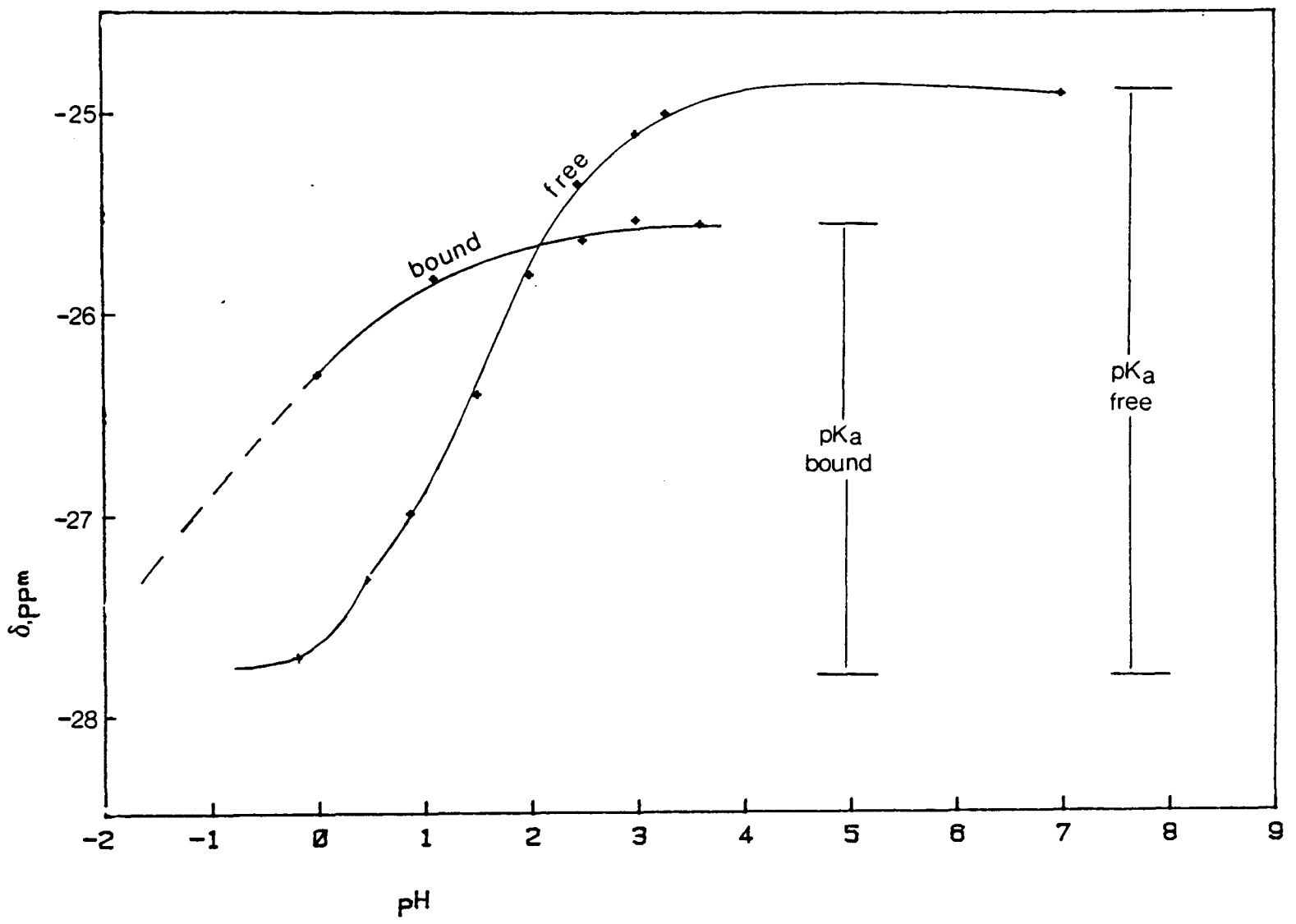

Figure 3.3 ^{31}P nmr pH profile of HMP with and without excess trien.

70mM Na^+
90mM Cl^-
pH 1.6: 25mM H^+
5mM HMP^{5-}/HMP^{6-}

$I = 172mM, \quad F = 0.123$

$\Delta z^2 = +12, \quad C = +1.48$

Thus the pK_a values for free HMP are as follws

equilibrium	pK_a	
	I	I→0
HMP 5-/6-	1.48	2.96

Trien with excess HMP

The pH profile for trien with excess HMP is shown in figure 3.2. pK_a's are evaluated as before, and ionic strength correction is as follows.

$trien^{1+}/trien^0$

45mM Na^+ 45mM HMP^{6-}
20mM Cl^- 5mM $complex^{5-}/complex^{6-}$

$I = 918mM, \quad F = 0.109$

$[trien^{1+}\ HMP^{6-}]^{5-} \rightleftharpoons [trien^0\ HMP^{6-}]^{6-} + H^+$

$n = -5; \quad \Delta z^2 = -2(n-1)$

$\Delta z^2 = +12, \quad C = +1.31$

$trien^{2+}/trien^{1+}$

45mM Na^+ 45mM HMP^{6-}
60mM Cl^- 5mM $complex^{4-}/complex^{5-}$

$I = 913mM, \quad F = 0.110$

$\Delta z^2 = +10, \quad C = +1.10$

$trien^{3+}/trien^{2+}$

45mM Na^+ 45mM HMP^{6-}
100mM Cl^- 5mM $complex^{3-}/complex^{4-}$

$I = 913mM, \quad F = 0.110$

$\Delta z^3 = +8, \quad C = +0.88$

$trien^{4+}/trien^{3+}$

45mM Na+ 45mM HMP^{6-}
160mM Cl- 5mM $complex^{2-}/complex^{3-}$

$I = 928mM, \quad F = 0.1085$

$\Delta z^2 = +6, \quad C = +0.65$

These corrections yield the following values

equilibrium	pK_a with excess HMP I	I→0	
$4^+/3^+$	6.70	7.35	(±0.02)
$3^+/2^+$	9.03	9.91	(±0.02)
$2^+/1^+$	9.89	10.99	(±0.07)
$1^+/0$	10.50	11.81	(±0.07)

HMP with excess trien

The pH profile of HMP with excess trien is shown in figure 3.2. Due to the low pH values involved considerable extrapolation is necessary. It is assumed that the chemical shift value of the protonated complex is the same as that of the protonated free phosphate and, indeed, in the subsequent studies, such a relationship is generally seen to be upheld. Correction to zero ionic strength is as follows.

lowest experimental pH:pH0.0 → 1,000mM H^+

45mM Na^+ } I = 1.536M

300mM Cl^- } F = +0.047

45mM $trien^{4+}$ }

5mM $complex^{1-}$/

$complex^{2-}$

$[trien^{4+}\ HMP^{5-}]^{1-}$ → n = -1

→ $\Delta z^2 = +3$

→ C = +0.14

The correction is applied here.

equilibrium	pK_a with excess trien	
	I	I → 0
HMP $5^-/6^-$	-0.21	-0.07(±.02)

pK_a summary

The completed set of pK_a's, free and complexed, corrected to I → 0, are as follows.

equilibrium		pK_a free	pK_a complexed	ΔpK_a
trien	$4^+/3^+$	2.57(±.02)	7.35(±.02)	+4.78(±.03)
	$3^+/2^+$	6.34(±.02)	9.91(±.02)	+3.57(±.03)
	$2^+/1^+$	9.16(±.07)	10.91(±.07)	+1.83(±.10)
	$1^+/0$	10.34(±.07)	11.81(±.07)	+1.47(±.10)
HMP	$5^-/6^-$	2.96(±.02)	-0.07(±.02)	-3.03(±.03)

Two observations are immediately made from these figures.

(i) As the charge on the amine decreases, so does the influence of the phosphate, measured here by ΔpK_a.

(ii) ΔpK_a for HMP^{5-}/HMP^{6-}, with or without $trien^{4+}$, is slightly less than ΔpK_a for $trient^{3+}/trien^{2+}$, with or without HMP^{6-}. Given the comparative isolation of charges in the linear amine molecule this might well be expected, that the "preference" (or increase in strength of interaction) of $trien^{4+}$ for HMP^{6-} over HMP^{5-} is less than that of HMP^{6-} for $trien^{4+}$ over $trien^{3+}$ and comarable, instead, to that of HMP^{6-} for $trien^{3+}$ over $trien^{2+}$.

3.2.2 Association constant evaluation

Incremental addition was made, as described in the materials and methods section, of trien to a 5mM HMP solution. The sample was maintained at pH8.00, ± 0.05, and the increase in volume did not exceed 2%. The addition is illustrated by figure 3.4A, which indicates the maximum error in δ of ± 0.01ppm. The association constant is calculated using the following data.

At mM	Δδ -	$At(\Delta\delta)^{-1} - Pt$ mM	$(1-\Delta\delta)^{-1}$ -
3	0.455	1.59	1.83
4	0.581	1.88	2.39
5	0.659	2.59	2.93
6	0.725	3.28	3.64
7	0.766	4.14	4.27
8	0.814	4.83	5.38
9	0.850	5.59	6.67

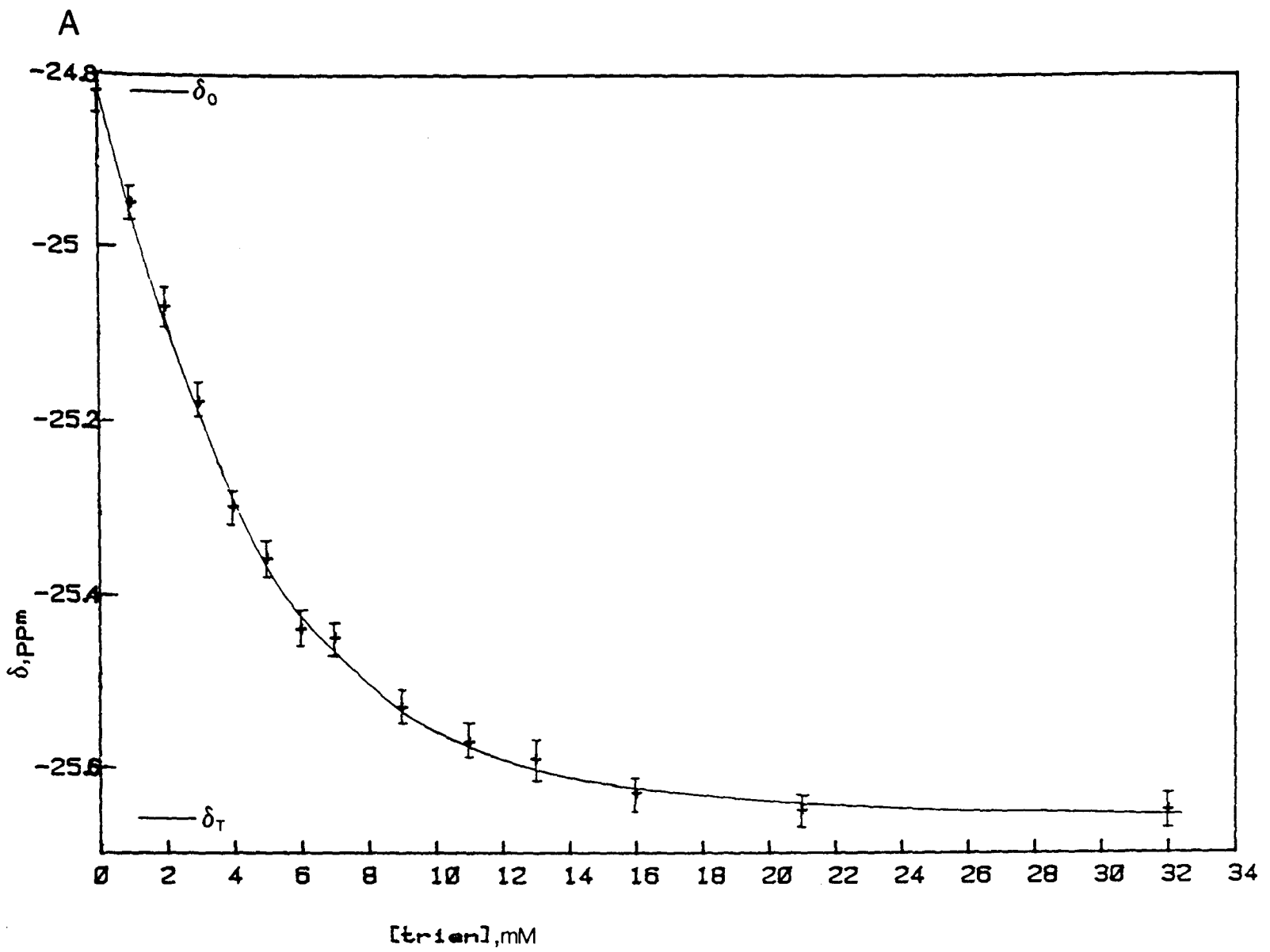

Figure 3.4 (A) The effect of the addition of trien on the ^{31}P nmr chemical shift of HMP. pH8.0.

(B) Evaluation of the dissociation constant.

The least squares computer programme was used to plot $(1-\Delta\delta)^{-1}$ against $\{At(\Delta\delta)^{-1}-Pt\}$ in figure 3.4B. The gradient of the plot indicated that K_b = 1.11mM^{-1} (±0.08mM^{-1}) or $\lg K_b$ = 3.05 (±0.03). The correction to zero ionic strength, evaluated at 5mM trien is as follows.

5mM $EDTA^{3-}$ 1.7mM $trien^{2+}$ I = 71mM, F = 0.096

3.3mM $complex^{3-}$ 1.7mM HMP^{6-}

$$trien^{2+} + HMP^{6-} + H^{+} = [trien^{3+}\ HMP^{6-}]^{3-}$$

$m = +2,\ n = -6,\ r = +1;$

$\Delta z^2 = 2mn + r(2m + 2n + r-1)$

$\rightarrow \Delta z^2 = -32 \qquad \rightarrow c(=-F\Delta z^2) = +3.07$

Thus $\lg K_b$(pH8.0, I→0) = 6.12 (±0.03)

3.2.3 Association constants at several pH values

The various complexes are set out in table 3.1, beginning with the most protonated on the left. The various pK_a values determined for each successive deprotonation of the various complexes are given, as are the ΔpK_a values determined above, where $\Delta pK_a = pK_{a2}$ (bound species) - pK_{a1} (free species) as expressed in the introductory section.

The experimentally determined association constant is for the complex $[trien^{3+}\ HMP_6{}^{-}]^{3-}$.

As an illustration of the calculations, $\lg K_b$ for the next, less protonated, complex in the series $[trien^{2+}\ HMP^{6-}]^{4-}$ is determined as follows

$$trien^{3+} = trien^{2+} + H^{+} \quad pK_{a1} = 6.34$$

$$trien^{3+}_{HMP^{6-}}{}^{3-} = trien^{2+}_{HMP^{6-}}{}^{4-} + H^{+} \quad pK_{a2} = 9.91$$

$\rightarrow \Delta pK_a = 9.91 - 6.34 = 3.57$ (as indicated)

Table 3.1 Trien/HMP-pK_a and lgK_b summary

The experimentally determined lgK_b value is underlined.

Where extent of association falls below 80%, a correction has been applied to the lgK_b values as described in the introductory section 3.13. In such cases, the estimated degree of binding is given alongside the lgK_b value.

complex	$[trien^{4+}\ HMP^{5-}]^{1-}$	⇌	$[trien^{4+}\ HMP^{6-}]^{2-}$	⇌	$[trien^{3+}\ HMP^{6-}]^{3-}$	⇌	$[trien^{2+}\ HMP^{6-}]^{4-}$	⇌	$[trien^{1+}\ HMP^{6-}]^{5-}$	⇌	$[trien^{0}\ HMP^{6-}]^{6-}$
pK_a			-0.07		7.35		9.91		10.91		11.81
ΔpK_a			-3.03(±.03)		4.78(±.03)		3.57(±.03)		1.83(±.10)		1.47(±.10)
lgK_b	7.87(±.05)	←	10.90(±.04)	←	<u>6.12</u>(±.03)	→	2.55(±.04)	→	1.12(±.11) (39%)	→	0.51(±.15) (14%)

But, see introduction,

$\Delta pK_a = lgK_{b1}$(protonated complex) $- lgK_{b2}$ (deprotonated complex)

$$\rightarrow lgK_b \left[\begin{matrix} trien^{2+} \\ HMP^{6-} \end{matrix} \right]^{4-} = lgK_b \left[\begin{matrix} trien^{3+} \\ HMP^{6-} \end{matrix} \right]^{3-} - \Delta pK_a$$

$$\rightarrow lgK_{b2} = 6.12 - 3.57$$

i.e. the association constant for $[trien^{2+}\ HMP^{6-}]^{4-}$ is expressed by lgK_b $(I \rightarrow 0) = 2.55$.

The remaining association constants are calculated in the same manner and the lgK_b values are presented in table 3.1. They are plotted against charge product in figure 3.5 which includes a reference plot of the average strength of interaction of seventeen spherical inorganic ion pairs. (Tam and Williams, 1984 (table 4)). This plot was found to show good agreement with the theoretical curves based on Bjerrum's theoretical treatment of ions as point charges with distance of cloest approach estimated to lie between 0.5 and 0.7nm.

An assessment in now made of the effects of the distribution of charge on the strength of association. These effects are minimal for $trien^{1+}$ which may be considered to act as a point charge, and will be less for the fully protonated $trien^{4+}$ than for the partially protonated species $trien^{3+}$ and $trien^{2+}$. Similarly, the effect may be expected to be less for the fully anionic HMP^{6-} than for the partially charged HMP^{5-}. On this basis a (broken) line is drawn on

figure 3.4 between the data points for the $trien^{1+}/HMP^{6-}$ and $trien^{4+}/HMP^{6-}$ interactions which indicates, for a given charge product, the value of lgK_b when association is least diminished by isolation of charges. This line indicates that, from the lgK_b value determined, the "effective" charge products of the various combinations are as follows.

complex	charge product	effective charge product
$trien^{4+}/HMP^{5-}$	20	18
$trien^{3+}/HMP^{6-}$	18	$15\frac{1}{2}$
$trien^{2+}/HMP^{6-}$	12	$8\frac{1}{2}$

The greatest discrepancy is seen for $trien^{2+}$, with its two charges held at the extremities of its linear structure. The apparent strength of its interaction indicates an effective charge of only $1\frac{1}{2}$ units. Similarly $trien^{3+}$ has an apparent effective charge of only $2\frac{1}{2}$ units.

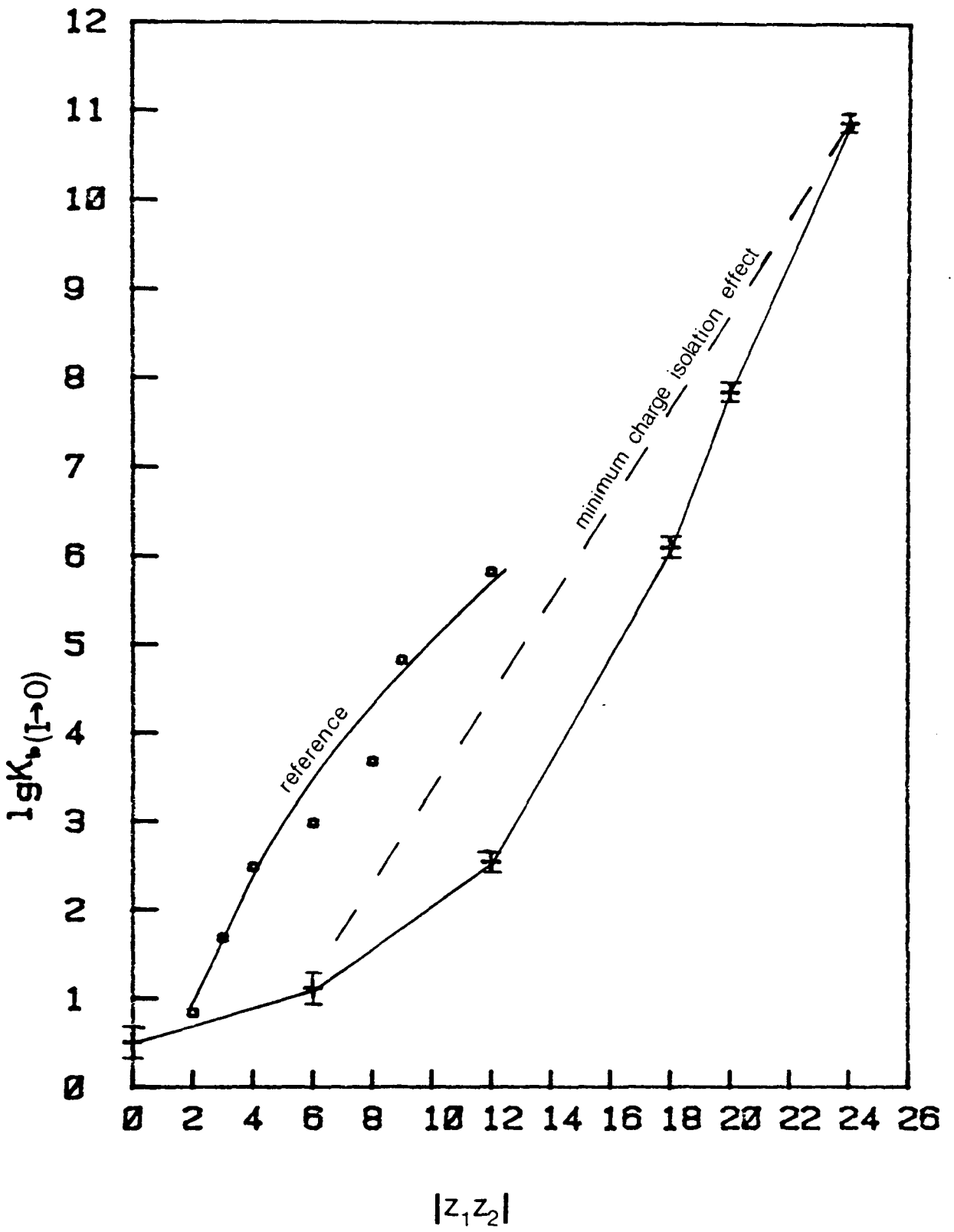

Figure 3.5 HMP/trien association: lgK_b vs charge product for various levels of protonation.

Also shown are

(i) strength of association for minimum charge isolation, represented by a broken line, and

(ii) a reference plot of spherical inorganic ion interaction (Tam and Williams, 1983).

3.3 PYROPHOSPHATE WITH TRIETHYLENETETRAMINE

3.3.1 pK_a evaluation

The pK_a values of free triethylenetetramine are recorded in the previous section.

The pH profiles of the amine in prsence of excess pyrophosphate and of the phosphate with and without the amine are shown in figures 3.6 and 3.7 respectively. Corrections for ionic strength are as follows. The various complexes are represented by AP^{n+}.

trien with excess PP

$trien^{1+}/trien^{0}$	45mM Na^+	45mM PP^{4-}	I=425mM, F=0.136
	20mM Ce^-	5mM AP^{3-}/AP^{4-}	

$[trien^{1+}\ PP^{4-}]^{3-} = [trien^{0}\ PP^{4-}]^{4-} + H^+$ $\Delta z^2=+8$, C=+1.09

$trien^{2+}/trien^{1+}$	45mM Na^+	45mM PP^{4-}	I=430mM,	F=0.136
	60mM Cl^-	5mM AP^{2-}/AP^{3-}	$\Delta z^2=+6$,	C=+0.82
$trien^{3+}/trien^{2+}$	45mM Na^+	45mM PP^{3-}/PP^{4-}	I=360mM,	F=0.136
	100mM Cl^-	5mM AP^{1-}/AP^{2-}	$\Delta z^2=+4$,	C=+0.54
$trien^{4+}/trien^{3+}$	45mM Na^+	45mM PP^{2-}/PP^{3-}	I=250mM,	F=0.131
	160mM Cl^-	5mM AP^{0}/AP^{1-}	$\Delta z^2=+2$,	C=+0.26

free PP

PP^{3-}/PP^{4-}	70mM Na^+	5mM $EDTA^{3-}$	I=103mM,	F=0.108
	30mM Cl^-	5mM PP^{3-}/PP^{4-}	$\Delta z^2=+8$,	C=+0.86
PP^{2-}/PP^{3-}	70mM Na^+	5mM $EDTA^{2-}/EDTA^{3-}$	I=97mM,	F=0.106
	60mM Cl^-	5mM PP^{2-}/PP^{3-}	$\Delta z^2=+6$,	C=+0.64

PP with excess trien

PP^{3-}/PP^{4-}	45mM Na^+	45mM $trien^{3+}/trien^{2+}$	$\Delta z^2=0$	
	70mM Cl^-	5mM AP^{1+}/AP^{0}		
PP^{2-}/PP^{3-}	45mM Na^+	45mM $trien^{3+}$	I=310mM,	F=0.134
	140mM Cl^-	5mM AP^{2+}/AP^{1+}		
	5mM $EDTA^{2-}$		$\Delta z^2=-2$,	C=-0.26

The corrected pK_a values are given below, together with the ΔpK figures.

species	equilibrium	pK_a free (uncorrected)	pK_a free I=0	pK_a bound (uncorrected)	pK_a bound I=0	ΔpK_a I=0
trien	$4^+/3^+$	-	2.57±.02	(6.55)	6.81±.02	4.24±.03
	$3^+/2^+$	-	6.34±.02	(8.84)	9.38±.02	3.04±.03
	$2^+/1^+$	-	9.16±.07	(9.85)	10.67±.07	1.51±.10
	$1^+/0$	-	10.34±.07	(10.42)	11.51±.07	1.17±.10
PP	$2^-/3^-$	(6.38)	7.02±.02	(4.68)	4.42±.02	-2.60±.07
	$3^-/4^-$	(8.73)	9.59±.02	(6.18)	6.18±.02	-3.41±.07

As before, it is seen that the influence of the phosphate on the amine decreases as the charge on the amine decreases. Also, the differences in strength of interaction (ΔpK_a) of $\underline{PP^{4-}}$ with $\underline{trien^{4+}\ over\ trien^{3+}}$ (4.24) and with $\underline{trien^{3+}\ over\ trien^{2+}}$ (3.04) are, respectively, greater than those of $trien^{4+}$ with $\underline{PP^{4-}\ over\ PP^{3-}}$ (3.41) and with $\underline{PP^{3-}\ over\ PP^{2-}}$ (2.60).

The average of the three pK_a values reported by Hogfeldt and Perrin (1979) for PP at 25° C, and corrected to zero ionic strength, has been taken and is compared below with the present values, corrected for deuterium isotope effects. The larger discrepancy is 0.12 and thus agreement is good.

equilibrium	pK_a (I→0) present work, -0.10	pK_a (I→0) literature
PP $2^-/3^-$	6.92	6.80
PP 3-/4-	9.49	9.50

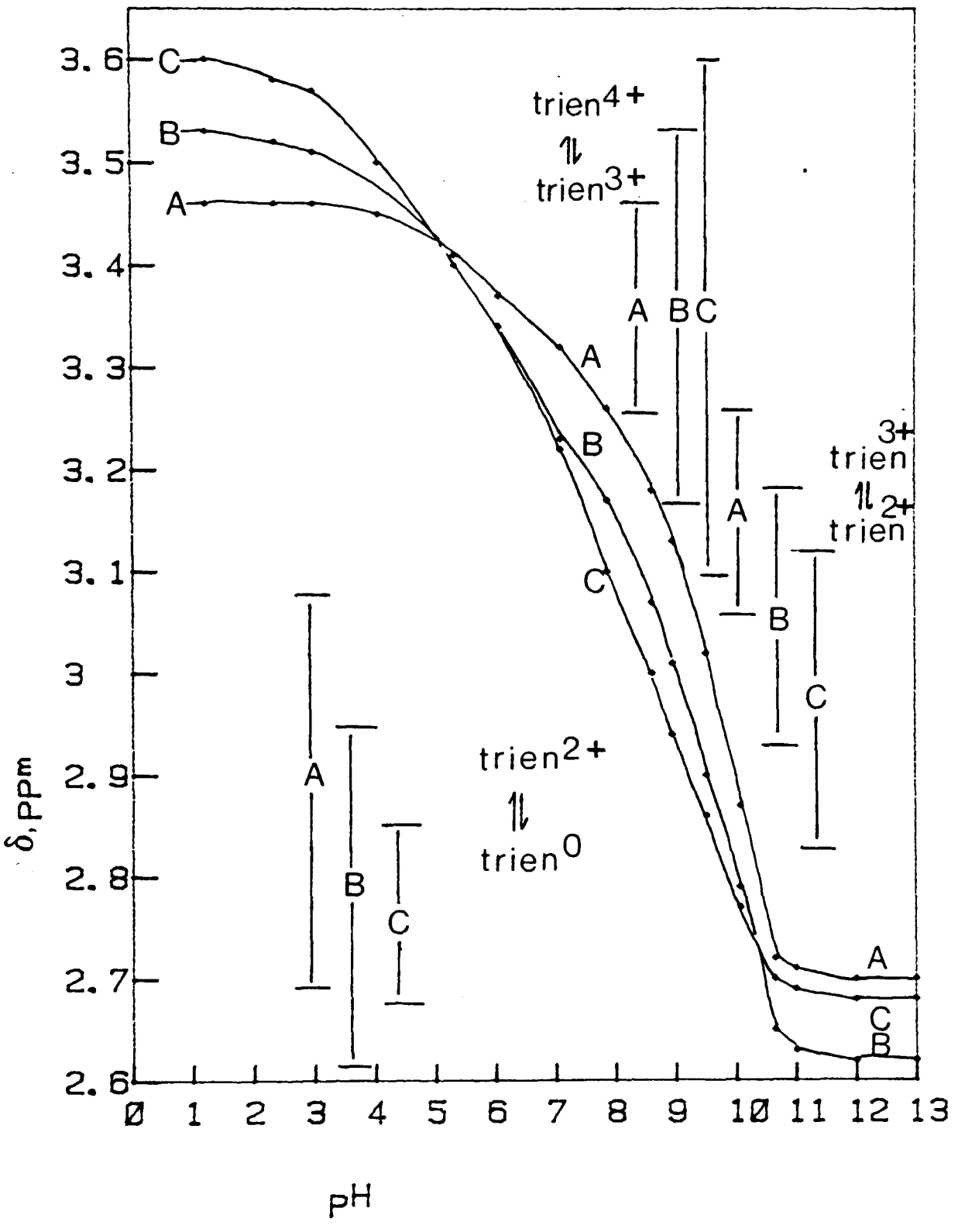

Figure 3.6 ^{1}H nmr pH profile of triethylenetetramine in the presence of excess pyrophosphate.

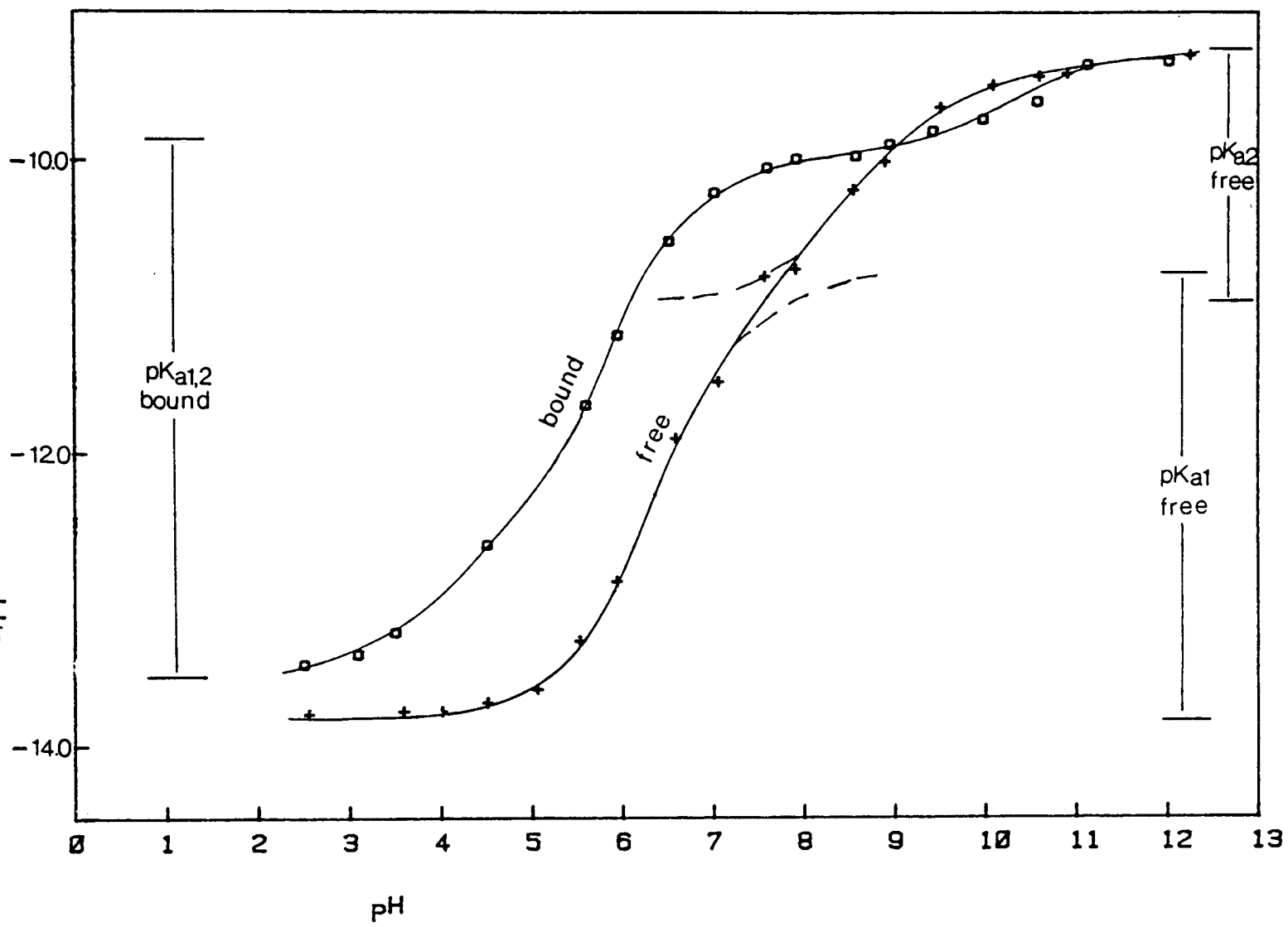

Figure 3.7 ^{31}P nmr pH profiles of pyrophosphate in the presence and absence of excess triethylenetetramine.

3.3.2 Association constant evaluation

Trien was added to a solution of 5mMPP kept constant at pH 3.0. The titration is illustrated by figure 3.8A. The association constant, K_b, is calculated from the following data.

At mM	$\Delta\delta$ -	$At(\Delta\delta)^{-1} - Pt$ mM	$(1-\Delta\delta)^{-1}$ -
3	0.264	6.36	1.36
4	0.325	7.31	1.48
5	0.387	7.92	1.63
6	0.434	8.82	1.77
7	0.491	9.26	1.96
8	0.538	9.87	2.16
9	0.585	10.38	2.41

The least squares programme was used to plot $(1-\Delta\delta)^{-1}$ against $\{At(\Delta\delta)^{-1}-Pt\}$ in figure 3.8B. The slope indicated that $K_b = 210(\pm 22)M^{-1}$, or $\lg K_b = 2.32(\pm.05)$. Correction to zero ionic strength, evaluated at 5mM trien, is as follows.

5mM $EDTA^{1-}/EDTA^{2-}$, 2mM AP^{2+}, 3mM $trien^{4+}$, 3mM PP^{2-} } I=19mM, F=0.058

$$trien^{4+} + PP^{2-} \rightleftharpoons [trien^{4+}\ PP^{2-}]^{2+} \quad \Delta z^2=-2mn=-16$$

C=+0.93

Thus, $\lg K_b(I\rightarrow 0, pH3.0)=3.25(\pm.05)$.

A

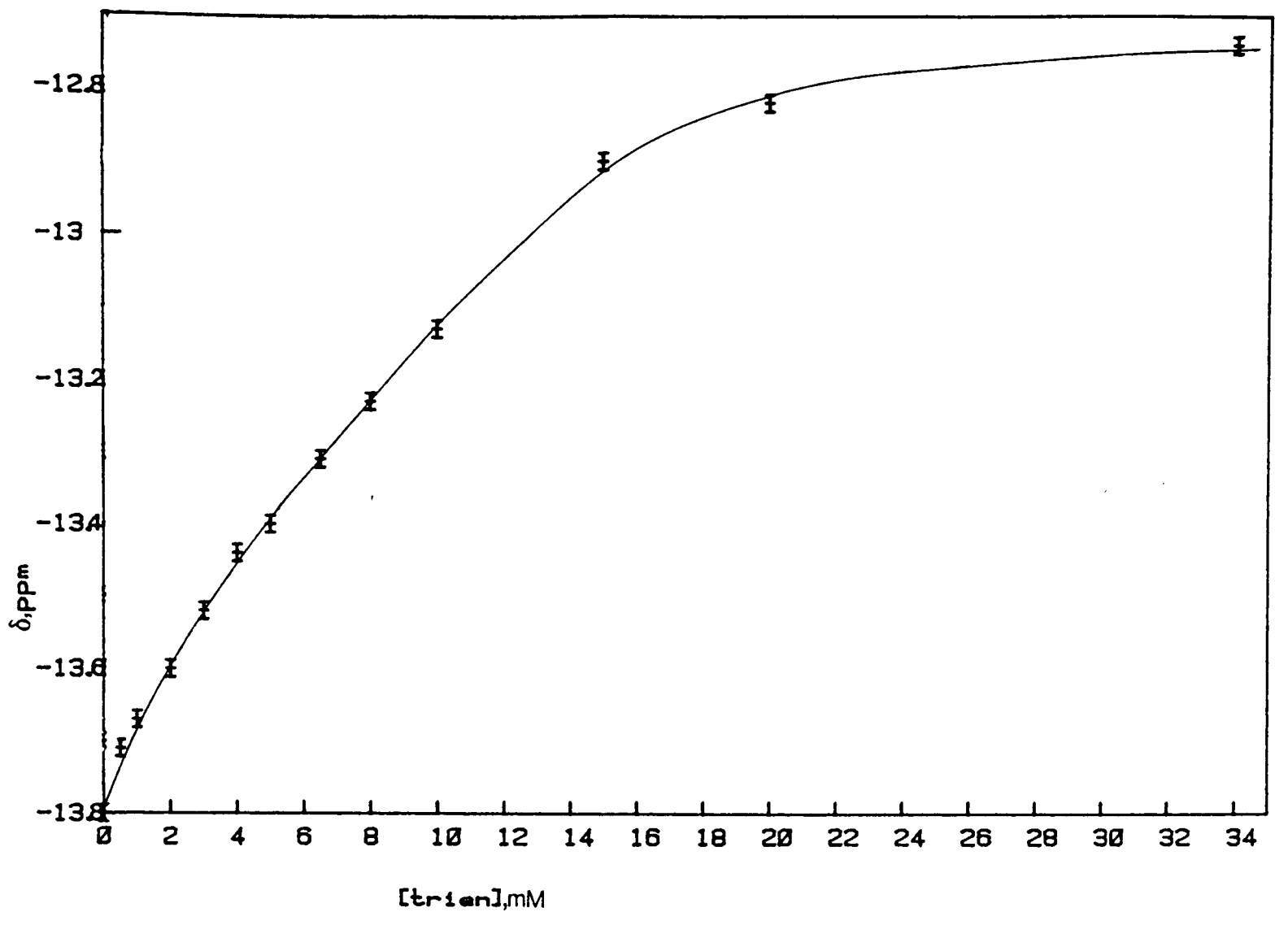

B

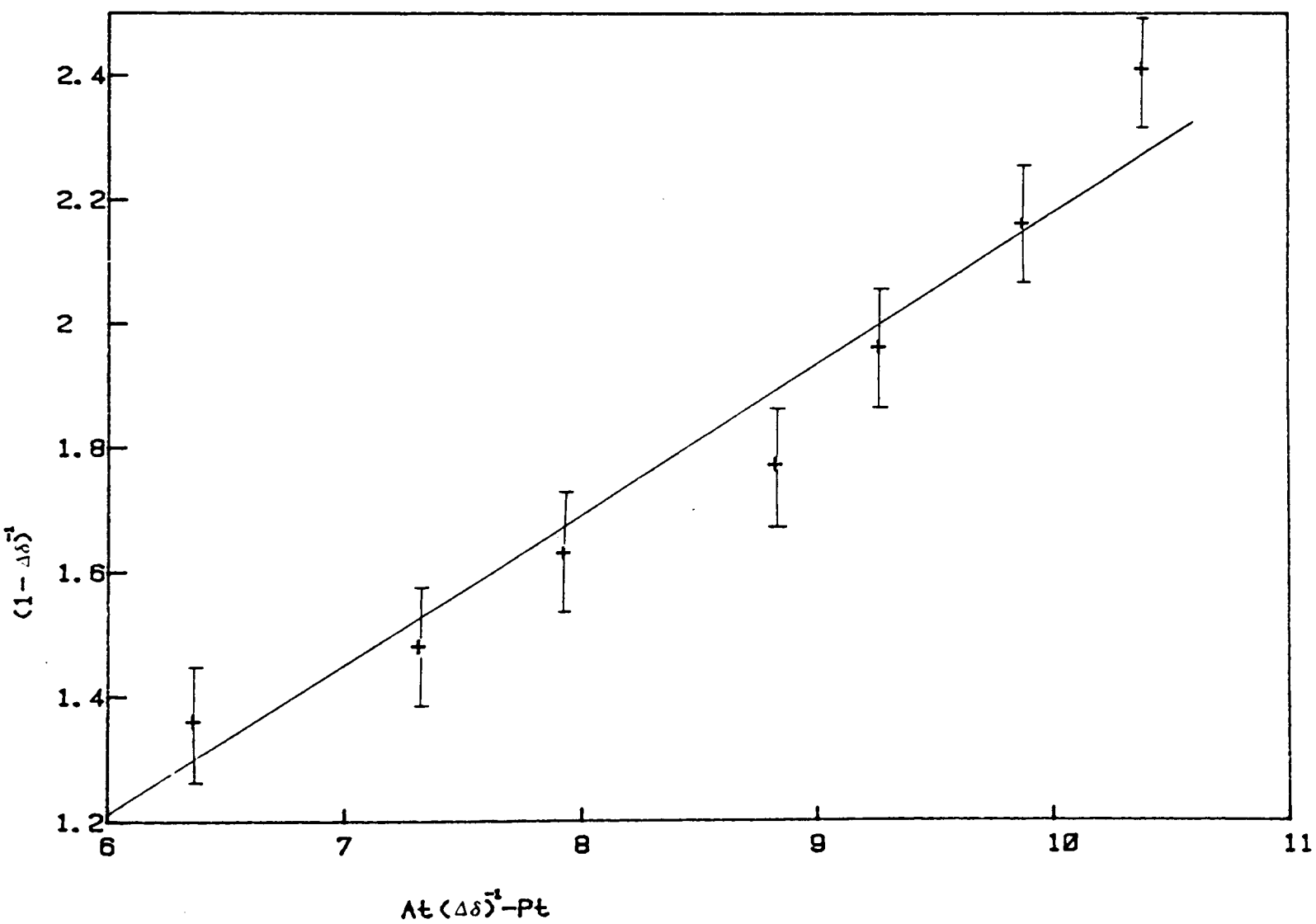

Figure 3.8 (A) The effect of the addition of trien on the ^{31}P nmr chemical shift of PP. (pH3.0)

(B) Evaluation of association constant.

3.3.3 Association constants at several pH values

The $lgK_b(I \rightarrow 0)$ values for the various complexes are calculated as before and the completed set is presented in table 3.2. The values are plotted against charge product in figure 3.9, which includes the inorganic ion pair reference line (Tam and Williams, 1983) and a line of minimum charge isolation effects, connecting the points for the $trien^{1+}/PP^{4-}$ and $trien^{4+}/PP^{4-}$ complexes. This line is used to determined the shortfalls of "effective charge product" calculated on the basis of strength of association.

interaction	charge product	effective charge product
$trien^{4+}/PP^{2-}$	8	$7\frac{1}{2}$
$trien^{4+}/PP^{3-}$	12	11
$trien^{3+}/PP^{4-}$	12	10
$trien^{2+}/PP^{4-}$	8	$5\frac{1}{2}$

As before, the greatest shortfall is seen for the $trien^{2+}$ complex, with its charge isolated of either end of its structure. The isolation effect is much less marked for the more compact PP molecule.

Table 3.2 Trien/PP - pK_a and lgK_b summary

complex	$\left[\begin{matrix}trien^{4+}\\PP^{2-}\end{matrix}\right]^{2+}$	⇌	$\left[\begin{matrix}trien^{4+}\\PP^{3-}\end{matrix}\right]^{1+}$	⇌	$\left[\begin{matrix}trien^{4+}\\PP^{4-}\end{matrix}\right]^{0}$	⇌	$\left[\begin{matrix}trien^{3+}\\PP^{4-}\end{matrix}\right]^{1-}$	⇌	$\left[\begin{matrix}trien^{2+}\\PP^{4-}\end{matrix}\right]^{2-}$	⇌	$\left[\begin{matrix}trien^{1+}\\PP^{4-}\end{matrix}\right]^{3-}$	⇌	$\left[\begin{matrix}trien^{0}\\PP^{4-}\end{matrix}\right]^{4-}$
pK_a			4.42		6.18		6.81		9.38		10.67		11.51
ΔpK_a			-2.60(±.07)		-3.41(±.07)		4.24(±.03)		3.04(±.03)		1.51(±.10)		1.17(±.10)
lgK_b	3.25(±.05)	→	5.85(±.09)	→	9.26(±.11)	→	5.02(±.11)	→	2.05(±.12)	→	1.01(±.16)	→	0.61(0.18)
			(84% bound)		(33% bound)		(17% bound)						

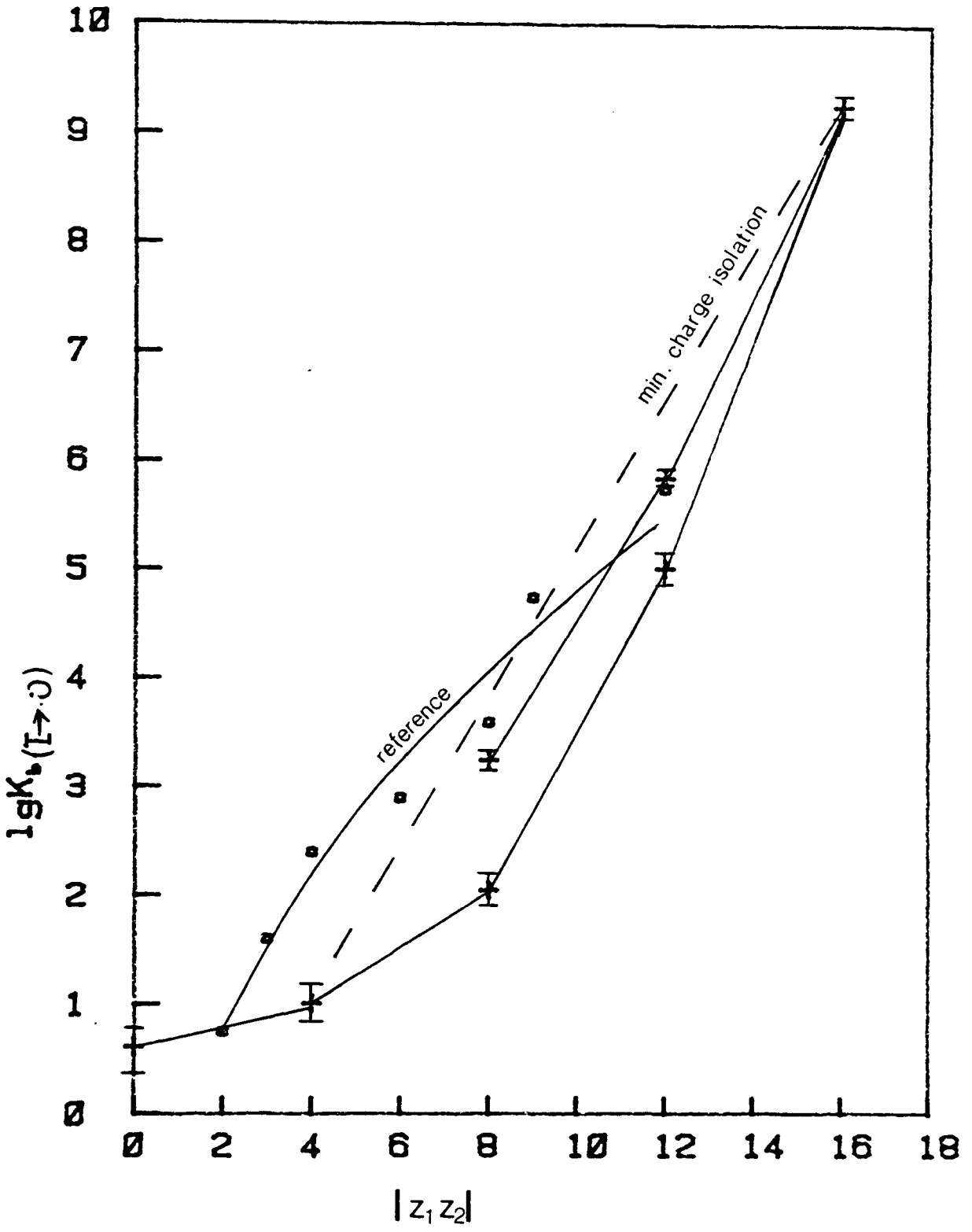

Figure 3.9 PP/trien:$\lg K_b$ against charge product. Reference and minimum charge isolation lines are shown.

3.4. TRIPOLYPHOSPHATE WITH TRIETHYLENETETRAMINE

3.4.1 pK_a evaluation.

The pH profile of triethylenetetramine in the presence of excess tripolyphosphate is given in figure 3.10. Titrations were also performed for PPP in the absence and presence of excess trien. Of the two phosphate signals, that of the α-phosphate was found to be more sensitive to changes in pH and thus it is the one monitored here. It is a doublet, and the average of its two chemical shifts was taken and is used throughout. The titrations are illustrated by figure 3.11. Corrections to zero ionic strength are as follows.

trien with excess PPP

$trien^{4}/trien^{0}$	45mM Na^+	45mM PPP^{5-}	I = 650mM, F = 0.129
	25mM Cl^-	5mM AP^{4-}/AP^{5-}	Δz^2 = +10, c = +1.29
$trien^{2+}/trien^{1+}$	45mM Na^+	45mM PPP^{5-}	I = 655mM, F = 0.129
	75mM Cl^-	5mM AP^{3-}/AP^{4-}	Δz^2 = +8, c = +1.03
$trien^{3+}/trien^{2+}$	45mM Na^+	45mM PPP^{5-}	I = 660mM, F = 0.129
	125mM Cl^-	5mM AP^{2-}/AP^{3-}	Δz^2 = +6, c = +0.77
$trien^{3+}/trien^{4+}$	45mM Na^+	45mM PPP^{4-}	I = 480mM, F = 0.135
	175mM Cl^-	5mM AP^{1-}/AP^{2-}	Δz^2 = +4, c = +0.54

PPP free

PPP^{4-}/PPP^{5-}	70mM Na^+	0.5mM $EDTA^{3-}$	I= 99mM, F = 0.107
	20mM Cl^-	5mM PPP^{4-}/PPP^{5-}	Δz^2=+10, c= +1.07

PPP^{3-}/PPP^{4-}	70mM Na^+	0.5mM $EDTA^{2-}/EDTA^{3-}$	I= 95mM, F = 0.111
	55mM Cl^-	5mM PPP^{3-}/PPP^{4-}	Δz^2= +8, c= +0.89

PPP with excess trien

PPP^{4-}/PPP^{5-}	45mM Na^+	45mM $trien^{3-}$	I= 260mM, F= 0.133
	50mM Cl^-	5mM AP^0/AP^{1-}	
	5mM $EDTA^{2-}$		Δz^2 =+2, c = +0.27

PPP^{3-}/PPP^{4-} - $\Delta z^2 = 0$

The pK_a results are summarised below.

species	equilibrium		pK_a free	pK_a bound	ΔpK_a
	(uncorrected)	I = 0	(uncorrected)	I = 0	I = 0
	$4^+/3^+$	-	2.57(±.02)	(6.67)	7.21(±.02)	4.64(±.03)
trien	$3^+/2^+$	-	6.34(±.02)	(9.20)	9.97(±.02)	3.63(±.03)
trien	$2^+/1^+$	-	9.16(±.07)	(10.06)	11.09(±.07)	1.93(±.10)
trien	$1^+/0$	-	10.34(±.07)	(10.60)	11.89(±.07)	1.55(±.10)
PPP	$3^-/4^-$	5.89	6.78(±.02)	(3.55)	3.55(±.06)	-3.23(±.06)
PPP	$4^-/5^-$	8.61	9.68(±.02)	(5.25)	5.52(±.06)	-4.16(±0.6)

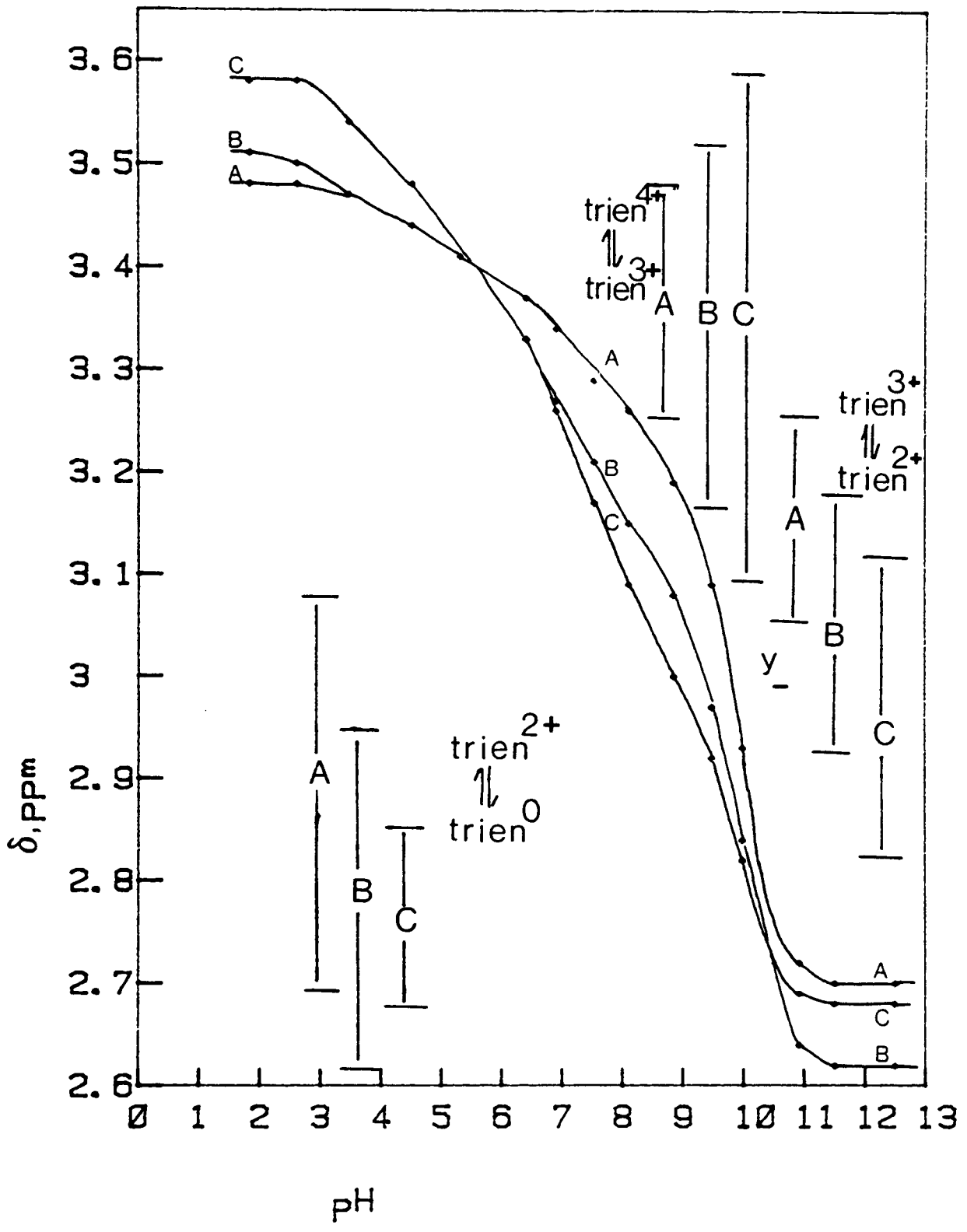

Figure 3.10 ^{1}H nmr pH profile of triethylenetetramine in the presence of excess tripolyphosphate.

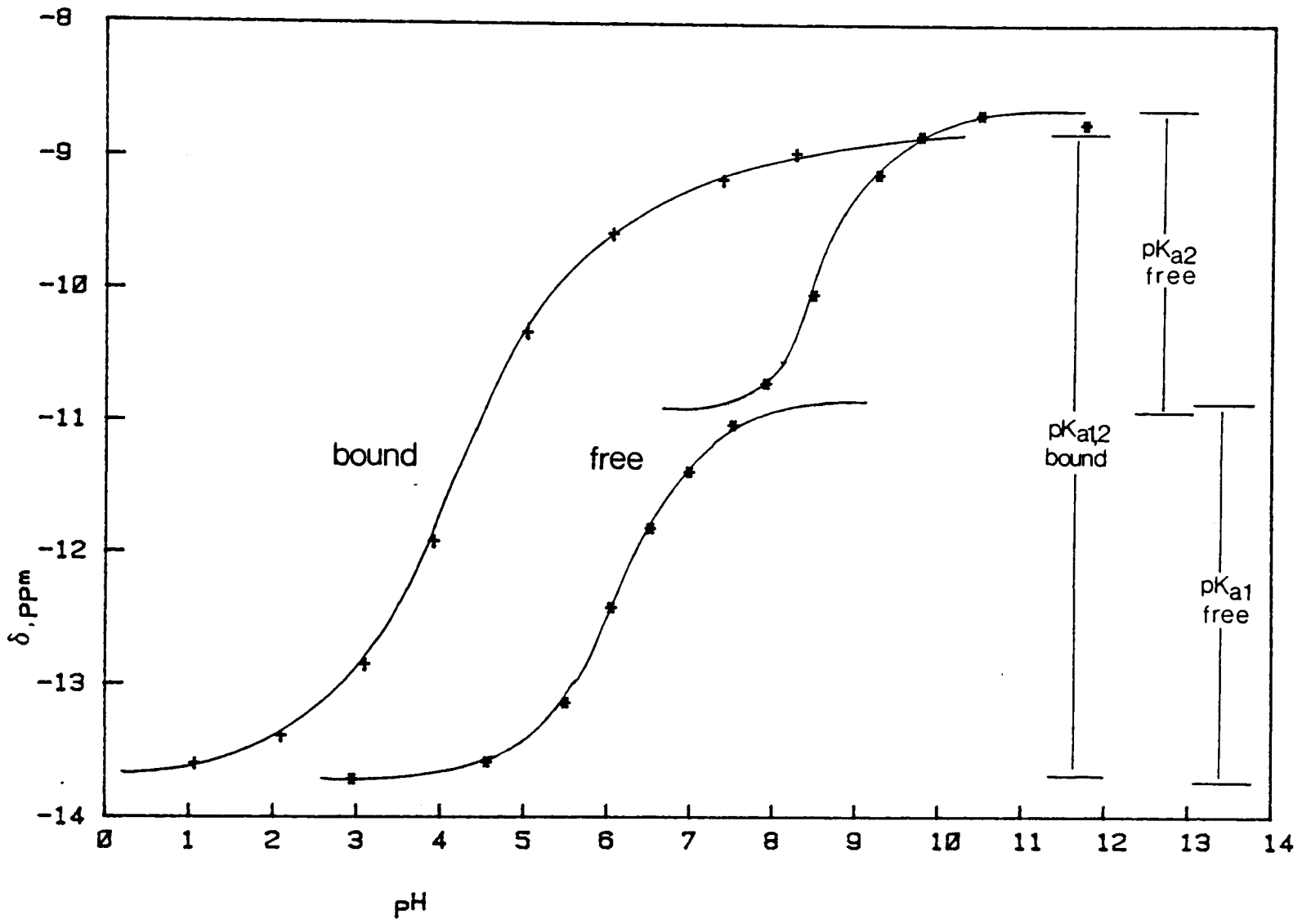

Figure 3.11 ^{31}P nmr pH profiles of tripolyphosphate (α-phosphate) in the absence and presence of excess triethylenetetramine.

It is noted that for trien^{4+} with PPP^{5-}/PPP^{4-}, ΔpK_a = 4.16,

while for PPP^{5-} with trien^{4+}/trien^{3+}, ΔpK_a = 4.64.

Similarly, for trien^{4+} with PPP^{4-}/PPP^{3-}, ΔpK_a = 3.23,

while for PPP^{5-} with trien^{3+}/trien^{2+}, ΔpK_a = 3.63.

As before, decrease in strength of interaction is less for the protonation of the comparatively compact phosphate molecule than for the deprotonation of the amine, which to leads to single positive charges held on their own at the end of the molecule.

The literature comparison shown below uses the average of the three (25°C) pK_a values reported by Högfeldt and Perrin (1979), corrected to zero ionic strength. Agreement is good.

equilibrium		pK_a ($I \to 0$) present work, -0.10	literature
PPP	$3^-/4^-$	6.68	6.72
	$4^-/5^-$	9.58	9.72

3.4.2 Association constant evaluation

Trien was added to a 5mM solution of PPP, kept constant at pH2.2. The titration is illustrated by figure 3.12A. the association constant, KG, is calculated from the following data.

At mM	Δδ -	$At(\Delta\delta)^{-1}$-Pt mM	$(1-\Delta\delta)^{-1}$ -
2	0.325	1.15	1.48
3	0.448	1.70	1.81
4	0.548	2.30	2.21
5	0.643	2.78	2.80
6	0.718	3.36	3.55
7	0.778	4.00	4.50

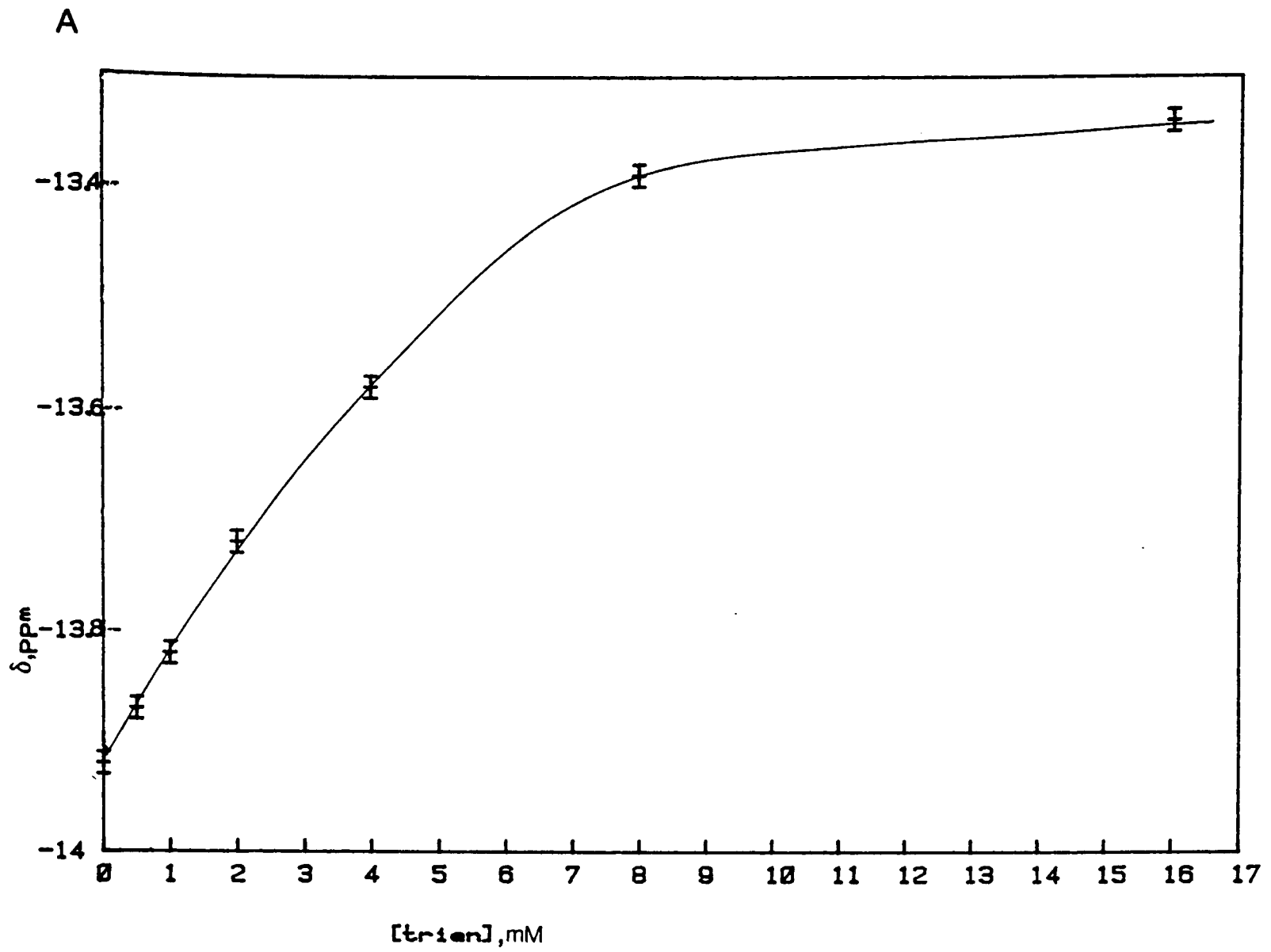

Figure 3.12 (A) The effect of the addition of trien on the ^{31}P nmr chemical shift of the α-phosphate of PPP. pH2.2.

(B) Evaluation of association constant.

The plot of $(1-\Delta\delta)^{-1}$ vs $\{At(\Delta\delta)^{-1}-Pt\}$ (figure 3.12B) indicated that $K_b = 1070(\pm 50)M^{-1}$, or $\lg K_b = 3.03(\pm .02)$. Correction to zero ionic strength, evaluated at a concentration of 5mM trien, is as follows

$$\left.\begin{array}{ll} pH2.2{:}6mM[H^+] & 1.8mM\ trien^{4+} \\ 3.2mM\ AP^{1+} & 1.8mM\ PPP^{3-} \end{array}\right\} \quad I = 27mM,\ F = 0.067$$

$$trien^{4+} + PPP^{3-} \rightleftharpoons [trien^{4+}PPP^{3-}] \quad \Delta z^2 = -24,\ C = +1.61$$

Thus, $\lg K_b(I\to 0, pH2.2) = 4.64(\pm .02)$

3.4.3 Association constants at several pH values

The completed set of $\lg K_b(I\to 0)$ values is given in table 3.3 and the values are plotted against charge poduct in fig. 3.13. The "effective charge products" are calculated from strength of association and are as follows.

interaction	charge product	effective charge product
$trien^{4+}/PPP^{3-}$	12	9
$trien^{4+}/PPP^{4-}$	16	14
$trien^{3+}/PPP^{5-}$	15	13
$trien^{2+}/PPP^{5-}$	10	$7\frac{1}{2}$

Loss of strength of association is greatest for PPP^{3-}, with its three charges strung out along its seven atom chain; and for $trien^{2+}$, as before.

Table 3.3 PPP/trien: pK_a and lgK_b summary

complex	$[trien^{4+}\ PPP^{3-}]^{1+}$	⇌	$[trien^{4+}\ PPP^{4-}]^{0}$	⇌	$[trien^{4+}\ PPP^{5-}]^{1-}$	⇌	$[trien^{3+}\ PPP^{5-}]^{2-}$	⇌	$[trien^{2+}\ PPP^{5-}]^{3+}$	⇌	$[trien^{1+}\ PPP^{5-}]^{4-}$	⇌	$[trien^{0}\ PPP^{5-}]^{5-}$
pK_a	3.55		5.52		7.21		9.97		11.09		11.89		
ΔpK_a	-3.23(±.06)		-4.16(±.06)		4.64(±.03)		3.63(±.03)		1.93(±.10)		1.55(±.10)		
lgK_b	4.64(±.02)	→	7.87(±.06)	→	12.03(±.09)	→	7.39(±.09)	→	3.76(±.10)	→	1.93(±.14)	→	0.93(±.17)
									(80% bound)		(29% bound)		

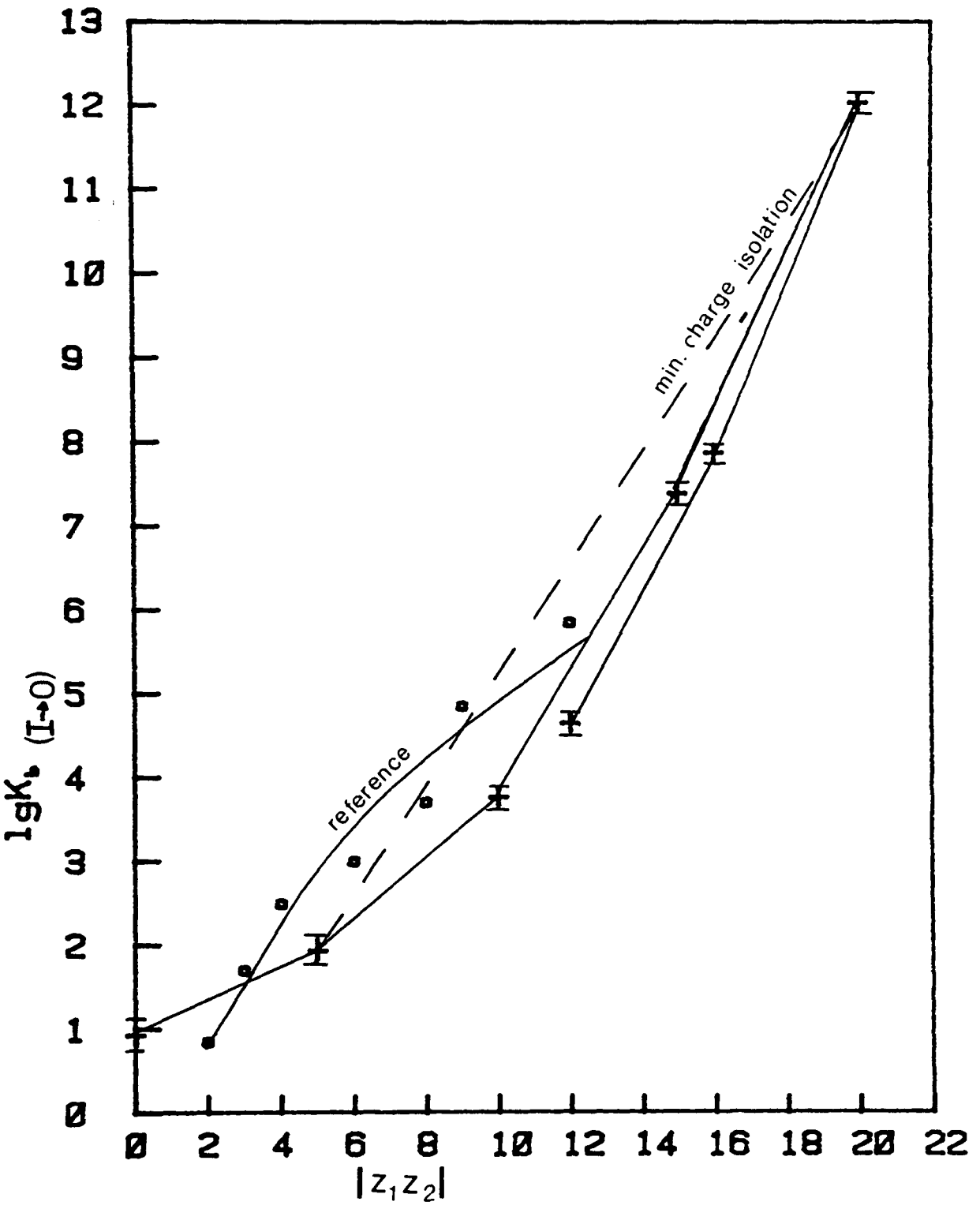

Figure 3.13 Trien/PPP: strength of association against charge product. Reference and minimum isolation lines are shown.

3.5 ADENOSINE DIPHOSPHATE WITH TRIETHYLENETETRAMINE

3.5.1 pK_a evaluation

pH profiles of trien with excess ADP, and of ADP, without and with excess amine are given in figures 3.14 and 3.15 respectively. Since it is the β-phosphate group that loses a proton as the pH is raised, it is the β-phosphate signal that is monitored here. Ionic strength corrections are as follows.

trien with excess ADP

$trien^{1+}/trien^{0}$	70mM Na^+	45mM ADP^{3-}	I=266mM, F=0.132
	25mM Cl^-	5mM AP^{2-}/AP^{3-}	Δz^2=+6, C=+0.79
$trien^{2+}/trien^{1+}$	70mM Na^+	45mM ADP^{3-}	I=281mM, F=0.133
	75mM Cl^-	5mM AP^{1-}/AP^{2-}	Δz^2=+4, C=+0.53
$trien^{3+}/trien^{2+}$	70mM Na^+	45mM ADP^{3-}	I=301mM, F=0.134
	125mM Cl^-	5mM AP^{0}/AP^{1-}	Δz^2=+2, C=+0.27
$trien^{4+}/trien^{3+}$	70mM Na^+	45mM ADP^{2-}	I=218mM, F=0.128
	175mM Cl^-	5mM AP^{2+}/AP^{0}	

$[trien^{4+}\ ADP^{2-}]^{2+} \rightleftharpoons [trien^{3+}\ ADP^{3-}]^{0} + 2H^+$

z^2	4	0	1,1 Δz^2=-2, C=-0.26

ADP free

ADP^{2-}/ADP^{3-}	70mM Na^+	0.5mM $EDTA^{3-}$	I=76mM, F=0.097
	45mM Cl^-	5mM ADP^{2-}/ADP^{3-}	Δz^2=+6, C=+0.58

ADP with excess trien

ADP^{2-}/ADP^{3-}	45mM Na^+	45mM $trien^{3+}$	I=281mM
	100mM Cl^-	5mM AP^{2+}/AP^{0}	F=0.133
	0.5mM $EDTA^{2-}$		

$[trien^{4+}\ ADP^{2-}]^{2+} \rightleftharpoons [trien^{3+}\ ADP^{3-}]^{0} + 2H^+$ Δz^2=-2

C=-0.27

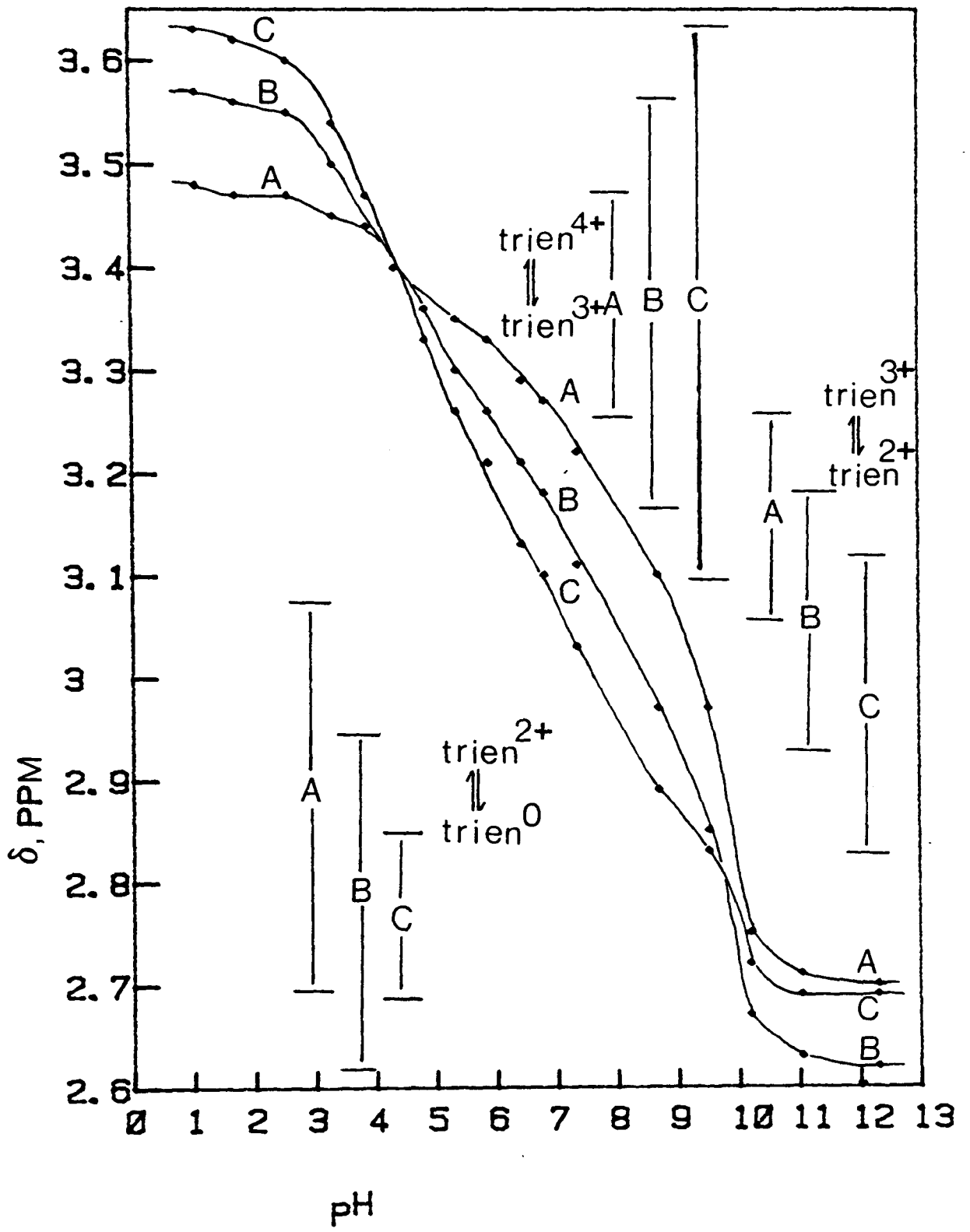

Figure 3.14 ^{1}H nmr pH profile of triethylenetetramine in the presence of excess adenosine diphosphate.

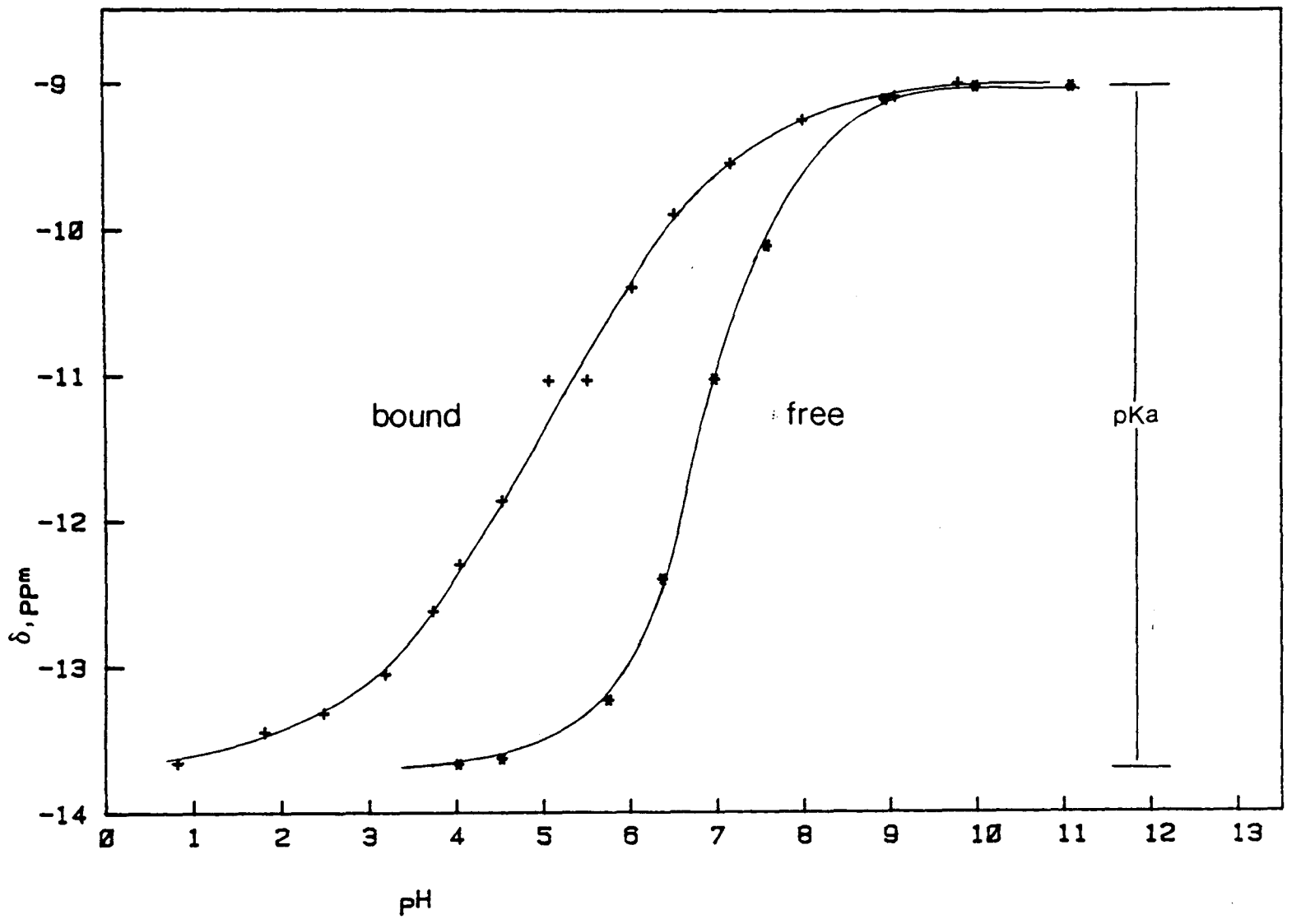

Figure 3.15 ^{31}P nmr pH profiles of ADP, β-phosphate signal, in the absence and presence of excess triethylenetetramine.

The pK_a values are presented below.

species	equilibrium		pK_a free (uncorrected)	I=0	pK_a bound (uncorrected)	I=0	ΔpK_a
trien	$4^+/3^+$	-	2.57(±.02)	(5.34)	5.08(±.02)		2.51(±.03)
	$3^+/2^+$	-	6.34(±.02)	(8.02)	8.29(±.02)		1.95(±.03)
	$2^+/1^+$	-	9.16(±.07)	(9.67)	10.20(±.07)		1.04(±.10)
	$1^+/0$	-	10.34(±.07)	(10.14)	10.93(±.07)		0.59(±.10)
ADP	$2^-/3^-$	(6.91)	7.49(±.02)	(5.08)	4.81(±.02)		-2.68(±.03)

The literature comparison below uses the pK_a of Weitzel and Spehr (1958), recorded at 25°C and I=100mM, and corrected here to zero ionic strength. Agreement is good.

equilibrium	pK_a(I→0) present work, -0.10	literature
ADP $2^-/3^-$	7.39	7.25

3.5.2 Association constant evaluation

Trien was added to a 5mM solution of ADP, kept constant at pH4.8. The interaction was monitored by following the change in the chemical shift of the β-phosphate signal, as shown in figure 3.16A. In association constant, K_b, is evaluated from the following data.

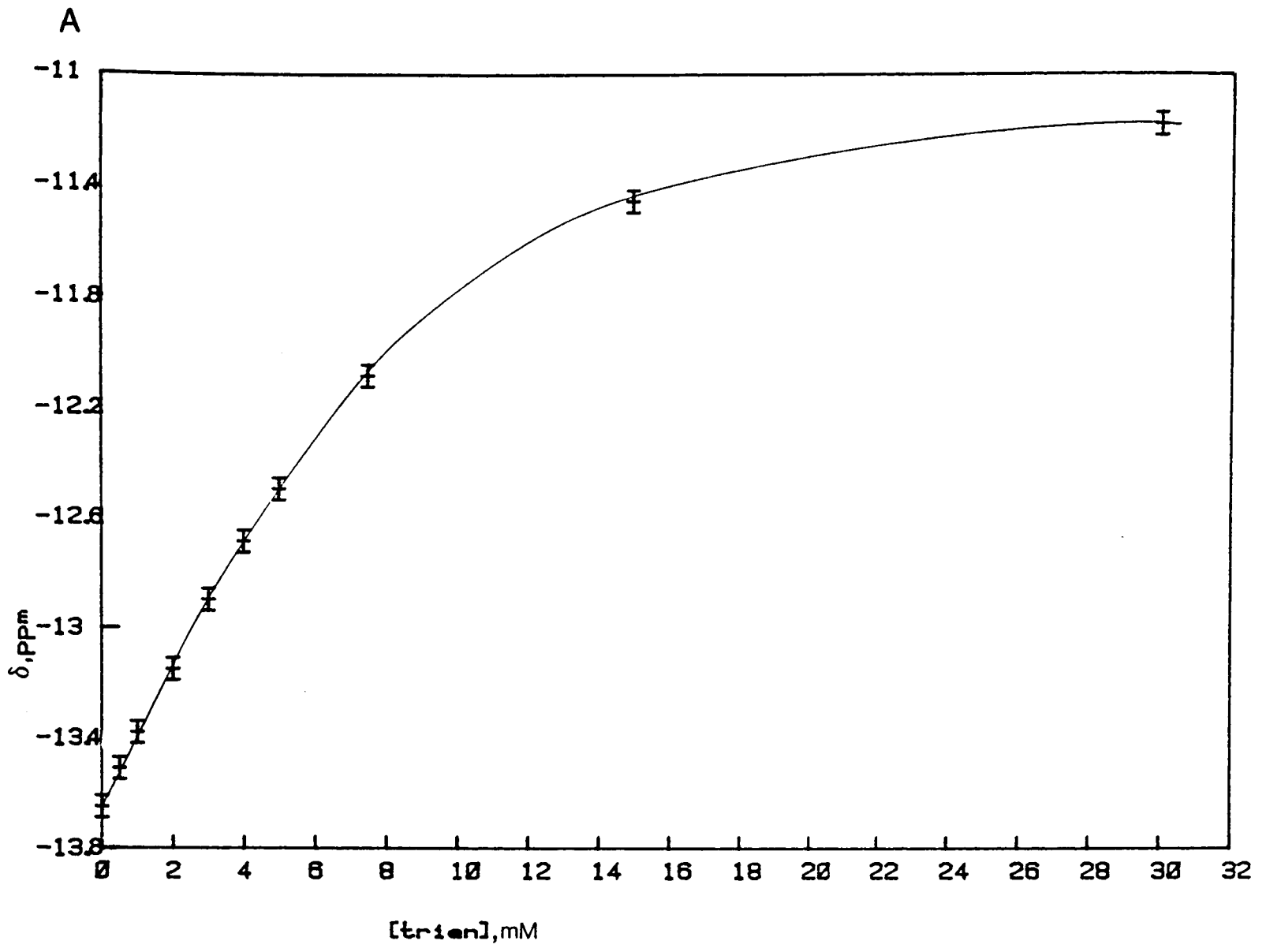

Figure 3.16 (A) The effect of the addition of trien on the ^{31}P nmr chemical shift of the β-phosphate of ADP. pH4.8

(B) Evaluation of association constant.

At mM	$\Delta\delta$ -	$At(\Delta\delta)^{-1}$ - Pt mM	$(1-\Delta\delta)^{-1}$ -
2	0.219	4.13	1.28
3	0.305	4.84	1.44
4	0.391	5.23	1.64
5	0.453	6.04	1.83
6	0.516	6.63	2.07
7	0.578	7.11	2.37

The plot of $(1-\Delta\delta)^{-1}$ vs$\{At(\Delta\delta)^{-1}-Pt\}$ in figure 3.16B indicated that $K_b = 316(\pm 60)M^{-1}$, or $\lg K_b = 2.50(\pm 0.10)$. Correction to zero ionic strength is as follows.

$trien^{3+} + ADP^{2-} \rightleftharpoons [trien^{3+}\ ADP^{2-}]^{1+}/[trien^{4+}\ ADP^{3-}]^{1+}$

5mM $EDTA^{2-}$ 2.7mM ADP^{2-} } I=29mM, F=0.069

2.3mM AP^{1+} 2.7mM $trien^{3+}$ } Δz^2=-12, C=+0.83

Thus $\lg K_b$(I-0,pH4.8) = 3.33(±0.10)

3.5.3 Association constants at several pH values

The completed set of $\lg K_b$(I-0) values is given in table 3.4 and the values are plotted against charge product in figure 3.17. The "effective" charge product of the $trien^{2+}$, ADP^{3-} complex is seen to be $4\frac{1}{2}$ rather than 6.

Table 3.4 Trien/ADP: pK_a and lgK_b summary

complex	$\left[\begin{matrix}trien^{4+}\\ADP^{2-}\end{matrix}\right]^{2+}$	⇌	$\left[\begin{matrix}trien^{3+}\\ADP^{3-}\end{matrix}\right]^{0}$	⇌	$\left[\begin{matrix}trien^{2+}\\ADP^{3-}\end{matrix}\right]^{1-}$	⇌	$\left[\begin{matrix}trien^{1+}\\ADP^{3-}\end{matrix}\right]^{2-}$	⇌	$\left[\begin{matrix}trien^{0}\\ADP^{3-}\end{matrix}\right]^{3-}$
pK_a	4.81/5.08		8.29		10.20		10.93		
ΔpK_a	-		1.95(±.03)		1.04(±.10)		0.59(±.10)		
lgK_b	3.33(±.10)	→	1.57(±.10)	→	1.01(±.14)	→	0.94(±.18)		
	(64% bound)		(33% bound)		(30% bound)				

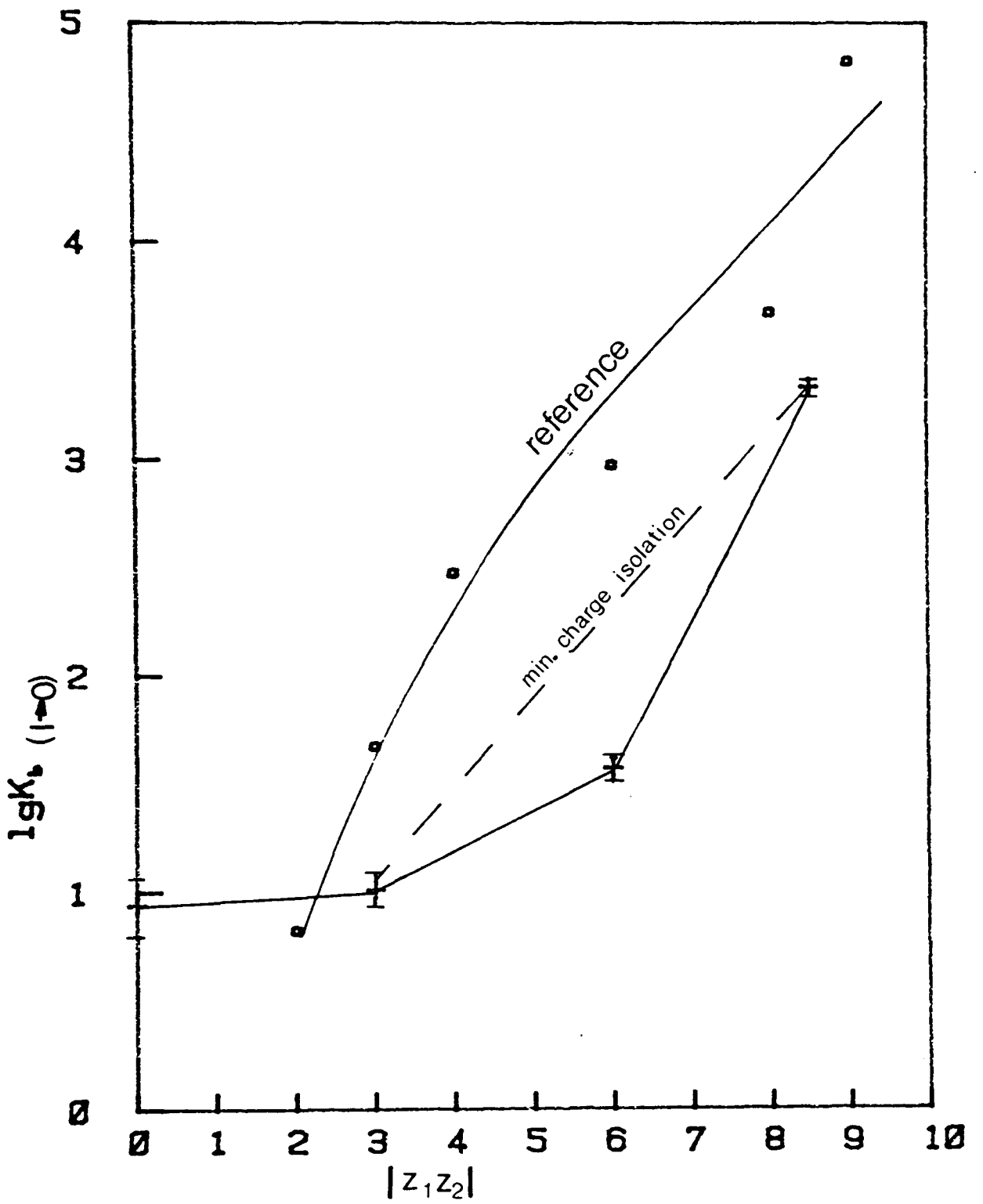

Figure 3.17 Trien/ADP: strength of association against charge product. Reference and minimum charge isolation lines are shown.

3.6 ADENOSINE TRIPHOSPHATE WITH TRIETHYLENETETRAMINE

3.6.1 pK_a evaluation

pH profiles of trien with excess ATP and of ATP without and with excess trien are given in figures 3.18 and 3.19 respectively. Since it is the γ-phosphate group that experiences deprotonation as the pH is raised, it is the γ-phosphate signal that is monitored here. Ionic strength corrections are as follows.

trien with excess ATP

$trien^{1+}/trien^{0}$	45mM Na^+	45mM ATP^{4-}	I=426mM, F=0.136
	25mM Cl^-	5mM AP^{3-}/AP^{4-}	Δz^2=+8, C=+1.09
$trien^{2+}/trien^{1+}$	45mM Na^+	45mM ATP^{4-}	I=436mM, F=0.136
	75mM Cl^-	5mM AP^{2-}/AP^{3-}	Δz^2=+6, C=+0.82
$trien^{3+}/trien^{2+}$	45mM Na^+	45mM ATP^{4-}	I=451mM, F=0.136
	125mM Cl^-	5mM AP^{1-}/AP^{2-}	Δz^2=+4, C=+0.54
$trien^{4+}/trien^{3+}$	45mM Na^+	45mM ATP^{3-}/ATP^{4-}	I=393mM, F=0.136
	175mM Cl^-	5mM AP^{0}/AP^{1-}	Δz^2=+2, C=+0.27

ATP free

ATP^{3-}/ATP^{4-}	70mM Na^+	5mM $EDTA^{3-}$	I=111mM, F=0.110
	45mM Cl^-	5mM ATP^{3-}/ATP^{4-}	Δz^2=+8, C=0.88

ATP with excess trien

ATP^{3-}/ATP^{4-} $[trien^{4+}\ ATP^{3-}]^{1+} \rightleftharpoons [trien^{4+}\ ATP^{4-}]^{0} + H^+$ Δz^2=0

The pK_a values are summarised as follows.

species	equilibrium	pK_a free (uncorrected)	pK_a free I→0	pK_a bound (uncorrected)	pK_a bound I→0	ΔpK_a I→0
trien	$4^+/3^+$	(-)	2.57(±.02)	(6.34)	6.61(±.02)	4.04(.03)
	$3^+/2^+$	(-)	6.34(±.02)	(8.69)	9.23(±.02)	2.89(±.03)
	$2^+/1^+$	(-)	9.16(±.07)	(9.85)	10.67(±.07)	1.51(±.10)
	$1^+/0$	(-)	10.34(±.07)	(10.71)	11.80(±.07)	1.46(±.10)
ATP	$3-/4-$	(6.52)	7.40(±.02)	(4.54)	4.54(±.02)	-2.86(±.03)

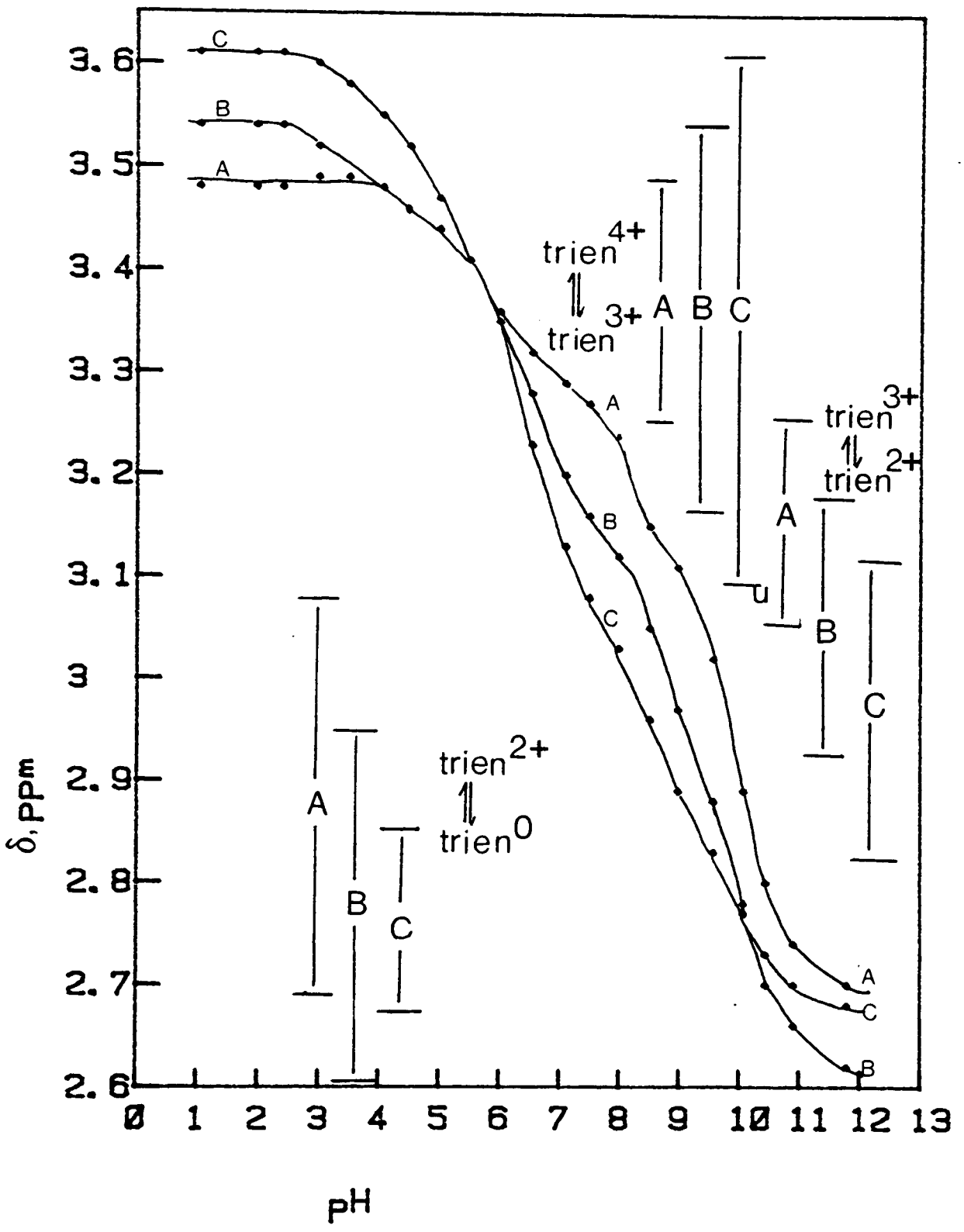

Figure 3.18 ^{1}H nmr pH profile of triethylenetetramine in the presence of excess adenosine triphosphate.

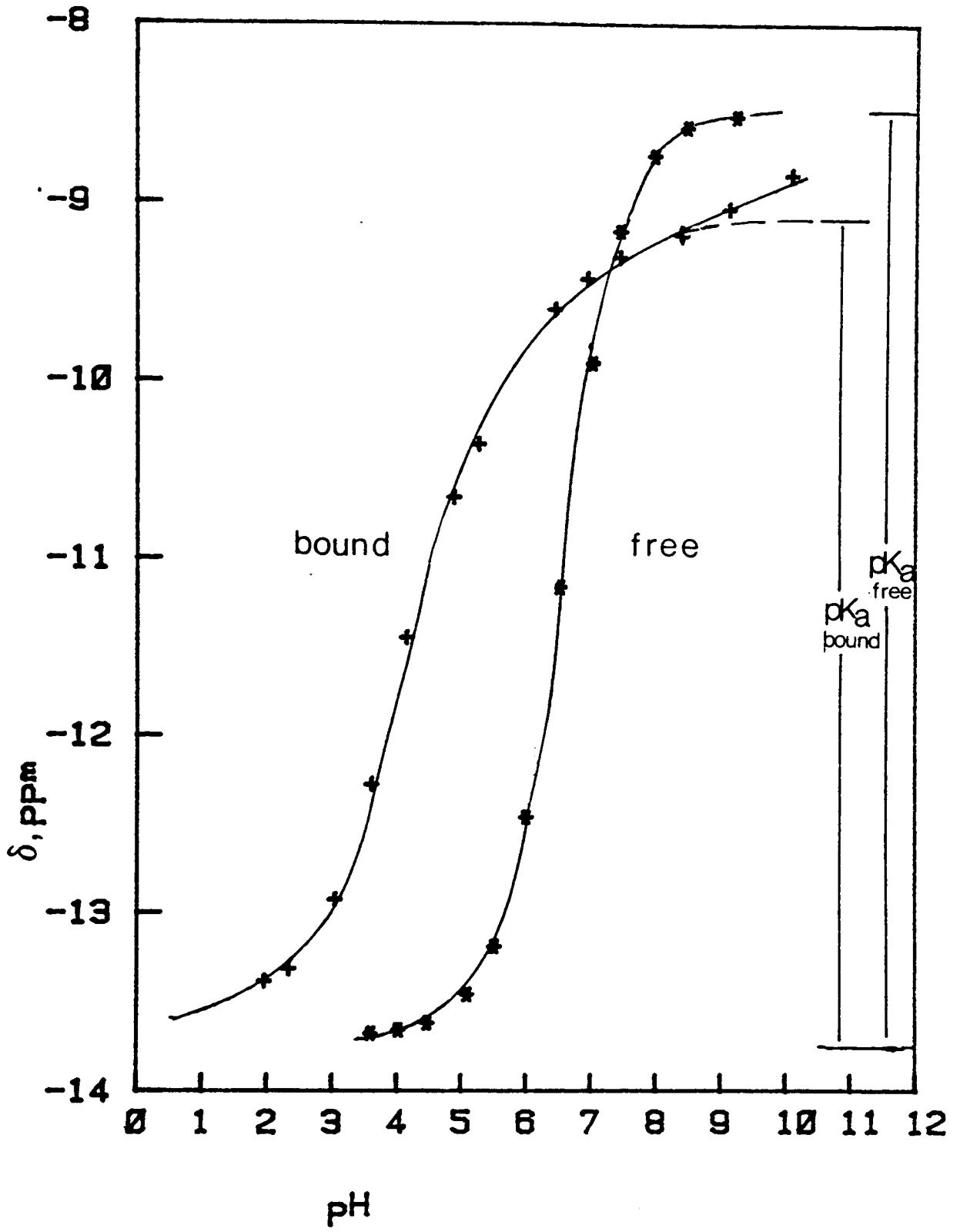

Figure 3.19 ^{31}P nmr pH profiles of ATP, γ-phosphate signal, in the absence and presence of excess triethylenetetramine.

The literature comparison below uses the value reported by Kahn and Martell (1966) at 25°C and I=100mM, corrected here to zero ionic strength. Agreement is good.

equilibrium	$pK_a(I\rightarrow 0)$ present work, -0.10	literature
ATP $3^-/4^-$	7.30	7.39

3.6.2 Association constant evaluation

Trien was added to a 5mM solution of ATP maintained at pH2.0. The interaction was monitored by following the change in chemical shift at the β-phosphate signed, as shown in figure 3.20A. The association constant is evaluated from the following data.

At mM	Δδ -	$At(\Delta\delta)^{-1} - Pt$ mM	$(1-\Delta\delta)^{-1}$ -
4	0.689	0.81	3.22
4.5	0.724	1.22	3.62
5	0.780	1.41	4.55
5.5	0.819	1.72	5.52
6	0.850	2.06	6.67
6.5	0.882	2.37	8.47

The plot of $(1-\Delta\delta)^{-1}$ vs $\{At(\Delta\delta)^{-1} - Pt\}$, figure 3.20B, indicated that K_b = 3,340(±600)M^{-1}, or $\lg K_b$=3.52(±.08).

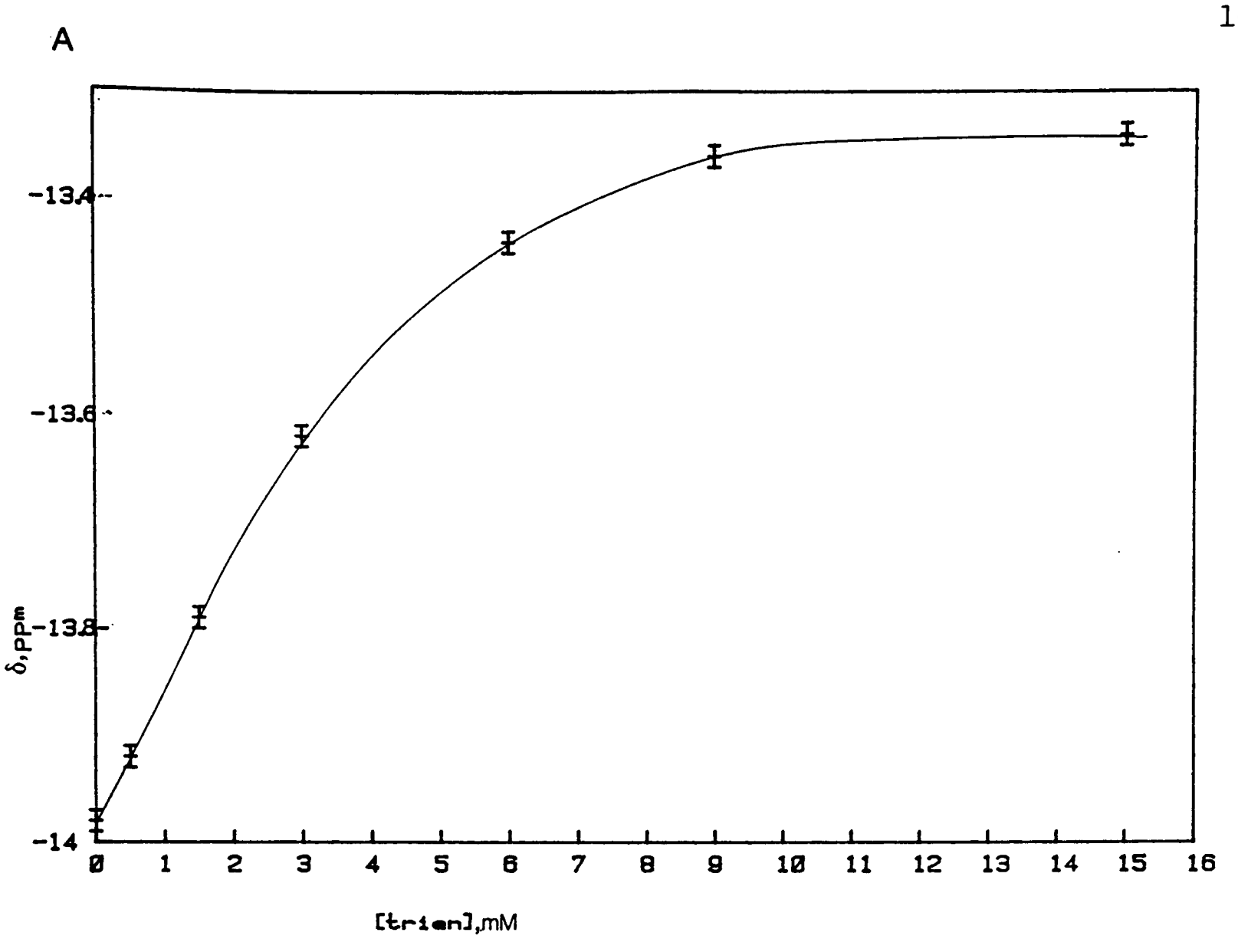

Figure 3.20 (A) The effect of the addition of trien on the ^{31}P nmr chemical shift of the γ-phosphate of ATP. (pH2.0).

(B) Evaluation of association constant.

Correction to zero ionic strength is as follows

$$trien^{4+} + ATP^{3-} \rightleftharpoons [trien^{4+}\ ATP^{3-}]^{1+}$$

pH2:10mM H^+	3.9mM AP^{1+}	I=21mM, F=0.061
0.5mM $EDTA^0/EDTA^{1-}$	1.1mM $trien^{4+}$	
	1.1mM ATP^{3-}	Δz^2=-24, C=+1.46

Thus $lgK_b(I\text{-}0,pH2.0) = 4.98\pm(.08)$.

3.6.3 Association constants at several pH values

The completed set of $lgK_b(I\rightarrow 0)$ values is presented in table 3.5 and the values are plotted against charge product in figure 3.21. Reference to the projection of minimal charge isolation indicates the following "effective charge products".

interaction	charge product	effective charge product
$trien^{4+}/ATP^{3-}$	12	$11\frac{1}{2}$
$trien^{3+}/ATP^{4-}$	12	$9\frac{1}{2}$
$trien^{2+}/ATP^{4-}$	8	5

The charge isolation effect for the comparatively compact structure of ATP is quite small, while the extended linear structure of trien leads to large shortfalls for the triply and, especially, the doubly protonated states.

Table 3.5 Trien/ATP - pK_a and lgK_b summary

complex $\begin{bmatrix}trien^{4+}\\ATP^{3-}\end{bmatrix}^{1+}$	= $\begin{bmatrix}trien^{4+}\\ATP^{4-}\end{bmatrix}^{0}$	= $\begin{bmatrix}trien^{3+}\\ATP^{4-}\end{bmatrix}^{1-}$	= $\begin{bmatrix}trien^{2+}\\ATP^{4-}\end{bmatrix}^{2-}$	= $\begin{bmatrix}trien^{1+}\\ATP^{4-}\end{bmatrix}^{3-}$	= $\begin{bmatrix}trien^{0}\\ATP^{4-}\end{bmatrix}^{4-}$
pK_a	4.54	6.61	9.23	10.67	11.80
ΔpK_a	2.86(±.03)	4.04(±.03)	2.89(±.03)	1.51(±.10)	1.46(±.10)
lgK_b	4.98(±.08) →	7.84(±.09) →	3.80(±.09) →	1.24(±.10) →	0.55(±.14) → 0.22(±.17)
			(46% bound)	(15% bound)	(8% bound)

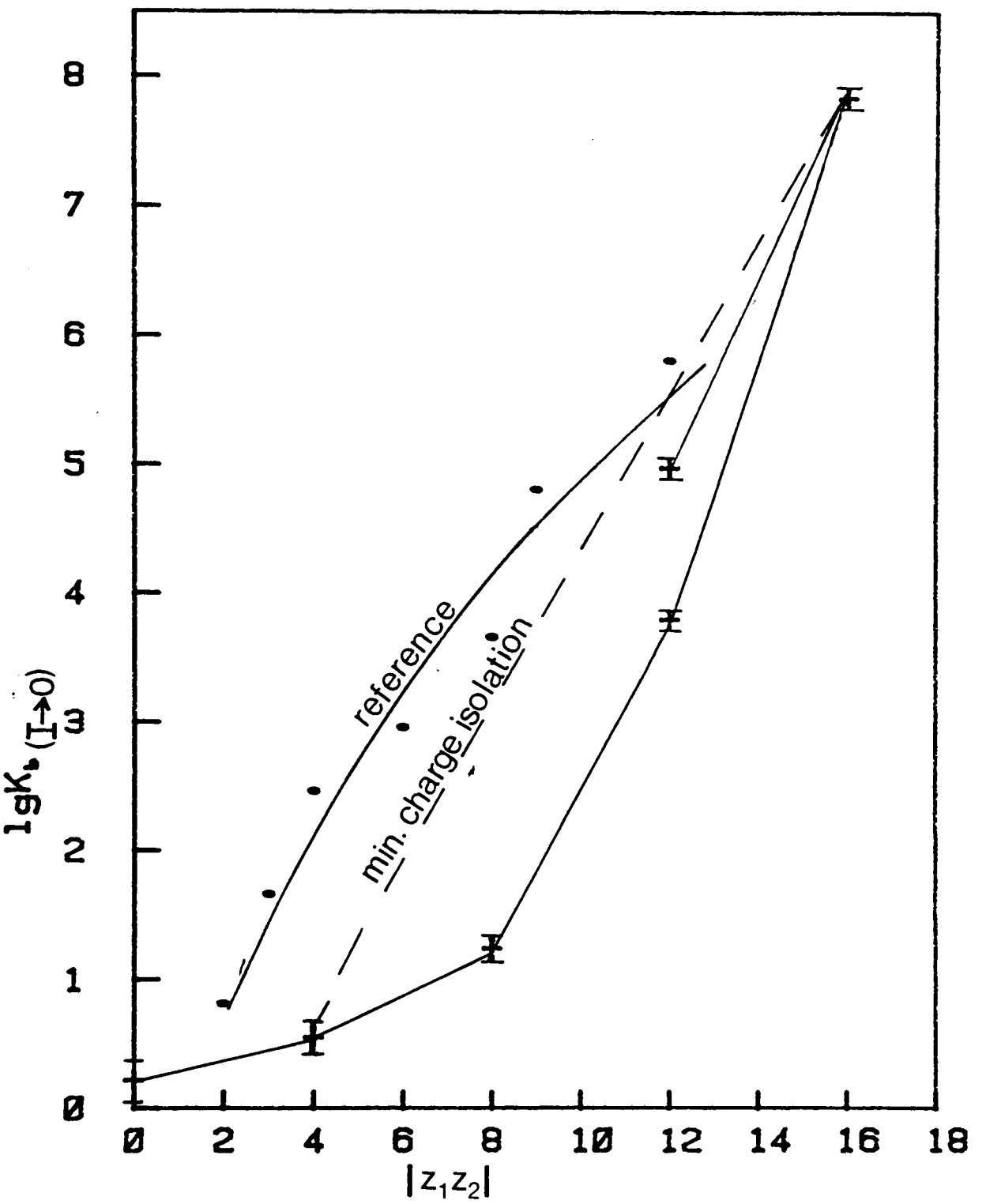

Figure 3.21 Trien, ATP: strength of asociation against charge product. Reference and minimum charge isolation lines are given.

3.7 HEXAMETAPHOSPHATE WITH CYCLIC TRIETHYLENETRIAMINE

3.7.1 pK_a evaluation

The pH profile of cyclic triethylenetriamine(nane) in the absence and presence of excess HMP is given in figure 3.22. The pK_a value of HMP was determined in section 3.2 to be 3.0 (I=0) and thus the phosphate can be regarded as fully deprotonated under the conditions of pH and ionic strength used here. Corrections to zero ionic strength for the nane titrations are as follows.

nane free

$nane^{1+}/nane^{0}$	-	$\Delta z^2=0$

$nane^{2+}/nane^{1+}$	70mM Na^+ 45mM Cl^- 5mM $nane^{2+}/nane^{1+}$	I = 64mM, F = 0.093 Δz^2 = -2, c = -0.19
$nane^{2+}/nane^{1+}$	70mM Na^+ 75mM Cl^- 5mM $nane^{3+}/nane^{2+}$	I = 89mM, F = 0.103 Δz^2 = -4, c = -0.41

nane with excess HMP

$nane^{1+}/nane^{0}$	45mM Na^+ 45mM HMP^{6-} 50mM Cl^- 5mM AP^{5-}/AP^{6-}	I = 259mM, F = 0.132 Δz^2 = +12, c = 1.58
$nane^{2+}/nane^{1+}$	45mM Na^+ 45mM HMP^{6-} 100mM Cl^- 5mM AP^{4-}/AP^{5-}	I = 259mM, F = 0.132 Δz^2 = +10, c = 1.32
$nane^{3+}/nane^{2+}$	45mM Na^+ 45mM HMP^{6-} 150mM Cl^- 5mM AP^{3-}/AP^{4-}	I = 251mM, F = 0.131 Δz^2 = +8, c = 1.05

The pK_a values are summarised as follows.

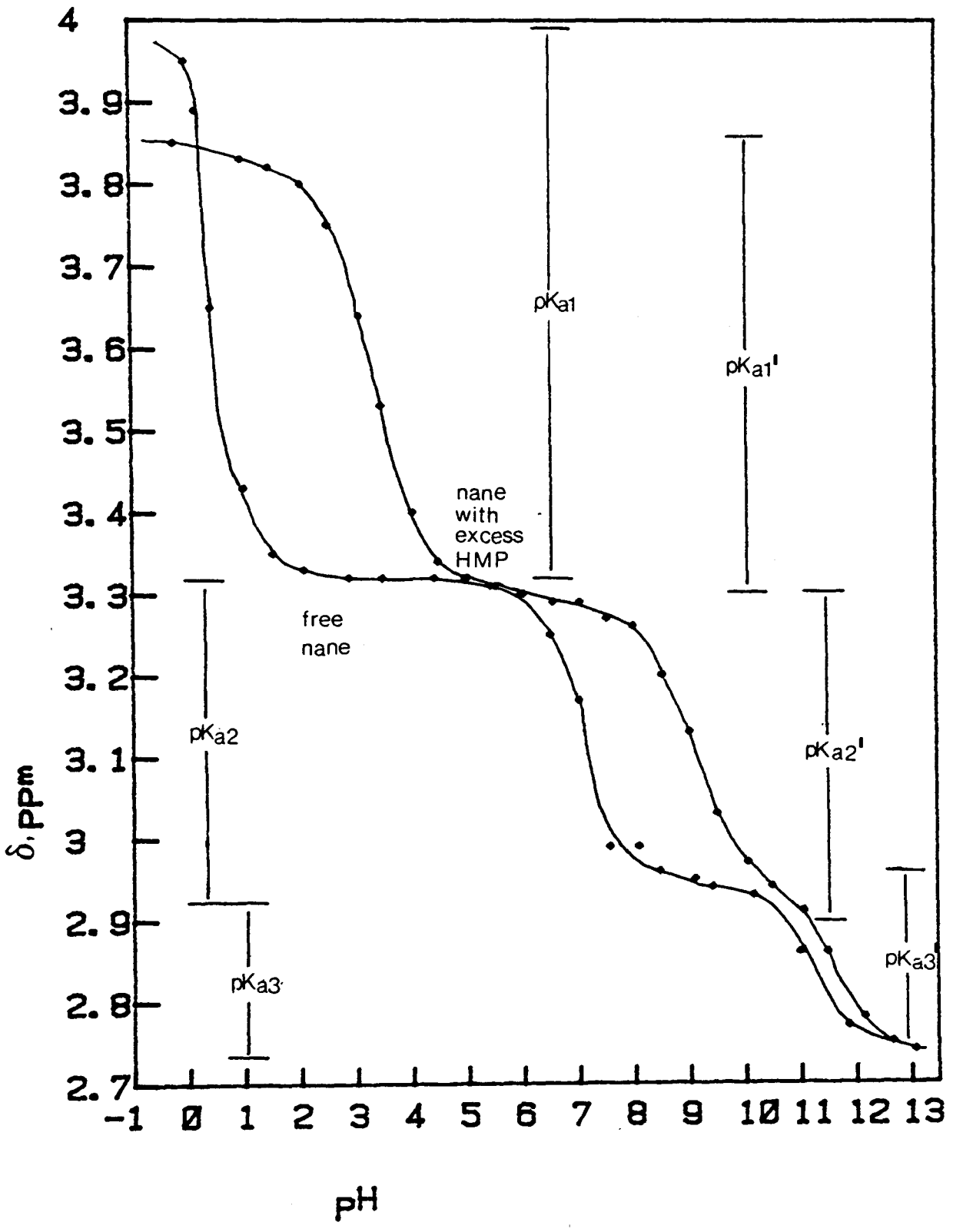

Figure 3.22 pH dependence of ^{1}H nmr chemical shift for (a) nane, (b) nane with excess HMP.

species	equilibrium	pK_a free (uncorrected)	pK_a free I = 0	pK_a bound (uncorrected)	pK_a bound I = 0	ΔpK_a I = 0
nane	$3^+/2^+$	(0.51)	0.10(±.02)	(3.28)	4.33(±.02)	4.23 (±.03)
nane	$2^+/1^+$	(7.31)	7.12(±.02)	(9.17)	10.49 (±.02)	3.37 (±.03)
nane	$1^+/0$	(11.18)	11.18(±.02)	(11.58)	13.16(±.02)	1.98 (±.03)
HMP	$5^-/6^-$	-	2.96(±.02)		-	-

3.7.2 Association constant evaluation

Trien was added incrementally to a solution of nane maintained at pH8.5. The chemical shift of the amine was monitored and is shown in figure 3.23A. Extrapolation of the initial slope to intersection of the line of limiting chemical shift yields an x-coordinate (in this case 6.3mM) which, assuming 1:1 stoichiometry, corresponds to the initial concentration of amine.

The association constant is evaluated from the following data.

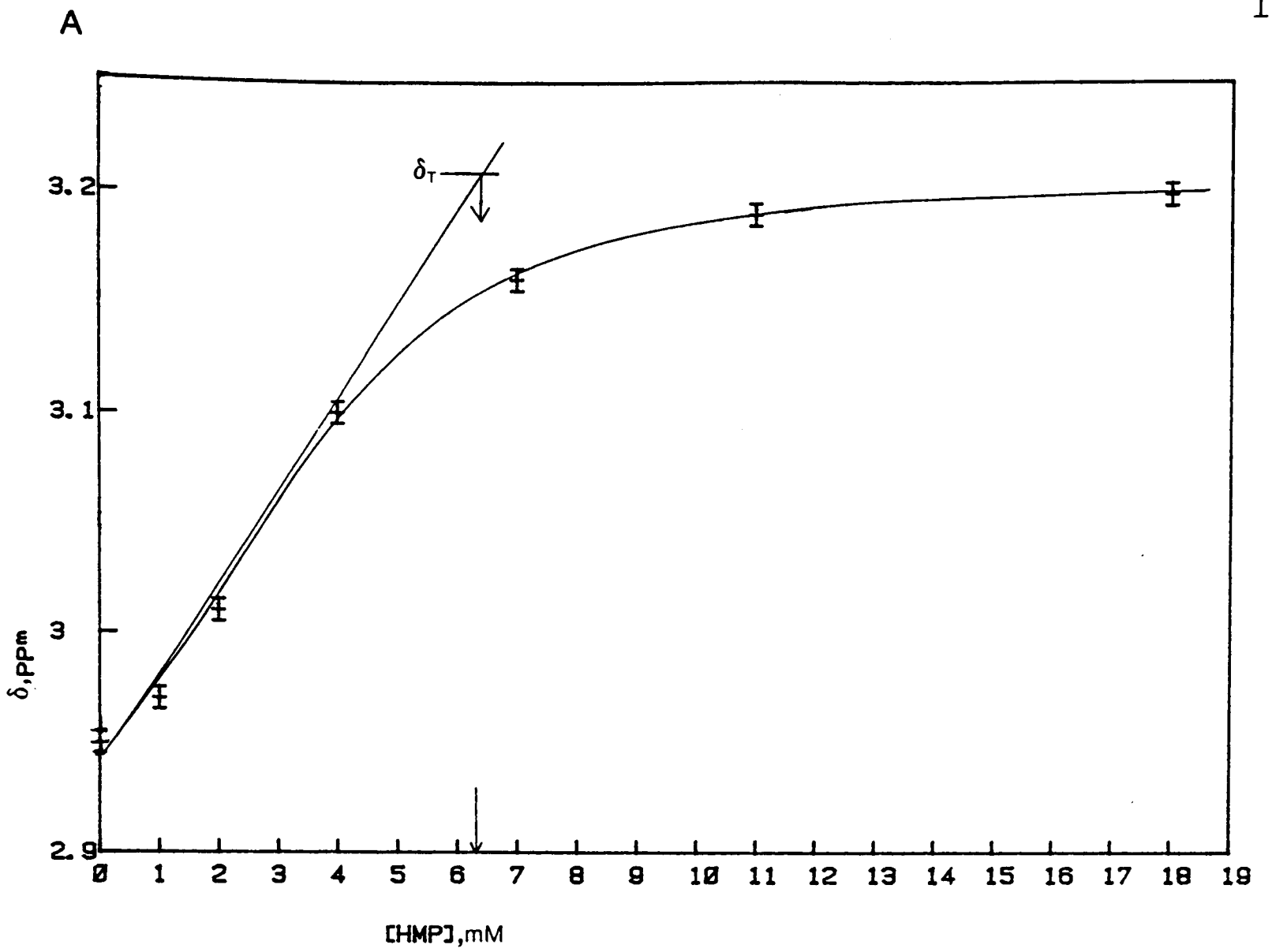

Figure 3.23 (A) The effect of the addition of HMP on the ^{1}H nmr chemical shift of nane at pH8.5.
Determination of [nane] is indicated.
(B) Evaluation of association constant.

Pt mM	Δδ -	$Pt(\Delta\delta)^{-1}-At$ mM	$(1-\Delta\delta)^{-1}$ -
4	0.566	0.77	2.30
5	0.660	1.28	2.94
6	0.726	1.96	3.65
7	0.783	2.64	4.61
8	0.821	3.44	5.59
9	0.858	4.19	7.04
10	0.877	5.10	8.13
11	0.896	5.98	9.62
12	0.915	6.81	11.76

The plot of $(1-\Delta\delta)^{-1}$ vs $\{Pt(\Delta\delta)^{-1}-At\}$, figure 3.23B, indicated that $K_b = 1{,}660(\pm 20)M^{-1}$ and that $\lg K_b = 3.22(\pm .03)$. Correction to zero ionic strength is as follows.

$$nane^{1+} + HMP^{6-} + H^{+} \rightleftharpoons [nane^{2+}HMP^{6-}]^{4-}$$

4.16mM AP^{4-}, 0.84mM HMP^{6-}, 2.14mM $nane^{1+}$: $I = 49mM$, $F = 0.084$

$\Delta z^2 = -22$, $c = +1.85$

Thus $\lg K_b(I\rightarrow 0, pH8.5) = 5.07(\pm .03)$

3.7.3 Association constants at several pH values

The completed set of $\lg K_b(I\rightarrow 0)$ values is presented in table 3.6 and the values are plotted against charge product in figure 3.24. Again a line is drawn between the points

corresponding to the fully charge complex and the complex with the singly charged amine. This line indicates that the effective charge product of the $nane^{2+}/HMP^{6-}$ complex is 11 rather than 12. Thus the effects of awkward charge distribution are minimal for the interaction of $nane^{2+}$ with HMP^{6-}.

Table 3.6 HMP/nane: pK_a, lg K_b summary

complex	$\left[\text{nane}^{3+}\right]^{3-}$ $\left[\text{HMP}^{6-}\right]$	⇌	$\left[\text{nane}^{2+}\right]^{4-}$ $\left[\text{HMP}^{6-}\right]$	⇌	$\left[\text{nane}^{1+}\right]^{5-}$ $\left[\text{HMP}^{6-}\right]$	⇌	$\left[\text{nane}^{0}\right]^{6-}$ $\left[\text{HMP}^{6-}\right]$
pK_a			4.33		10.49		13.16
ΔpK_a			4.23(±.03)		3.37(±.03)		1.98(±.03)
lgK_b	9.30(±.04)	←	5.07(±.03)	→	1.82(±.04)	→	0.61(±.05)
	(76% bound)				(17% bound)		

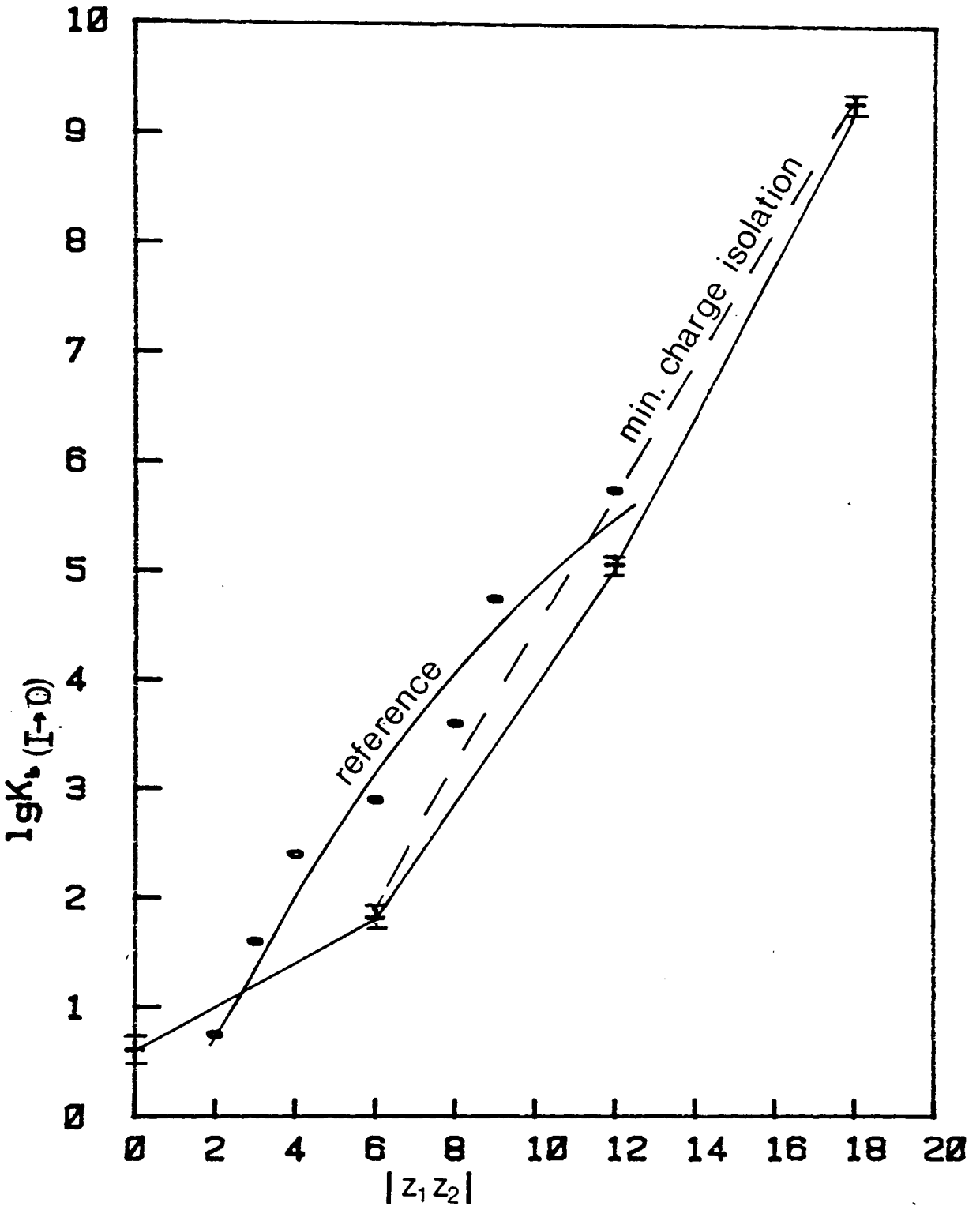

Figure 3.24 HMP/nane: strength of association against charge product. Reference and minimum charge isolation lines are given.

3.8 SUMMARY AND CONCLUSIONS

3.8.1 Effect of phosphate/amine interaction on chemical shift

The changes in chemical shift observed in the various interactions studied here are summarised in table 3.7 and are as follows. It is noted that for all the complexes that show a significant change in chemical shift, strength of association is sufficient to assume that the complexes are fully formed under the conditions used. The effect of phosphate interaction on the chemical shift values of trien varies with the strength of phosphate/amine interaction and is greatest for trien^{4+} and least for trien^{0}. (The trien^{0} complexes are not, of course, fully formed but a rough estimate of the fully formed shift shows it to be very small). Thus the trien^{4+} chemical shift values, for resonances A, B and C, are increased, with each phosphate, by an average of about 0.04ppm and the trien^{3+} resonances are moved downfield by HMP and ADP (but not by the other phosphates) by the same amount. When the charge carried by trien is less, strength of association decreases and phosphate interacts with only a small proportion of the trien molecules. Under the fast exchange conditions of the interaction the nmr signal represents an average of all the molecules and reveals little if any effects of interaction. The trien^{0} resonances are virtually unaffected by phosphate. The trien^{2+} resonances, not clearly definable in the presence of phosphate, are assumed to be not significantly affected and are given the same chemical shift values as those determined for the free species.

The interaction of nane with HMP shows the chemical shift of the fully protonated species, $nane^{3+}$, moved 0.13ppm upfield and shows negligible effects for the other species.

Under the conditions used in the present work the charge of the phosphates does not drop below 2, and the presence of amine is generally seen to influence the chemical shift of the phosphate. The effect is, again, least for the least ionized species and, on average, the ^{31}P nmr resonance is shifted 0.1ppm downfield at the low pH end of the titration and 0.4ppm upfield after deprotonation. This could be the basis of a useful diagnostic tool for phosphate/protein interaction.

3.8.2 Comparative strengths of phosphate/amine complexes

A summary of charge products and calculated strengths of association for the various phosphate/amine complexes investigated in this work is given in table 3.8. These data are now analyzed in three ways.

Comparison is made, in figure 3.25, of the strengths of association of the two amines, in their variously charged states, with the various phosphates, in their fully deprotonated states. The following observations are made.

(i) As amine charge incrases, so does lgK_b.

(ii) As phosphate charge increases, up to 5-, so does lgK_b.

(iii) The cyclic, compact amine nane, interacts more strongly with HMP^{6-} than does (similarly charged) trien.

(iv) For trien, the decrease in lgK_b with amine charge, is <u>not</u> linear, there being a definite shortfall in lgK_b for the intermediately charged 3+ and 2+ species.

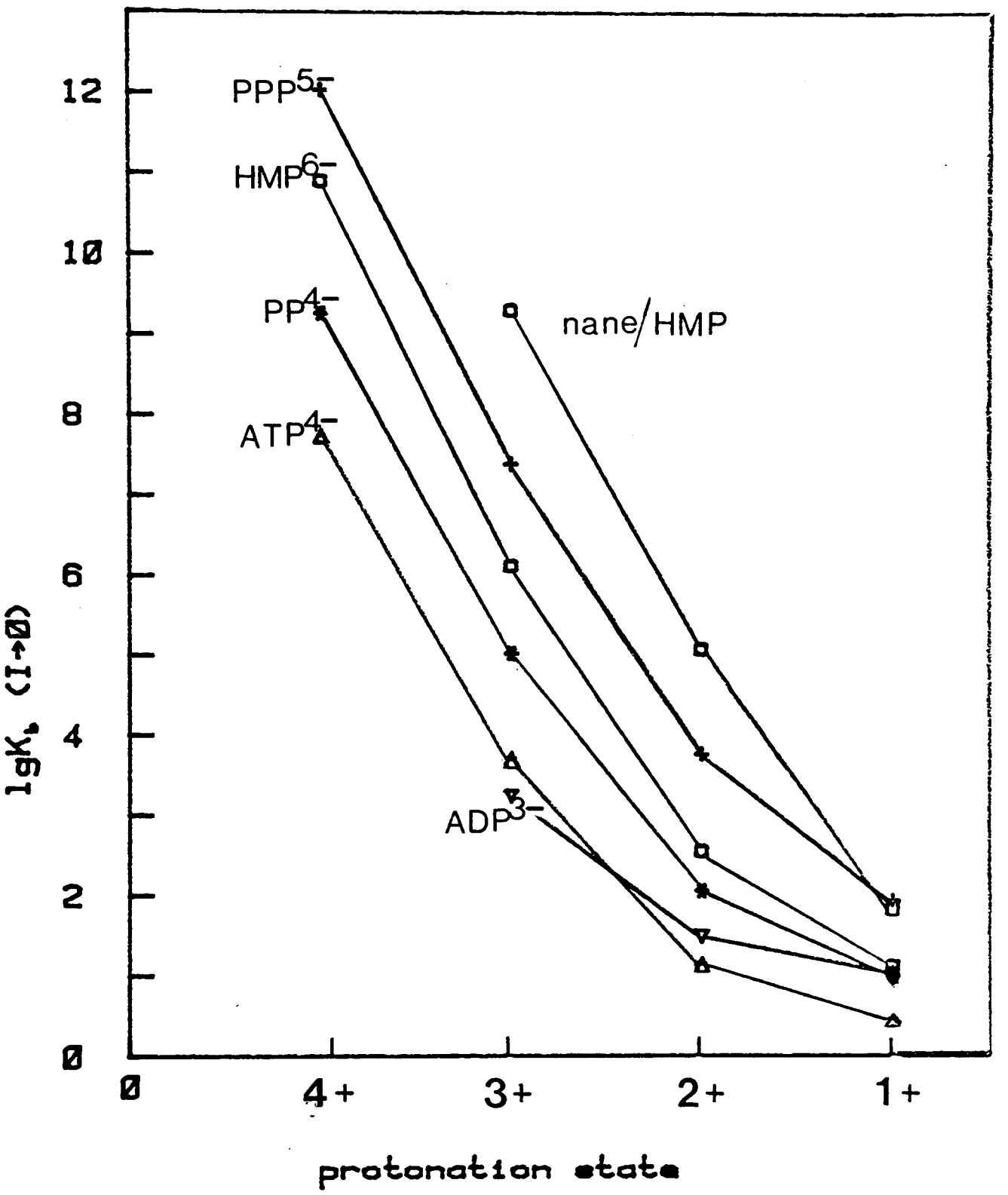

Figure 3.25 Summary of lgK_b values for trien with various phosphates and for nane with HMP^{6-}.

Symbols: HMP^{6-} (□)

PP^{4-} (✳), PPP^{5-} (+)

ADP (▽), ATP (△).

This is the effect of charge isolation along the extended linear structure of the amine. The shortfall, and the effect, are negligible for nane.

A comparison is made in figure 3.26, of strength of asociation of $trien^{4+}$ with the various phosphates. The following observations are made.

(i) As phosphate charge increases so does lgK_b.

(ii) There is very little shortfall for the intermediately charged PP^{3-} and PPP^{4-} species and thus there is little evidence of the charge isolation effect.

(iii) The strength of interaction for the various phosphates follows the sequence

$$PP > \begin{matrix} PPP \\ ATP \end{matrix} > HMP$$

Thus it appears that interaction is weaker for the larger structures, possibly because while the more widely dispersed charge is more easily accommodated by individual solvent molecules in the free solution, it is generally less likely to be closely matched by a particular conformation of triethylenetetramine. In general, stronger association is seen for the flexible, linear phosphates than for the more rigidly structured cyclic phosphates and it is remembered that, in the previous section, no evidence of association was observed for trimetaphosphate. In addition, it is noted that doubly charged phosphate forms much stronger H-bonds than the singly charged ring phosphate.

Finally, in figure 3.27, a comprehensive plot is made of strength of association against charge product for the trien complexes.

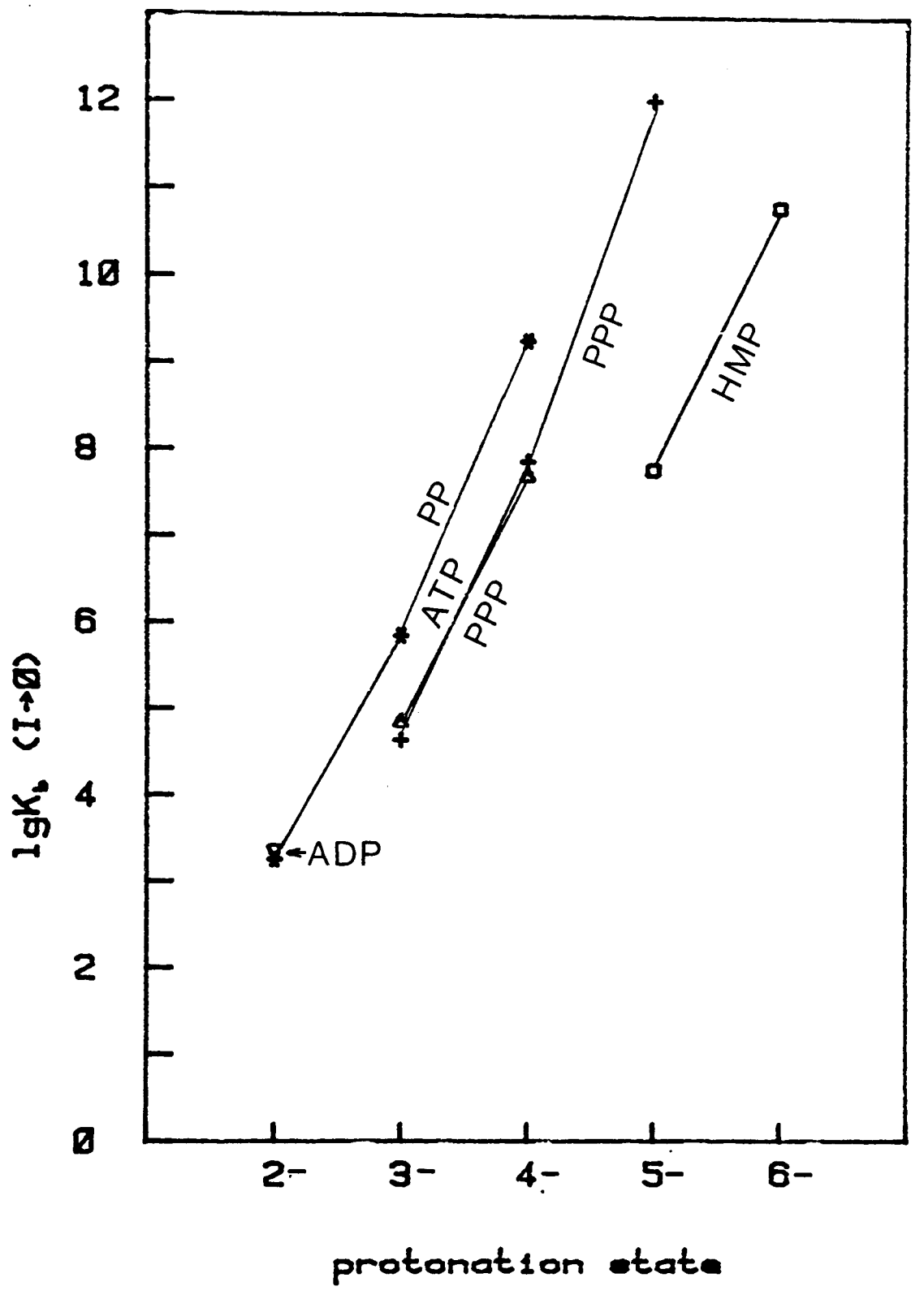

Figure 3.26 Summary of lgK_b values for various phosphates with $trien^{4+}$.

Symbols as for figure 3.25.

It has already been observed that the greatest shortfall in lgK_b is seen with the complexes of intermediate charge product which involve triethylenetetramine in its 2+ and 3+ states when its charges are well separated. Strengths of association of singly charged triethylenetetramine are generally close to the reference plot based on the interactions of spherical inorganic ions.

At the other end of the scale, the most highly charged species interact more strongly than predicted from simple consideration of point charges. It is remembered that the lgK_b values have been corrected to zero ionic strength conditions. The corrections are most significant when two highly charged species interact which reflects the thermodynamically unfavourable nature of individual highly charged species. Entropy effects are involved here since a higher degree of order is implicit in the solvation of a highly charged molecule by several singly charged or uncharged molecules than in the mutual neutralisation of just two highly charged molecules.

When there is the possibility of a good fit of positive and negative charges, certain complexes are stronger than others. An example is provided by the comparatively strong association of HMP^{5-} and $trien^{4+}$. This selectivity of association allows for biochemical specificity.

The strength of the associations studied here is seen to be less than that of the binding of Mg^{2+} and Ca^{2+} to the various phosphates. Thus biological amines do not compete with Mg^{2+} for nucleotides or pyrophosphate when both are

about 10^{-3}M in solution. Unlike the metal ions, however, they do bind to DNA, with its spread charge pattern, and this is an integral part of their function.

Finally, it is noted that, when of equal charge, the strength of the association of ADP with trien^{4+} is similar to that of PP. A corresponding similarity is seen for ATP and PPP. Thus no effect is observed for the presence of the adenosine moiety.

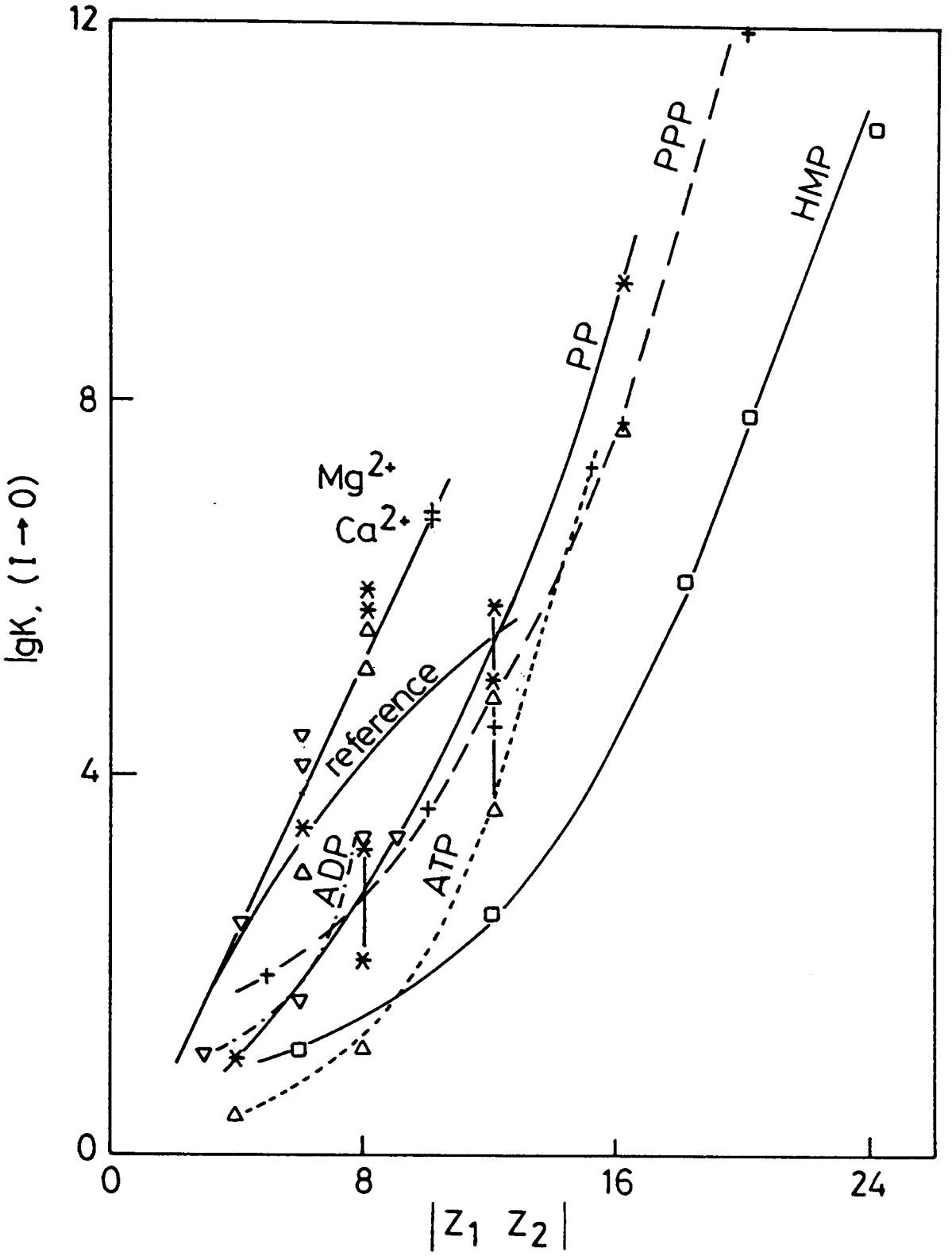

Figure 3.27 Association of phosphates with trien: lgK_b vs charge product

(i) for the present series;

(ii) for Mg^{2+} and Ca^{2+} with phosphates (Sillén & Martell, 1971);

(iii) for spherical inorganic ions (reference).

Key: HMP (□), PP (✳), PPP (+), ADP (▽), ATP (△).

Table 3.7 The effect of interaction on chemical shift

(a) Change in proton nmr chemical shift of amine in presence of excess phosphate

amine	signal	phosphate HMP^{6-}	PP^{4-}	PPP^{5-}	ADP^{2-}/ADP^{3-}	ATP^{4-}
$trien^{4+}$	A	+0.075	+0.02	+0.04	+0.035	+0.04
	B	+0.05	+0.02	-	+0.055	+0.035
	C	+0.035	+0.005	-	+0.035	+0.025
$trien^{3+}$	A	+0.075			+0.035	
	B	-	-	-	+0.065	-
	C	-			+0.03	
$nane^{3+}$	-	-0.13	-	-	-	-
$nane^{2+}$	-	-0.01	-	-	-	-

(b) Change in ^{31}P nmr chemical shift of phosphate in presence of excess $trien^{4+}$. Phosphate charge is indicated.

charge state	phosphate HMP	PP	PPP(α)	ADP(β)	ATP(γ)
protonated	(5-)(not available)	(2-) +0.3	(3-) +0.1	(2-) 0.0	(3-) 0.0
deprotonated	(6-) -0.6	(4-) -0.7	(5-) -0.1	(3-) 0.0	(4-) -0.65

Table 3.8 Association of phosphates and amines:
charge product (in parentheses) and lgK_b values for the interactions of the present study. (I→0,T=300K)

phosphate	charge	trien^{4+}	trien^{3+}	trien^{2+}	trien^{1+}
HMP	5-	(20) 7.87	-	-	-
	6-	(24) 10.90	(18) 6.12	(12) 2.55	(6) 1.12
PP	2-	(8) 3.25	-	-	-
	3-	(12) 5.85	-	-	-
	4-	(16) 9.26	(12) 5.02	(8) 2.05	(4) 1.01
PPP	3-	(12) 4.64	-	-	-
	4-	(16) 7.87	-	-	-
	5-	(20) 12.03	(15) 7.39	(10) 3.76	(5) 1.93
ADP	2-	(8) 3.33			
	3-	-	(9) 3.33	(6) 1.57	(3) 1.01
ATP	3-	(12) 4.98	-	-	-
	4-	(16) 7.84	(12) 3.80	(8) 1.24	(4) 0.55
			nane^{3+}	nane^{2+}	nane^{1+}
HMP	6-	-	(18) 9.30	(12) 5.07	(6) 1.82

Chapter 3 References

Bundi, A. and Wüthrich, K. (1979) Biopolymers, 18, 285-297.

Högfeldt, E. and Perrin, D.D. (1979) "Stability constants of metal-ion complexes, parts A and B", IUPAC Chemical Data Series nos.21 and 22, Pergamon Press, Oxford.

Rorabacher, D.B., MacKellar, W.J., Shu, F.R., and Bonavita, Sister M. (1971) Anal.Chem., 43, 4, 561-573.

Rossotti, H. (1978) "The study of ionic equilibria." Longman, London.

Tam, S-C. and Williams, R.J.P. (1984) J.Chem.Soc., Faraday Trans. 1, 80, 2255-2267.

Taqui Khan, M.M. and Martell, A.E. (1966) J.Amer.Chem.Soc., 88, 668-671.

Weitzel, G. and Spehr, T. (1958) Hoppe-Seyler's Z.Physiol.Chem., 313, 212-226.

CHAPTER 4.

YEAST PHOSPHOGLYCERATE KINASE
STRUCTURE AND PROTON NMR SPECTRUM

Chapter 4 Contents

4.1 INTRODUCTION

4.1.1 Introduction

Phosphoglycerate kinase (PGK) catalyzes the high-energy Mg^{2+}-dependent phosphoryl transfer from 1,3-P_2G to ADP in the first ATP-producing step of the glycolytic pathway.

$$1,3\text{-}P_2G + ADP \overset{Mg^{2+}}{\rightleftharpoons} 3\text{-}PG + ATP$$

The enzyme is a monomer of approximate molecular mass 45,000a.m.u. It is found in both aerobes and anaerobes and is necessary for carbon fixation in plants.

The amino acid sequences of yeast, horse and human PGK have been compared with two trypanosome PGKs (Osinga et al., 1985), a fungal PGK has been sequenced, and work is in progress on PGK from the prokaryote Thermus thermophilus (Littlechild et al., 1986). Regions of the molecule which are seen to be highly conserved are considered to be of specific structural significance, as are those amino acids whose substitution causes a decrease in enzyme activity (Fujii and Yoshida, 1980). More generally, similarities in sequence and in catalytic properties indicate a highly conserved structure.

The crystal structures of horse PGK (Banks et al., 1979) and yeast PGK (Watson et al., 1982) have been determined by high resolution X-ray crystallography. The yeast PGK molecule is seen to consist of two equally-sized, well

separated domains, each of which, in turn, consists of six parallel β-sheets, surrounded by α-helices. The two lobes are connected by a narrow waist region comprising two peptide strands. One, helix V, runs from the N-terminal domain to the C-terminal domain, while the other, β-sheet N and helix XIII, doubles back from the C-terminal lobe to the N-terminal lobe to form the C-terminus (see figure 4.1). It is noted that glu190 of helix V is connected by a hydrogen bond to his388. This region may well belong to some form of hinge system (see later). Both of these residues are completely conserved and, in fact, β-sheet N and helix XIII, from ser387 to lys403 provide the longest conserved stretch of the protein. Conservation is also noted from ile367 to asp372 which could well provide a link between the nucleotide binding site and this "hinge" region.

Yeast PGK crystals soaked in MgADP or MgATP have been shown to bind nucleotides at a single site. High resolution X-ray difference maps have revealed the conformation of the bound nucleotide (Watson et al., 1982) and its location is shown in figure 4.2. The adenosine moiety lies in a shallow hydrophobic cleft, above val339 and gly338 and between ala212 and gly211 on one side and leu311 on the other. The ribose ring lies over pro336 and its 2'- and 3'-OH groups coordinate with glu341 and asp372 respectively. The phosphate chain lies across the peptide backbone of pro336 and gly335. The α and β phosphates coordinate with lys213 and lys217 respectively, while the γ-phosphate interacts with the main chain NH of asp372 and, probably, with that of gly371 as well. It

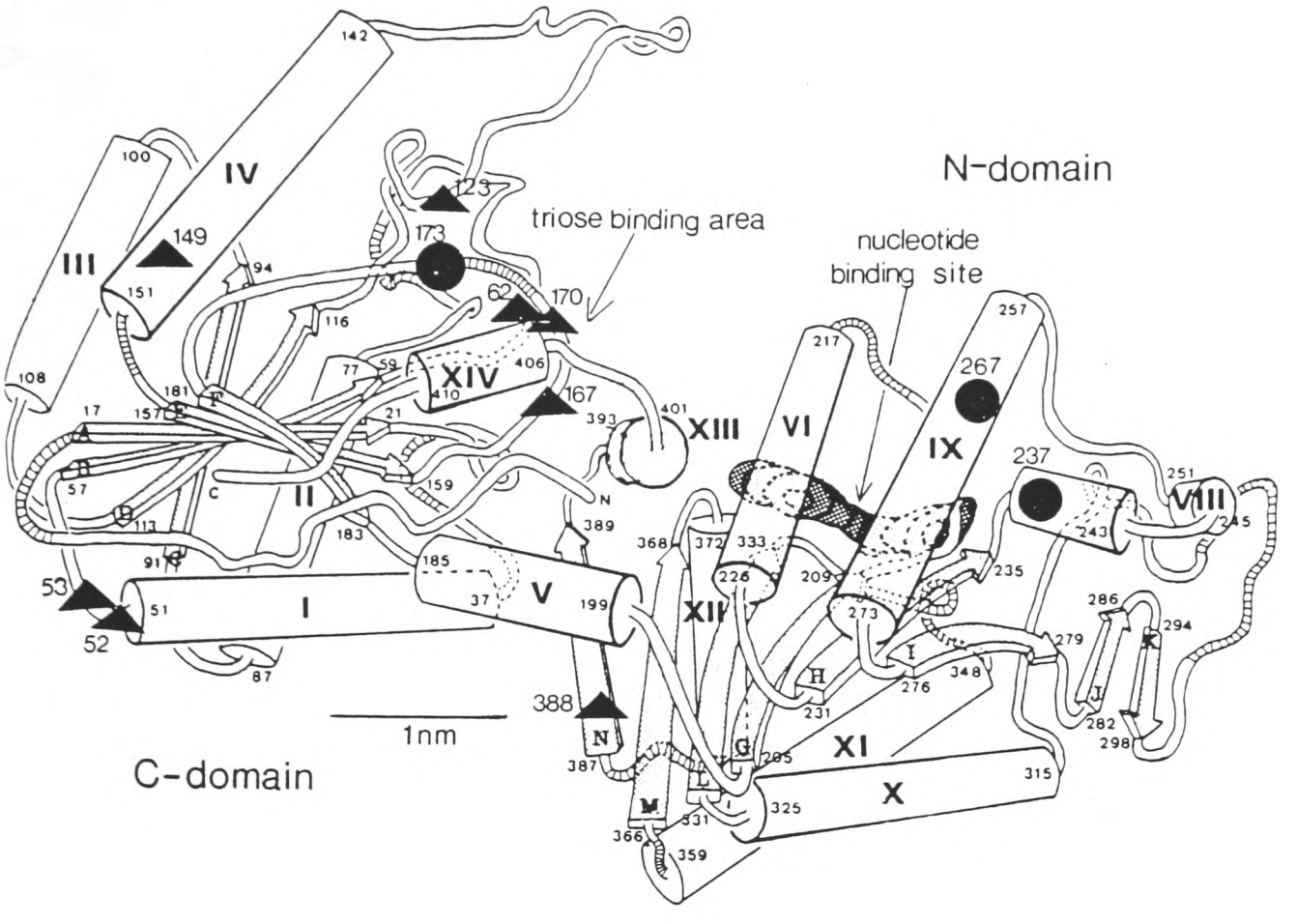

Figure 4.1 A diagram of the crystal structure of yeast PGK, with the N-terminal domain on the left. α-helices are denoted by red cylinders, β-sheets by blue arrows. (After Watson et al., 1982). Symbols: histidine residue (Δ), methionine residue (O).

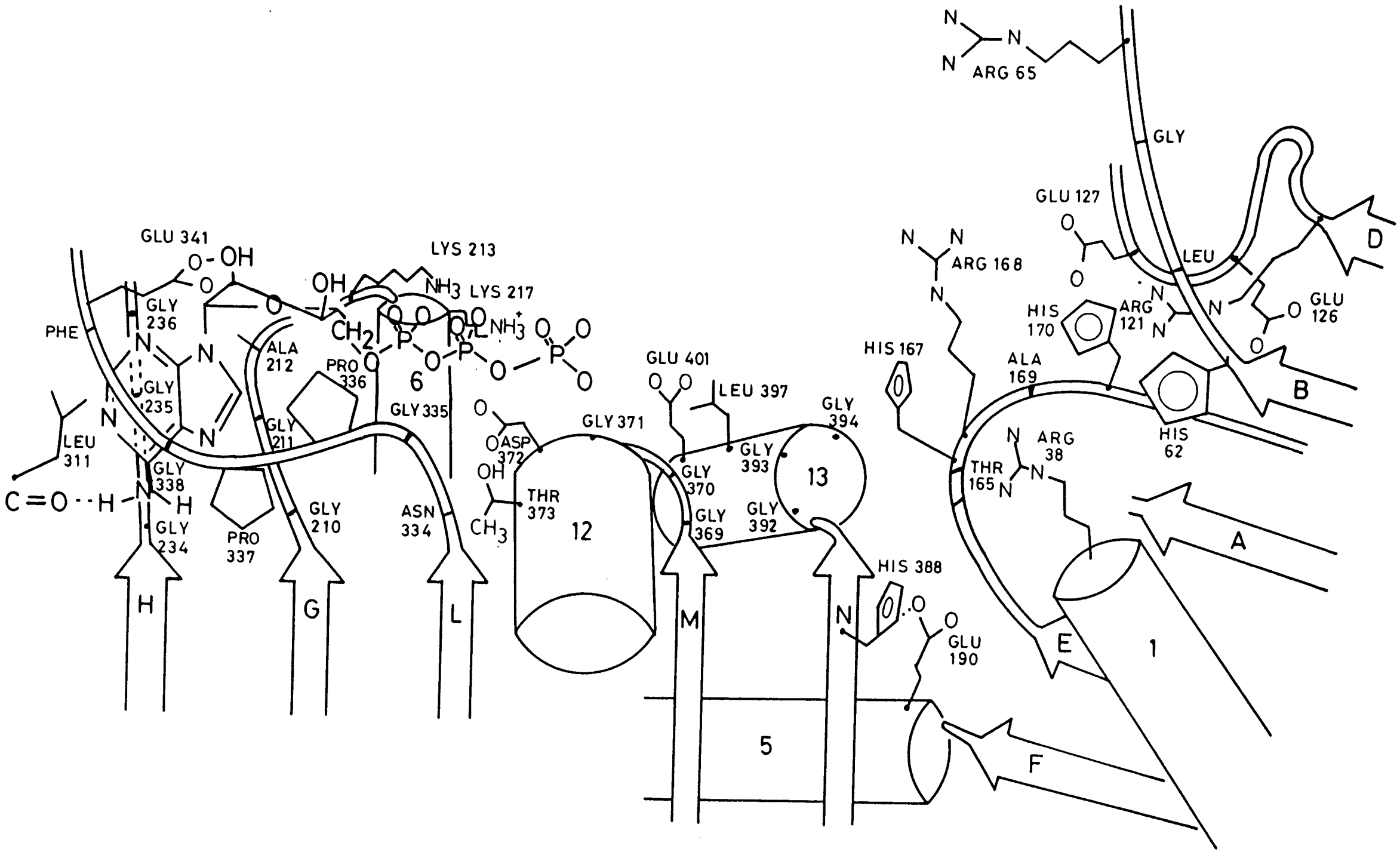

Figure 4.2 Schematic drawing of the active site of yeast PGK, with ATP bound.

is noted here that all of these residues are completely conserved and that no aromatic residues appear to be directly associated with bound ATP.

The triose substrate appears to bind in a single site in the N-terminal domain, facing the nucleotide site (figures 4.1 & 4.2 ~~and 2b~~) but the definition of this binding is poor. A phosphate group is expected to be attracted to this area of positive charge which comprises a triangle of histidine residues (62, 167 and 170) as well as four arginine residues (168, 21, 65 and 121). There are several acidic residues in the vicinity (glu118, 125 and 126, and asp23). It is observed here that, with the exception of his170 and glu125, these are conserved residues, and that this area is 1.2nm distant from the γ-phosphate of bound nucleotide, at least in the crystal structure studied. If this is, indeed, the site of triose phosphate binding, then this "open" form of the protein must be converted to a "closed" form for the possibility of phosphate transfer to arise. We shall test these structural considerations further in this thesis.

Small angle x-ray studies (Pickover et al., 1979) have suggested that the radius of gyration of the enzyme decreases only on binding <u>both</u> substrates, MgATP and 3-PG. Using computer modelling this has been tentatively linked to a cleft closure when the two domains of the "open" structure described above move towards each other, to form a "closed" structure. Work by Roustan et al. (1980) and by Rice and Blake (1984) has provided further evidence of the closure of PGK (see chapter 7, introduction).

An examination (Wrobel and Stinson, 1978) of the binding of various anions indicated the presence of a non-specific anionic site and suggested that this anionic binding was involved in catalytic activation. Kinetic studies (Scopes, 1978a) demonstrated that the sulphate ion caused an increase in PGK activity. Further work (Scopes, 1978b), with gel filtration, showed the anion to compete with 1,3-P_2G and to promote dissociation of this very tightly bound substrate. There has also been some suggestion (Roustan et al., 1980) that sulphate displaces the conformational equilibrium towards the closed form.

All of the above suggestions about changes in conformation, binding site of anions and substrates can be tested by nmr. The first detailed proton nmr analyses (Tanswell et al., 1976) were done before there was a sequence and showed, independent of X-ray diffraction studies, that when MgATP is bound to the enzyme, the divalent metal ion was between the β and γ phosphates of ATP, as in free solution. Using paramagnetic metal ion probes, three histidines (at that stage completely unassigned) of the presumed 3-PG site were found to be less than 0.6nm away from the metal of ATP. This suggests that, in the 15mM ammonium sulphate solutions used, the enzyme adopts the closed conformation at least to some degree (nmr gives averaged conformational data for dynamic systems), since the open form has the sites at some 1.2nm distance in a crystal. We return to the exact measuring of probe studies later. On binding one substrate there was the suggestion that the enzyme was in a more "open"

conformation but binding of both substrates gave a marked change in the spectrum involving resonances in both the aromatic and aliphatic regions, indicative of some degree of closure.

In this work, new nmr data will be analysed and the problems of substrate, anion and metal ion binding and of conformational equilibria will be reconsidered. We use both ^{31}P and ^{1}H nmr spectroscopy, and we keep in mind the findings of the model studies in Chapters 2 and 3.

4.1.2 The histidines

The downfield proton nmr chemical shift of the histidine resonance and its pH dependence makes the histidine residue a convenient probe point for nmr study. Moreover, the aromaticity and positive charge of histidine have important structural and functional implications in their own right. The positions of the eight histidines of yeast PGK are shown in figure 4.3 which shows that seven are found in the N-terminal lobe while his388 is located in the hinge region.

Three of the histidines are located in the positively charged face of the triose phosphate binding site facing across the cleft towards the nucleotide site. This triangle of histidines is illustrated by figure 4.4. Arg168 lies between his167 and his170 within 0.4nm of each. These histidines are in turn flanked by glu398 (not in the diagram) and by glu125. Positioned between his170 and his62 is arg21 and another arg, arg65, lies below his62 to the right. Below his62 lies phe24 and to its left lies asp23. Thus, each of

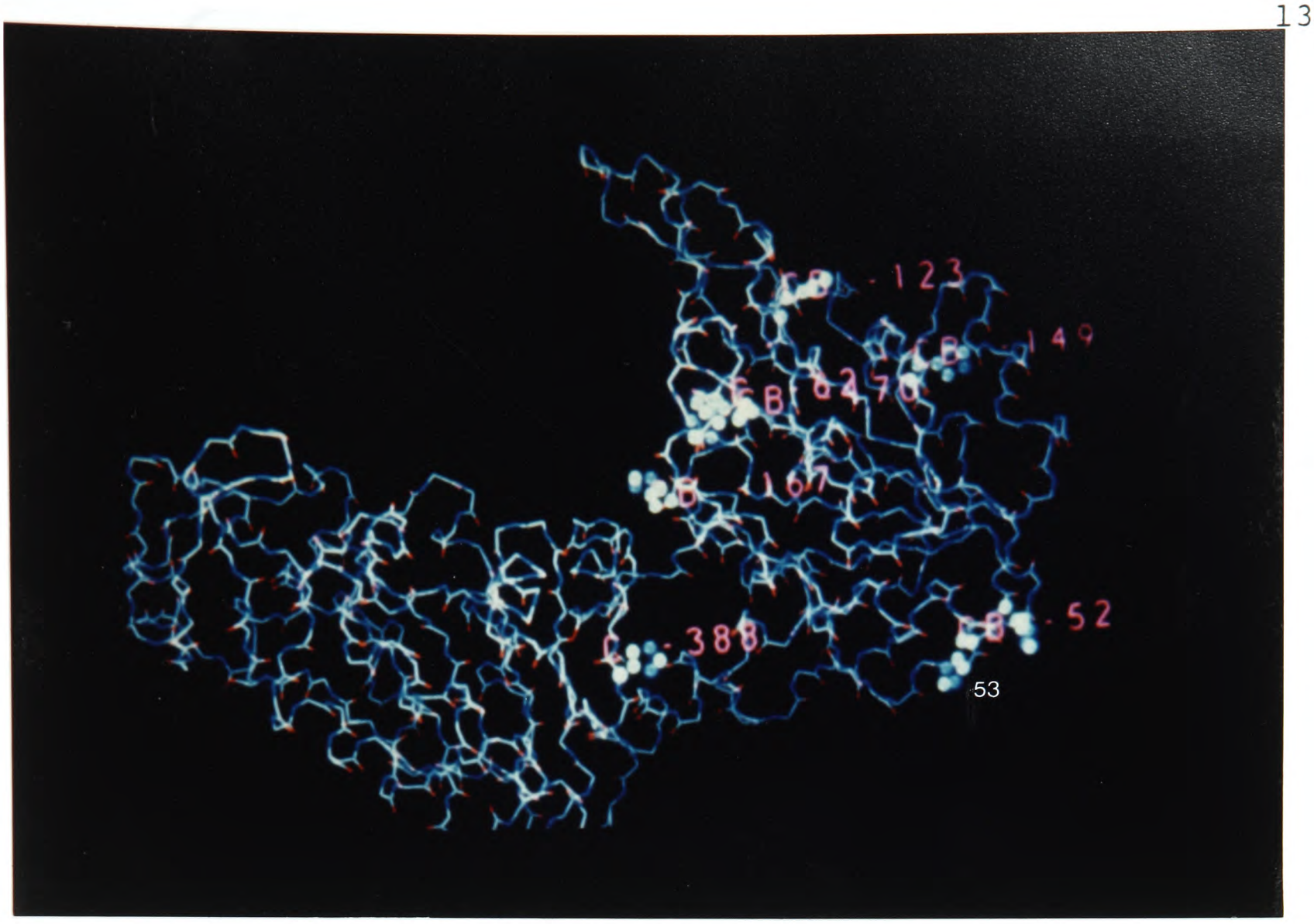

Figure 4.3 The crystallographic structure of yeast PGK showing the peptide backbone. The C-terminal lobe is on the left, the N-terminal on the right. The positions of the eight histidine residues are indicated.

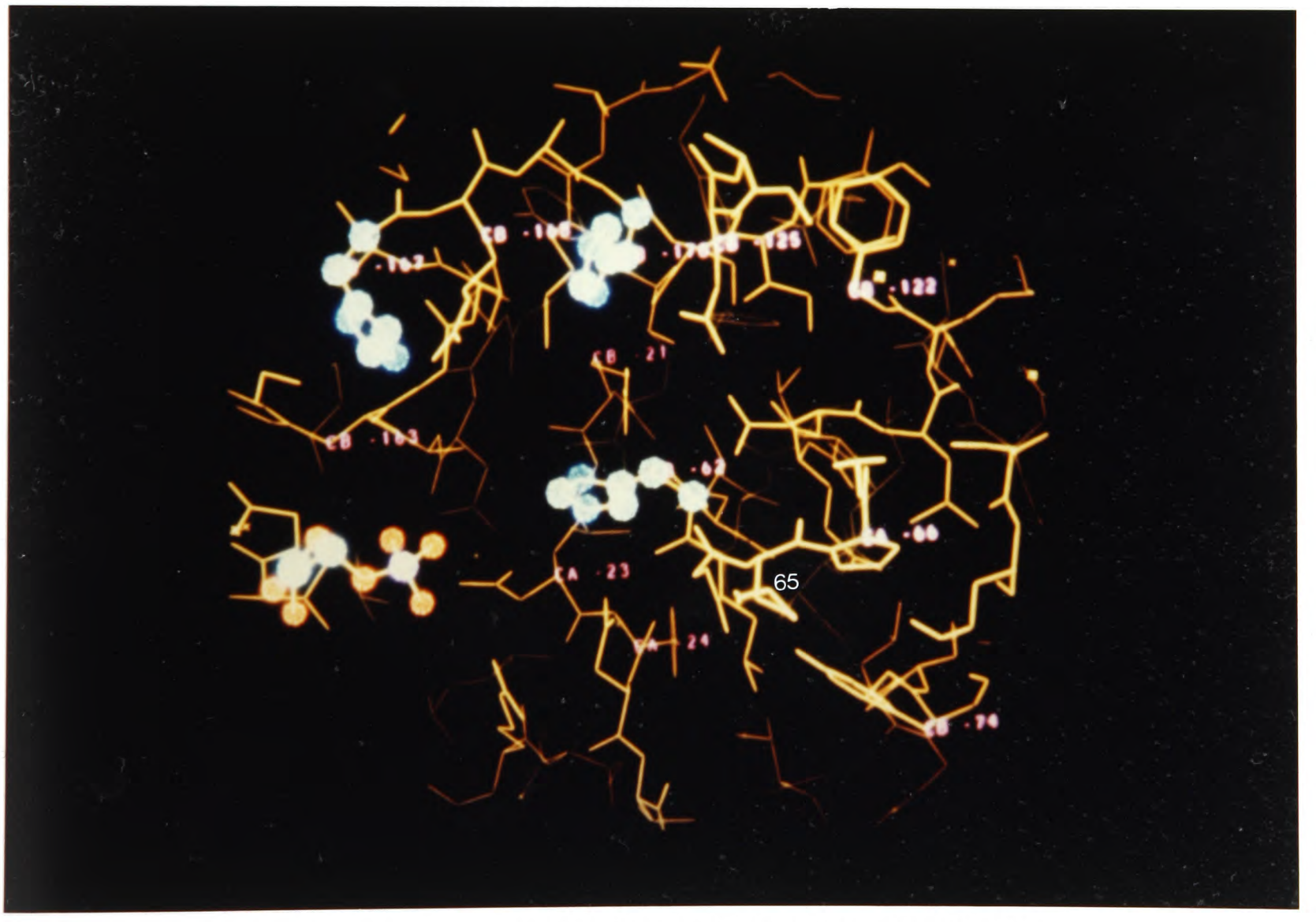

Figure 4.4 The environment of histidines 62, 167 and 170 included in the diagram is a ~~seemingly unlikely~~ position of triose phosphate sufficiently close to the nucleotide-binding site (to the left, out of the picture) to allow interaction with bound nucleotide.

the three histidines is near both positively and negatively charged residues with the positive element slightly predominant. From the conformation shown, his167 appears most likely to interact with arg168. More generally, from its position opposite the known nucleotide binding site this surface is implicated in triose phosphate binding and the excess of basic residues commends the area as an anion binding site. These features are used in the nmr studies to identify the resonances of these histidines. Note also that there is only one other aromatic residue in this region.

The environment of his52 and his53 is shown in figure 4.5. The situation of lys14 between the two histidines defines this as an area of positive charge. Another lysine, lys89 (not shown), lies about 0.3nm to the left of his53. His52 lies between leu13 and tyr48, while his53 is totally exposed on the surface. Within a 0.6nm radius are found arg55 and lys16 above, asp12 to the right, and gly51 and lys47 below.

The hydrogen bond between his388 and glu190 is shown in figure 4.6. The histidine residue is seen to provide a link between helix V and the completely conserved β-sheet areas N and M. The residue is seen to be closely sandwiched between tyr193 below and phe194 above. Phe163 ends this completely conserved aromatic corridor. Aside from glu190, charged groups within 0.5nm are lys189 below and lys385 to the left.

Histidine 123 and its environment is displayed in figure 4.7. As with histidine 388, the residue lies between two aromatic residues, in this case phe147, at 0.5nm distance on

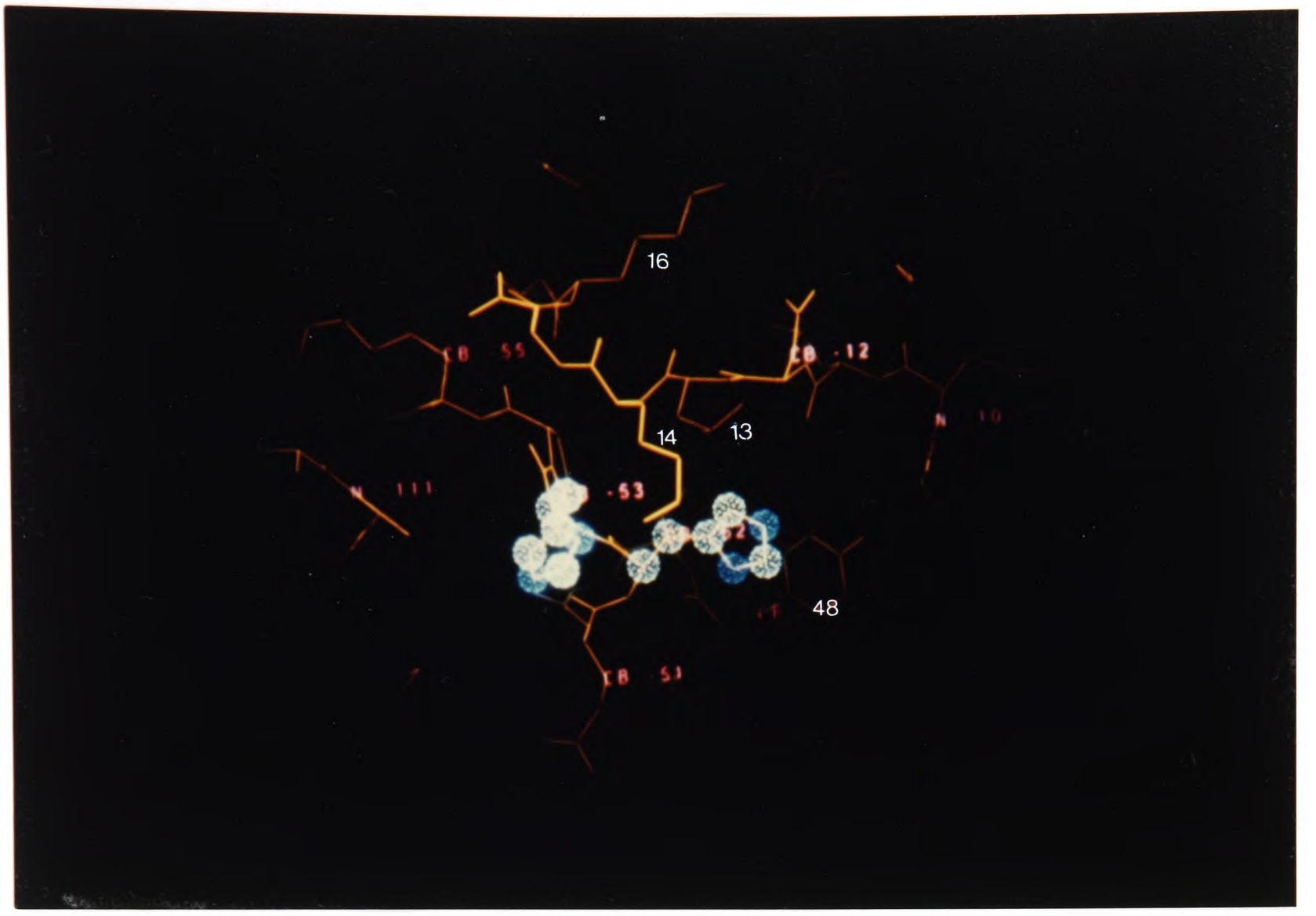

Figure 4.5 The environment of histidines 52 and 53.

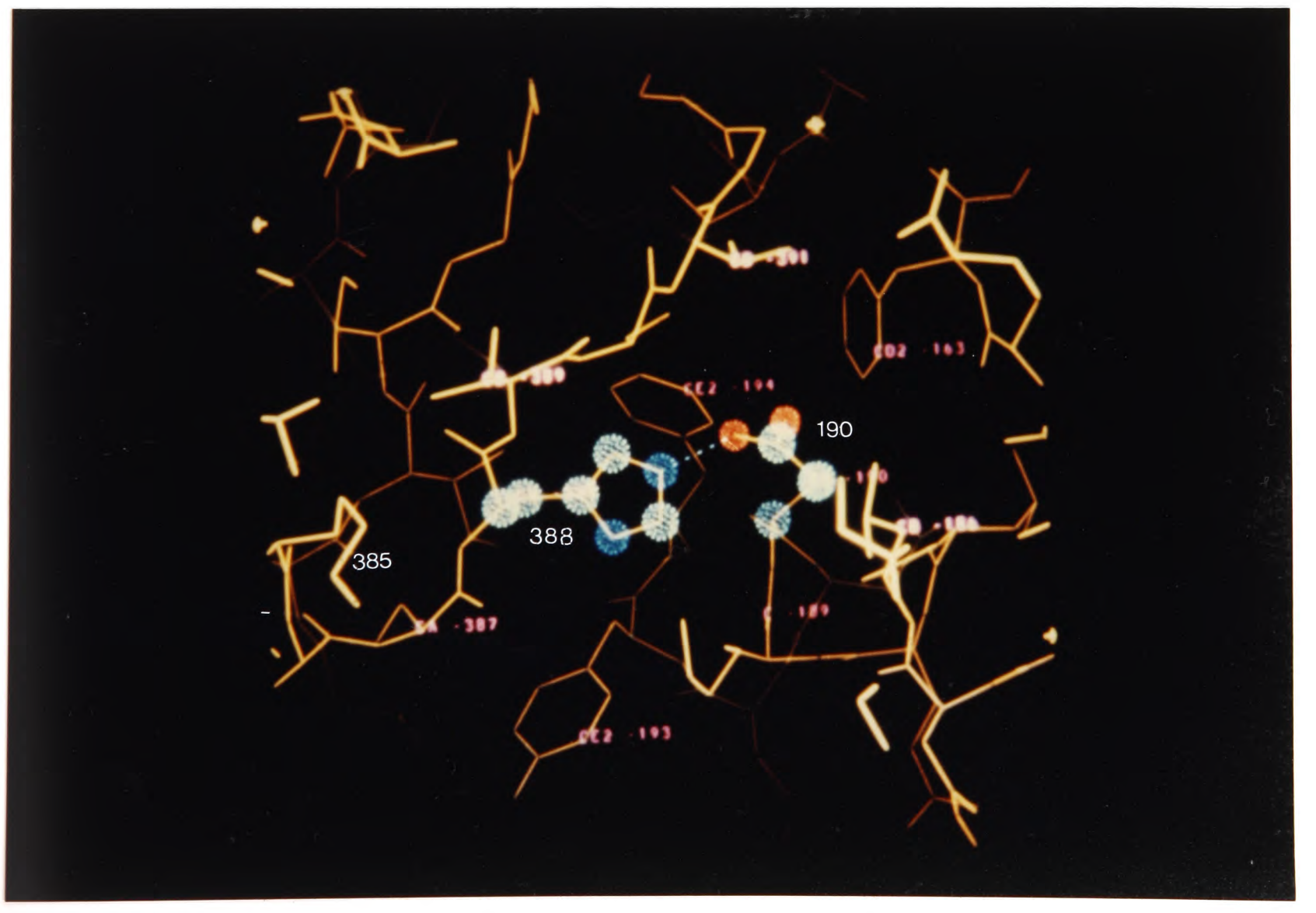

Figure 4.6 The environment of histidine 388.

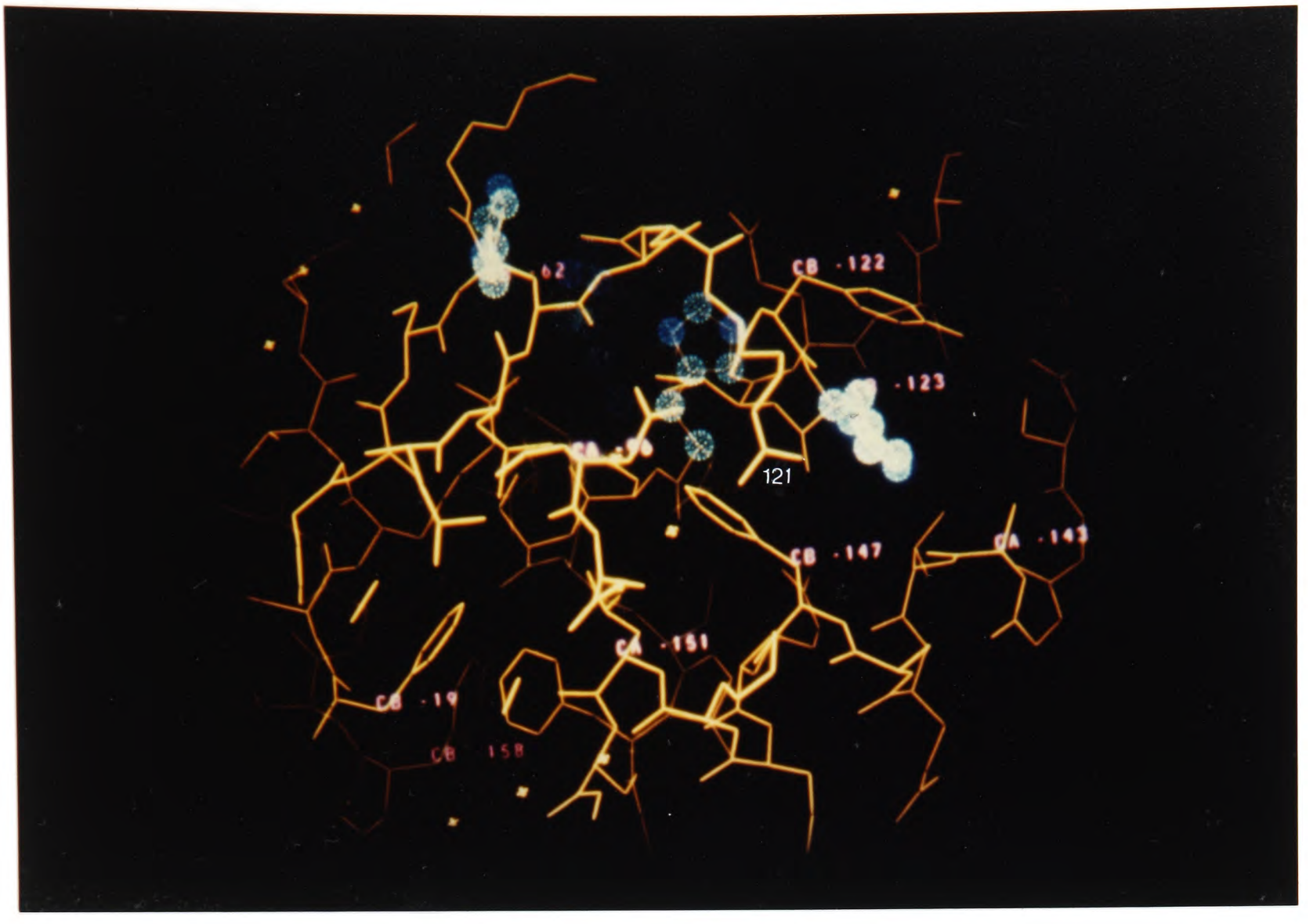

Figure 4.7 The environment of histidine 123.

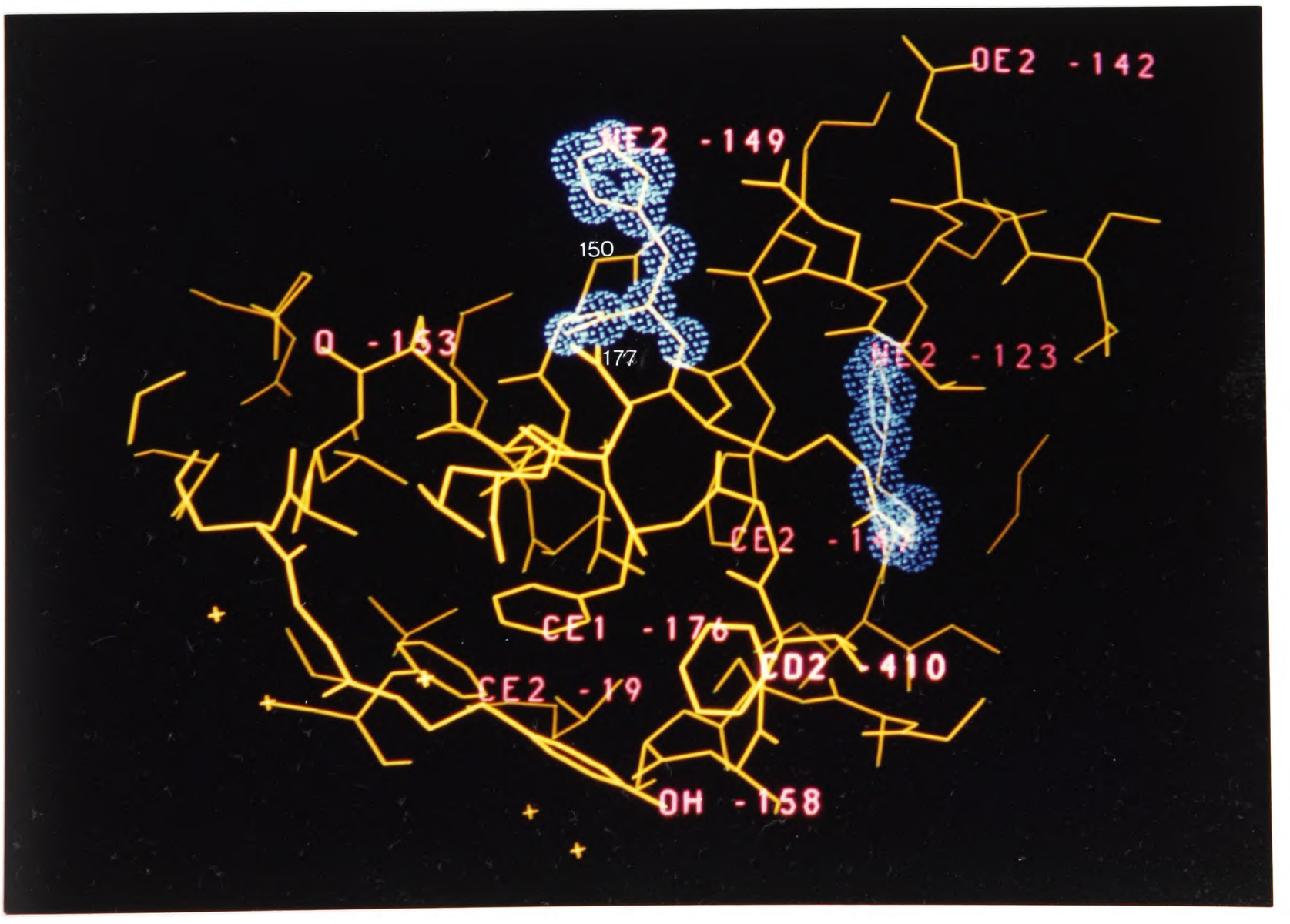

Figure 4.8 The environment of histidine 149.

one side, and tyr122 0.4nm distance on the other. The ring of the latter exactly overlaps the histidine ring and is likely to give rise to ring current shifts in the nmr spectrum. Arg121 is at 0.3nm distance on the left in the diagram, while the α-carbon of asp143 is at a similar distance to the bottom right, close enough to allow the formation of a hydrogen bond. Finally, glu126 lies within 0.5nm of his123, behind and to the right. Generally, his123 is at the surface of the molecule but not completely exposed, and is seen to be liable to the influence of the negative charge nearby basic residues while, together with arg121, forming a local area of positive charge.

Finally, histidine 149 is portrayed in figure 4.8. This is the most exposed of the histidines, with no evident nearby aromatic residues. Two acidic residues, glu150 and asp177, are at 0.4 and 0.6nm respectively, from this histidine.

4.2 MATERIALS AND METHODS

4.2.1 The sample

Fresh, wet bakers' yeast was purchased from Distillers plc, United Yeast Company Ltd., Brislington, Bristol, in 1kg blocks. The preparation of the enzyme followed the methods of Fifis and Scopes (1978), the resulting PGK being maintained in the relatively stable form of a pellet of enzyme in ammonium sulphate. The bulk of the enzyme was kindly supplied, in this form by the group of Dr. M. C. Watson, University of Bristol.

Activity was determined at various stages throughout the preparation by coupling the kinase reaction to removal of NADH with the enzyme GAPDH.

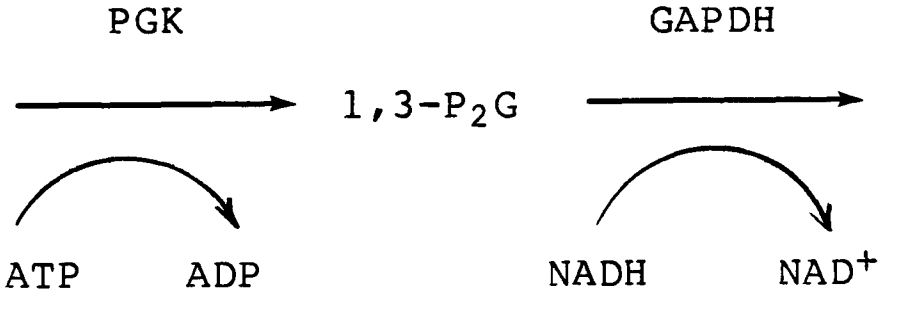

The concentration of NADH was monitored with a Pye Unicam SP-1800 double beam UV-visible spectrometer. A value of $6.22 mM^{-1} cm^{-1}$ was used for the extinction coefficient of NADH at 340nm, and the enzyme activity was expressed as the initial velocity, in μmoles of substrate converted per minute, at 25° C. The assay mixture was buffered at pH7.5 and contained 10mM 3-PG, 4mM ATP, 0.15mM NADH, $30 \mu g ml^{-1}$ GAPDH and 5mM $MgCl_2$. The PGK to be assayed was diluted such that an addition of 5μl to 1ml of the assay mixture caused a rate of decay of optical density of about 0.2 units per minute. Only those preparations with high activity were used.

Protein concentration was determined using an extinction coefficient of A 1%/1cm = 4.9 at 278nm. Checks on the purity of the enzyme were carried out by SDS/PAGE separation.

ADP, ATP and 3-PG were all obtained as sodium salts of the highest grade from Sigma Chemical Company. AMPPNP was purchased as its tetralithium salt from Boehringer Mannheim GmbH. Sodium d_3-acetate was bought from Aldrich Chemical Company.

In the preparation of a sample for proton nmr spectroscopy, the enzyme/ammonium sulphate pellet was taken up into solution buffered at pH 6.5, and the sulphate removed using dialysis in the Amicon Centricon 30 apparatus. Typically, 5ml of solution, in two Centricon tubes, were reduced to a volume of 200µl. This was repeated three or four times - sufficient to reduce the ammonium sulphate to negligible levels. The sample was buffered at pH5.9 with 100mM sodium d_3-acetate and made up to a final volume of 350µl. The enzyme was present at a concentration of 1 to 2mM. The chemical shift zero reference, TMS, is known to interact with PGK and so acetone was used as an internal standard (δ=2.214ppm).

4.2.2 Proton nmr

Proton nmr spectra were recorded either on a Bruker WH300 spectrometer, with a sweepwidth of 3kHz and 2,000 accumulations per spectrum, or on a Bruker AM500 spectrometer, with a sweepwidth of 5kHz and 128 accumulations. A memory size of 8K was used, and the pulse

angle was adjusted to 60 . When necessary, solution enhancement of the spectra was achieved using a Gaussian multiplication, with a Gaussian broadening of 0.10 and a line broadening of -10Hz.

Hahn echo experiments were carried out at 500MHz using the pulse sequence

$$D1 - 90^{\circ} - \tau - 180^{\circ} - \tau - FID$$

The experiment made use of the available Bruker Aspect 3000 software microprogram and included solvent suppression applied during D1 at the usual power level. D1 was set to 1 second, long enough to allow complete relaxation, and the number of scans per accumulation 64. τ was increased from 0 to 80ms, and thus the total time T between the 90° pulse and FID accumulation was varied from 0 to 160ms. This gave rise to a series of spectra where the tendency is for odd multiplet resonances to appear as positive peaks compared to the negative peaks of even multiplicity resonances. More importantly, intrinsic differences in relaxation times afford selective observation of peaks (Campbell et al., 1975), and only resonances of groups with long T_2 relaxation times appear in the spectra. Typically such peaks include C2 and C4 proton resonances of histidines exposed to solvent and ε-CH_2 proton resonances of lysine residues.

To obtain further multiplet selection, the Carr Purcell Meiboom Gill sequence was used:

$$D1 - 90^{\circ} - (\tau - 180^{\circ} - \tau).C - FID$$

This eliminates J-modulation and gives spectra where even and odd multiplet resonances are in phase. Again, the available software was used, modified to include solvent suppression. τ was set to 1ms and variable constant C to values of 60 and 75. This gave T values of, approximately, 120 and 150ms. By addition to and substraction of Hahn echo accumulations of equal T values spectra are obtained showing only doublet and only singlet and triplet peaks respectively.

4.2.3 Phosphorus-31 nmr

The phosphorus spectra (chapter 8) were recorded on a Bruker AM-250 spectrometer operating at a frequency of 101MHz. Typical parameters were a 40° pulse angle, together with a relaxation delay of 0.7s; 2,000 accumulations over a 6kHz sweepwidth; a 4K memory size and a line broadening of 9Hz. Chemical shifts were measured against an external standard of TMP (δ=0ppm) and upfield shifts are given a negative sign.

4.3 THE ^{1}H NMR SPECTRUM OF YEAST PGK

4.3.1 General description and pH dependence

The proton nmr spectrum of yeast PGK at 500MHz is shown in figure 4.9. The spectrum is totally reproducible though not very well resolved and it is easy to recognise peaks found earlier at 270MHz. There are extra resolved peaks which are also labelled. The absorption peaks are numbered starting from the low field region, generally according to the system of Tanswell et al. (1976), except that resonance 5 and 6 are reversed. Spectra were obtained at a variety of pH values from 5.9 to 10.6. The aromatic regions of the 500MHz spectra are shown in figure 4.10, and the chemical shift pH dependence is plotted in figure 4.11, from which certain conclusions may be drawn. First to be considered are the resonances which appear to come from singlet peaks several of which have been assigned by Tanswell et al. to histidines.

Peak 1 corresponds to a C-2 histidine resonance showing pK_a 8.3. This is high for a histidine pK_a and suggests the influence of a negatively charged environment. In the nmr work carried out on the horse enzyme in collaboration with this group (Delepierre, 1983), a C-2 histidine resonance of very similar chemical shift and pH dependence was observed. By comparison of histidine residues of the two molecules (see table 4.1), it is seen that there are only two residues, common to each protein, and known to be in areas of negative charge, numbers 123 and 388 in the yeast sequence. Further work on mutant yeast PGK, with histidine 388 replaced

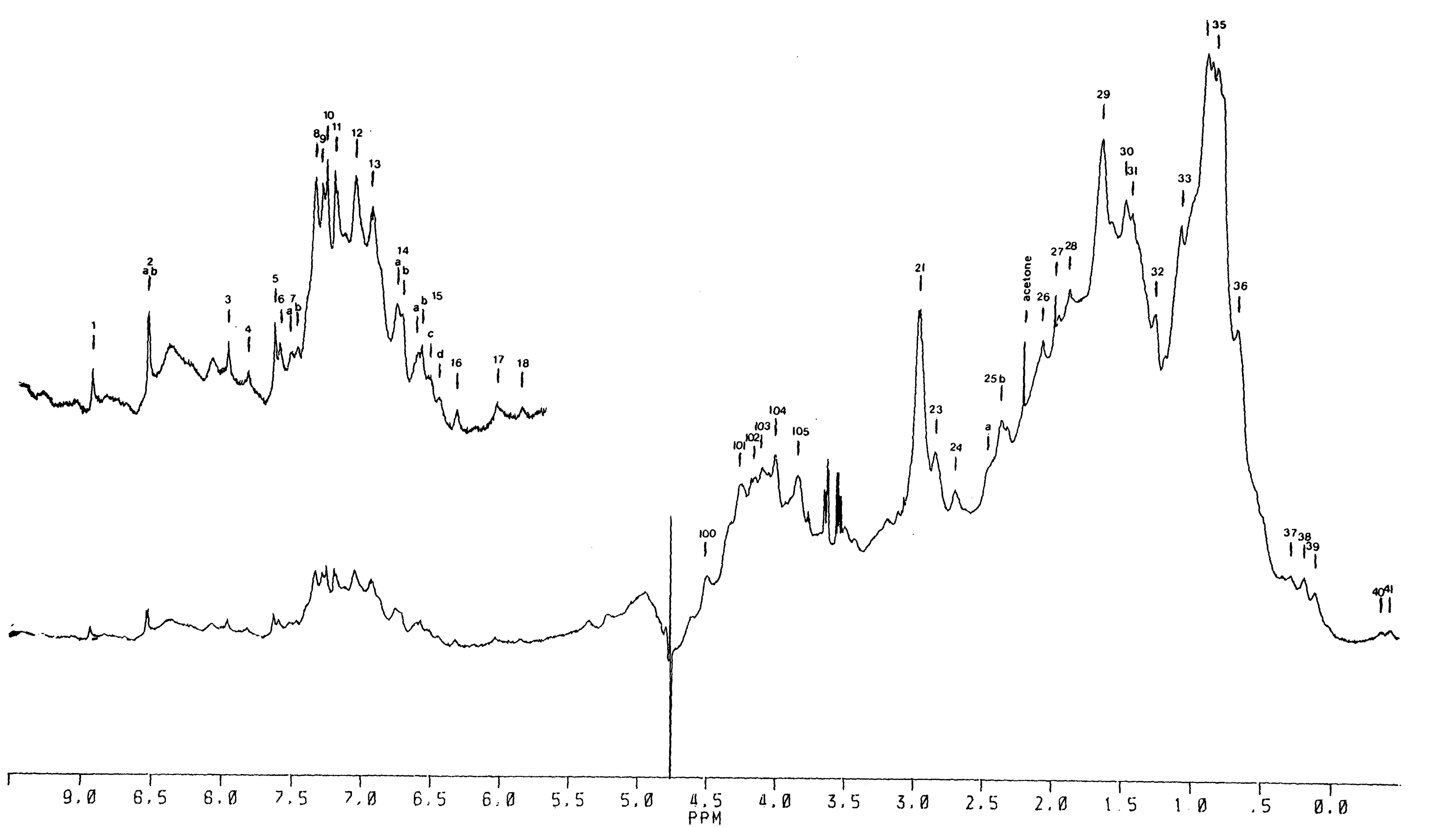

Figure 4.9 500 MHz proton nmr spectrum of 1mM yeast PGK. pH5.8.

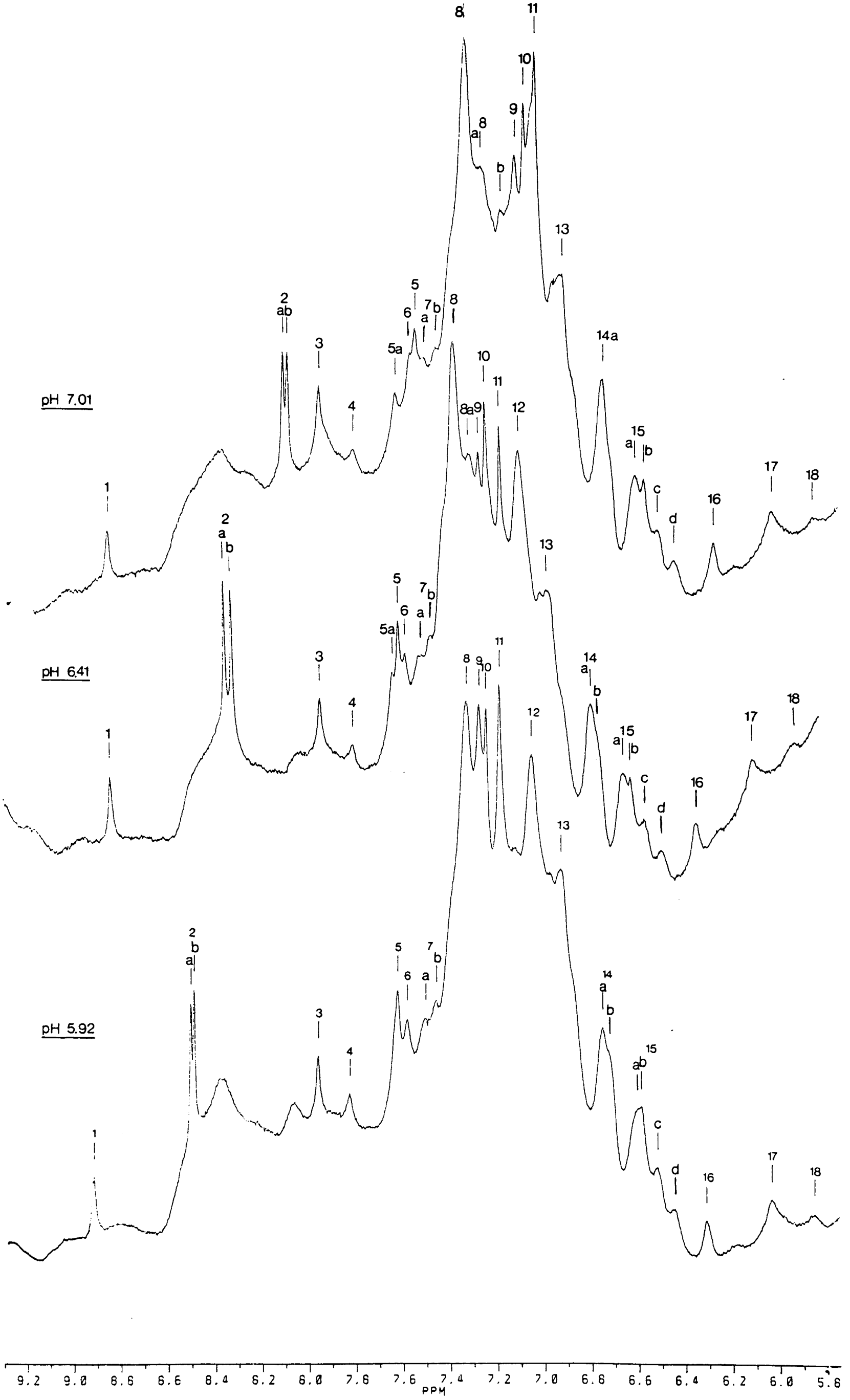

Figure 4.10 The aromatic region of the 500 MHz ^{1}H nmr spectrum of yeast PGK at various pH values.

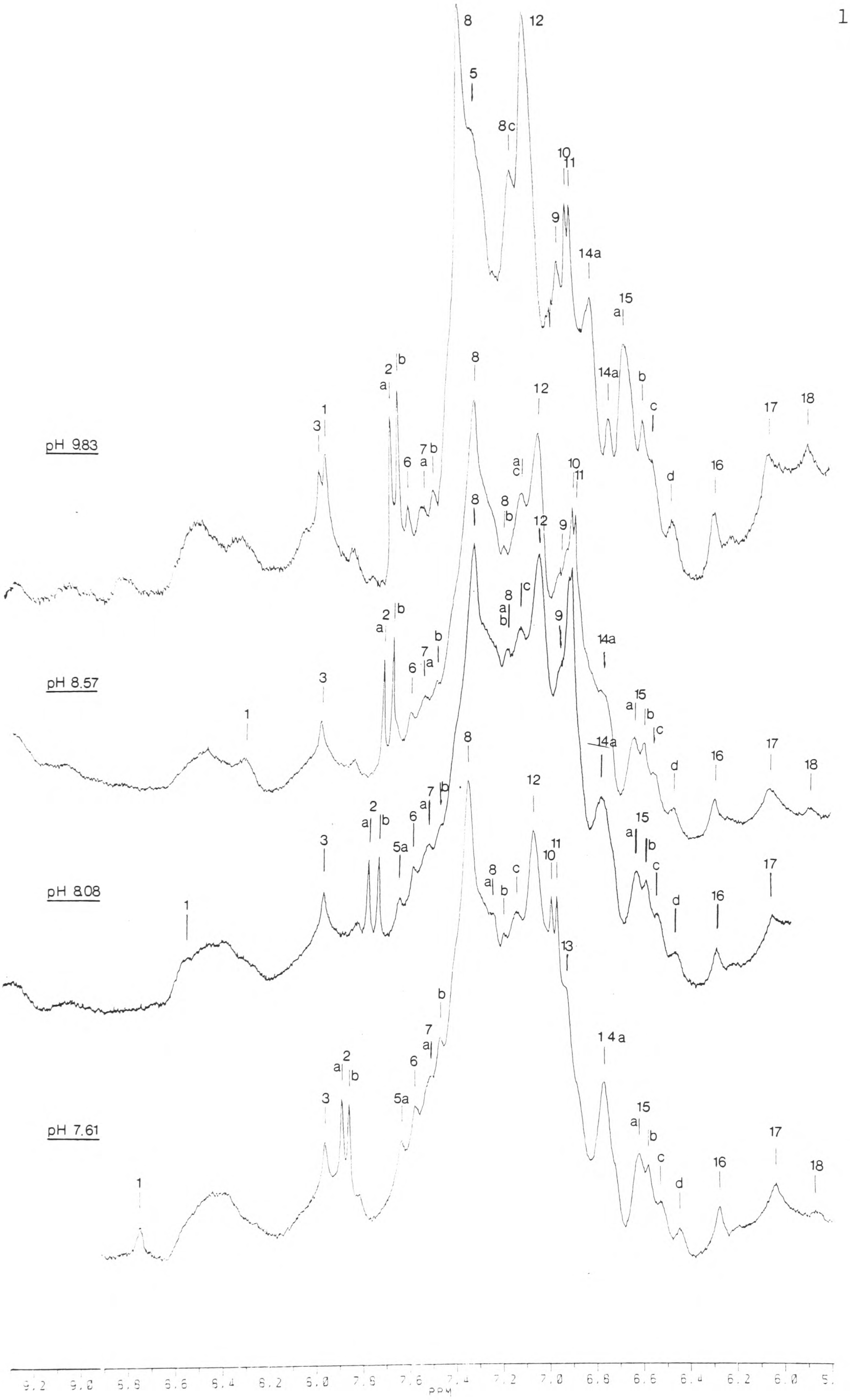
pH 9.83
pH 8.57
pH 8.08
pH 7.61
PPM

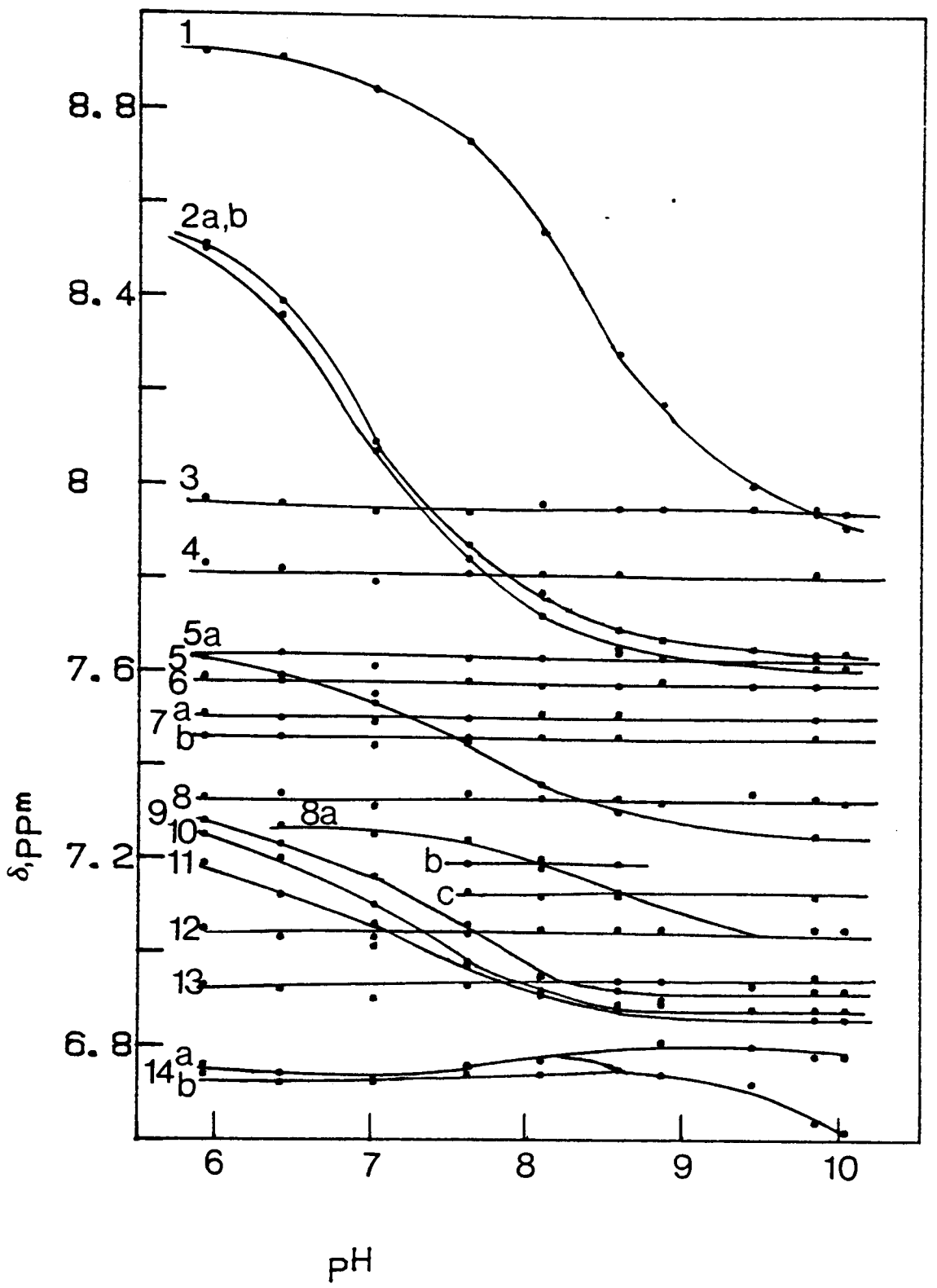

Figure 4.11 The proton nmr spectrum of yeast PGK: variation of chemical shift with pH.

by glutamine 388, revealed that peak 1, observed in the mutant spectrum, could not relate to resonance 388, and, therefore, it does correspond to histidine 123.

Peaks 2a and b have pK_a's about pH7 and thus show the characteristics of C-2 resonances of histidine groups totally exposed to solvent. Their chemical shift positions are those for unperturbed histidine resonances. In yeast PGK the three remaining possible candidates for these two resonances are residues number 52, 53 and 149. With horse PGK, only one peak of these characteristics is observed and it is likely to correspond to residue 294 which is the only exposed surface histidine of the horse PGK structure.

Peaks 3, 4, 5a and b of yeast PGK, all of which are apparently one proton peaks, are independent of pH over the range studied. Their chemical shift values indicate that they could represent either C-2 protons of deprotonated histidine residues or protons of the two tryptophan resonances found in yeast PGK, and also present in the horse enzyme. Peaks 3, 4 and 6 are consistently found to be influenced by addition of 3-PG and anionic shift or broadening reagents, and, given the knowledge of the structure, and, therefore, good indications of the binding sites of these agents, it can be stated confidently that these resonances correspond to histidines 62, 167 and 170. Peak 5a is not assigned as yet. Peaks similar to 3, 4 and 6 are also observed in the spectrum of horse PGK and they are also found to be influenced by addition of anions. Horse PGK has the identical three active site histidines.

Peak 12 is pH independent. Its size indicates that it represents two protons and its chemical shift suggests that it represents tryptophan, tyrosine or deprotonated histidine residues. The investigation in the following two chapters of the interaction of nucleotides, triose phosphates and other anions to yeast PGK show the sharper component of peak 12 is broadened or shifted by the same interactions that broaden or shift peak 3. This indicates that peak 12 represents the C4 proton of an active site histidine - the same histidine that is represented by peak 3.

Peaks 5, 8a, 9, 10 and 11 show pH dependence over the range studied corresponding to that expected of C4 protons of histidine residues as judged by the magnitude of their shifts with pH. Peak 5 appears to have a pK_a of about 8.1, approaching the pK_a value of peak 1. Furthermore, both peak 5 and peak 1 are located 0.25ppm downfield of the random coil histidine position (Bundi and Wüthrich, 1979), suggesting that they may be influenced by the same ring current shift. Examination of the effect of substrate and anion binding (see later) on the nmr spectrum confirms that peaks 1 and 5 are from the same residue. Thus peak 5 represents the C4 proton of histidine 123. A similar resonance is seen in the horse PGK spectrum and, by direct analogy, corresponds to his124 in the horse PGK sequence. Peak 8a shows a pK_a of 8.1, but it is not obviously a singlet belonging to a histidine. Peaks 9,10 and 11 display pH dependence (pK_a=7.1) typical of exposed histidines, together with C2 peaks 2a and b, they represent residues 52,

53 and 149. Anion binding studies in this work do, indeed, establish a link between peak 11 and peak 2. Only one C4 peak of this type is seen in the horse PGK spectrum and, as for the C-2 resonance, it apparently corresponds to residue 294 in the horse PGK sequence.

A summary of these assignments (which can not be absolutely certain) is given in table 4.1.

sequence	position	environment	assignment	
yeast	horse		C2	C4
52,53,149	(294)	exposed	2a,b	9,10,11
62,167,170	62,169,172	area of positive charge	3,4,6	12
123	124	aromatic basic, acidic influence	1	5
388	390	H-bond to glutamic acid	-	-

Table 4.1 The histidine residues of yeast PGK: assignment of peaks in the proton nmr spectrum. Equivalent (or similar) horse PGK residues are indicated.

resonance number	description	pH 5.9	6.4	7.0	7.6	8.6	9.1	9.8
100a						+	+	+
101	αCH			x	xx	xxx	xxx	xxx
102						+	++	+++
108/9	-							++
21						X, +.05	X, +.05	X, +.05
23	ε-lysine						-0.3	-.17
24					+.01	+.01	+.01	+.08
31a	-					x	x	xxx
33a	methyl					+	++	++
35					x	x	xx	xx

Table 4.2 The proton nmr spectrum of yeast PGK: pH dependence observed in the aliphatic region.

Symbols: X, broadening; +, increased intensity. Figures refer to changes in chemical shift. The use of these symbols is continued throughout the work.

The remainder of the aromatic region of the spectrum is as follows. A broad aromatic envelope centred about 7.2ppm represents the bulk of the 19 phenylalanine, 7 tyrosine and 2 tryptophan residues. Downfield of this envelope, as well as the histidine C-2 signals, broad resonances due to buried non-exchanging NH protons are observed.

On the upfield side of the region, several relatively well resolved peaks are noted: 14(a and b), 15(a,b,c, and d), 16, 17 and 18. They are all present in horse PGK. These aromatic resonances have been shifted upfield, probably by ring current effects of other nearby aromatic residues. It is recalled here that a highly conserved aromatic cluster surrounds his388 in the hinge region (figure 2d). Their relaxation behaviour will be investigated later. If any of these upfield peaks corresponds to this region it may well be influenced by opening or closing of the protein.

pH dependent behaviour is observed for peak 14a, which titrates with a pK_a of about 9.6, suggesting that it probably corresponds to a surface tyrosine residue. In a spectrophotometric/nitration study of the tyrosine residues of yeast PGK, Hjelmgren et al. (1976) found that one had a pK_a of about 9.3, while the remaining six had pK_a's of 11.0 or more. Selective nitration of the exposed tyrosine did <u>not</u> reduce the Km values for MgATP or for 3-PG, but it did reduce the enzyme activity considerably. The most exposed tyrosine of the yeast PGK structure is tyr193 and the evidence suggests that this is the one located by selective nitration and represented by peak 14a of the nmr spectrum.

Tyr 193 is located in helix V, close to his388 in the hinge region of the protein (see figures 4.1 and 4.6).

In the aliphatic region, only limited areas of the spectrum reveal pH dependence. At higher pH values, some rearrangement is observed among the αCHs and part of the methyl peak appears to shift downfield at about pH9. Various shifts and broadenings are observed among the lysine ε-CH_2 peaks, 21,23 and 24, as the lysine pK_a is approached. These and other pH dependencies in the aliphatic region are summarised in table 4.2. It is remarkable that no well-defined pK_a effects are seen opposite to the histidine titrations, but the structure indicates that the histidines tend to be isolated from hydrophobic groups.

Three sharp peaks, 26, 27 and 28, are noted around 2.0ppm. The long T_2 values of these signals, confirmed in subsequent relaxation studies, and their chemical shift position strongly suggest that they represent the methyl resonances of methionine residues. The location of the three methionine residues of yeast PGK is as follows. Met 173 is found above the positively charged face of the N-terminal domain, semi-exposed in a deep cleft; met 237 lies close to the position of the adenine moiety of bound nucleotide, buried rather than exposed on the surface, and met 267 is found close to both met 237 and bound nucleotide, but is in a much more exposed situation. In nmr spectra, peak 17 is consistently seen as the sharpest of the three, and it seems reasonable to assign it to the most exposed methionine, met 267.

Upfield shifted methyl resonances are observed in both the yeast and the horse PGK spectra. Three peaks are clearly seen around +0.2ppm (numbered 37-39 in the yeast spectrum) and another three much broader peaks are seen around -0.4ppm (40-42). These shifted resonances must be associated with ring current shifts in regions of conserved secondary structure, and the nucleotide binding studies of the next chapter links them with the upfield shifted resonances of the aromatic region.

After the completion of this work a pre-print was received of a photo-CIDNP nmr study of yeast and horse PGK by Scheffler and Cohn (1986). As in the present work, their numbering system for the yeast PGK resonances is based on that introduced by Tanswell et al. (1976) and they confirmed that peaks 2a, 2b, 10 and 11 represent exposed histidine residues. On the basis of differences in intensity of the CIDNP spectra, peaks 2b and 11 were assigned to the most exposed his53 residue and peaks 2a and 10, tentatively, to his149 ("his151" after the convention of Perkins et al., 1983). Resonances corresponding to peaks 7a and 8b of the present thesis were assigned to trp308 (see figure 4.1), as was a small peak at 6.84ppm. Apart from trp308, there is only one other tryptophan residue in yeast PGK, trp333, and it is completely buried; and so the location of three tyrptophan resonances, including the furthest downfield C4 resonance, helps to confirm the present assignment, to histidine residues, or resonances 3, 4 and 6. Two emission signals at 6.73 and 7.31ppm (pH7.0) confirmed that peak 14a

represents a tyrosine residue and indicated that a component of peak 8 represents another one. The investigation of horse PGK identified two pairs of histidine residues. One corresponds to peaks 2 and 11 of the yeast spectrum and was assigned to the exposed his294 as given in this thesis, (Table 4.1). The other did not correspond to any of the yeast signals and was tentatively assigned to his172. This is not obviously related to our data (Table 4.1). No other histidine residues were observed, at least not in the absence of substrates. Finally, peaks corresponding to 7 and 8b of the yeast spectrum were observed and were assigned to trp308. In most respects these data are in full agreement both with the data of Tanswell et al. (1976) and with those reported in this thesis.

4.3.2 T_2 relaxation studies

The first relaxation study used the Hahn echo pulse sequence described above in the materials and methods section. For low values of T the following effects are observed.

At T=5msec, there is no loss of intensity in the spectrum. At T=10msec, the bulk of the broad CH_2/CH aliphatic signal, but not the individual peaks, from 2.5 to 1.0ppm, diminishes by 10%. At T=20msec it has dropped by half while the bulk of the broad aromatic envelope has fallen by 40%. At T=30msec, the two areas have fallen to a third of their original values and, finally, at T=40msec the bulk has gone and only the individual peaks remain. Thus it is seen

that the peaks of the nmr spectrum represent surface residues of relatively high mobility and long relaxation time while the broad mass of the spectrum, which accounts for 90% of the total spectral intensity, represents the core of the protein and particularly of the two lobes.

The upfield shifted methyl peaks are very broad, even at T=0msec and are no longer visible at T=20msec. The upfield aromatic signals, on the other hand, remain visible up to T=40msec. Thus, while the relaxation rate of these residues is not as long as those of the surface or active site histidines whose signals persist at higher T values, they are longer than those of the majority of the protein. This intermediate relaxation rate is indicative of a region of high mobility in the protein and provides further evidence that resonances 14 to 18 relate to the hinge region of the protein.

At higher values of T, individual peaks only are observed, and the spectra recorded as T increases from 40 to 160msec are shown in figure 4.12. The reference, TMS, is a small molecule with a long relaxation time and its peak height is used as an internal standard. The relative peak height is calculated by dividing the actual peak height by that of the standard, and multiplying the result by ten. These values are recorded in table 4.3.

As has been previously observed, (Campbell et al., 1975) C2 and C4 proton resonances of histidines exposed to solvent have particularly long relaxation times. At the selective value of T 120msec, resonances 1 and 5 are evident, as are

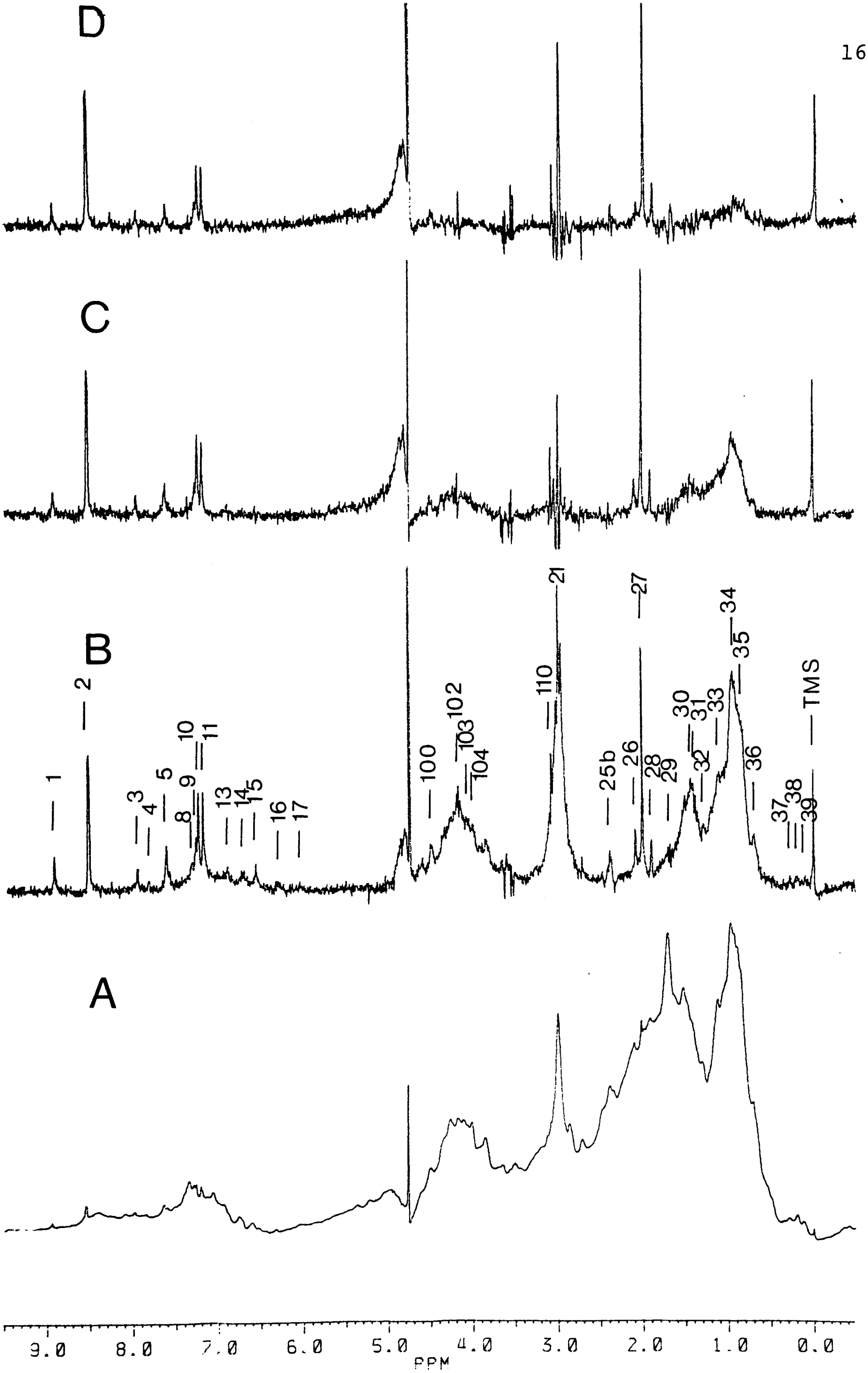

Figure 4.12 Relaxation study of yeast PGK (at 500MHz). 2mM PGK, TMS present. (A) normal nmr spectrum; (B) Hahn echo experiments, T values (msec): (B) 40; (C) 60; (D) 80; (E) 100; (F) 120; (G) 140; (H) 160.

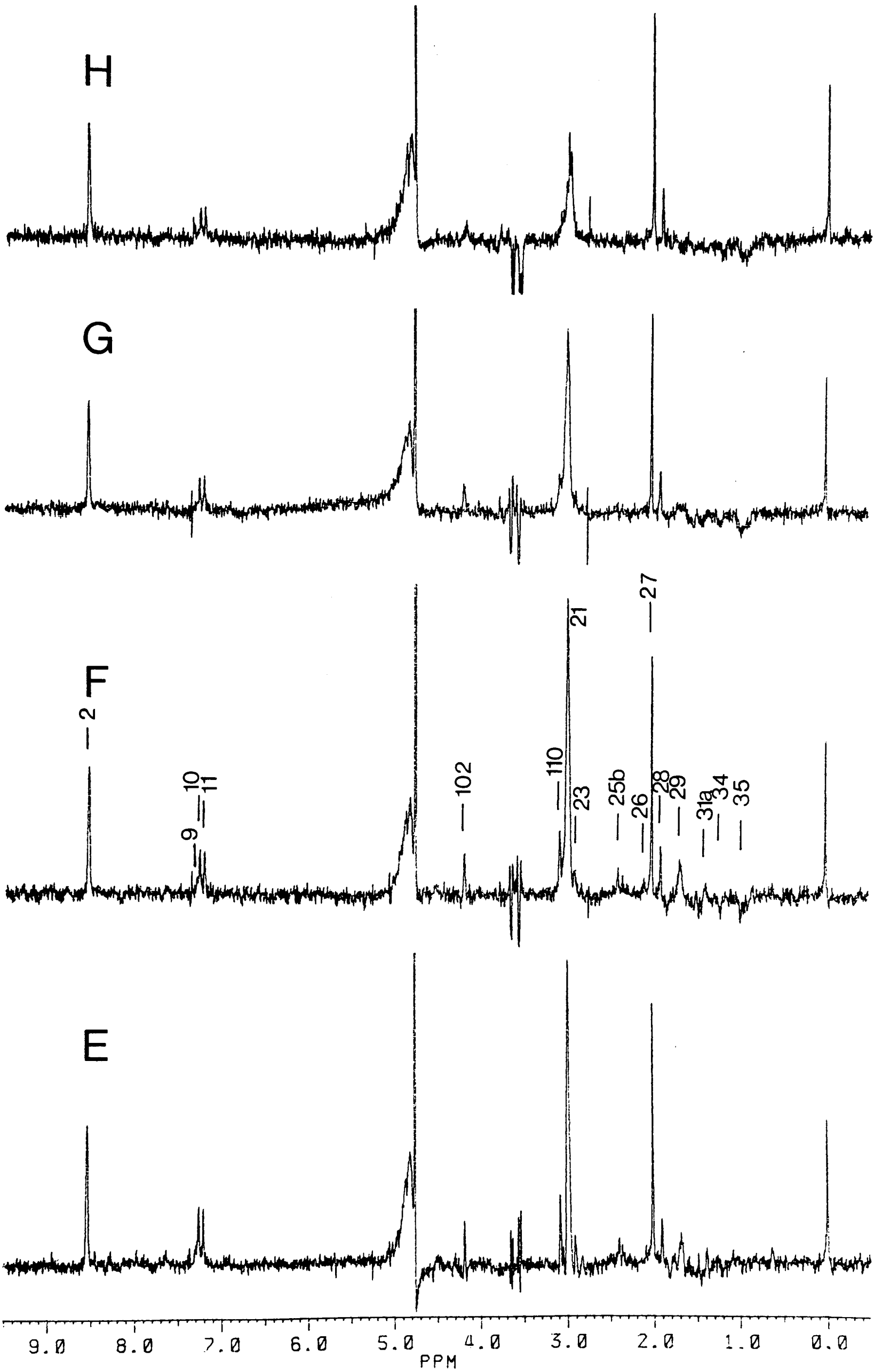
H
G
F
E
2
9
10
11
102
110
21
23
25b
26
27
28
29
31a
34
35
9.0
8.0
7.0
6.0
5.0
4.0
3.0
2.0
1.0
0.0
PPM

Table 4.3 T_2 relaxation study of yeast PGK.
Relative peak heights are shown against T for the Hahn echo experiment. Multiplicity was determined by CPMG/Hahn echo difference spectroscopy.

AROMATIC RESONANCE

ADDITION	1	5		3	4	6	12		2	9	10	11		7	8	13			14	15	16	17	18					
40 msec	3.0	3.6		2.0	0.8	1.3			10.8	3.8	6.7	6.7			1.8	1.2			0.8	1.5	0.6							
60 "	1.9	3.0		1.6	0.7	0.8			11.1	2.8	6.3	5.5			0.9					0.9								
80 "	1.8	2.1		1.1					10.0	1.8	4.5	4.5																
100 "	1.0	1.0		0.8					10.0	1.5	3.8	3.8																
120 "	0.5								8.1	0.9	2.8	2.8																
140 "									7.7	0.8	2.6	2.7																
160 "									7.2	0.5	1.8	2.0																
multiplicity									odd	odd	odd	odd																

ALIPHATIC RESONANCE

ADDITION	100	102	110		21	22	23		24	25b		26	27	28		29	30	31	31a	32a		33	34	35	36	37	38	39
40 msec	1.8	5.2	10.0		22.9		2.9			3.2		3.7	18.3	2.9		2.7	7.7		6.5	4.2		8.3	16.3	13.1	3.7	0.4	0.4	0.5
60 "	1.1	3.5	6.6		13.8		2.2			2.9		2.1	18.0	2.8		2.3	2.5		3.0				5.6	5.4				
80 "	1.1	3.7	6.9		19.1		2.5			2.6		1.1	15.9	3.0		2.8	0.9		2.1				1.4	1.6				
100 "		3.5	5.0		19.1		2.2			2.2		0.9	17.5	2.8		2.8			1.5				-1.1	-0.6				
120 "		2.8	3.8		19.5		1.7			1.7			15.1	3.2		2.6			0.9				-1.0	-1.3				
140 "		2.3	2.9		13.5		1.7						14.9	3.1		1.7							-1.1	-1.3				
160 "		1.8	2.3		8.1		1.4						14.1	3.4														
multiplicity		odd	odd		odd					odd		odd	odd	odd		odd/even	even		even	even			odd/even	odd/even				

peaks 2(a) and (b) and peaks 9, 10 and 11. These histidine peaks are confirmed as surface histidines.

In the aliphatic region, peaks 110, 21 and 23 are observed at around 3.0ppm and they could well correspond to ε-CH_2 groups of lysines with particularly long T_2 values, as observed in the lysozyme spectrum (Campbell et al., 1975). A comparison of the intensity with peak 2 indicates that peaks 110 and 21 represent at least $3CH_2$ groups. Resonances 27 and 28, and to a lesser extent 26, appear as sharp singlet-type peaks and, together with their chemical shift values, this suggests that they represent methyl resonances of the three PGK methionine residues. Peak 27, the sharpest, is assigned to met267, the most exposed methionine peak 28 to the semi-exposed met173 and peak 26 to the buried met237. Further peaks observed of odd multiplicity include the αCH peak 102, which may be a singlet glycine resonance, and broader peaks 29 and 31, which are in the CH_2 region of the spectrum. Negative peaks, associated with signals of even multiplicity, appear at positions 34/35, corresponding to methyl groups of leucine, isoleucine and valine; at position 32a, corresponding to a threonine or alanine methyl group; and at position 30. The two sharp negative peaks at 3.6ppm are attributed to an impurity.

For the Hahn echo sequence, as T increases resonances decay exponentially with a time constant equivalent to their T_2 relaxation time. Therefore, in order to classify the observed peaks on the basis of T_2 values, the relative peak heights, of table 4.3 , have been expressed as natural

logarithms and plotted against T, in figure 4.13(i)-(iii). For each resonance, the reciprocal of the slope is equivalent to its T_2 value.

Of the aromatic resonances (figure 4.13.(i)), resonance 2 and resonances 9, 10 and 11 have the longest T_2 values, of 250 and 80msec respectively, consistent with their previous assignment to exposed, surface histidine; resonance 3, which previous evidence located in the cleft of the protein, but still at its surface, has a T_2 value of 60msec, and resonances 1 and 5, assigned to the partly exposed residue 123, have the shortest T_2 value, of 40msec. These results can be compared with T_2 relaxation work with horse PGK which showed resonances equivalent to yeast PGK peaks 2 and 10 to have T_2 values of 80 and 50msec respectively; a resonance equivalent to peak 3 to have a T_2 value of 10msec, and one equivalent to peak 1 to have a T_2 value of 40msec. All these observations are fully consistent with the assignments in Table 1a.

The decay of the aliphatic peaks with T is shown in parts (ii) and (iii) of figure 4.13. The longest relaxation times are seen to be those of the surface methionine resonances 27 and 28 ($\geq$400msec), and of resonance 29. The third methionine resonance, peak 26, has the comparatively short T_2 value of 30msec, which suggests that it corresponds to the most buried of the three methionine residues, met237. Long relaxation times are observed for the lysine ε-CH_2 resonances, peaks 110, 21 and 23 which are found to have T_2 values of 90, 180 and 170msecs respectively. The T_2 value for methyl peaks 34 and 35 is calculated as 20msecs.

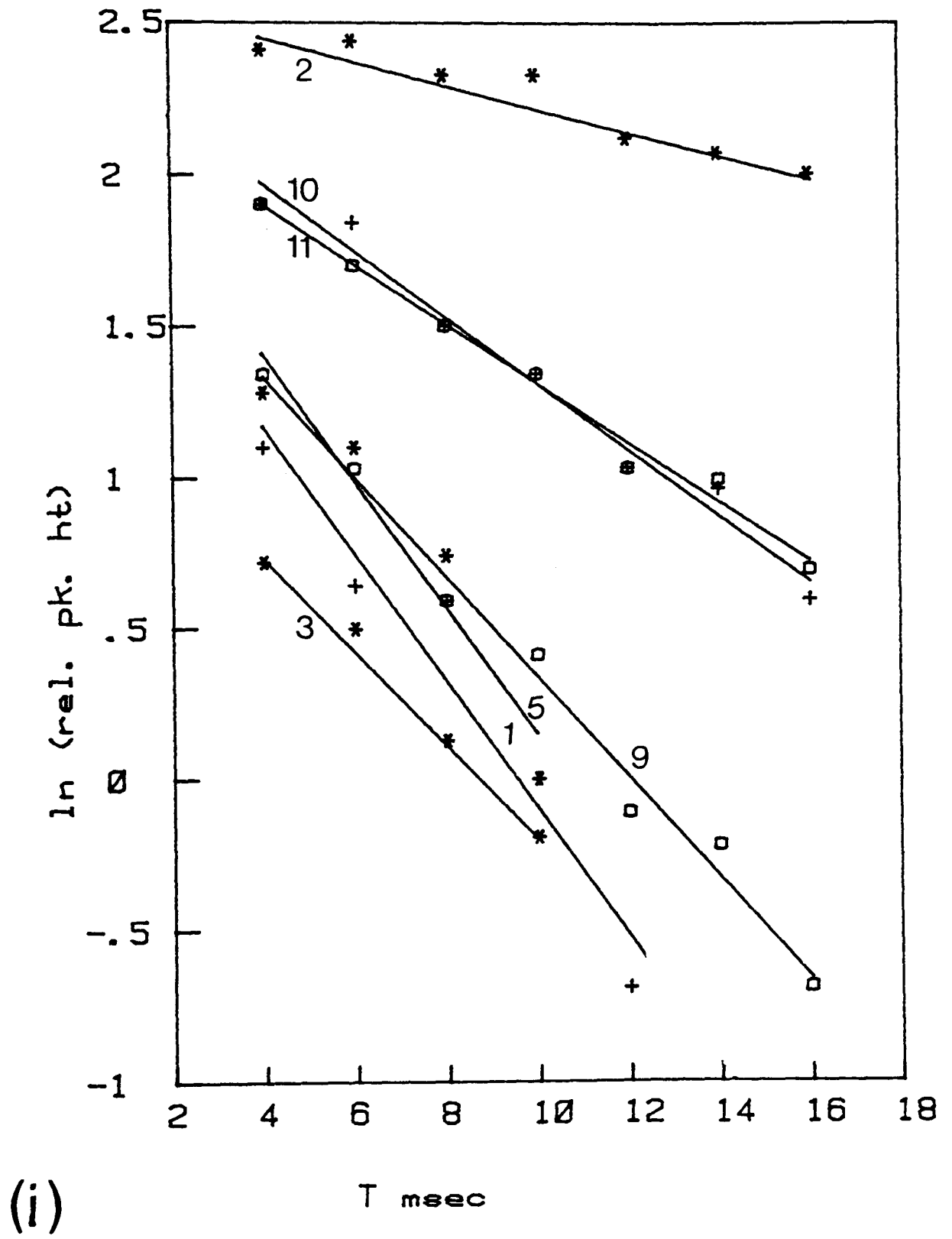

(i)

Figure 4.13 Hahn echo sequence of yeast PGK spectrum: ln (relative peak height) against T(msec). (i) aromatic, (ii) aliphatic, (iii) aliphatic.

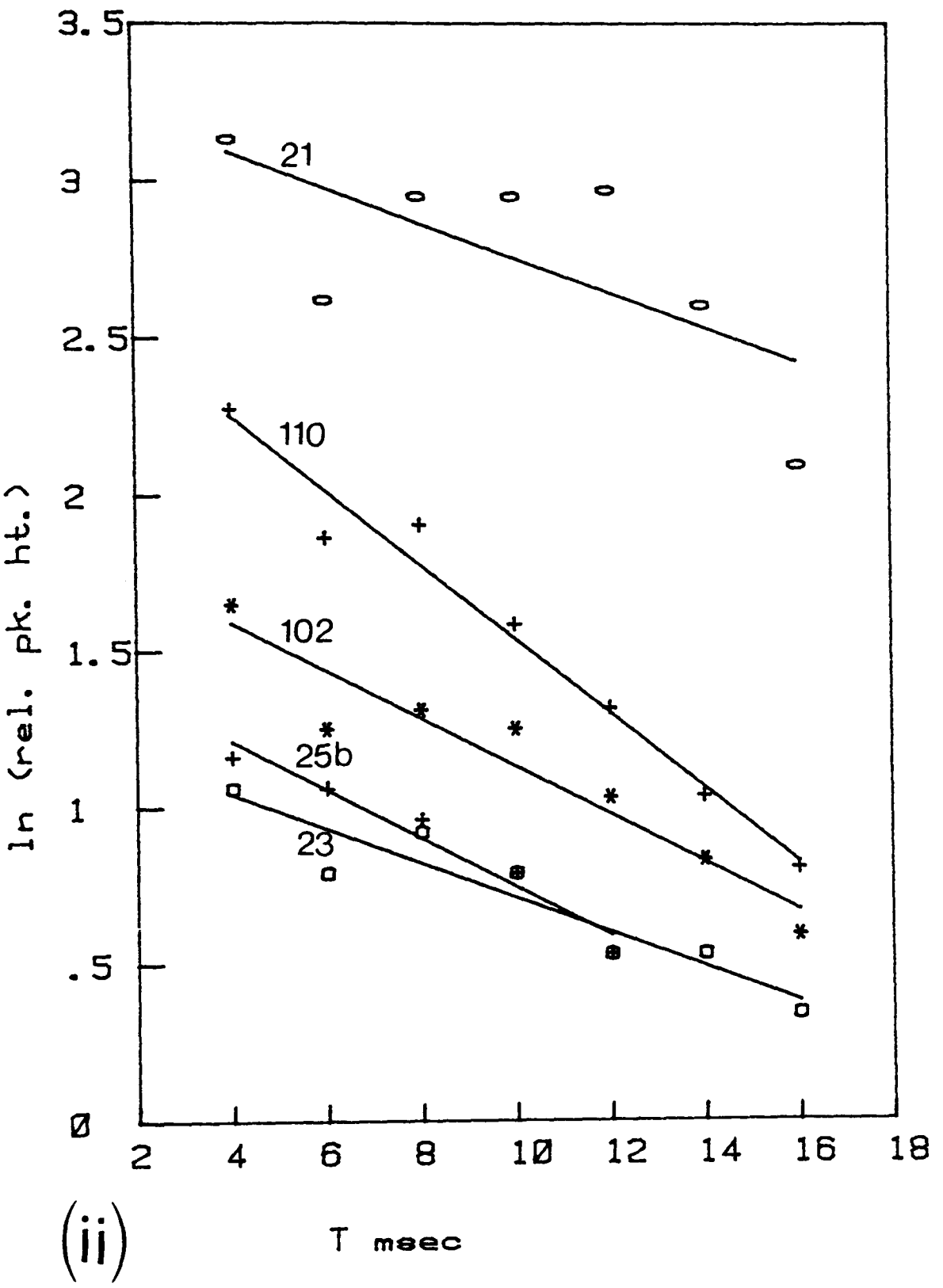
3.5
3
2.5
2
1.5
1
.5
Ø
ln (rel. pk. ht.)
21
110
102
25b
23
2
4
6
8
10
12
14
16
18
T msec

(ii)

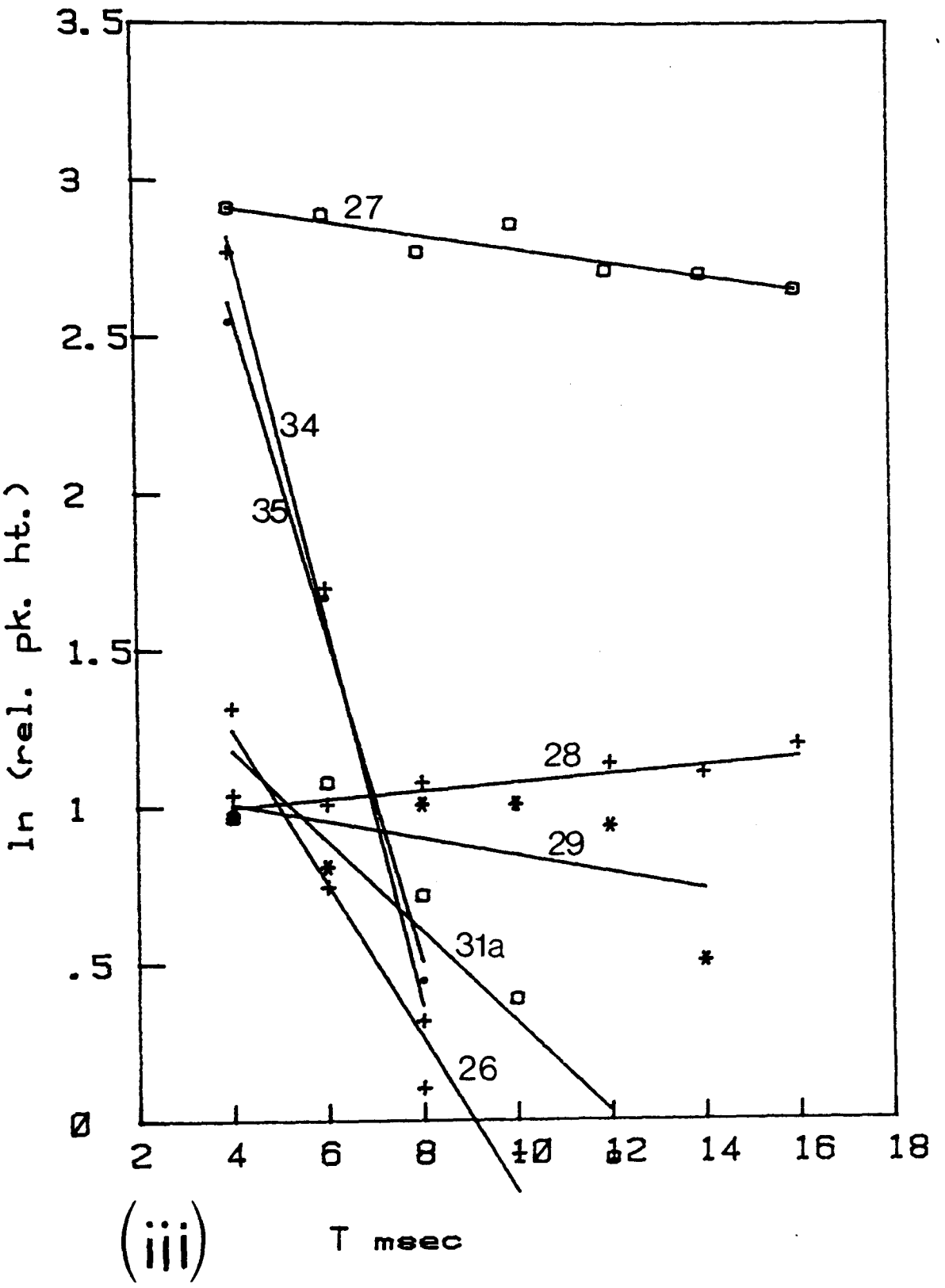
3.5
3
2.5
2
1.5
1
.5
0
ln (rel. pk. ht.)
27
34
35
28
29
31a
26
2
4
6
8
10
12
14
16
18
T msec

(iii)

The second part of the relaxation studies involved the CPMG pulse sequence detailed in Materials and Methods. The most selective value for T was found to be 120msec, and the Hahn echo and CPMG spectra obtained at this value, together with the difference spectra showing multiplet selection are given in figure 4.14. Part (C) of the figure shows the resonances of even multiplicity, mainly doublets, while part (D) shows singlets and triplets, resonances of odd multiplicity. The peaks in the aromatic region assigned to histidines are confirmed as singlets, but a doublet contribution is noted in the aromatic envelope. In the aliphatic region, the αCH resonance 102, the ε-lysine resonances triplets and the methionine singlet resonances are confirmed as odd multiplets. Peak 29 is seen to have a significant doublet component; peaks 30, 31a, 32a, and 33a are essentially of even multiplicity and could be associated with surface alanine or threonine methyl groups, and the peak 34/35 is predominantly of even multiplicity as expected for a leucine/isoleucine/valine methyl resonance. These findings are summarised in the bottom line of table 4.3 .

Finally, Hahn echo, CPMG and difference spectra with T=120msec, were obtained for yeast PGK in presence of equimolar adenosine tetraphosphate, A4P. Evidence presented in subsequent chapters indicates that interaction with this nucleotide causes a significant conformational change in the protein. Here, the effect of the presence of A4P on the doublet (subtraction) spectrum (figure 4.15) and on the singlet and triplet (addition) spectrum (figure 4.16) is

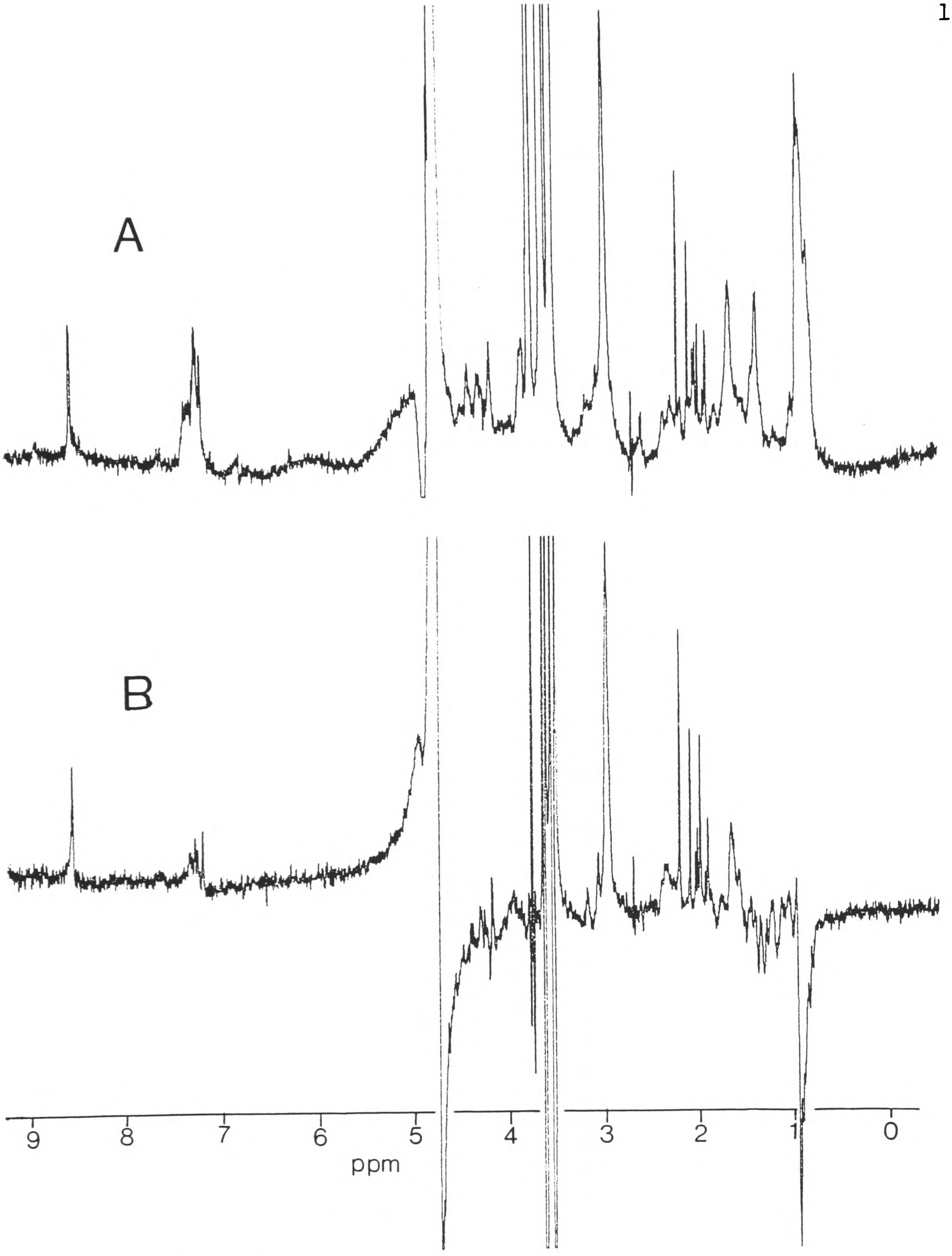

Figure 4.14 Multiplet selection spectra of yeast PGK. 2mM PGK, TMS present, T=120msec.

(A) Spectrum obtained with CPMG sequence

(B) Spectrum obtained with Hahn echo sequence

(C) Spectrum (A) minus spectrum (B), showing doublets

(D) Spectrum (A) plus spectrum (B), showing singlets and triplets.

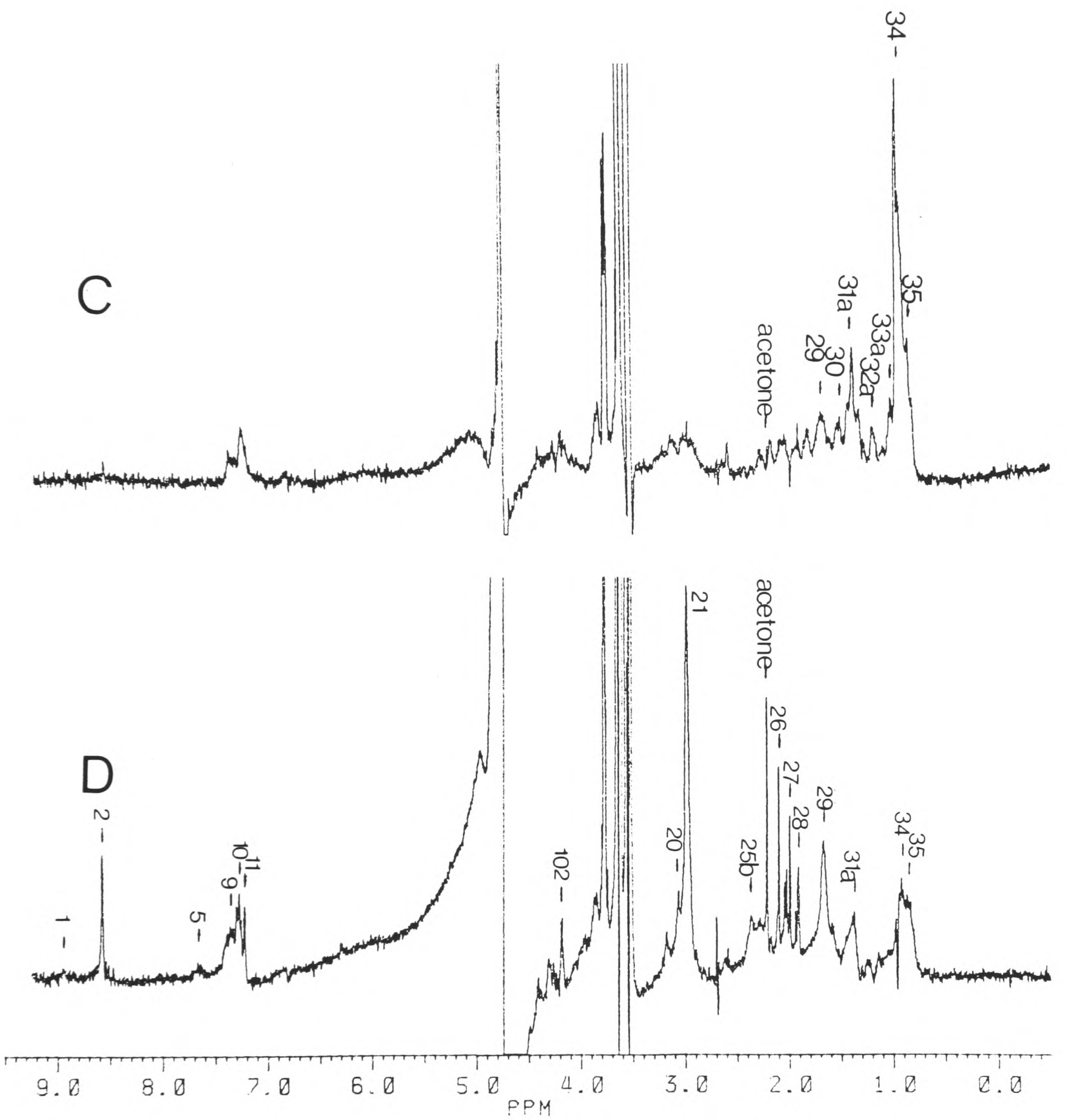
C
34
35
33a
32a
31a
30
29
acetone
D
2
1
5
10
11
9
102
21
20
25b
26
27
28
29
31a
34
35
acetone
9.0
8.0
7.0
6.0
5.0
4.0
3.0
2.0
1.0
0.0
PPM

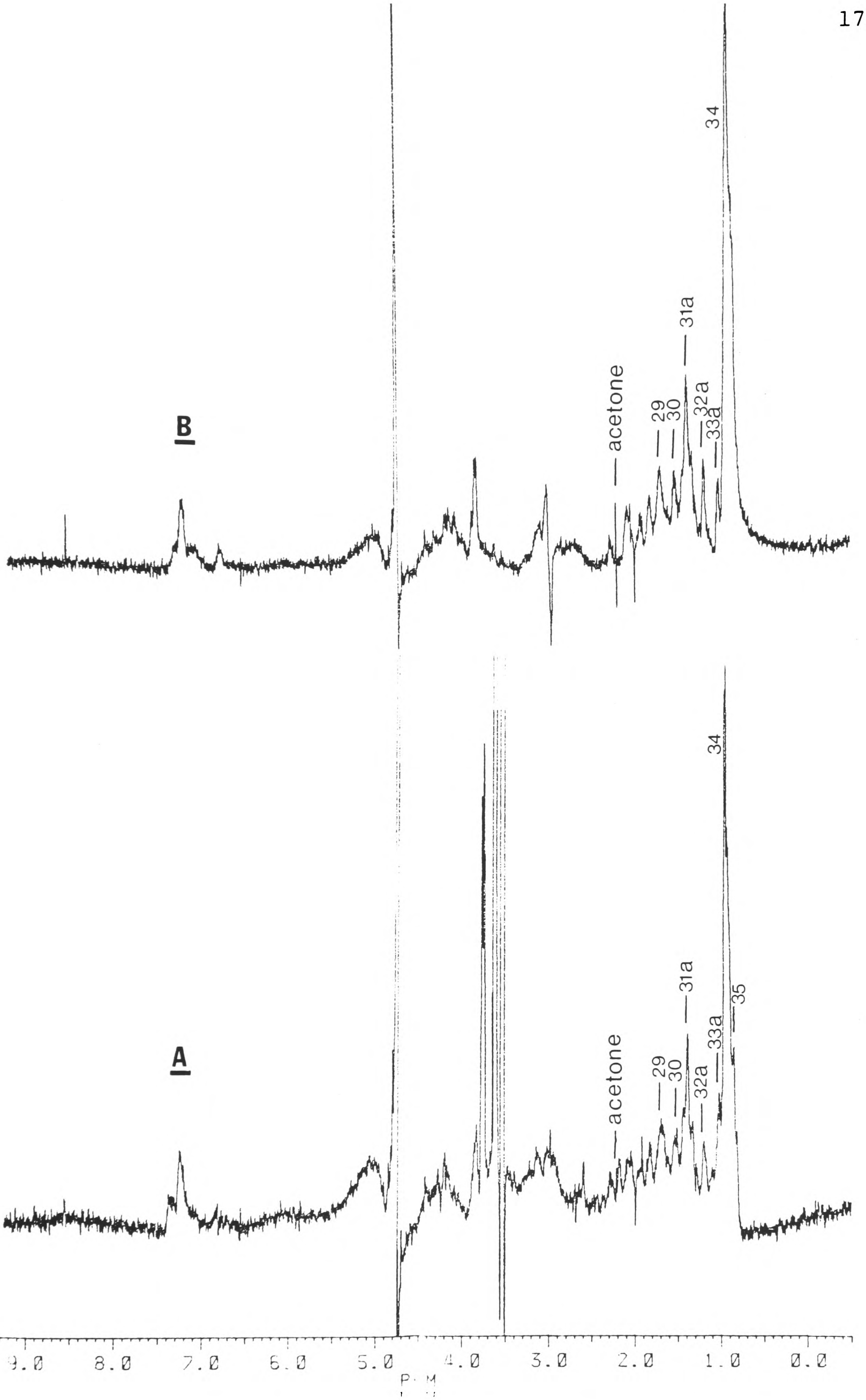

Figure 4.15 Multiplet selection spectra, showing doublets. (A) 1mM PGK; (B) as (A), with 1mM A4P.

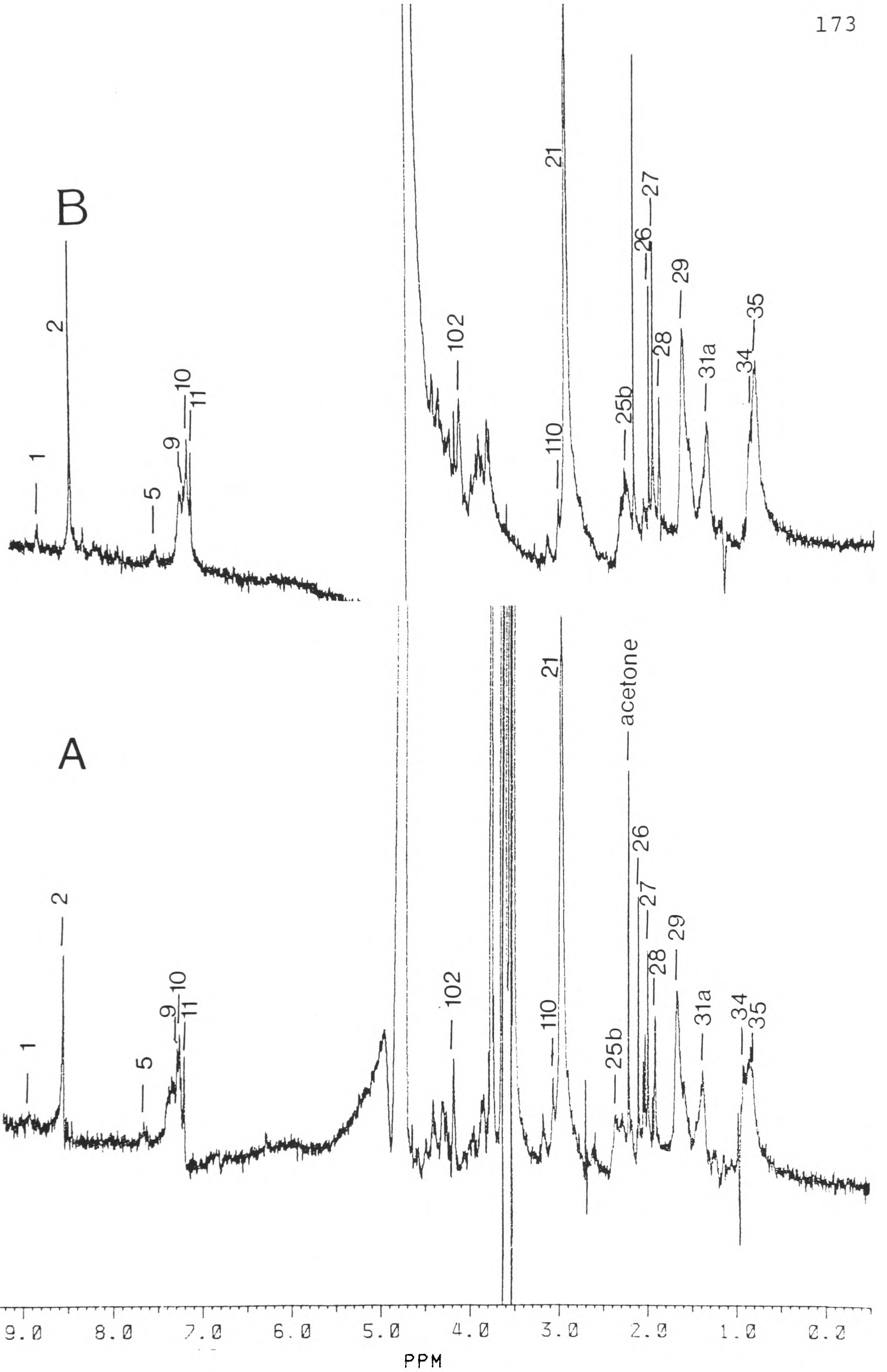

Figure 4.16 Multiplet selection spectra, showing singlets and triplets.

(A) 1mM PGK; (B) as (A), with 1mM A4P.

examined. In the former, the nucleotide has the effect of removing peak 35, while in the latter, peak 35 is increased, but apart from this slight rearrangement of the methyl peak, interaction with A4P has little effect on the spectra. This demonstrates that while A4P produces changes in the spectrum compatible with conformational changes in the protein, it has very little effect on the resonances of longer T_2 relaxation times, that is on those resonances associated with the surface of the protein.

Summary

The relaxation data confirm the results of the analysis of the pH dependence of the spectrum. They show too that there is a large part of the protein which has a very short relaxation time. This is the bulk of the interior of the two lobes and includes the ring current shifted methyls as expected. There is also a zone of intermediate relaxation time associated with the moderately resolved peaks, numbers 14-18. It is immediately likely that this is the region between the two lobes i.e. the hinge region.

Chapter 4 References

Banks, R.D., Blake, C.C.F., Evans, P.R., Haser, R., Rice, D.W., Hardy, G.W., Merrett, M. and Phillips, A.W. (1979) Nature, 279, 773-777.

Bundi, A. and Wüthrich, K. (1979) Biopolymers, 18, 285-297.

Campbell, I.D., Dobson, C.M., Williams, R.J.P. and Wright, P.E. (1975) FEBS Lett., 57, 1, 96-99.

Delepierre, M. (1983) Personal communication, Université René Descartes, 4, Avenue de l'Observatoire, Paris.

Fifis, T. and Scopes, R.K. (1978) Biochem.J., 175, 311-319.

Fujii, H. and Yoshida, A. (1980) Proc.Natl.Acad.Sci. USA, 77, 9, 5461-5465.

Hjelmgren, T., Arvidsson, L. and Larsson-Raźnikiewicz, M. (1976) Biochim.Biophys.Acta, 445, 342-349.

Littlechild, J., Rohll, J., and Watson, H.C. (1986) Personal communication, University of Bristol.

Osinga, K.A., Swinkels, B.W., Gibson, W.C., Borst, P., Veeneman, G.H., Van Boom, J.H., Michels, P.A.M. and Opperdoes, F.R. (1985) EMBO J., 4, 13B, 3811-3817.

Perkins, R.E., Conroy, S.C., Dunbar, B., Fothergill, L.A., Tuite, M.F., Dobson, M.J., Kingsman, S.M. and Kingsman, A.J. (1983) Biochem.J. 211, 199-218.

Pickover, C.A., McKay, D.B., Engelman, D.M. and Steitz, T.A. (1979) J.Biol.Chem., 254, 11323-9.

Rice, D.W. and Blake, C.C.F. (1984) J.Mol.Biol. 175, 219-223.

Roustan, C., Fattoum, A., Jeanneau, R. and Pradel, L-A. (1980) Biochemistry, 19, 5168-5175.

Scheffler, J.E. and Cohn, M. (1986) Biochemistry, 25, 3788-3796.

Scopes, R.K. (1978a) Eur.J.Biochem., 85, 503-516.

Scopes, R.K. (1978b) Eur.J.Biochem., 91, 119-129.

Tanswell, P., Westhead, E.W. and Williams, R.J.P. (1976) Eur.J.Biochem., 63, 249-262.

Watson, H.C., Walker, N.P.C., Shaw, P.J., Bryant, T.N., Wendell, P.L., Fothergill, L.A., Perkins, R.E., Conroy, S.C., Dobson, M.J., Tuite, M.F., Kingsman, A.J. and Kingsman, S.M. (1982) EMBO J., 1, 12, 1635-40.

Wrobel, J.A. and Stinson, R.A. (1978) Eur.J.Biochem., 85, 345-350.

CHAPTER 5.

INTERACTION OF PGK WITH NUCLEOTIDE SUBSTRATES

Chapter 5 Contents

5.1. INTRODUCTION

The primary, catalytic nucleotide binding site of yeast PGK has been determined by X-ray crystallographic studies (Banks et al., 1979; Watson et al., 1982) and is described fully in the previous chapter, and in figure 5.1. Electrostatic interactions are identified between the ribose ring, the phosphate chain, the divalent metal ion and the protein but various investigations show that the nucleotide binds principally through the anchoring of the adenine moiety in the hydrophobic cleft. Thus, comparative studies (Krietsch and Bücher, 1970; Roustan et al, 1973) of nucleotide binding show a specificity for nucleotides with purine bases and demonstrate the hydrophobicity of the binding site spectrophotometrically. In addition, fluorimetric work (Wiksell and Larsson-Raźnikiewicz, 1982) with 1-anilino-8-naphthalenesulphonate confirms the existence of a strongly hydrophobic site. Thiol reactivity studies (Tompa et al., 1986) with pig muscle PGK quantify the interaction of adenosine and enzyme (Kd = 1.0mM, I = 0.1M) but also reveal conformational changes brought about by interaction with MgAMP, MgATP and especially MgADP, which are not occasioned by interaction with adenosine. Finally, early crystallographic work (Bryant et al., 1974) demonstrates the location of adenosine at the binding site and examination of the effect of adenosine on the proton nmr spectrum (Tanswell, 1976) shows that peaks 8, 12 and 13, which are only some of those broadened and shifted by interaction with the nucleotide substrate, were also broadened and shifted by adenosine on its own.

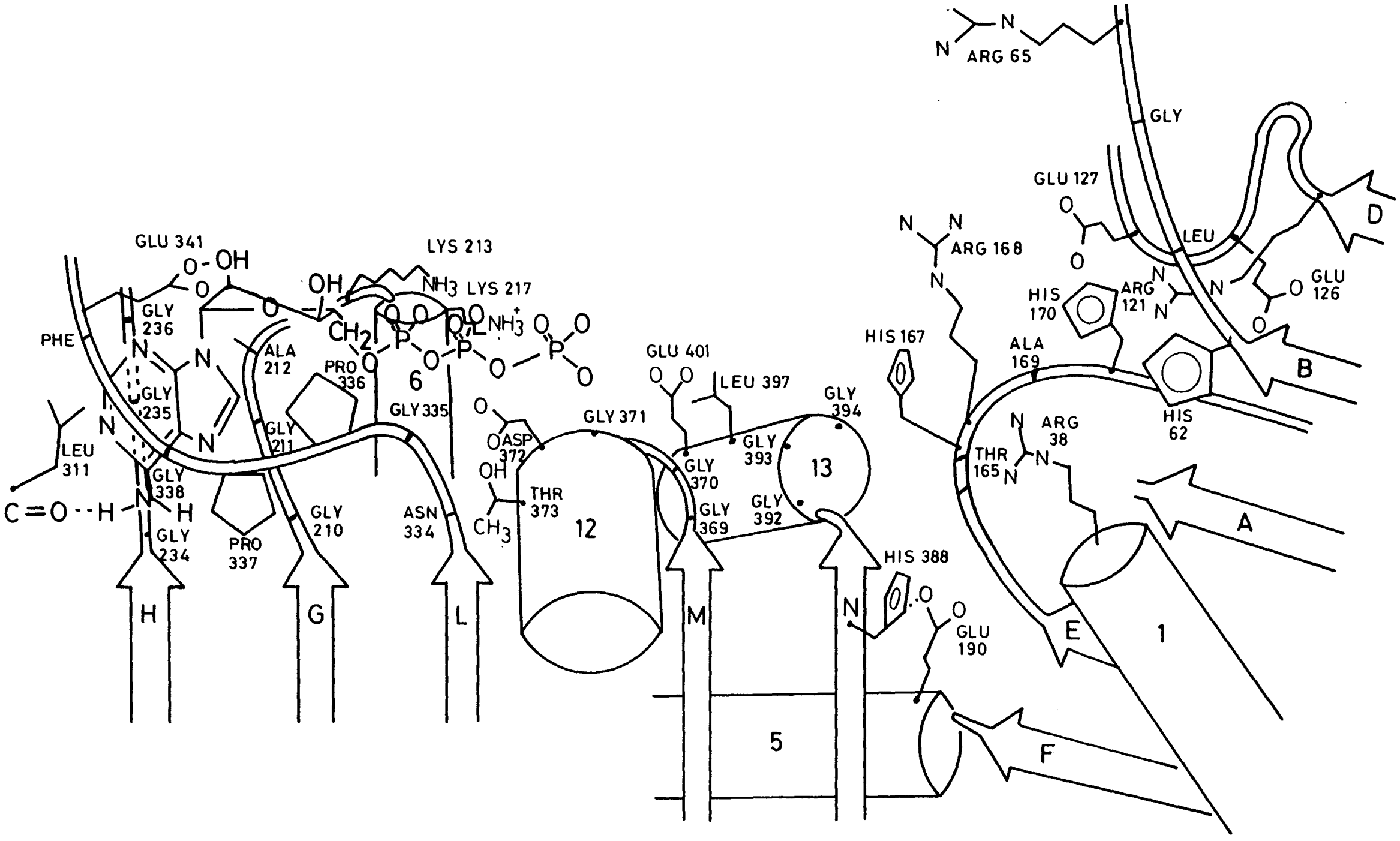

Fig.5.1 Schematic drawing of the active site of yeast PGK, with ATP bound

The strength of nucleotide binding has been calculated from the gel filtration (Scopes 1978b) data and from the thiol reactivity (Tompa et al, 1986) data, giving Kd values of about 50μM and 150μM (I = 150mM) for MgADP and MgATP respectively.

Interaction at a second site, up to fifty fold weaker than at the primary site is revealed in the gel filtration study. Product inhibition studies (Schierbeck and Larsson-Raźnikiewicz, 1979) confirm the existence of a low affinity site and suggest a regulatory role, possibly involving the removal of 1,3-P_2G. As yet, it is not clear whether the second site is located in the protein cleft, near the primary sites and the hinge region, or if it is found elsewhere on the surface of the protein. The nature of binding at this site is also unclear. The spectrophotometric study (Roustan et al., 1973) indicates that the hydrophobic interaction between the protein and the adenine ring occurs only at the active site, which suggests that binding at a second site is predominantly electrostatic, presumably involving the phosphate groups. In the next chapter it will be shown that indeed simple polyphosphate binds to this active site region.

In the present work proton nmr is used to monitor the interaction of PGK with the nucleotide and phosphate chain components of ATP, with both the substrate nucleotides, and with the substrate analogue, MgAMPPNP. The line broadening reagent Gd^{3+}, which displaces Mg^{2+} from the nucleotide complex, is used to probe the area of interaction. As a preliminary experiment, the interaction of the protein with Gd^{3+} on its own is investigated.

5.2 RESULTS AND DISCUSSION

5.2.1 Interaction with the cationic probe, Gd^{3+}

In this preliminary experiment, 70μM $GdCl_3$ was added to a 1.3mM sample of PGK, buffered at pH7.0 with 20mM Tris. The effects on the protein spectrum are illustrated by figure 5.2 summarised in table 5.1, and are as follows.

Resonances 1 and 5, assigned to his 123 and peaks 2,9,10 and 11, collectively assigned to his 52, 53 and 149, are considerably broadened, and with the exception of peak 2, are no longer visible. This indicates that Gd^{3+} is dispersed over the surface of the protein (see table 5.2 and figure 5.3). Peaks which are assigned to surface residues because of their comparatively long relaxation times and which are also broadened are the methionine peaks, 26, 27 and 28 and peaks 25b and 29. In addition, slight broadening is observed at peaks 25a and 30, and in the aromatic region, at peaks 4, 5a, 8a, 8b and 15b. Apart from the slight broadening of peak 4, there is no evidence of interaction at the active site.

5.2.2 Interaction with adenosine and adenosine plus tripolyphosphate.

A 25mM solution of adenosine, buffered at pH5.8 with 100mM sodium d_3-acetate, was added to a 1.35mM solution of yeast PGK, similarly buffered, to give nucleoside:enzyme ratios of 1:1 and 5:1. Using the adenosine/PGK dissociation constant of 1.0mM, determined by Tompa et al (1986), it is calculated that in the equimolar mixture about 40% of the total enzyme present interacts with 40% of the total adenosine present, and that with a 5:1 excess of adenosine, 85% of the enzyme interacts with 17% of the total nucleoside.

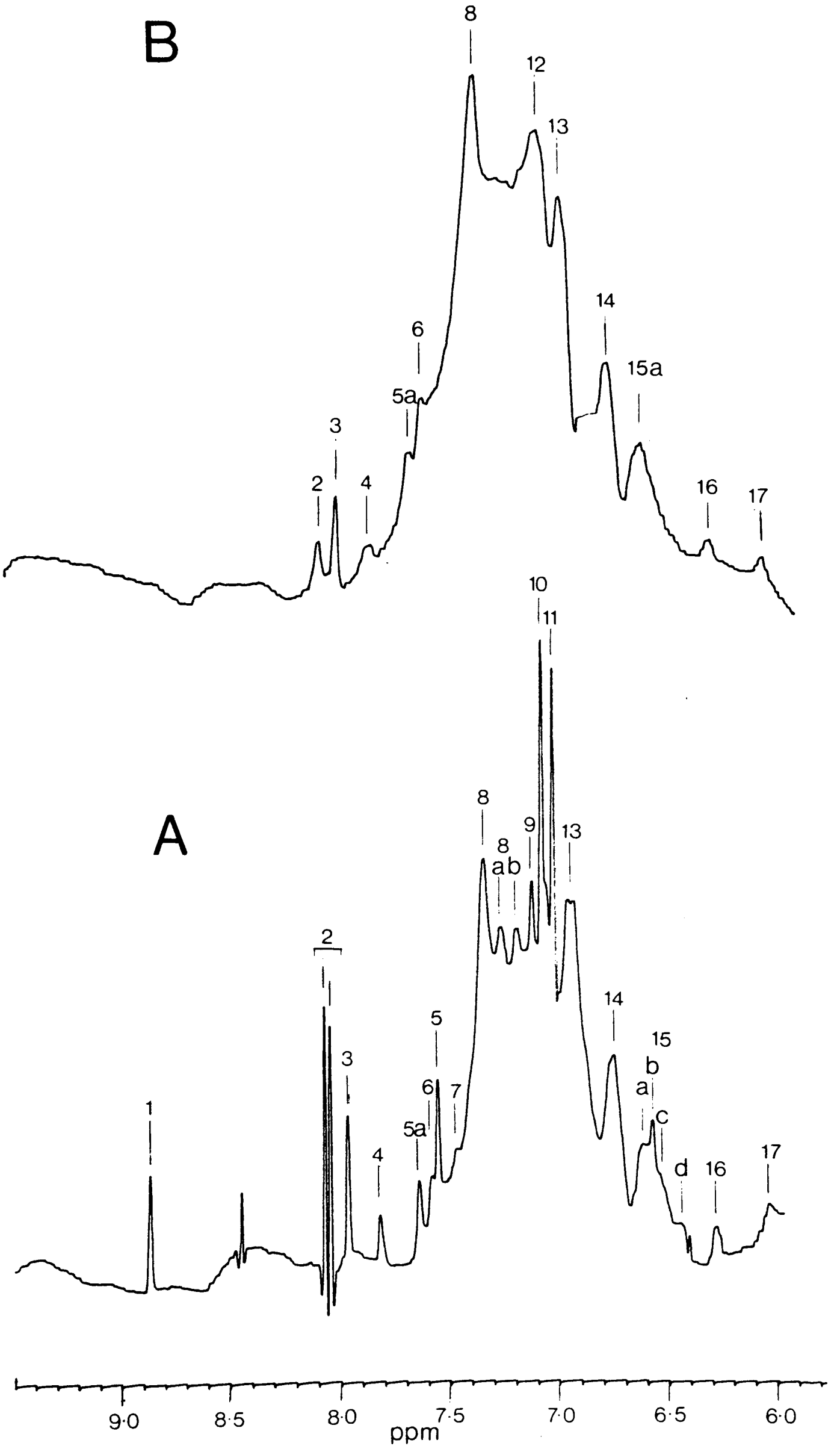

Fig.5.2 The effect of Gd^{3+} on the aromatic region of te 300MHz spectrum of yeast PGK.

(A) 1.3mM PGK, pH7.0;

(B) as (A) plus 70μM $GdCl_3$.

Table 5.1 The effect of the addition of $GdCl_3$ on the 300MHz spectrum of a 1.3mM solution of PGK. Key: broadening: (x) slight; (xx) conisderable; (xxx) complete. Figures refer to change in chemical shift.

AROMATIC RESONANCE

ADDITION	1	5		3	4	6	12		2	9	10	11		5a	8	8a	8b			13	14	15a	b	16	17			
70 M Gd^{3+}	xxx	xxx			x				xx	xxx	xx	xx		x		xx	xx						xx					

ALIPHATIC RESONANCE

ADDITION	21	23	24		25a	b		26	27	28		29	30	31	32	33	34	35	36		38							
70 M Gd^{3+}					x	xx		xx	xxx	xx		xx	x					-.02										

Table 5.2 Nmr resonances assigned to histidine and methionine residues of yeast PGK. The methionine assignments are not confirmed.

type	position	environment	resonance			
			C2	2a,b	C4	9,10,11
histidine	52,53,149	exposed				
	62,167,170	area of positive charge		3,4,6		12
	123	aromatic, basic, acidic		1		5
	388	H-bond to glutamic acid		-		-
methionine	173	semi-exposed		28		
	237	buried		26		
	267	exposed		27		

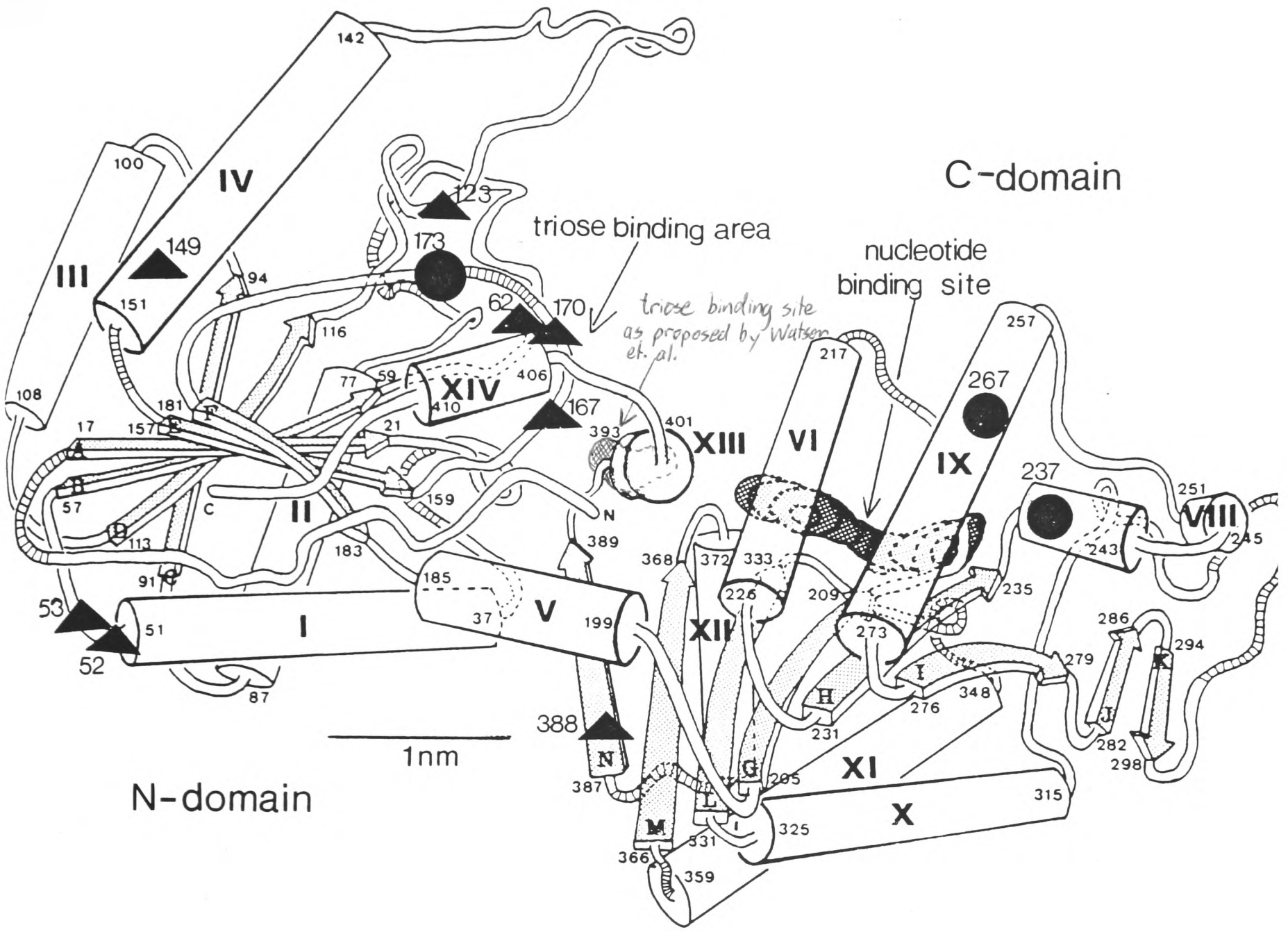

Fig.5.3 Scheme of the open form of the yeast PGK molecules. The helices are denoted by cylinders, the sheet strands by arrows.
Histidine residues (▲) and methionine residues (●) are indicated.

In the final step of the titration sufficient 30mM sodium tripolyphosphate was added to the sample to give an equimolar tripolyphosphate concentration. The titration is illustrated in figures 5.4 and 5.5, the enzyme structure is represented in figure 5.3 and a summary of assigned and partly assigned histidine and methionine residues is given in table 5.2. The effects of the interaction on the nmr spectrum of the protein and nucleoside are summarised in table 5.3 and are as follows.

In the presence of an equimolar concentration of adenosine, peak 8 of the aromatic region of the protein spectrum appears to shift upfield to merge with peak 10, while peak 11a broadens. This is consistent with a contained local interaction between the nucleoside and the protein, perhaps involving phe 340 or trp 308. In the aliphatic region of the spectrum peak 30 is seen to shift slightly upfield. The relaxation studies of the previous chapter link this peak to a surface alanine or threonine residue, and it is noted here that ala 212 lies close to the ribose ring of bound adenosine. Further effects in the aliphatic region are the slight broadening of methyl peaks 35 and 39.

The strong hydrophobic interaction is illustrated by the effect of the protein on the adenine signals, H8 and H2, which are both broadened considerably and which shift upfield and downfield respectively. The ribose signals are also affected: H1' broadens and shifts upfield and H3', H4' and H5' broaden and are barely visible above the αCH peaks of the protein spectrum.

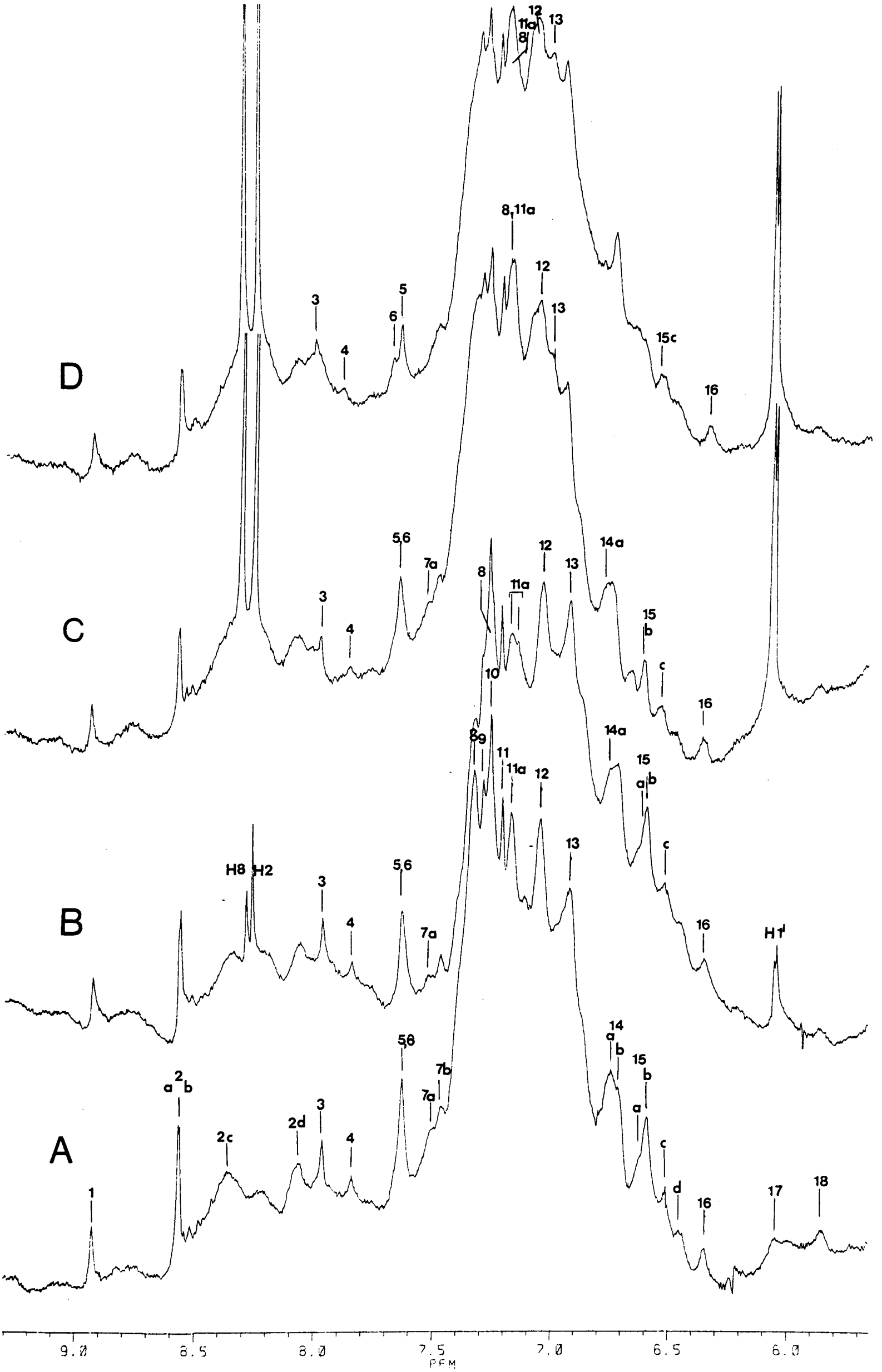

Fig.5.4 The effect of enzyme/nucleoside/ triphosphate interaction on the aromatic region of the 500MHz spectrum of yeast PGK.
(A) 1.4mM PGK; (B) as (A) with 1.4mM adenosine; (C) as (A) with 7.0mM adenosine; (D) as (C) with 1.4mM PPP.

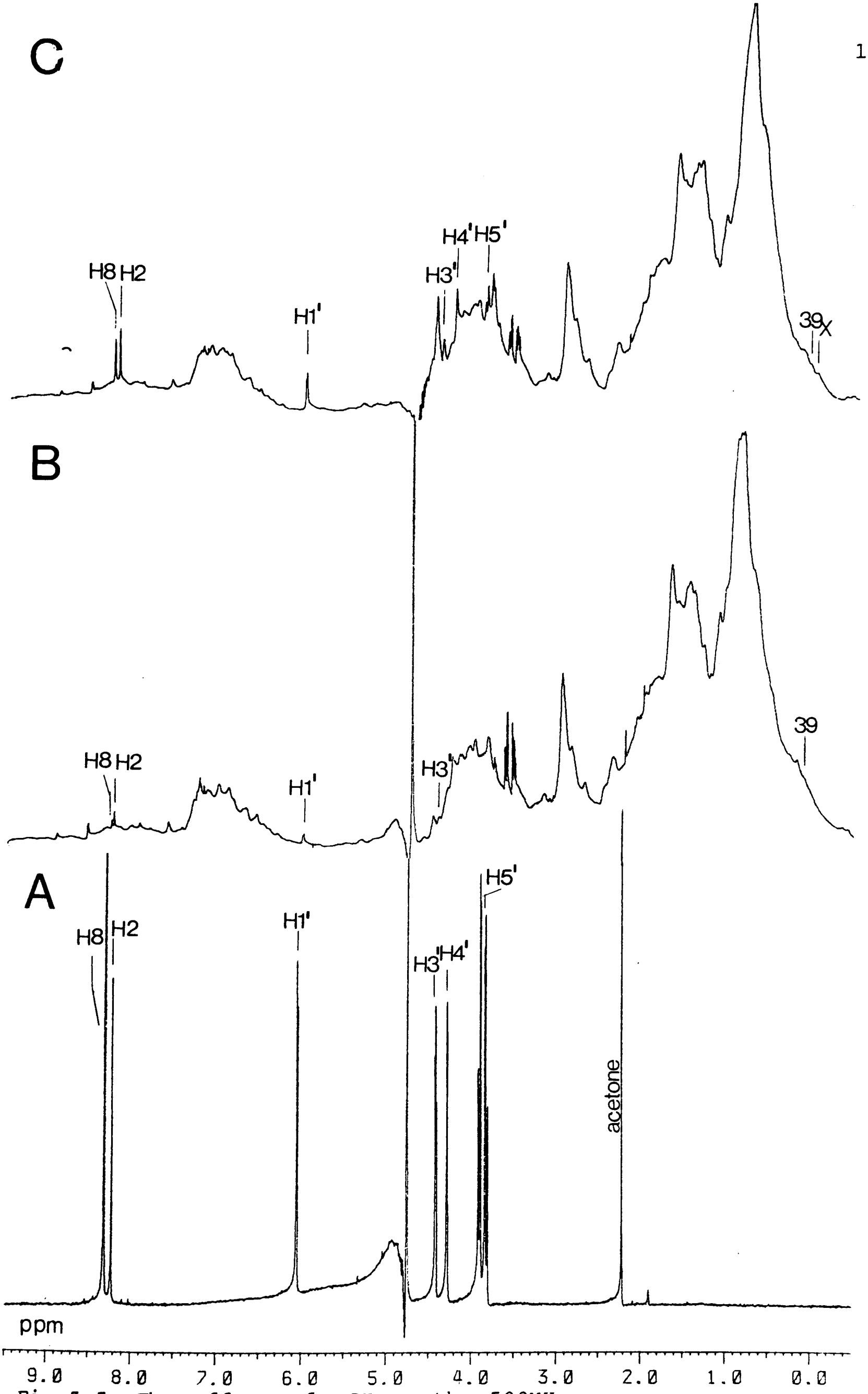

Fig.5.5 The effect of PGK on the 500MHz spectrum of adenosine.

(A) 5mM adenosine; (B) 1.4mM 1.4mM PGK; (C) 7.0mM adenosine, 1.4mM PGK.

AROMATIC RESONANCE

ADDITION	1	5		3	4	6		2	9	10	11	12	7a	b	8	11a		13		14a	b	15a	b	c	d	16	17	18
(i) 1:1 adenosine: PGK															-.05	-.03												
(ii) 5:1 adenosine: PGK												+.03			-.15	-.03		+.06				xxx		x		-.02		
(iii)as(ii) plus 1:1 PPP:PGK				+.03	+.05 x	+.04						+.02	x		-.15	-.03		+.06		xxx		xxx	xxx	x		-.03		

ALIPHATIC RESONANCE

ADDITION	21	23	24		25a	b		26	27	28		29	30	31	32	33	34	35	36		37	38	39		40	41	42	
(i) 1:1 adenosine: PGK													-.03					x				x						
(ii) 5:1 adenosine: PGK													-.04									x -.09						
(iii)as(ii) plus 1:1 PPP:PGK		+.01 x	+.01		x	-.01		x		x			-.04		xxx							x -.09						

Table 5.3 The effect of the addition of adenosine and then sodium tripolyphosphate on the 500MHz spectrum of a 1.35mM solution of yeast PGK; the effect of the interaction on the nucleoside resonances. Symbols as for table 5.1. A diagonal indicates the splitting of a peak.

NUCLEOTIDE RESONANCE

ADDITION		H8	H2	H1'	H3'	H4'	H5'
(i) 1:1 adenosine:PGK		-.03 x	+.02 x	-.02 x	xxx	xxx	xxx
(ii) 5:1 adenosine:PGK		-.01	±.00	±.00	xx	x	x
(iii)as(ii) plus 1:1PPP:PGK		-.01			xx	x	x

In the next step, the adenosine:PGK ratio is increased to 5:1. It is now seen that, in the aromatic region of the protein spectrum, peak 8 shifts further upfield to the position of peak 11a, and that peak 13 and a broad component of peak 12 shift downfield. In the upfield section of both the aromatic and aliphatic regions the effects are as follows. Peak 16 shifts upfield, peak 15a broadens out completely, peak 15c broadens slightly and a component of peak 39 shifts 0.09ppm upfield. These changes indicate either a direct influence or a more remote, conformational influence on an aromatic, hydrophobic region of the enzyme. A prime contender for such a region is the hinge area around his 388, which includes phe 194, tyr 193 and phe 163 (figure 4.6).

The increase in adenosine concentration has the effect of sharpening up the nucleoside peaks which return towards their original positions. This behaviour is consistent with fast exchange kinetics of adenosine binding.

In the third stage of the experiment, tripolyphosphate is added. Peaks 3, 4, 6 and 12 all shift downfield. This relates to the histidines of the positively charged N-terminal face of the protein cleft and the downfield shift would be consistent with protonation of these residues. It certainly demonstrates an interaction between the polyanion and this positive surface, interaction which is seen again in the anion binding studies (in the absence of adenosine) of the next chapter. Further effects in the aromatic region, are the broadening of peak 7a and, in the upfield section, peaks 14a and 15b. It is recalled here that peak 7a has been

assigned by Scheffler and Cohn (1986) to trp 308 which lies at a distance of 0.4nm from the adenosine binding site.

Several effects are seen in the aliphatic region of the spectrum. The methionine peaks 26 and 28 broaden slightly and it is noted here that of the three methionine residues of yeast PGK, one, met 237, lies near the nucleoside binding site while another, met 173, lies behind the positive anion-binding surface of the N-terminal domain. In addition, peaks 32 and 36 broaden, and some slight effects are seen at peaks 101, 23, 24 and 25. No effect is seen on the spectrum of the nucleotide.

5.2.3 Interaction with MgADP and MgADP/Gd^{3+}

A 1mM solution of yeast PGK, a 35mM solution of ADP and $MgCl_2$, and a 2mM solution of $GdCl_3$ were made up in 100mM sodium acetate, pH 5.8. Spectra were obtained for a 1mM MgADP solution; a 1mM enzyme solution; a 1mM enzyme solution with equimolar MgADP; the equimolar solution with 50μM Gd^{3+}, and finally, the equimolar solution with 150μM Gd^{3+}. It is estimated that in these equimolar solutions, 80% of the enzyme interacts with 80% of the nucleotide. The aromatic regions of the spectra are shown in figure 5.6 and the effects of the interaction are summarised in table 5.4 and are as follows.

In the 1mM enzyme/nucleotide solution, some evidence of interaction with the active site histidines is afforded by downfield shifts of peaks 3 and 12, consistent with but not necessarily reflecting protonation, and by the slight broadening of peaks 4 and 6. Peak 11a splits and shifts

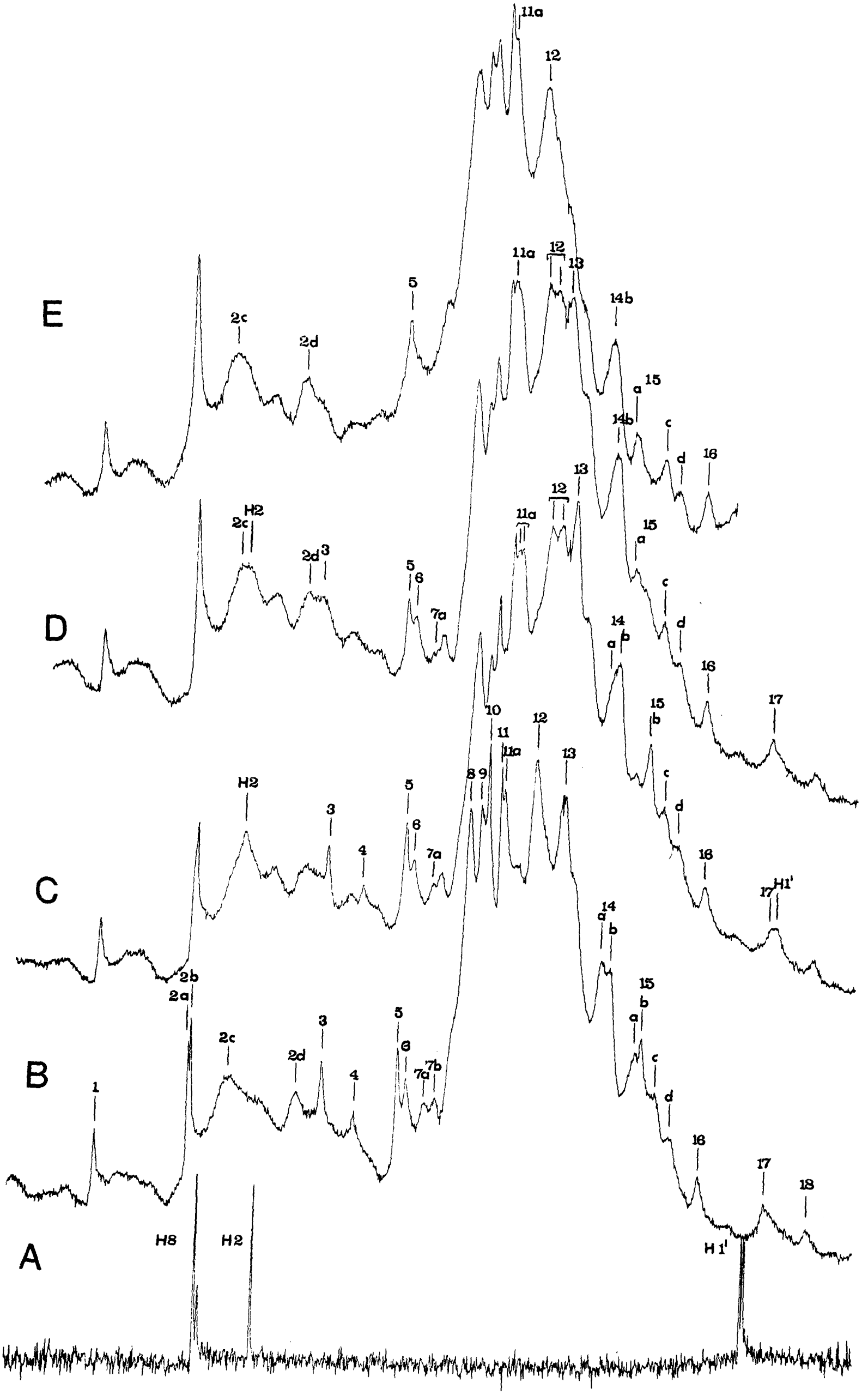

Fig.5.6 The effect of enzyme/nucleotide/metal interaction on the aromatic region of the 500MHz spectrum of MgADP and of yeast PGK. (A) 1mM MgADP; (B) 1mM PGK; (C) 1mM MgADP, PGK; (D) as (C) plus 50μM Gd^{3+}; (E) as (C) plus 150μM Gd^{3+}.

AROMATIC RESONANCE

ADDITION	1	5		3	4	6	12		2	9	10	11		7a	b	8	11a	13		14a	b	15a	b	16	17	18		
1mM MgADP				+.01	x	x	-.03 -.06							x			-.03			xx		xxx		+.01				
1mM MgADP + 50μM Gd^{3+}		x		xxx	xxx	x	-.03 -.06							xx			-.03	x		xxx		xxx	xxx	±.00				
1mM MgADP + 150μM Gd^{3+}				xxx	xxx	xxx	-.03 xxx							xxx			-.03	xxx		xxx		xx	xxx					

ALIPHATIC RESONANCE

ADDITION	21	23	24		25a	b		26	27	28		29	30	31	32	33	34	35	36		37	38	39		40	41	42	
1mM MgADP													-.04				x					-.02	x -.10			+.05		
1mM MgADP + 50μM Gd^{3+}													x -.04		x							-.02	x -.10			+.05		
1mM MgADP + 150μM Gd^{3+}													x -.04		xx		+	x				-.02	x -.10			+.05		

NUCLEOTIDE RESONANCE

ADDITION		H8	H2	H1'			
1mM PGK		xxx	+.08 xx	-.13 xx			
1mM PGK + 50μM Gd^{3+}		xxx	xxx	xxx			
1mM PGK + 150μM Gd^{3+}		xxx	xxx	xxx			

Table 5.4 The effect of MgADP and then $GdCl_3$ on the 500MHz spectrum of a 1mM solution of PGK; the effect of the interaction on the nucleotide resonances.

upfield and peak 15a broadens out completely. Both these last two effects were observed on addition of adenosine to the protein. In addition, broadening is observed at peaks 14a and 7a. Peak 14a has been assigned to a tyrosine residue and since none is found in the immediate vicinity of the nucleotide site this effect is indicative of conformational change, including involvement of a somewhat hydrophobic region of the enzyme. Peak 7a, it is recalled, has been assigned by Scheffler and Cohn (1986) to trp308, which lies, near the surface, 0.4nm behind the adenine end of the nucleotide binding site. In the aliphatic region, further evidence of such changes is provided by the upfield shifted methyl peaks. Peak 38 and a component of peak 39 shift upfield, while peak 41 moves downfield to merge with peak 40.

The strong interaction of the adenosine moiety in the hydrophobic cleft is evidenced by the considerable shifts and broadenings of the three aromatic nucleotide peaks. The three ribose peaks are also considerably broadened and are not visible above the protein spectrum.

On the addition of 50μM Gd^{3+}, the expected replacement of Mg^{2+} by the line-broadening reagent is confirmed by the considerable broadening of the nucleotide peaks. Of the protein resonances, active site histidine peak 4 broadens out completely, and peaks 3 and 6, and the upfield component of peak 12, all broaden. Peak 15b broadens out completely, and slight broadening is observed at peaks 7a and 13, and at peak 5. This last effect is evidence of binding of free Gd^{3+} at the surface near his 123, as observed in the previous section. In the aliphatic region only very slight broadening is observed, at resonances 30 and 32.

Finally, at a Gd^{3+} concentration of 150μM, of the remaining peaks assigned to active site histidines, peaks 3 and 6 and the upfield component of peak 12 broaden out completely. Broadening already observed at peaks 7a and 13 also increases.

5.2.4 Interaction with MgATP and MgATP/Gd^{3+}

In this study, conditions identical to the previous section were used, but with MgATP replacing MgADP. It is estimated that in the equimolar PGK, MgATP solutions, 70% of the total enzyme present is bound to 70% of the total substrate present. The spectra are shown in figure 5.7 and the spectral effects, summarised in table 5.5, are as follows.

As with MgADP, peaks 3 and 6 are affected by the addition of equimolar nucleotide. Peak 3 moves 0.06ppm downfield and broadens slightly, peak 4 broadens slightly, peak 6 shifts 0.05ppm downfield and peak 12 shifts 0.02ppm downfield. The downfield shifts are consistent with histidine protonation on interaction with the phosphate. As with the diphosphate, peak 7a is broadened, this time completely, and so is peak 14a. Effects common to interaction with MgADP and with adenosine are the upfield shift of peak 11a, the downfield shift of peak 13 and the upfield shift of upfield aromatic peak 16. As with adenosine, peak 8 is affected, this time being slightly broadened. In addition, and not previously observed with adenosine or MgADP, upfield aromatic peaks 15b and 17 shift downfield.

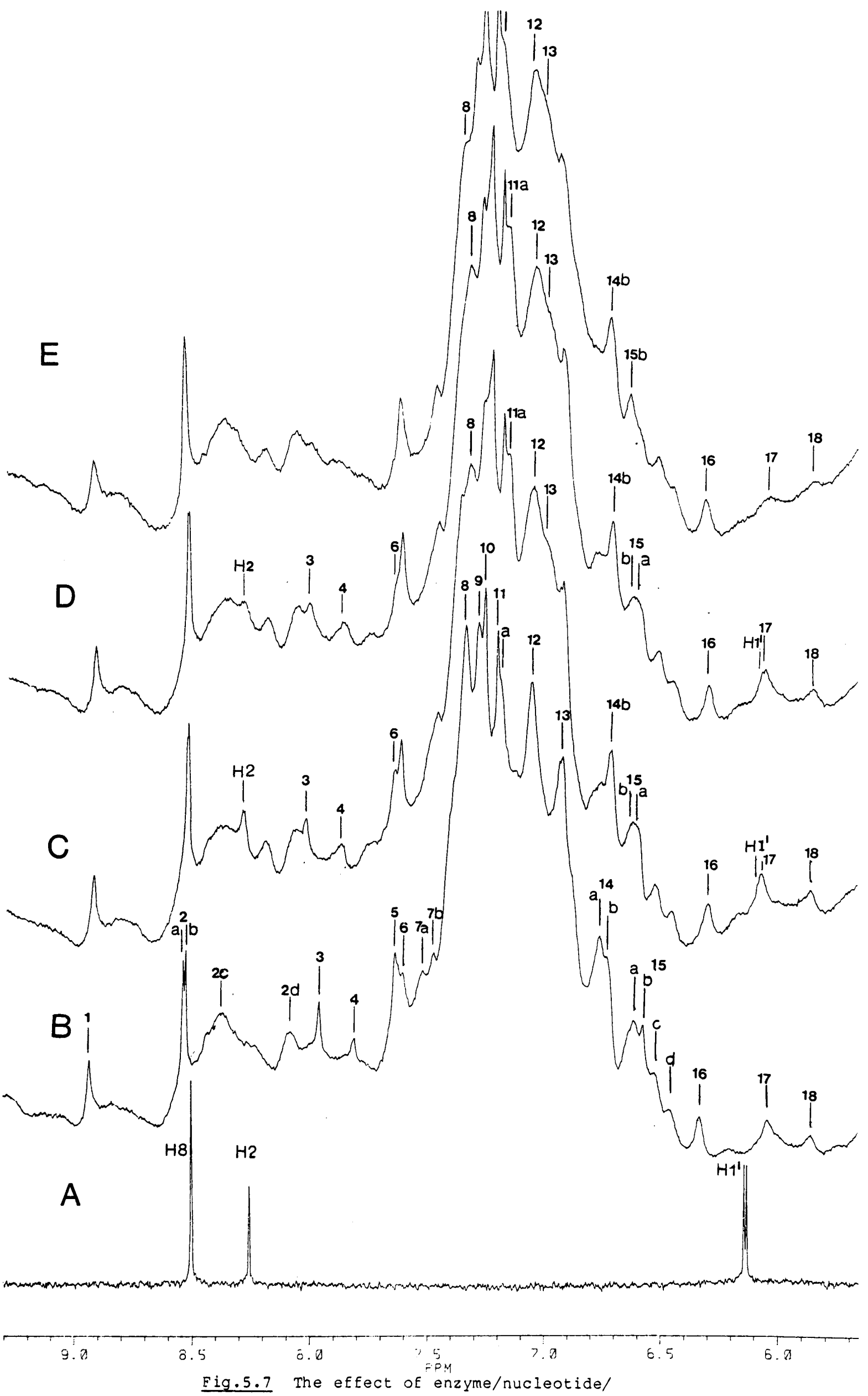

Fig.5.7 The effect of enzyme/nucleotide/metal interaction on the aromatic region of the 500MHz spectrum of MgATP and of yeast PGK.

(A) 1mM MgATP; (B) 1mM PGK; (C) 1mM MgATP, PGK; (D) and (C) plus 50μM Gd^{3+}; (E) as (C) plus 150μM Gd^{3+}.

AROMATIC RESONANCE

ADDITION	1	5		3	4	6	12		2	9	10	11		7a	b	8	11a	13		14a	b	15a	b	16	17	18		
1mM MgATP				+.06 x	x	+.05	+.02							xxx		x	-.02	+.08		xxx			-.08	-.02	+.03			
1mM MgATP + 50μM Gd^{3+}				+.06 xx	x	+.05 xx	+.02							xxx		x	-.02	+.08		xxx			+.08	-.02	+.03			
1mM MgATP + 150μM Gd^{3+}				xxx	xxx	xxx	+.02							xxx		xx	-.02	+.08		xxx		xxx	+.08	±.00	xx	xx		

ALIPHATIC RESONANCE

ADDITION	21	23	24		25a	b		26	27	28		29	30	31	32	33	34	35	36		37	38	39		40	41	42	
1mM MgATP			xxx		+	-.02		-.01					-.04		x			x					-.04 -.10			+.04		
1mM MgATP + 50μM Gd^{3+}			xx		+	-.02		-.01					-.04		x			xx	x				-.04 -.10			+.04		
1mM MgATP + 150μM Gd^{3+}		x	xx		0	-.02		-.01	xx				-.04		x			x	x				xx xxx		xx	+.04 x	x	

NUCLEOTIDE RESONANCE

ADDITION		H8	H2		H1'		
1mM PGK		xxx	+.02 xx		-.03 xx		
1mM PGK + 50μM Gd^{3+}		xxx	xxx		xxx		
1mM PGK + 150μM Gd^{3+}		xxx	xxx		xxx		

Table 5.5 The effect of MgATP and then $GdCl_3$ on the 500MHz spectrum of a 1mM solution of PGK; the effect of the interaction on the nucleotide resonances.

All the aromatic peaks which are affected by addition of adenosine and of MgADP are influenced, also, by the addition of MgATP, with the sole exception of peak 15a.

In the aliphatic region, shifts at upfield shifted methyl peaks 39 and 41, observed on addition of MgADP, are repeated here as in the upfield shift of peak 30. The downfield shifts of peak 25b and of methionine peak 26, and the loss of peak 24 are among the aliphatic effects not previously observed.

As with adenosine and with MgADP all three nucleotide peaks are broadened, H2 is shifted downfield and $H1^1$ is shifted upfield.

On addition of 50μM Gd^{3+}, peaks 3, 4 and 6 and the nucleotide peaks broaden considerably. On increasing the Gd^{3+} concentration to 150μM, they are lost completely. In addition, the broadening of peak 8 increases, and both the upfield aromatics 15a and 18 and the upfield shifted methyl peaks 39 and 40 broaden considerably. Linewidth increases are also observed for peaks 41 and 42 and for methionine peak 27. At least some of these effects are due to the binding of excess Gd^{3+} to the surface of the proton.

5.2.5 Interaction with MgAMPPNP and MgAMPPNP/Gd^{3+}

The third study of nucleotide binding involves the addition of MgAMPPNP, which is used as a non-reacting substrate analogue in studies of the complete enzyme-substrate system. A 2mM PGK sample is used, together with a 1mM solution of $GdCl_3$, a 3.5M solution of $(NH_4)_2SO_4$ and a 20mM solution of $MgCl_2$, AMPPNP. All the solutions were buffered at pH5.9 with 100mM sodium d_3-acetate.

In the first stage of the experiment, three incremental amounts of MgAMPPNP were added to the PGK sample such that 30% of the total enzyme present binds 94% of the total nucleotide present, then 60% enzyme binds 88% nucleotide and finally 90% enzyme binds 67% nucleotide. In the next stage the line-broadening reagent $GdCl_3$ is added to levels of 30 and 100μM. In the final stage, ammonium sulphate is added to levels of 15, 80 and 350mM. Scopes (1978b) gel filtration studies indicate that ammonium sulphate competes with the binding of MgATP but not of MgADP, and its addition here is an attempt to remove Gd^{3+}/MgAMPPNP from the protein, and reverse the effects on the spectrum of the interaction.

The changes produced in the spectra of the protein and the nucleotide by the various additions are illustrated in figure 5.8 and summarised in table 5.6. They are as follows.

On the first addition of MgAMPPNP, when only a calculated 30% of the enzyme interacts, active site histidine resonances 3 and 6 move slightly downfield. Peaks 7a and 14a, broadened by equimolar MgADP and MgATP, are both shifted upfield, and peak 8, broadened by MgATP, is shifted slightly downfield. In the aliphatic region, effects common to the three nucleotides are the splitting and upfield shifts of peaks 30 and 39 and the movement of peak 41. In addition peak 37 moves slightly upfield. Peaks 37, 39 and 41 are upfield shifted methyl resonances and, as before, the effects are indicative of movement in a hydrophobic region of the protein. Effects common to the two triphosphate nucleotides are the broadening of peak 24, the intensity increase of peak 25a, the upfield shift of peak 25b and the slight upfield

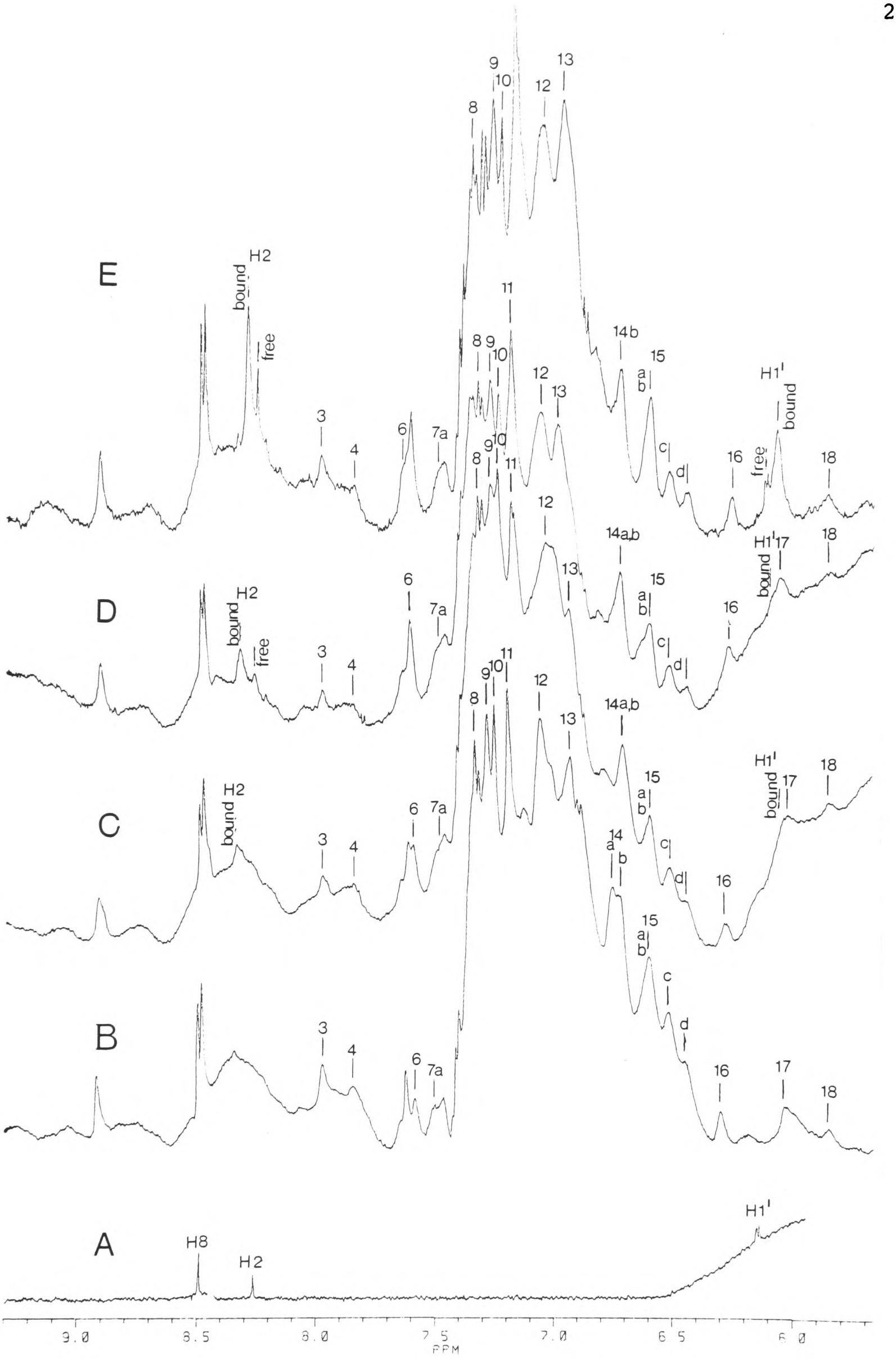

Fig.5.8 The effect of enzyme/nucleotide/metal sulphate interaction on the aromatic region of the 500MHz spectrum of MgAMPPNP and yeast PGK.

(A) 1mM MgAMPPNP; (B) 2.0mM PGK, pH5.9; (C), (D) amd (E) as (B) with 0.6, 1.4 and 2.8mM MgAMPPNP; (F) and (G) as (E) plus 30 and 100μM $GdCl_3$; (H), (I) and (J) as (G) plus 15, 80 and 350mM $(NH_4)_2SO_4$.

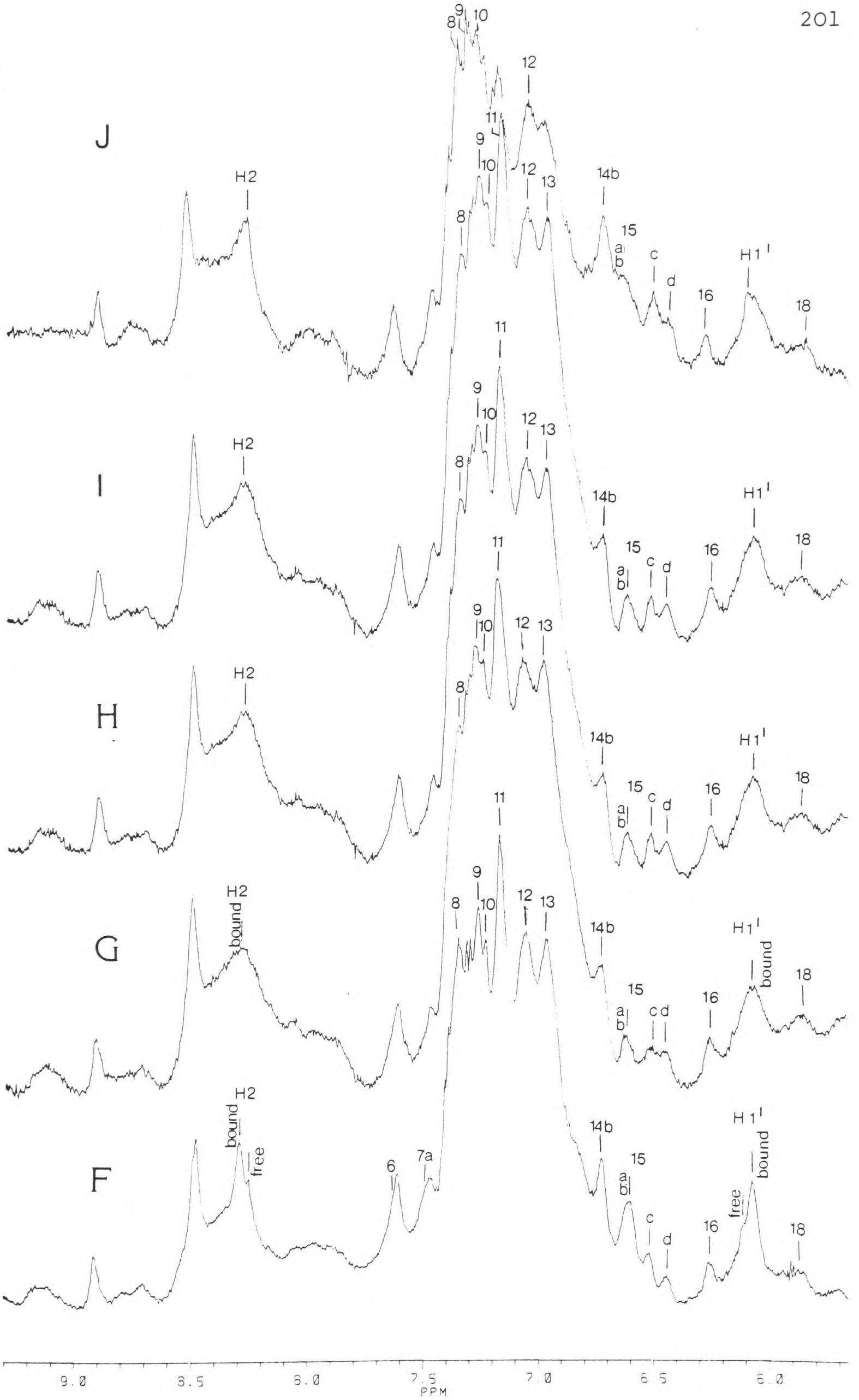
J
I
H
G
F
H2
H1'
8
9
10
11
12
13
14b
15
a
b
c
d
16
18
H2 bound
H2 free
H1' bound
H1' free
6
7a
9.0
8.5
8.0
7.5
7.0
6.5
6.0
PPM

AROMATIC RESONANCE

ADDITION	1	5		3	4	6	12		2	9	10	11		7a	b	8	13		14a	b	15a	b	c	d	16	17	18	
(i) 0.6mM MgAMPPNP				+.01		+.02								-.01		+.01			-.03						-.03	+.02		
(ii) 1.4mM MgAMPPNP				+.01		+.04								-.01		+.01	+.05		-.03		-.01				-.03	+.07		
(iii) 2.8mM MgAMPPNP				+.02	+.01	+.07	+.02							-.01		+.02	+.05		xxx	+.02	-.01				-.03	+.08	x	
(iv) as (iii) plus 30μM $GdCl_3$				xxx	xxx	+.07 xx	+.02							-.01		+.02	+.05		xxx	+.02		+.02		+.01 x	-.03	+.08	x	
(v) as (iii) plus 100μM $GdCl_3$				xxx	xxx	xxx	+.02			x	xx			xxx		+.02	+.05		xxx	+.02		+.04	x	+.01 x	-.03 x	-.08	x	
(vi) as (v) plus 15mM amm.sul.				xxx	xxx	xxx	+.02				xx			xxx		+.02	+.06		xxx	+.02		+.04			-.02	+.08	x	
(vii) as (v) plus 80mM " "				xxx	xxx	xxx	+.02				xx			xxx		+.02	+.06		xxx	+.02		+.04			±.00	+.08	x	
(viii) as (v) plus 350mM" "				xxx	xxx	xxx	+.02				xx	xxx		xxx		+.02	xxx		xxx	+.02		+.04			-.02	+.08	x	

ALIPHATIC RESONANCE

ADDITION	21	23	24		25a	b		26	27	28		29	30	31	32	33	34	35	36		37	38	39		40	41		
(i) 0.6mM MgAMPPNP			x		+	-.02		-.01					-.04						x		-.01		-.05 -.10			+.03		
(ii) 1.4mM "			xx		++	-.03		-.01					-.04		x						-.01 -.05		-.08			+.03		
(iii) 2.8mM "			xxx		++	-.03		-.02					-.04						xx		-.01 -.05		-.08 x		-.01 x	+.05 xx		
(iv)as(iii) plus 30μM $GdCl_3$		x	xxx		+	-.05		-.02					-.04		x						-.01 -.05 x		-.08 x		-.01 x	+.05 xxx		
(v)as(iv) plus 100μM "		xxx	xxx		+	-.05		-.02	x				-.04		xx				xxx		-.01 -.05 x		-.08 x		-.01 xx	+.05 xxx		
(vi)as(v) plus 80mM amm.sulph		xxx	xxx		xx	-.05		-.02	x				-.04		xx				xxx		-.01 -.05 x		-.08 x		-.01 xx	+.05 xxx		
(vii)as(v) plus 350mM " "		xxx	xxx		xxx	-.05		-.02	x				-.04		xx				xxx		-.01 -.05 x		-.08		-.01 xx	+.05 xxx		
(viii)as(v) plus 350mM" "		xxx	000		xxx	-.05		-.02	x				-.04		xx				xxx		-.01 -.05 x		-.08		-.01 xx	+.05 xxx		

NUCLEOTIDE RESONANCE

ADDITION	H8		H2	FREE	FREE	H1'	
(i) 94% bound to enzyme	xxx		+.08 xx			-.09 xx	
(ii) 88% " " "	xxx		+.06 x	x		-.05 x	
(iii) 67% " " "	xxx		+.04 0	0	x	-.05 x	
(iv) plus 30μM $GdCl_3$	xxx		+.04 x	x	xx	-.05 xx	
(v) " 100μM "	xxx		+.04 xx	xxx	xxx	-.05 xx	
(vi)as(v) plus 15mM amm.sulph.	xxx		+.04 xx	xxx	xxx	-.05 xx	
(vii)" " " 80mM " "	xxx		+.04 xx	xxx	xxx	-.05 x	
(viii)as(v) " 350mM " "	xxx		+.03 xx	xxx	xxx	-.02 x	

Table 5.6 The effects of the addition of MgAMPPNP, $GdCl_3$ and finally ammonium sulphate on the 500MHz spectrum of a 2mM solution of PGK; the effect of the interactions on the nucleotide spectrum.

shift of buried methionine 26 (tentatively assigned to residue 237). In addition some slight alteration is seen among the peaks near 4.2ppm which may be αCH peaks.

The three aromatic nucleotide peaks are broadened considerably. Peak H8 is lost and peaks H2 and H1' appear as single broad peaks 0.08ppm downfield and 0.09ppm upfield, respectively, of their original positions. The remaining ribose peaks of the nucleotide do not appear above the protein spectrum.

On increasing the nucleotide concentration to 1.4mM, active site resonance 6 moves a further 0.02ppm downfield; peak 13 moves downfield, which is an effect shared with adenosine and MgATP, and upfield aromatic peaks 16 and 17 move away from each other, which is an effect shared with MgATP. In the aliphatic region, movement increases among the αCH signals; the intensity increases at peak 25a continues; 25b moves further upfield, and a rearrangement at peak 39 produces a single peak 0.08ppm upfield from the original position.

The concentration of free nucleotide is calculated to have doubled and a small peak is now observed upfield of the H2 resonance with a chemical shift value corresponding to free nucleotide. This is consistent with the nucleotide/ enzyme interaction having slow exchange kinetics on the nmr time scale. Meanwhile, both the H2 and H1' resonances move towards the free nucleotide chemical shift positions, and the linewidth of the H2 resonance decreases. The H5' resonance appears for the first time, at 4.28ppm.

On the final increase of nucleotide concentration, to 2.8mM, resonances 3,4,6 and 12 all move downfield, consistent with some degree of protonation of the active site. In the upfield aromatic region, peak 14a broadens out completely (an effect seen with both the substrate nucleotides), peak 14b is seen to have shifted 0.02ppm upfield and peak 17 moves further downfield. In addition, upfield shifted methyl resonance 37 splits with a component moving 0.05ppm upfield. These effects reveal further conformational change in the hydrophobic region of the proton. Other effects on the upfield region include the complete broadening out of peak 24 and the continuing shift of the methionine peak 26.

One third of the nucleotide is now calculated not to interact with the enzyme and the free species is represented by comparatively sharp H2 and H1' peaks. Meanwhile, the H2 peak of the bound species sharpens up and moves 0.02ppm upfield, towards its original position.

The similarities between the effects on the spectrum of the interaction of PGK and MgAMPPNP and those caused by interaction between the substrate nucleotides and the enzyme confirm the expected similarities of interaction and support the use of MgAMPPNP as a substrate analogue.

On the addition of 30μM Gd^{3+}, all three active site histidine C2 resonances broaden considerably, as expected. Among the upfield aromatics, peak 15b shifts downfield, an effect noted with MgATP. In addition, peak 17 moves slightly further downfield and peak 18 broadens slightly. Of the

upfield shifted methyl resonances, peak 39 broadens, and peaks 40 and 41 move downfield. Other effects in the aliphatic region include the broadening of ε-lysine peak 23 and of peaks 25a, 32 and 36, all of which are effects observed with MgATP/Gd^{3+}. All of the observed nucleotide peaks show some degree of broadening.

On increasing the Gd^{3+} concentration to 100μM, peak 7a, shifted by the nucleotide alone, is now completely broadened out. In addition, titratable histidine peaks 9 and 10 and exposed methionine peak 27 broaden slightly, giving evidence of binding of the cation on the surface of the protein, independent of the nucleotide. Of the upfield shifted resonances, aromatic peaks 15b,c and d are broadened and/or shifted while methyl peaks 40, 41 and a component of 39 broaden. The linewidth increases already noted at peaks 23, 25a, 32 and 36 continue and αCH peak 103 broadens also. The broadening of the nucleotide peaks increases and the H5' peak, the free H2 peak and the free H1' peak completely broaden out.

The first two additions of ammonium sulphate, to concentrations of 15 and then 80mM, have no significant effect on the spectrum apart from producing a new peak between position 8 and 9. At a level of 350mM ammonium sulphate, peaks 11 and 13 broaden out completely, causing a dramatic change in the overall shape of the aromatic envelope; upfield aromatic peak 16 moves downfield; upfield shifted methyl peak 39 sharpens up, and peak 24 reappears. This indicates a limited conformational change in the

protein. The two (bound) nucleotide peaks move closer to their positions in the free nucleotide but apart from this there is no strong indication that the sulphate removed the nucleotide from the protein.

5.2.6 The location of Gd^{3+} in enzyme/nucleotide/metal complexes

Using spectra from the above experiments, a comparison is made of the Gd^{3+} induced broadening of the enzyme's three active site histidine C2 resonances with that of the nucleotide H2 resonance. It is shown in table 5.7. The broadening factor is simply the difference between the linewidths in the presence of Gd^{3+} and in its absence, while the broadening ratio is that factor divided by the factor of the reference H2 resonance. The distance ratio is the inverse of the sixth power of the broadening ratio. Using the H2-metal ion distance calculated by Tanswell et al., (1975) of 1.1nm, these results indicate that in the Gd^{3+}-nucleotide-enzyme complex the peak 3 histidine residue lies 0.9nm from the metal ion and the peak 4 and peak 6 histidine residues are about 1.2nm from the metal ion.

5.2.7 Summary of spectral effects

Yeast PGK is a large protein by nmr standards with the attendant problems of broad signals and low resolution. Thus the experiments carried out here were originally performed at 300MHz and then repeated, whenever possible, at 500MHz to ensure that any observations made are genuine rather than artificial.

Table 5.7 Linewidth increases and metal-proton distances in PGK/nucleotide, Gd^{3+} complexes

nucleotide	proton	linewidth(Hz)		broadening factor	broadening ratio	distance ratio	separation (nm)
		$0\mu MGd^{3+}$	$50\mu MGd^{3+}$				
MgADP	his3	3.90	18.6	14.7	1.67	0.918	1.01
	his6	13.2	14.7	1.5	0.17	1.34	1.47
	H2	17.4	26.2	8.8	1.0	1.0	1.1
		$0\mu MGd^{3+}$	$50\mu MGd^{3+}$				
MgATP	his3	10.5	21.2	10.72	2.10	0.884	0.97
	his4	13.2	17.4	4.2	0.82	1.03	1.14
	his6	8.10	10.8	2.7	0.53	1.11	1.22
	H2	8.10	13.2	5.1	1.0	1.0	1.1
		$0\mu MGd^{3+}$	$30\mu MGd^{3+}$				
MgAMPPNP	his3	7.80	33.0	4.23	5.60	0.750	0.83
	his4	7.80	10.4	1.33	0.58	1.10	1.21
	his6	11.40	13.2	1.16	0.40	1.16	1.28
	H2	6.00	10.5	1.75	1.0	1.0	1.1

A comparison of the effects of adenosine and nucleotide binding is presented in table 5.8. The main features are as follows.

(a) All of the active site histidine resonances, 3,4,6 and 12 are affected by all of the nucleotides. None is influenced by adenosine. (The apparent effect of the latter on peak 12 concerns a broad component of the peak rather than the principal resonance). The phosphate chain of the nucleotide is necessary to cause an effect across the cleft from its anchorage by the adenosine moiety in the C-domain to the active site of the N-domain. Its negative charge is necessary for this interaction to occur. Adenosine and polyphosphate ions have a similar effect.

(b) Peak 7a is also sensitive only to nucleotides. On the addition of Gd^{3+} to nucleotide/enzyme complexes, it broadens, suggesting a direct influence. Scheffler and Cohn (1986) assign this peak to trp 308.

(c) Resonances 2,9,10 and 11 are completely unperturbed indicating that there is no interaction with surface histidines 52,53 and 149.

(d) Three of the peaks of the main aromatic envelope are influenced by adenosine and thus may represent a continued local nucleotide interaction. Peak 11a does not appear in the original protein spectrum of the MgAMPPNP binding study but otherwise it is consistently shifted upfield. It may correspond to phe 340 or trp

AROMATIC RESONANCE

ADDITION	1	5		3	4	6	12		2	9	10	11		7a	b	8	11a	13		14a	b	15a	b		16	17	18	
5:1 adenosine							+.03									-.15	-.03	+.06				xxx			-.02			
1:1 MgADP				+.01	x	x	-.03							x			-.03			xx		xxx			+.01			
1:1 MgATP				+.06 x	x	+.05	+.02							xxx		x	-.02	+.08		xxx			+.08		-.02	+.03		
1:1 MgAMPPNP				+.02	+.01	+.07	+.02							-.01		.02		+.05		xxx	+.02	-.01			-.03	+.07		

ALIPHATIC RESONANCE

ADDITION	21	23	24		25a	b		26	27	28		29	30	32	33	34	35	36		37	38	39		40	41	42		
5:1 adenosine													-.04									-.09						
1:1 MgADP													-.04			x					-.02	x -.10			+.05			
1:1 MgATP			xxx		+	-.02		-.01					-.04	x			x					-.04 -.10			+.04			
1:1 MgATP			xxx		++	-.03		-.02					-.04							-.01 -.05		-.08			+.03			

NUCLEOTIDE RESONANCE

ADDITION		H8		H2		H1'	
Adenosine		+.03 x		+.02 x		-.02 x	
MgADP		xxx		+.08 xx		-.13 xx	
MgATP		xxx		+.02 xx		-.03 xx	
MgAMPPNP		xxx		+.04		-.05 x	

Table 5.8 A summary and comparison of the effects of enzyme/nucleotide (or nucleoside)/ metal interaction on the 500MHz spectra of both enzyme and liigand.

308, which are close to the site of adenosine binding. Peaks 8 and 13, otherwise consistently perturbed, are not affected by MgADP interaction. This requires further investigation.

(e) Upfield shifted peaks 16 and 39 are shifted by each ligand and peaks 14a and 41 are affected by each nucleotide. It is recalled that peak 14a represents an exposed tyrosine residue, possibly tyr 193 of the hinge region. Peaks 15a and b, 17 and to a lesser extent 37 and 38 also reveal the conformational influence of ligand interaction.

(f) Peak 30 is consistently shifted upfield. It may represent ala 212.

(g) Lysine ε-CH_2 peak 24, buried methionine resonance 26, peaks 25a and b and peak 17 are influenced by both the triphosphate nucleotides. Peaks 24 and peaks 25a and b are also affected by the addition of tripolyphosphate and this evidence of anionic influence indicates that the latter may also represent lysine ε-CH_2 peaks. It is noted here that lys 213 is known to interact with the γ-phosphate of ATP but not with ADP.

(h) Of the nucleotide peaks, H8 is broadened out completely and H2 and H1' are shifted downfield and upfield respectively. These effects are most marked with MgADP. With MgAMPPNP, H2 and H1' peaks corresponding to free nucleotide are seen, giving evidence of slow exchange.

The general pattern of perturbations at the active site and upfield aromatic resonances and none at the surface histidine resonances is also found with horse PGK (Delepierre, 1983), where, on the addition of nucleotide, resonances equivalent to 3,4 and 6 broaden out completely, upfield aromatic resonances are seen to broaden and peaks equivalent to 1,2 and 10 are unaffected.

A striking feature of this study is that about 70% of the upfield aromatic peaks, associated by their intermediate relaxation times with a region of high mobility, are influenced by nucleotide binding. This is seen as a conformational effect on the hinge region of the protein. It appears to be a fortunate circumstance that so much of the interesting region of the enzyme is observed in the nmr spectrum.

Chapter 5 References

Banks, R.D., Blake, C.C.F., Evans, P.R., Haser, R., Rice, D.W., Hardy, G.W., Merrett, M. and Phillips, A.W. (1979) Nature, 279, 773-777.

Bryant, T.N., Watson, H.C. and Wendell, P.L. (1974) Nature, 247, 14-17.

Delepierre, M. (1983) Personal communication, Université René Descartes, 4, Avenue de l'Observatoire, Paris.

Krietsch, W.K.G., and Bücher, T. (1970) Eur.J.Biochem., 17, 568-580.

Roustan, C., Brevet, A., Pradel, L-A. and van Thoai, N. (1973) Eur.J.Biochem., 37, 248-255.

Scheffler, J.E. and Cohn, M. (1986) Biochemistry, 25, 3788-3796.

Schierbeck, B. and Larsson-Raźnikiewicz, M. (1979) Biochim.Biophys.Acta, 568, 195-204.

Scopes, R.K. (1978b) Eur.J.Biochem., 91, 119-129.

Tanswell, P., Thornton, J.M., Korda, A.V. and Williams, R.J.P. (1975) Eur.J.Biochem., 57, 135-145.

Tanswell, P., Westhead, E.W. and Williams, R.J.P. (1976) Eur.J.Biochem., 63, 249-262.

Tompa, P., Hong, P.T., and Vas, M. (1986) Eur.J.Biochem., 154, 643-649.

Watson, H.C., Walker, N.P.C., Shaw, P.J., Bryant, T.N., Wendell, P.L., Fothergill, L.A., Perkins, R.E., Conroy, S.C., Dobson, M.J., Tuite, M.F., Kingsman, A.J. and Kingsman, S.M. (1982) EMBO J., 1, 12, 1635-40.

Wiksell, E. and Larsson-Raźnikiewicz, M. (1982) J.Biol.Chem., 257, 21, 12672-7.

CHAPTER 6.

INTERACTION OF PGK WITH TRIOSE PHOSPHATE AND ANIONS

Chapter 6 Contents

6.1 INTRODUCTION

Examination of the crystal structure of yeast PGK (Watson et al., 1982) reveals a generally conserved surface of positive charge in the N-terminal domain, facing the phosphate chain of bound nucleotide across the hinge region (figures (6.1) and (6.2)). The electrostatic charge of the area strongly suggests that it is a primary anion-binding site and its position in the cleft indicates that it is the active site for triose phosphate binding, provided of course, that the lobes of the protein are free to fold towards each other in solution.

Studies with 3-phosphoglycerate analogues have probed the way in which the substrate binds to the enzyme. Orr and Knowles (1974) showed that replacement of the phosphate group with a phosphonomethylene group has little apparent effect on binding to the enzyme at high pH, but at low pH, when the phosphate group is monoanionic, binding is much weaker. Similarly, the sulphate analogue, of comparable size but missing one negative charge, does not act as a substrate for PGK. Adams et al. (1985) showed that it is possible to replace the phosphate group with an arsonomethylene group and retain enzyme-binding ability - but to lose most of the catalytic property. Thus it appears that the main contribution to triose phosphate binding is the electrostatic interaction.

A study of pig muscle PGK by Tompa et al (1986) measured enzyme activity with several phosphoglycerate analogues and showed that while the phosphate group of the substrate was

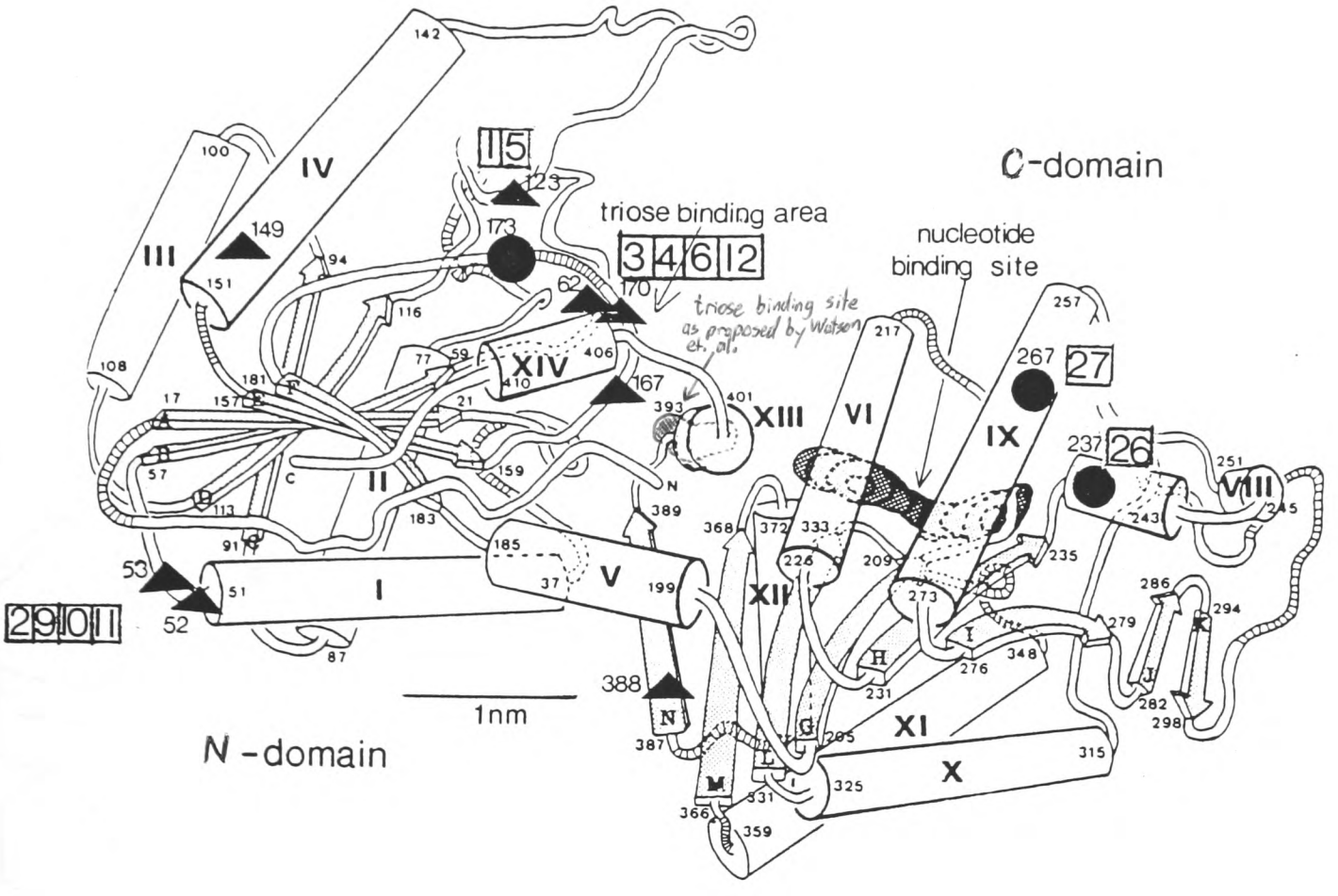

Figure 6.1 Scheme of the open form of the yeast PGK molecule. The helices are denoted by cylinders, the sheet strands by arrows. Histidine residues, ▲, and methionine residues, ●, are indicated, and the associated resonances are displayed in boxes.

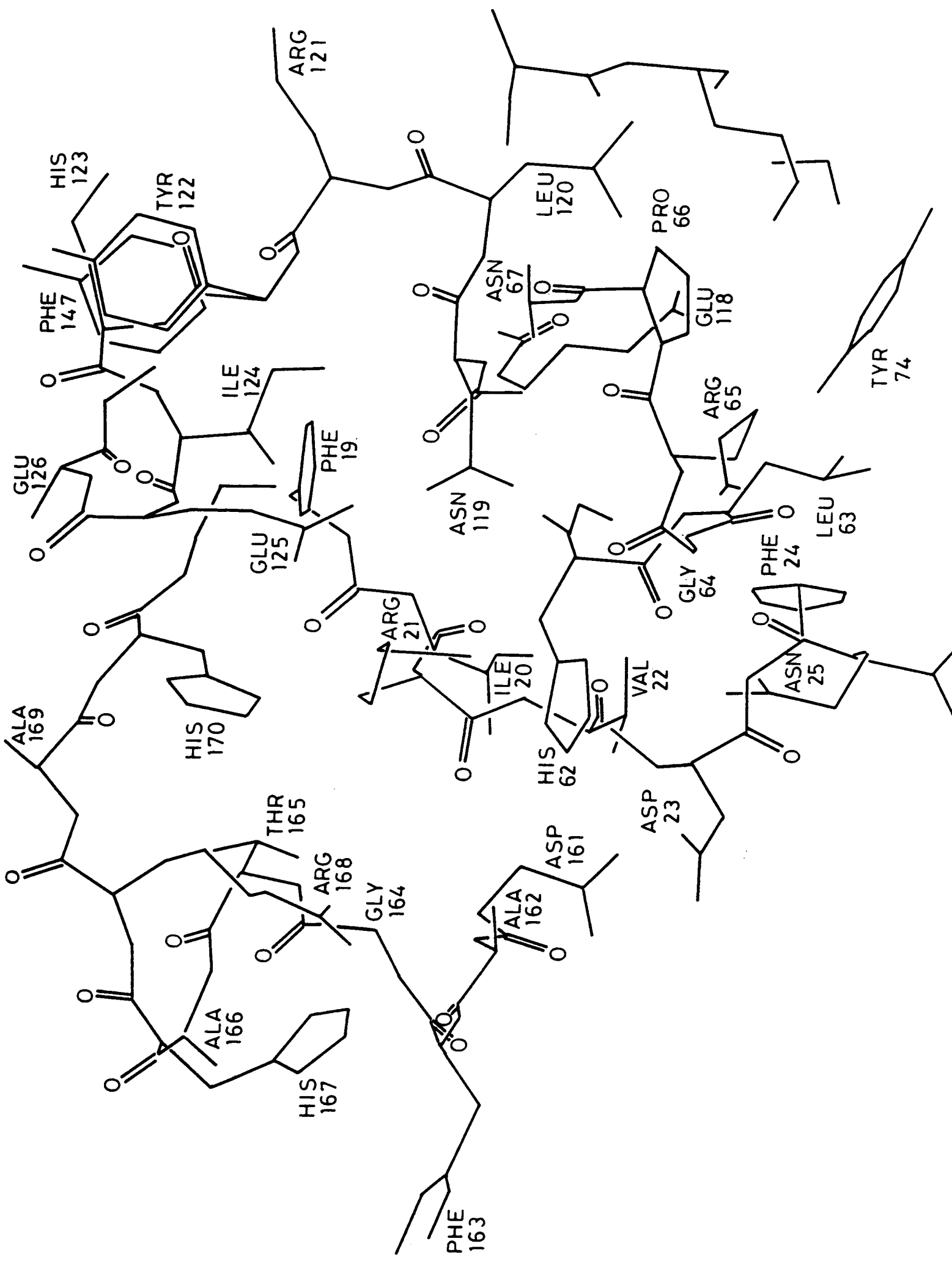

Figure 6.2 The positively charged face of the N-domain of yeast PGK.

essential for its interaction, the carboxyl group appeared to strengthen the binding in a synergic manner. Further work in the investigation concerned the reactivity of thiol groups remote from the active site of the protein and monitored conformational changes brought about by substrate binding. This work confirmed that the phosphate group is specifically involved in the interaction.

Scopes' (1978b) gel filtration study of yeast PGK identified a single site for phosphoglycerate binding with dissociation constants of 32μM for 3-PG and 50nM for 1,3-P_2G (I=150mM). The binding of SO_4^{2-} and HPO_4^{2-} was also evaluated (Kd's of 1.6mM and 1.1mM respectively, I=150mM).

A previous work by Scopes (1978a) investigated the effects of salts on the activity of PGK. It showed that most salts cause activation of the enzyme at low concentrations but cause inhibition at high concentrations. The effect was attributed to the anions and it was established that the greater the anionic charge, the lower the concentration needed for maximum activation. Thus there is evidence of binding of an electrostatic nature at the active site. Scopes (1978b) proposed the mechanism that the anion site is close to, or at, the site of phosphoglycerate binding and that at the lower concentration the anion activates the enzyme by dislodging the very tightly bound product 1,3-P_2G, while at higher concentrations the more dominant effect is its inhibition of the enzyme by competition with the initial binding of the substrate.

Wrobel and Stinson (1978) used the single thiol of yeast PGK, located 3nm distant from the acitive site in the N-terminal domain, to probe anion binding. They demonstrated a binding stoichiometry of 1:1 and established a linear energy relationship between the charge of various anions including substrate and the negative logarithm of the Kd of their complexes with the enzyme. The Kd values do not correspond to substrate Km values nor do they relate to competitive inhibition of the enzyme and thus it was thought that the site under investigation was not the active site but rather a second anionic binding site. The effect on the thiol reactivity was considered to be due to a local conformational change rather than a direct steric influence.

Further evidence for a second anionic binding site was provided by the product inhibition studies of Schierbeck and Larsson-Raźnikiewicz (1979) which demonstrated the presence of a second, low affinity phosphoglycerate site and suggested that it has a regulatory role.

The present nmr study considers the interaction of yeast PGK with various anions, including simple hexacyanide probes, polyphosphates and 3-phosphoglycerate itself in order to describe the anion binding in more detail.

6.2 INTERACTION WITH 3-PHOSPHOGLYCERATE

A titration of yeast PGK with 3-phosphoglycerate was carried out and followed using proton nmr at 300MHz. Both the enzyme and the substrate solution were buffered at pH 5.8 with 100nM sodium d_3-acetate. At first, 5µl of the 21mM phosphoglycerate solution were added to the 350µl 1mM enzyme sample, to give a substrate concentration of 300µM. Using Scopes' dissociation constant of 32µM (I=150mM), it was calculated that 29% of the total enzyme present would be bound to the substrate at these levels. Further additions of substrate were made to give levels of 0.6 and 1.2mM, corresponding to 56% and 90% of total enzyme bound. The effects on the aromatic region of the spectrum are shown in figure 6.3 and summarised in table 6.1, and figure 6.4.

On the first addition of phosphoglycerate the three peaks which are present in the original spectrum and which are associated with the triangle of histidines found in the positive surface in the cleft are seen to be affected: peak 3 broadens and shifts 0.06ppm downfield, peak 12 shifts 0.01ppm downfield, and peak 6, an upfield shoulder on peak 5, shifts 0.01ppm upfield. In addition, upfield aromatic peak 14a shifts 0.01ppm upfield. On increasing the substrate conentration to 600µM, the effects observed on peaks 3, 12 and 6 increase. Peak 3 broadens more and, together with peak 12, shifts a further 0.04ppm downfield, and peak 6 shifts a further 0.02ppm upfield. In addition, peak 7a shifts 0.01ppm downfield and upfield aromatic peak 16 moves 0.02ppm

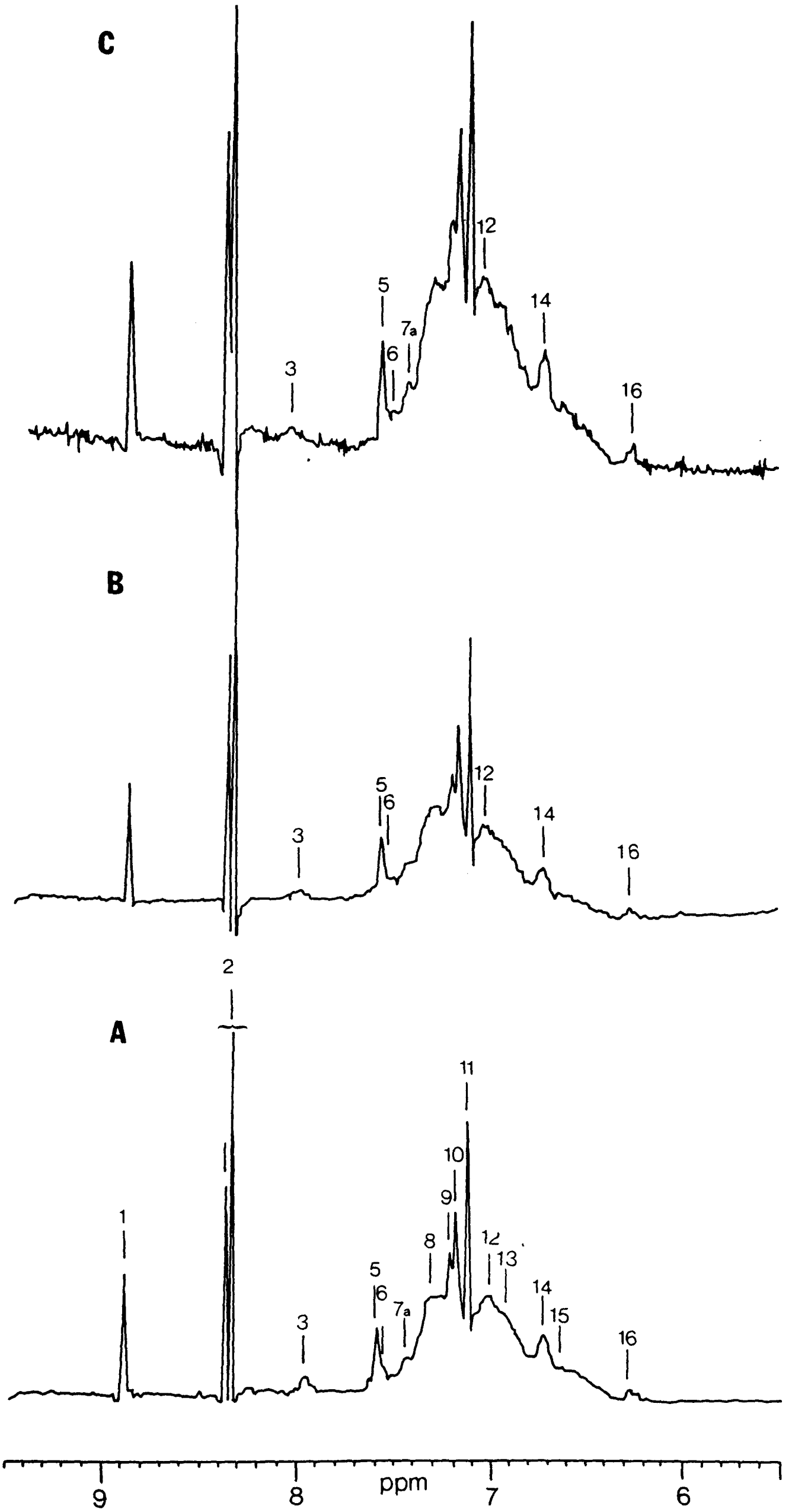

Figure 6.3 The effect of the 3-PG interaction on the aromatic region of the 300MHz spectrum of yeast PGK.

(A) 1mM PGK, pH6.2;

(B) with 0.3mM 3-PG;

(C) with 0.6mM 3-PG;

(D) with 1.2mM 3-PG;

(E) with 100mM ammonium sulphate, and 1.2mM 3-PG;

(F) with 400mM ammonium, sulphate, and 1.2mM 3-PG.

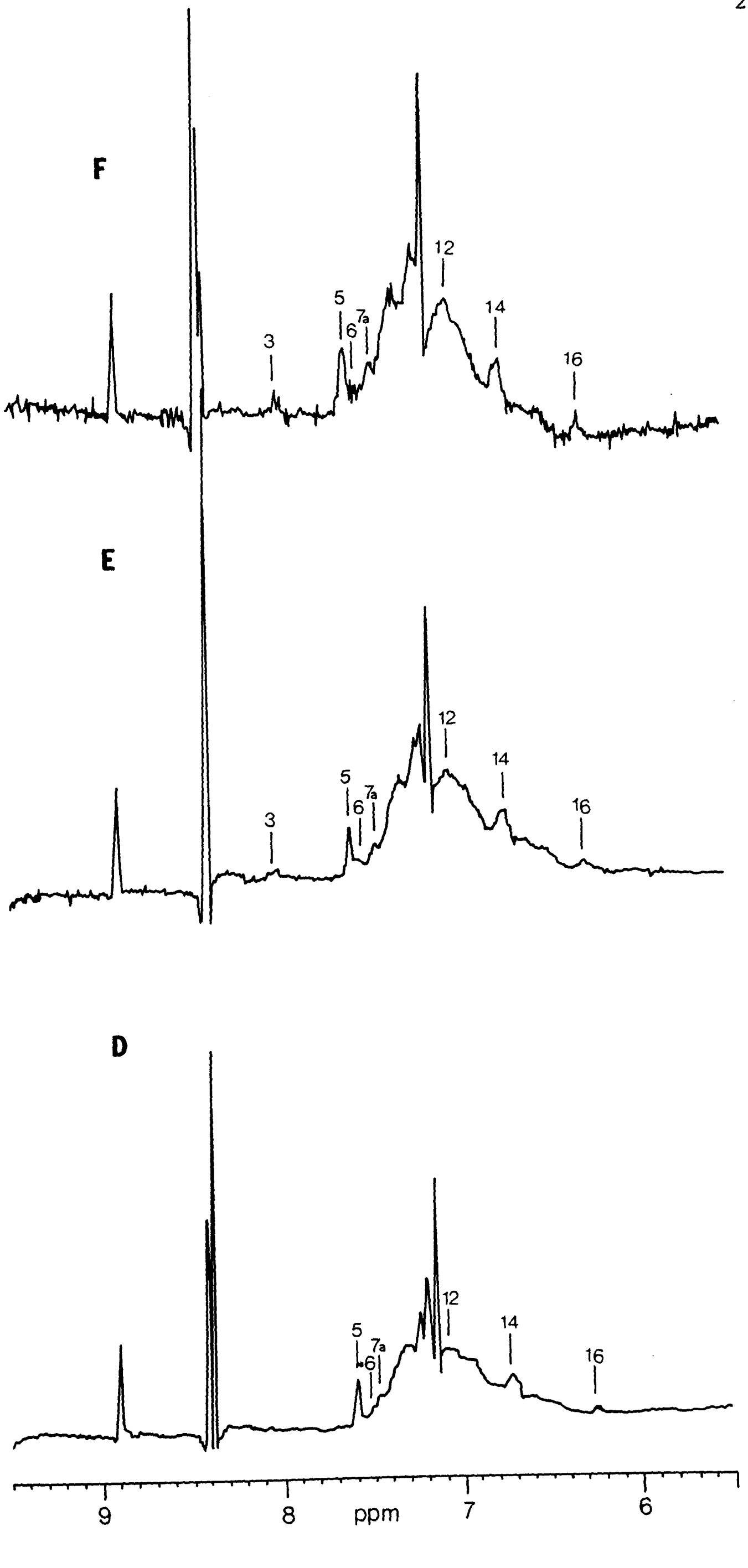
F
3
5
6
7a
12
14
16
E
3
5
6
7a
12
14
16
D
5
6
7a
12
14
16
9
8
ppm
7
6

Table 6.1 The effect of the addition of 3-phosphoglycerate and then ammonium sulphate on the 300MHz spectrum of 1mM PGK. Symbols as for table 5.1. "amm.sulph." = ammonium sulphate.

AROMATIC RESONANCE

ADDITION		1	5		3	6	12		2	9	10	11		7a	8	14a	16												
(i) 0.3mM 3-PG					+.06 x	-.01	+.01									-.01													
(ii) 0.6mM 3-PG					+.10 xx	-.03	+.05							+.01		-.01	-.02												
(iii) 1.2mM 3-PG			-.01		xxx	-.03	+.05							+.01		-.02	-.02												
(iv) as (iii) plus 100mM amm.sulph.					+.08 x	-.02	+.03							±.00		+.01	-.01												
(v) as (iii) plus 400mM amm.sulph.					+.01 x	±.00	+.01									±.00	-.01												

ALIPHATIC RESONANCE

ADDITION	21		23	24	25		26	27	28		29	30	31	32		33	34	35	36		37	38	39		40	41	42	
(i) 0.3mM 3-PG																												
(ii) 0.6mM 3-PG																			x									
(iii) 1.2mM 3-PG																			x									
(iv) as (iii) plus 100mM amm.sulph.																			xx									
(v) as (iii) plus 350mM amm.sulph.																			xx									

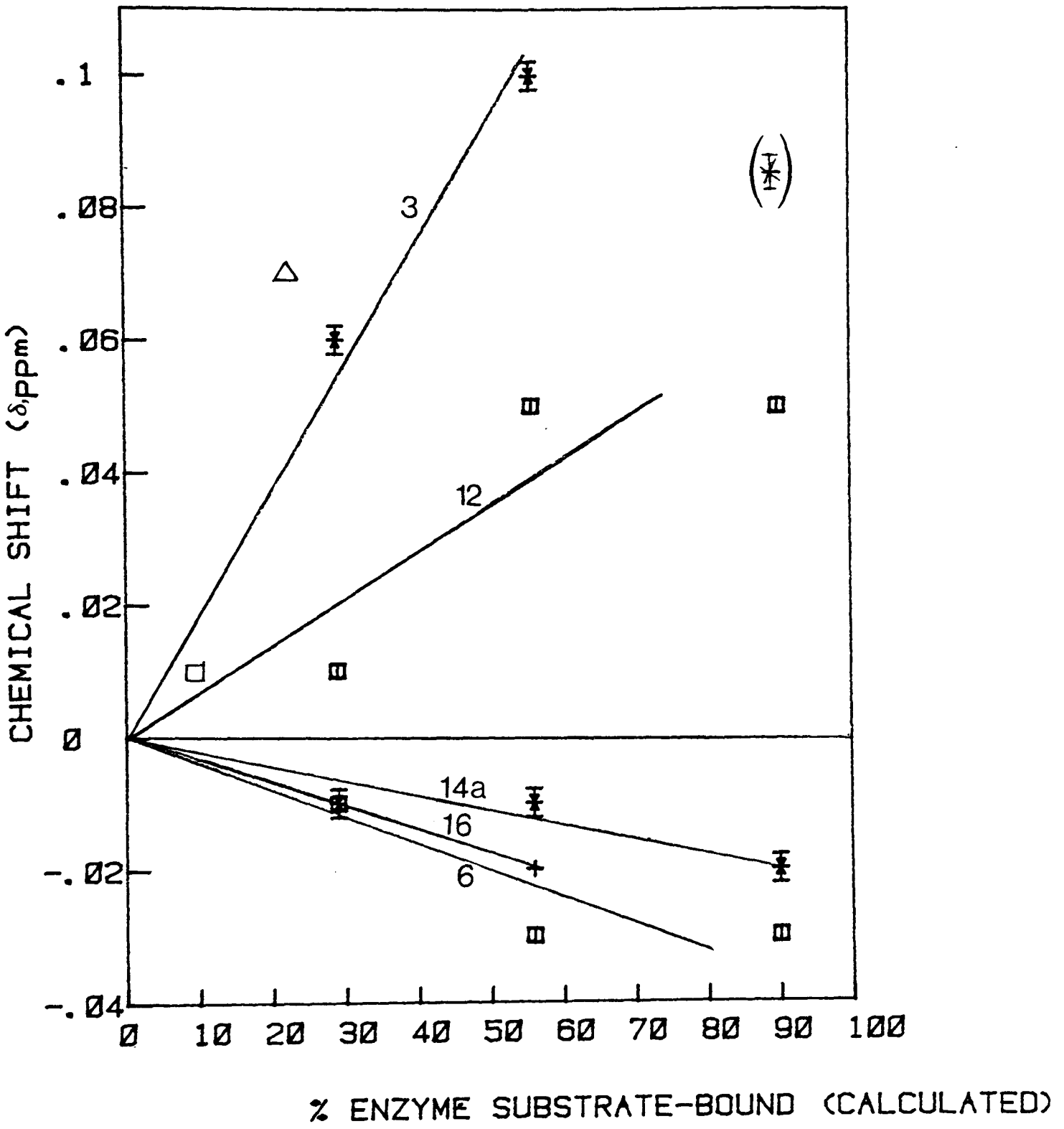

Figure 6.4 The effect of 3-PG interaction on four proton nmr resonances of yeast PGK.

Key: peak 3 (⊼); peak 12 (⊞); peak 6 (⊞); peak 14a (⊼); peak 16 (+);

(△) peak 3 in presence of 100mM ammonium sulphate, and

(□) peak 3 in presence of 400mM ammonium sulphate.

upfield. In the aliphatic region, peak 36 broadens slightly. Finally, at a phosphoglycerate concentration of 1.2mM, peak 3 broadens out completely.

An examination of Tanswell's less detailed spectra (1974) reveals similar effects on the addition of an excess of 3-PG to the enzyme as reported. Peak 3 broadens, peak 12 shifts downfield and a component of peak 16 shifts upfield. In addition, peak 4 is seen to broaden out completely and peaks 8 and 15 to move downfield.

It is further remarked that the type of effects observed here are consistent with fast exchange kinetics for the binding of the triose substrate.

The effect of a higher concentration of phosphoglycerate was examined in a second experiment, illustrated in figure 6.5 and summarised in table 6.2. 10µl of the 80mM substrate solution were added to the 400µl 8mM enzyme sample to give a substrate concentration of 2mM. This corresponds to 98% of the enzyme binding phosphoglycerate at the active site with an excess of substrate available to bind at secondary sites. As before, the substrate binding is seen to affect histidine peaks 3, 12 and 6, and peaks 12, 14a and 16. In addition, the third peak of the histidine triangle, peak 4, here visible in the original spectrum, is seen to broaden completely on the addition of substrate (see Tanswell et al. 1976). Evidence of binding at a second site is seen most clearly in the upfield movement of peaks 1 and 5, which have already been assigned to titratable histidine 123. This shift may well represent a partial deprotonation of the

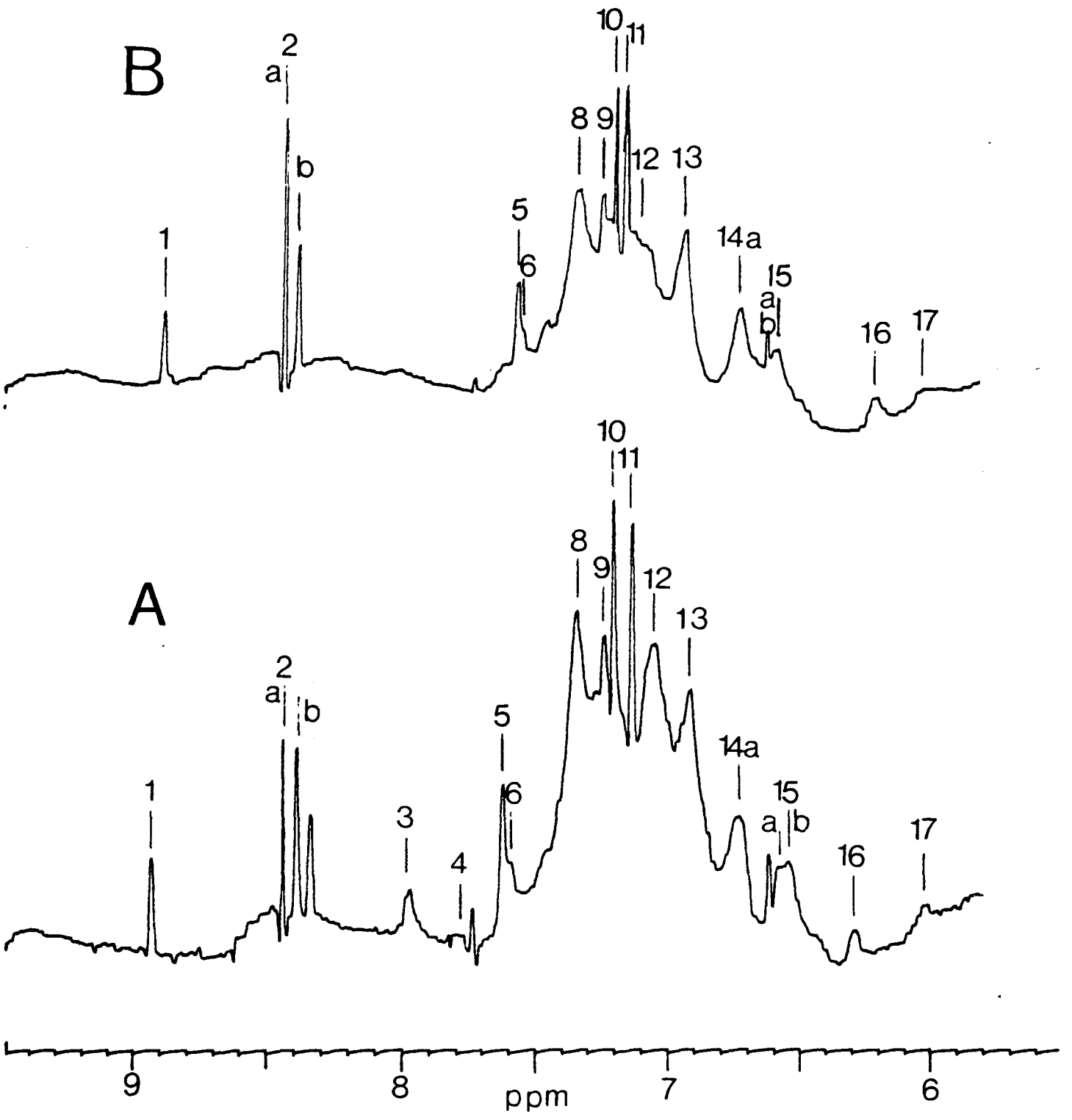

Figure 6.5 Resolution enhanced 300MHz spectra.

(A) 0.8mM PGK

(B) as (A) with 2mM 3-PG

Table 6.2 The effect of the addition of 3-phosphoglycerate on the 300MHz spectrum of 0.8mM PGK.

AROMATIC RESONANCE

ADDITION		1	5		3	4	6	12		2	9	10	11		7a	8	13		14a	14b	15a	15b	16	17	18			
2mM 3-PG		-.05	-.05		+.07 xx	xxx	-.04	+.05 x			+.01	-.01	+.03			+.01			-.03			+.03	-.10					

ALIPHATIC RESONANCE

ADDITION		21		23	24	25b		26	27	28		29	30	31	32		33	34	35		38							
2mM 3-PG						x												x										

histidine by the binding phosphate group. Other effects that appear to be connected to secondary binding, reflecting either a direct influence or a conformation change, are the upfield shifts of peaks 10 and 16 and the downfield shifts of peaks 9, 11 and 15b.

Work by Scopes (1978b) showed that ammonium sulphate increases the dissociation constant of PGK and 3-phosphoglycerate by competition, from a value of 30μM in its absence to about 600μM in the presence of 20mM sulphate, the ionic strength constant at 150mM. This effect was investigated here by addition of ammonium sulphate to the enzyme sample which had been titrated to a level of 1.2mM 3-PG and is illustrated by figure 6.3 and summarised in table 6.1. At a level of 100mM ammonium sulphate the histidine triangle peaks revert towards their original linewidths and positions. Thus peak 3 sharpens up and together with peak 12 shifts back 0.02ppm upfield and peak 6 shifts 0.01ppm upfield. In addition, upfield shifted resonances 14a and 16 return towards their original positions. None of the other histidine resonances is significantly affected and no effects are seen in the aliphatic region of the spectrum apart from a slight increase in broadening at position 36. When the level of ammonium sulphate is increased to 400mM, peak 3 sharpens further and, together with peaks 12 and 6, it returns to its original position. In short, all the effects of phosphoglycerate addition are reversed as the sulphate displaces the substrate. Notice that while phosphate forms strong H-bonds, sulphate does not.

Extrapolation of Scopes' figures gives phosphoglycerate-enzyme dissociation constants of about 3 and 13mM at respective ammonium sulphate concentrations of 100 and 400mM. This corresponds to 23% and 8% of the enzyme binding substrate and these values are used to compare the actual and theoretical chemical shifts of peak 3 in figure 6.4. These observations show that, as for the substrates, free and bound sulphates are in fast exchange on the nmr time scale.

Using the assignments of the previous chapter it is now seen that:

(1) Phosphoglycerate binds so as to affect the histidines in the "active site" i.e. resonances 3, 6, 12. This does not, however, prove that binding involves these histidines.

(2) Excess 3-PG binds so as to affect other histidines not at the active site

(3) SO_4^{2-} binds where 3-PG binds but does not have the same effect.

To locate the binding and to eliminate the possibility of all observations relating only to conformational change we now use paramagnetic probes.

6.3 A PARAMAGNETIC INVESTIGATION

The binding of triose phosphate is seen largely as the electrostatic interaction of an anion with a positively charged site on the enzyme. To define the sites of such anionic binding, the paramagnetic shift reagent $[Fe(CN)_6]^{3-}$ and the relaxation probe $[Cr(CN)_6]^{3-}$ were added to the protein. The former has been shown (Huang and Moore, 1983) to induce shifts predominantly by a contact interaction, while the effets of the latter extend beyond its immediate sphere of contact through long-range dipolar relaxation. As a preliminary experiment, diamagnetic $[Co(CN)_6]^{3-}$ was added to the protein. This diamagnetic probe has no direct shift or broadening effect in the region of its binding site but will show rather the effects of any conformational change it brings about in the protein. Thus it acts as a diamagnetic blank for the paramagnetic probes.

A preliminary investigation was made of the effect of $[Cr(CN)_6]^{3-}$ on the enzyme activity, measured spectrophotometrically as described in the materials and methods section. Two assay samples, containing 10mM 3-PG and 4mM ATP, were made up and 5mM $K_3Cr(CN)_6$ was added to one of them. To avoid spurious pH effects, the $K_3Cr(CN)_6$ stock solution had been buffered at pH7.5 and the pH of the assay mixture was checked at the end of the experiment. The activity of each sample was measured on the addition of 3µM fresh enzyme. Finally, the whole experiment was repeated. In both cases, the presence of $[Cr(CN)_6]^{3-}$ was found to increase the activity by about five fold.

This result is consistent with the findings of Scopes (1978a) that anions, and especially polyvalent anions, in moderate concentration, increase the activity of the enzyme, perhaps by helping to dislodge the otherwise very strongly bound product 1,3-P_2G. Furthermore, it confirms that $[Cr(CN)_6]^{3-}$ and, therefore, $[Fe(CN)_6]^{3-}$ and $[Co(CN)_6]^{3-}$, bind at the active site.

6.3.1 With $[Co(CN)_6]^{3-}$ and $[Fe(CN)_6]^{3-}$

In the first experiment, 1mM $K_3Co(CN)_6$ was added to a 1mM PGK solution, buffered at pH5.8 with 100mM sodium d_3-acetate. The effects on the spectrum are shown in figure 6.6 and summarised in table 6.3. Of the histidine triangle peaks, peak 4 broadens out completely, peak 6 shifts 0.02ppm downfield onto peak 5, but peaks 3 and 12 are unaffected. Other effects are observed at upfield shifted aromatic peak 15b, which shifts slightly downfield, and at upfield shifted methyl peak 37, which broadens slightly. On increasing the anion concentration to 10mM, peak 15b moves a further 0.03ppm downfield and fellow upfield shifted aromatic peaks 14a and 17 move 0.02ppm upfield and 0.03ppm downfield respectively. Some slight broadening is observed in the aliphatic region at lysine ε-CH_2 resonance 23, at surface methionine peak 27, (probably associated with residue 267) and at peaks 31 and 36.

In the second part of this experiment $K_3Fe(CN)_6$ was added to the sample. At a level of 1mM, it causes histidine triangle peaks 3 and 6 to shift 0.02ppm downfield, consistent

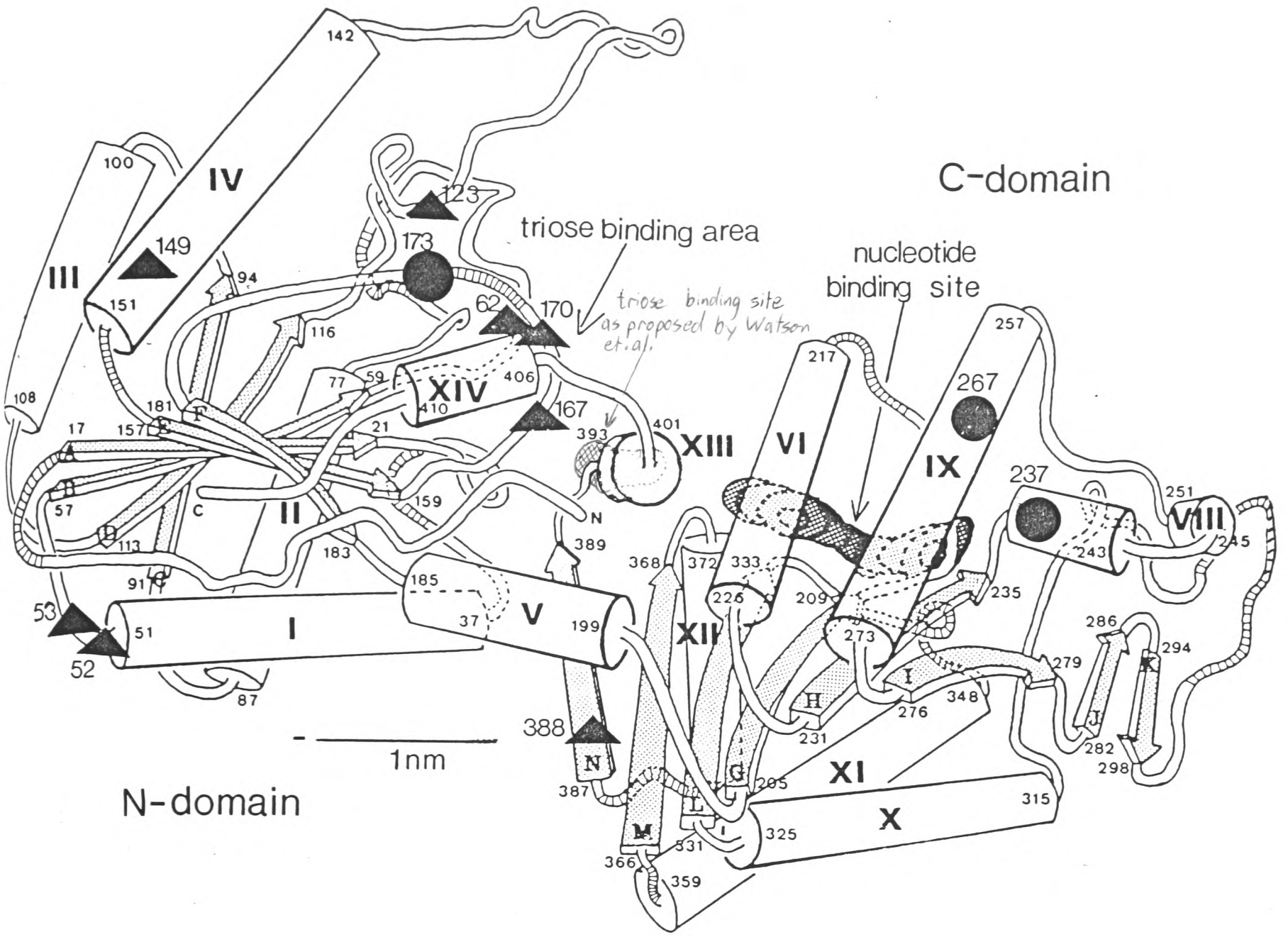

Fig. 6.6(i) Scheme of the open form of the yeast PGK molecules. The helices are denoted by cylinders, the sheet strands by arrows.
Histidine residues (▲) and methionine residues (●) are indicated.
(To assist interpretation of figure 6.6.)

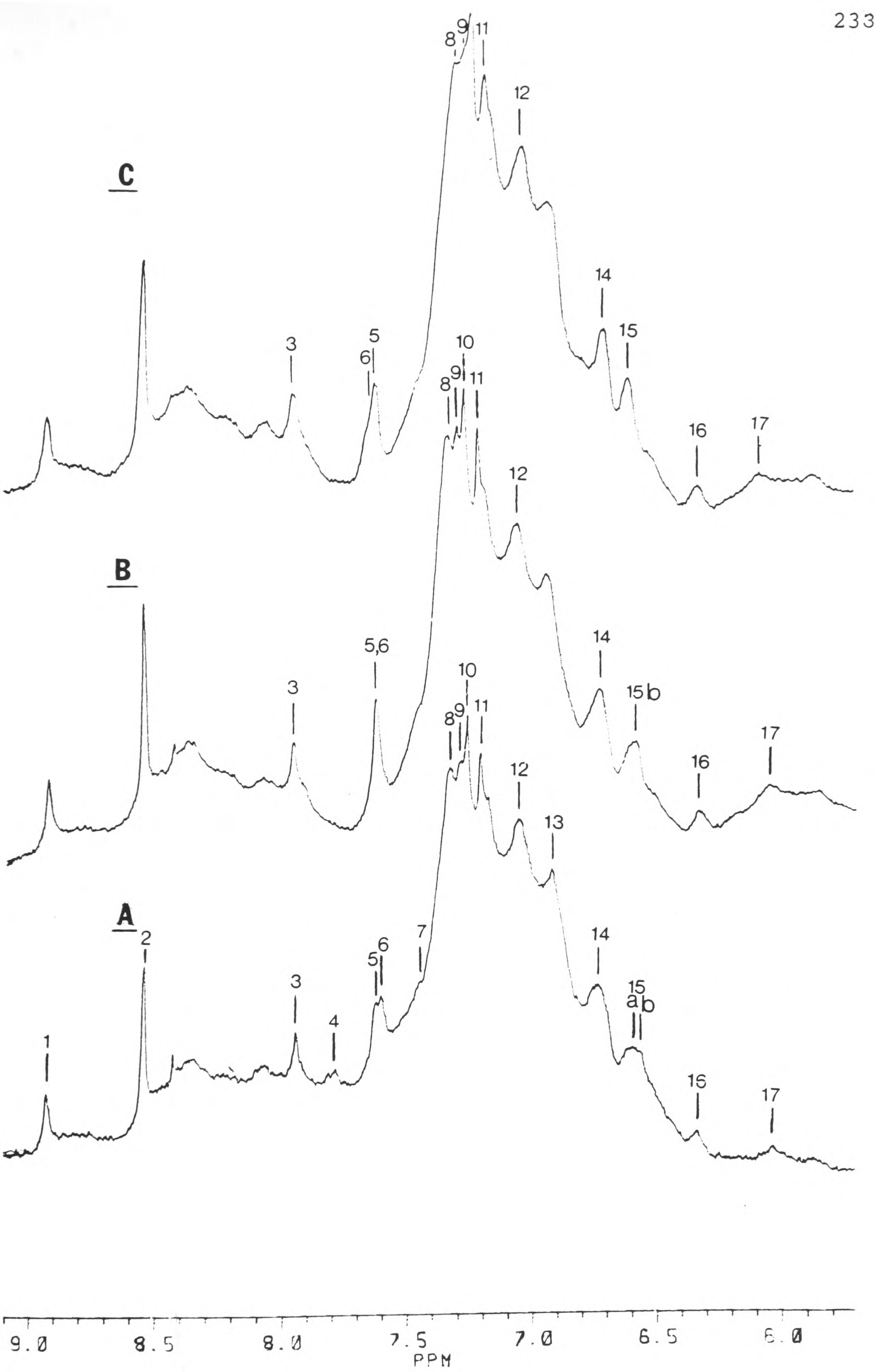

Figure 6.6 The aromatic region of the 300MHz spectrum showing the effect of $[Co(CN)_6]^{3-}$ and $[Fe(CN)_6]^{3-}$

(A) 1mM yeast PGK; (B) with 1mM $K_3Co(CN)_6$;

(C) with 10mM $K_3Co(CN)_6$; (D) as (C) with 1mM $K_3Fe(CN)_6$;

(E) as (C) with 10mM $K_3Fe(CN)_6$.

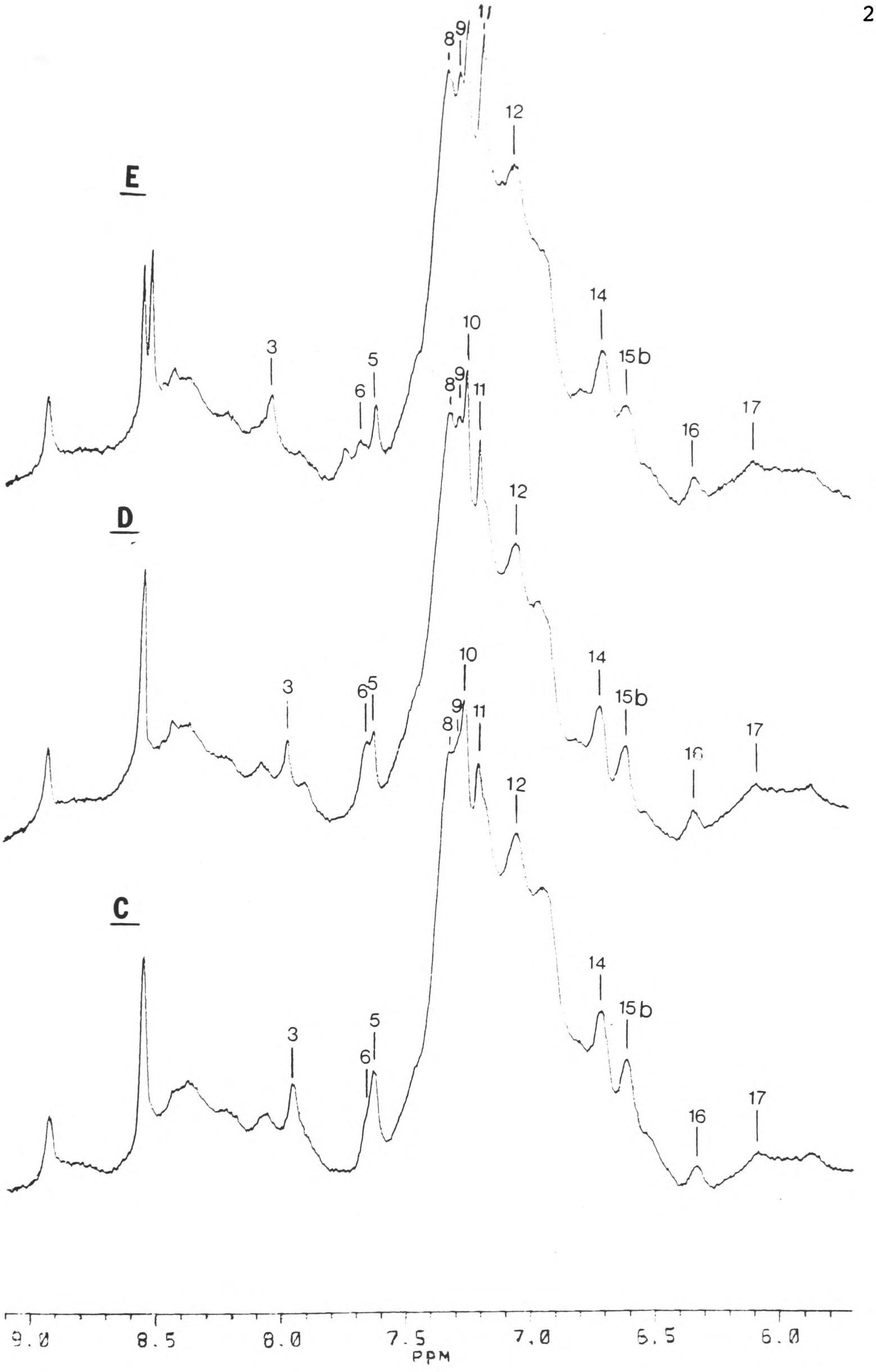
E
D
C
8
9
11
12
14
10
3
5
6
15b
16
17
9.0
8.5
8.0
7.5
7.0
6.5
6.0
PPM

Table 6.3 The effect of an addition of $K_3Co(CN)_6$ and then $K_3Fe(CN)_6$ on the 300MHz spectrum of a 1mM solution of yeast PGK.

AROMATIC RESONANCE

ADDITION		1	5		3	4	6	12		2	9	10	11		7a	8	13		14a	15a	15b	16	17	18				
(i) 1mM $[Co(CN)_6]^{3-}$						xxx	+.02														+.01							
(ii) 10mM $[Co(CN)_6]^{3-}$						xxx	+.02	+.01								x			-.02		+.04		+.03				
(iii) as (ii) + 1mM $[Fe(CN_6)]^{3-}$					+.02	xxx	+.04	±.00											-.02		+.03		+.03				
(iv) as (ii) + 10mM $[Fe(CN)_6]^{3-}$					+.10	-.03	+.04	+.03		-.03			-.01			+.02			-.02		+.03	+.02	+.07 x				

ALIPHATIC RESONANCE

ADDITION		101	102	104	105		21	23	24		25a	b		26	27	28		29	30	31	32		33	34	35	36	37	38
(i) 1mM $[Co(CN)_6]^{3-}$																											x	
(ii) 10mM $[Co(CN)_6]^{3-}$								x							x					x						x	x	
(iii) as (ii) + 1mM $[Fe(CN)_6]^{3-}$								x							x					x						x	x	
(iv) as (ii) + 10mM $[Fe(CN)_6]^{3-}$			+.01	+.03	+.03		+.10	x							x					x			+.30					+.02

with a limited displacement of $[Co(CN)_6]^{3-}$ from the binding site by the shift probe. On increasing the $[Fe(CN)_6]^{3-}$ level to 10mM, peak 3 is shifted further downfield, peak 4 re-appears, 0.03ppm upfield from its original position, and peak 12 shifts 0.03ppm downfield. A component of peak 2, and peak 11 shift upfield, providing evidence of secondary binding near the surface histidines 52 and 53 or 149. Peak 8 moves downfield as do upfield shifted aromatic peaks 16 and 17. In the aliphatic region, part of the lysine ε-CH_2 peak moves about 0.10ppm downfield and components of the methyl peak 34/35 show a downfield shift of up to about 0.3ppm downfield. Three of the αCH peaks and the upfield shifted methyl peak 38 also display downfield shifts.

In conclusion, it is seen that:

(i) resonances 3 and 12 are shifted by the paramagnetic but not by the diamagnetic reagent in what is, therefore, a direct influence of the anion rather than a long range conformational influence;

(ii) resonances 4 and 6 <u>are</u> influenced by the diamagnetic probe but nevertheless reveal the effect of the paramagnetic probe, again suggesting a direct rather than a long range influence.

Thus anionic binding is located at the active site of the molecule

(iii) Binding at high concentrations reveals additional site(s) not at the substrate region.

The effects at the upfield aromatic and methyl peaks reveal conformational influence, perhaps linked to closure of the molecule.

6.3.2 With $[Fe(CN)_6]^{3-}$ only

In the second anionic probe experiment, the effect of $[Fe(CN)_6]^{3-}$ on the 300MHz spectrum of yeast PGK was considered in detail. The potassium salt of the anion was added to a 1.1mM solution of the enzyme buffered at pH5.8 with sodium d_3-acetate. The addition took the form of a titration giving ratios of $[Fe(CN)_6]^{3-}$: protein of 1,2,5 and 10. The effects are illustrated in figures 6.7 and 6.8, summarised in table 6.4 and displayed graphically in figure 6.9.

At the 1:1 ratio, strong evidence of binding at the primary anionic site is provided by the shifts of histidine triangle peaks 3,12,4 and 6. Resonances 3 and 12 were unaffected by equimolar $[Co(CN)_6]^{3-}$ while resonance 4 was broadened, rather than shifted, and resonance 6 was shifted only 0.02ppm, downfield. Further effects in the aromatic region are at peak 7 and in the upfield shifted region at peaks 14a,15b,17 and 18. Peaks 14a,15b and 17 are all affected by the diamagnetic $[Co(CN)_6]^{3-}$, and the effect of $[Fe(CN)_6]^{3-}$ on these peaks indicates a conformational influence rather than a direct paramagnetic influence. In the aliphatic region a component of peak 21, the lysine ε-CH_2 resonance, moves 0.03ppm upfield and the upfield components of peaks 30/31 and 34/35 increase in intensity. Broadening is seen at peak 108, and this resonance may, therefore, represent the βCH_2 group of one of the active site histidines.

At the 2:1 ratio, the effects at active site histidine peaks 3,12 and 6 increase, but peak 4 moves downfield, back

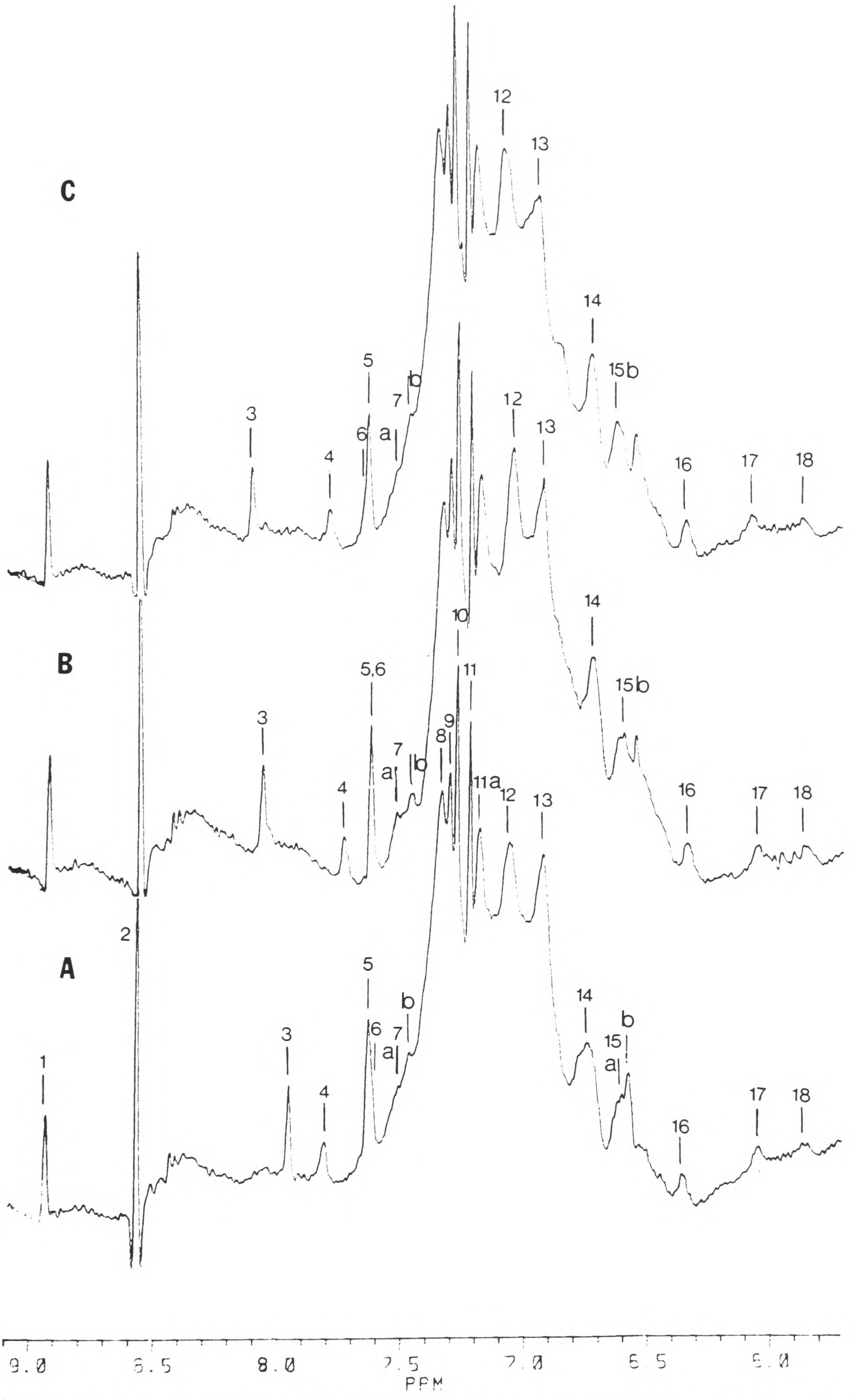

Figure 6.7 The aromatic region of the spectrum showing the effect of the addition of $K_3Fe(CN)_6$ to 1.1mM yeast PGK in 100mM sodium d_3-acetate at pH5.8. Resolution enhanced, 300MHz. $[Fe(CN)_6]^{3-}$:protein ratio:

(A) 0:1, (B) 1:1, (C) 2:1, (D) 5:1, (E) 10:1.

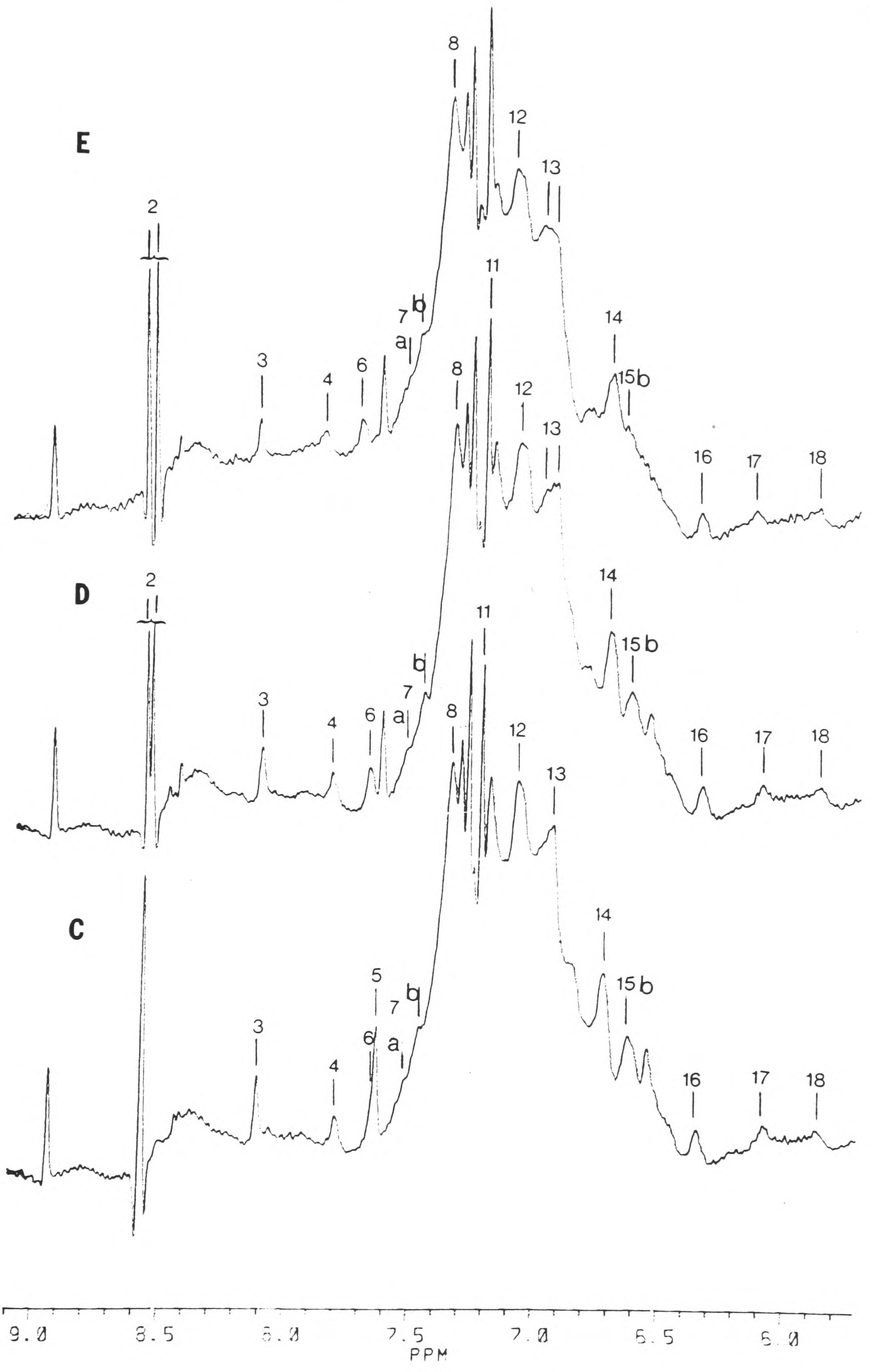
E
D
C
2
3
4
6
7
a
b
8
11
12
13
14
15b
16
17
18
5
9.0
8.5
8.0
7.5
7.0
6.5
6.0
PPM

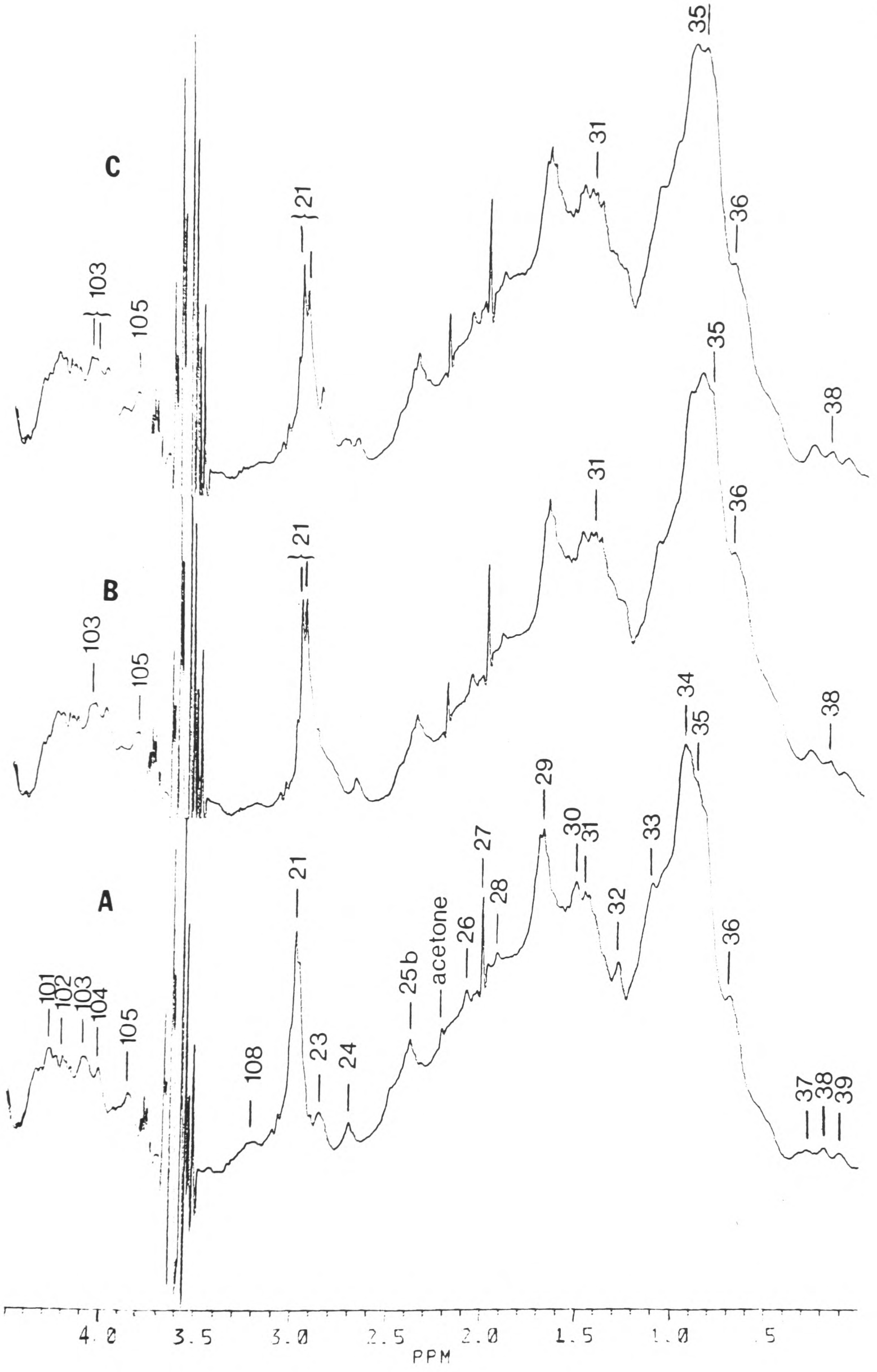

Figure 6.8 The aliphatic region as for figure 6.7.

$[Fe(CN)_6]^{3-}$:protein ratio:

(A) 0:1, (B) 1:1, (C) 2:1, (D) 5:1, (E) 10:1.

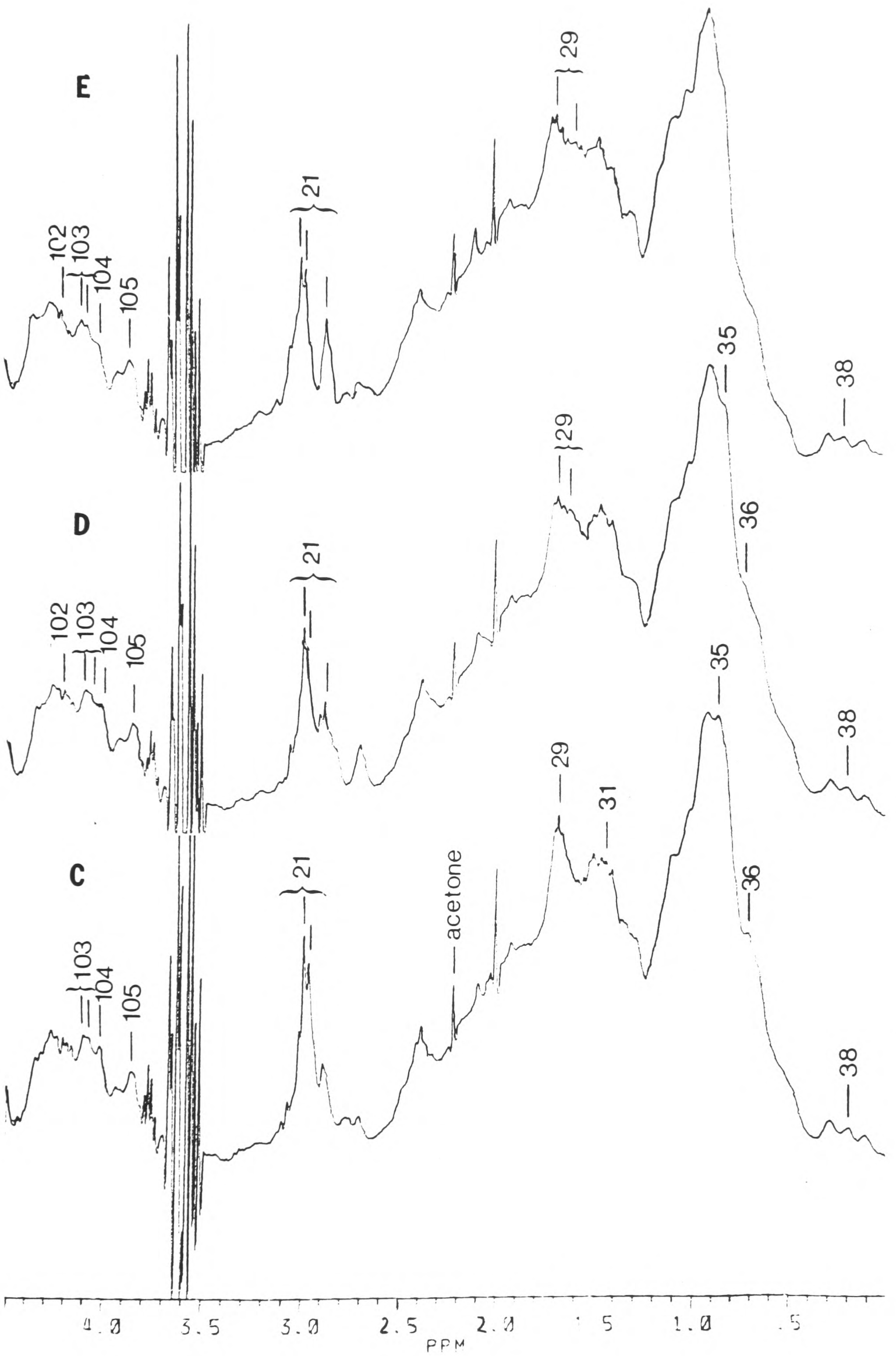
E
102
103
104
105
21
29
35
38
D
102
103
104
105
21
29
31
35
36
38
C
103
104
105
21
acetone
29
31
35
36
38
4.0
3.5
3.0
2.5
2.0
1.5
1.0
.5
PPM

Table 6.4 The effect of the addition of $K_3Fe(CN)_6$ on the 300MHz spectrum of a 1.1mM solution of yeast PGK. (+) signifies an increase in intensity.

AROMATIC RESONANCE

RATIO $[Fe(CN)_6]^{3-}$: PGK	1	5	3	4	6	12	2	9	10	11	7a	b	8	13	14a	15a	b	16	17	18
1:1			+.11	-.06	+.03	-.01					+.02	-.01			-.02		+.05		+.01	-.01
2:1			+.15	-.02	+.05	+.02					.00	.00	+.01	xx	-.02		+.07	-.02	+.03	-.01
5:1			+.15	+.02	+.08	+.02	-.02			-.01	+.03	-.01	+.01	+.03 xx	-.03		+.07	-.02	+.05	-.01
10:1	+.01	+.01	+.16	+.05	+.11	+.04	-.04			-.02	+.04	+.01	+.02	+.04 xx	-.04		+.09	-.02	+.08	.00

ALIPHATIC RESONANCE

RATIO $[Fe(CN)_6]^{3-}$: PGK	100	101	102	103	104	105	108	21	23	24	25	26	27	28	29	30	31	32	33	34	35	36	37	38
1:1							xx	-.03									++				++			
2:1				-.01 -.02			xx	-.10									+++				+	+.02		+.01
5:1				+.01 -.02		+.01	xx	-.11							-.07		+++				0	+.03		+.01
10:1			+.03	+.02 -.01	+.03	+.02	xx	-.13							-.10		+++					+.03		+.02

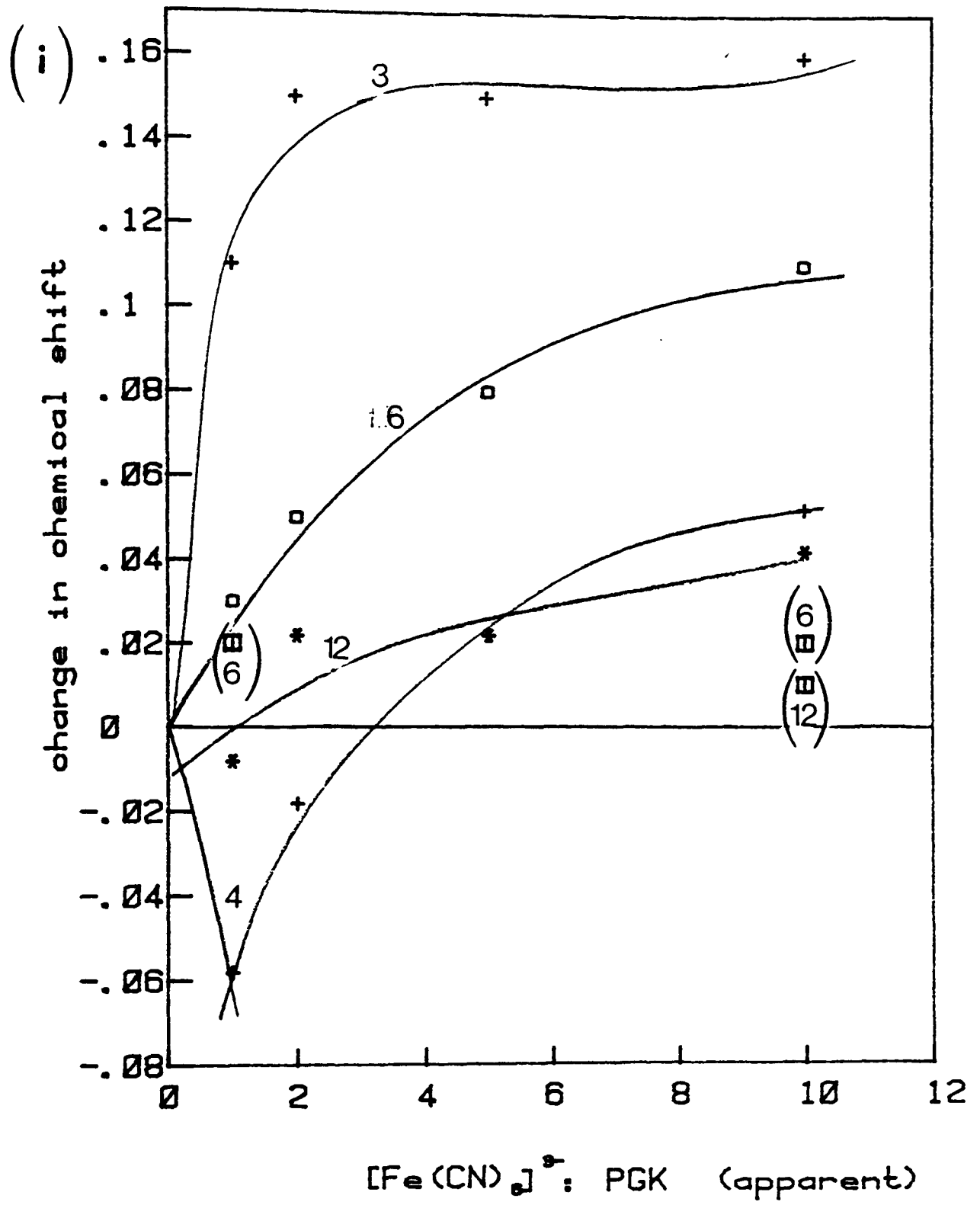

Figure 6.9 The change in chemical shift of various resonances of the protein spectrum as a function of the $[Fe(CN)_6]^{3-}$:PGK ratio. The purely diamagnetic influence of $[Co(CN)_6]^{3-}$ is indicated in boxes.

(i) The active site histidines.

Symbols: (+) 3,4; (□) 6; (*) 12, and $\left(\frac{\square}{n}\right)$ shift induced by diamagnetic blank $[Co(CN)_6]^{3-}$.

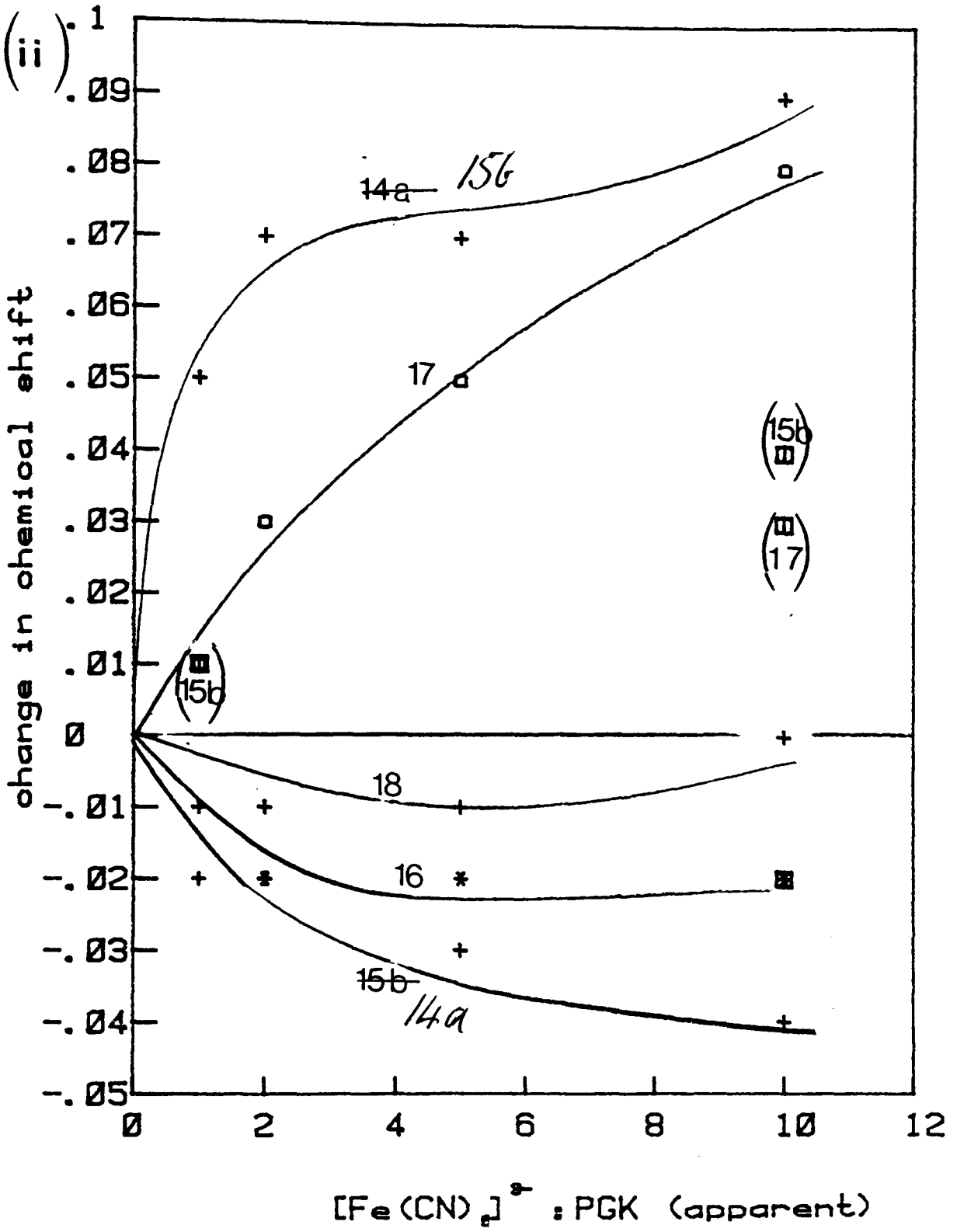

Figure 6.9(ii) The upfield aromatic resonances.

Symbols: (+) 14a, 15b, 18;

(*) 16, and

(□) 17.

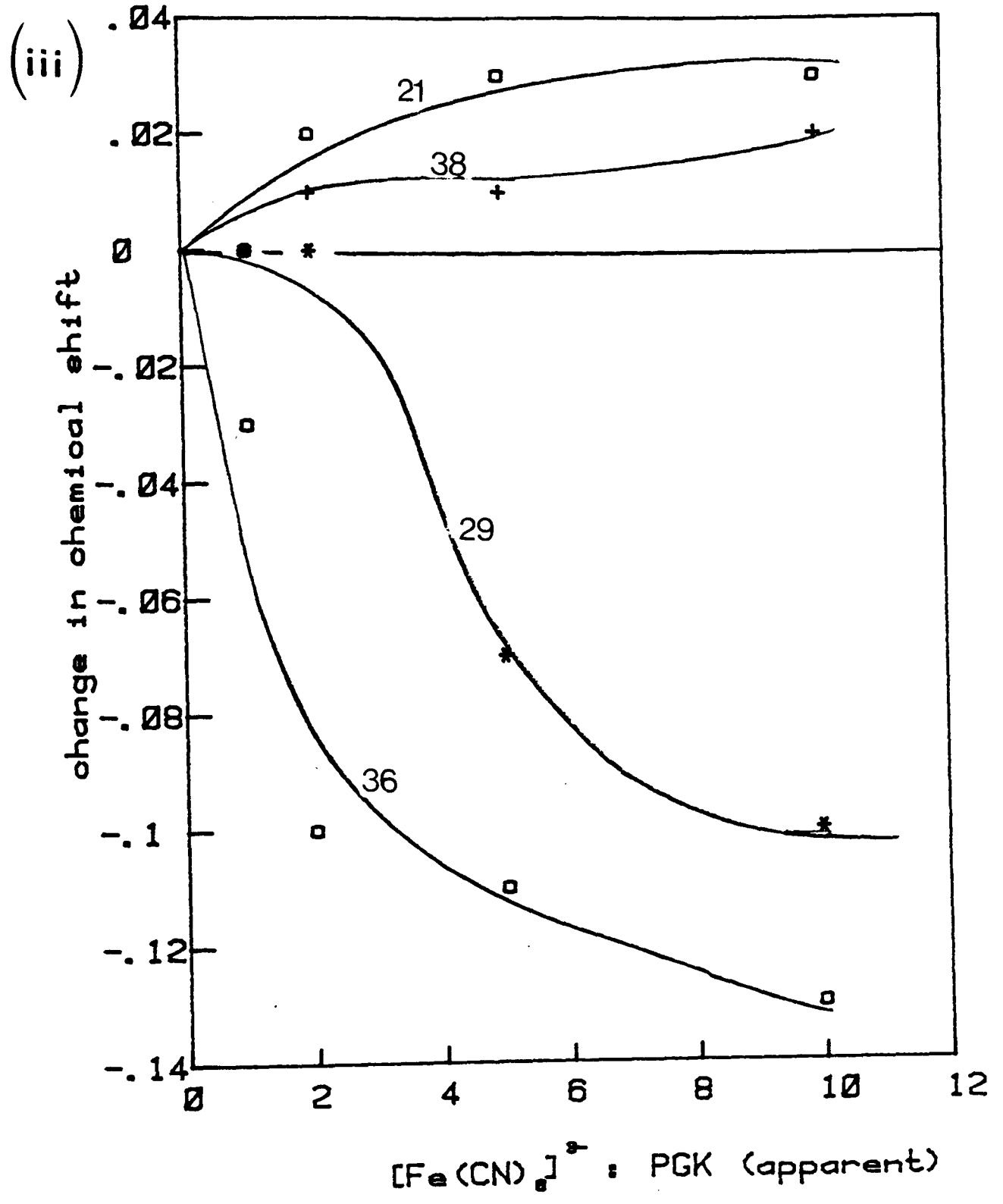

Figure 6.9(iii) Aliphatic resonances.

Symbols: (□) 21,36; (*) 29, and (+) 38.

towards its original position. This suggests that more of the paramagnetic anion is binding in the cleft of the protein, but at a different site from the first equivalent. Other effects observed are that peaks 7a and 7b return to their original positions, that peak 8 shifts downfield and that peak 13 broadens. Peak 15b shifts further downfield, 0.07ppm from its original position and peaks 16 and 17 shift in opposite directions. Among the aliphatics, the upfield movement at surface lysine peak 21 increases as does the increase in intensity at peak 31, while peak 35 diminishes slightly. Peak 36, which was broadened by the addition of $[Co(CN)_6]^{3-}$, is now shifted slightly downfield as is the upfield shifted methyl peak 38. Finally, peak 103 at 4.1ppm, a possible αCH resonance, splits.

At the 5:1 ratio, the following effects are observed. Peak 4 continues to shift downfield, indicative of more secondary binding in the cleft of the protein. Peak 6 also continues to move downfield. Upfield shifts are noted for a component of peak 2 and for peak 11, which are both surface, titratable histidine resonances, assigned to residues 52,53 or 149. In addition, peak 7a and a component of peak 13 shift 0.03ppm downfield, while peaks 7b and 14a move slightly upfield. Upfield aromatic peak 17 continues to move downfield. In the aliphatic region a component of peak 29 moves 0.07ppm upfield, αCH peak 105 shifts slightly and the effects already observed at peaks 21,31 and 36 increase very slightly. The intensity of peak 35 returns to its original value.

Finally, at a ratio of 10:1 anion:protein the following effects were observed. The shifts already noted for peaks 3,12,4 and 6 increase and peak 11 and the upfield component of peak 2 move further upfield. Peaks 7a and b and peak 8 shift slightly while peaks 1 and 5 shift for the first time, suggesting that excess anion is now binding on the surface of the protein near histidine 123. The shifts at peaks 13 and 14a increase slightly, as do those of the upfield aromatic area at peaks 15b and 17. In the aliphatic region, the movement at peaks 21,29 and 38 continues, and further alterations are seen in the αCH region.

The dependence of chemical shift of the nmr spectrum of PGK on the concentration of $[Fe(CN)_6]^{3-}$ seen in this titration is presented graphically in figure 6.9 which includes an indication of the purely diamagnetic effects observed on the addition of $[Cr(CN)_6]^{3-}$. The shape of the various plots indicates that there are at least two binding sites for the anion. Peaks 3 and 15b are seen to be those most clearly influenced by binding at the first site and are replotted in figure 6.10. To determine the $[Fe(CN)_6]^{3-}$:PGK ratio more accurately, the initial slope of each curve is extrapolated and its point of intersection with the limiting (y) value of the curve is noted. This gives the position of anion/enzyme equimolarity, and the scale of the x-axis is adjusted accordingly.

Using the data from figure 6.10, the dissociation constant of $[Fe(CN)_6]^{3-}$ from its primary site on PGK is evaluated. The theoretical basis of the calculation is given in appendix II and the figures are presented in table 6.5.

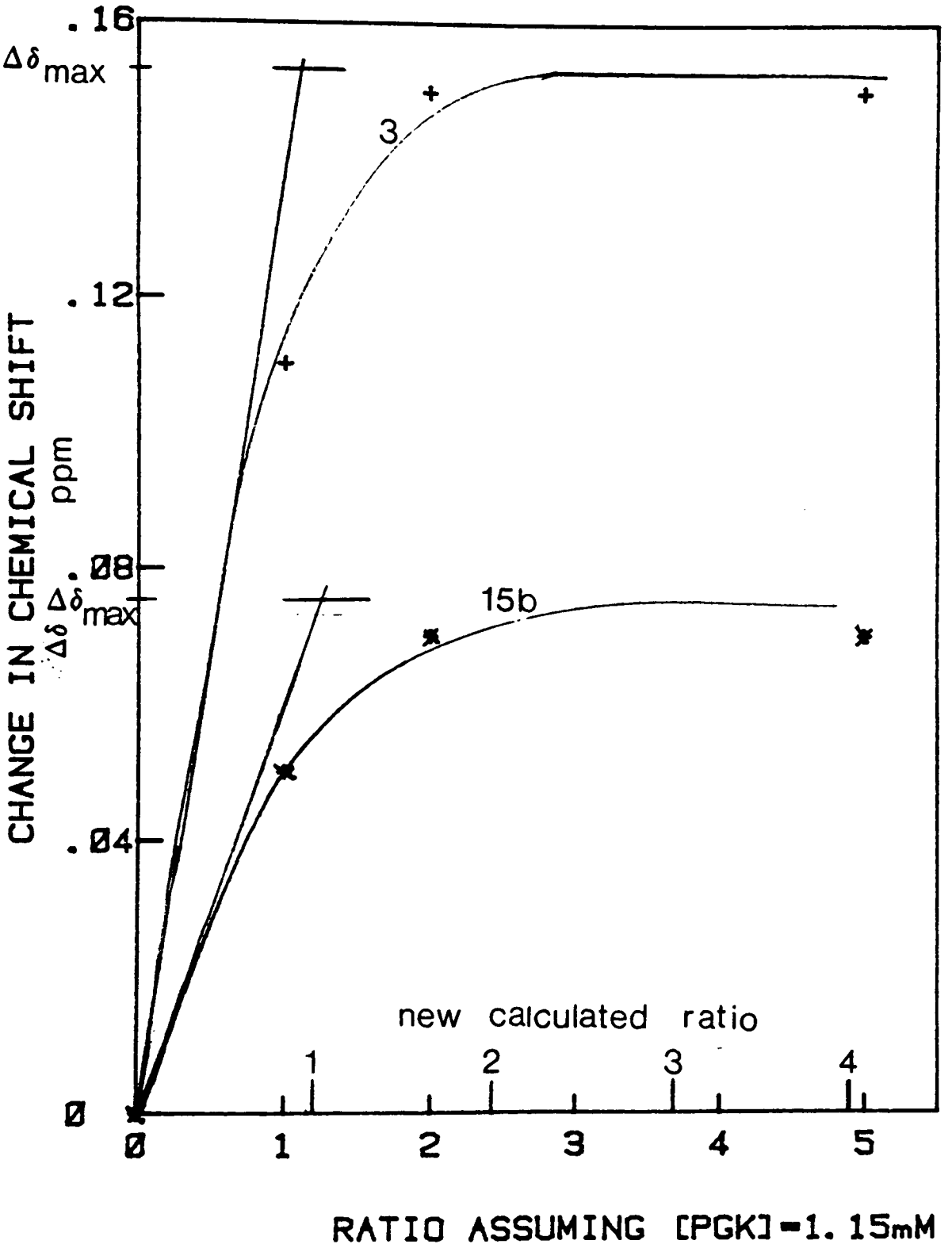

Figure 6.10 The chemical shift of peaks 3 and 15b plotted as a function of both the observed and the calculated $[Fe(CN)_6]^{3-}$:PGK ratio.

Table 6.5 Evaluation of the primary dissociation constant of $[Fe(CN)_6]^{3-}$ PGK from the change in chemical shift of peaks 3 and 15b

$[Fe(CN)_6]^{3-}$:PGK	vol.70mM $K_3Fe(CN)_6$ µl	$[[Fe(CN)_6]^{3-}]_t$ mM	$[PGK]_t$ mM	peak 3			peak 15b		
				$\Delta\delta/\Delta\delta max$ -	x -	y mM	$\Delta\delta/\Delta\delta max$ -	x -	
0.25	1.67	0.333	1.33	0.273	0.376	-0.030	0.240	0.316	0.01
0.50	3.33	0.660	1.32	0.487	0.949	0.017	0.443	0.795	0.07
0.75	5.00	0.986	1.31	0.687	2.195	0.086	0.643	1.801	0.14
1.00	6.67	1.308	1.31	0.807	4.181	0.251	0.800	4.000	0.26
1.25	8.33	1.629	1.30	0.893	8.346	0.468	0.914	10.628	0.44
1.50	10.00	1.944	1.29	0.960	24.00	0.706	0.971	33.483	0.69

$x = \Delta\delta/\Delta\delta max(1-\Delta\delta/\Delta\delta max)^{-1}$

$y = [[Fe(CN)_6]^{3-}]_t - [PGK]_t.\Delta\delta/\Delta\delta max$

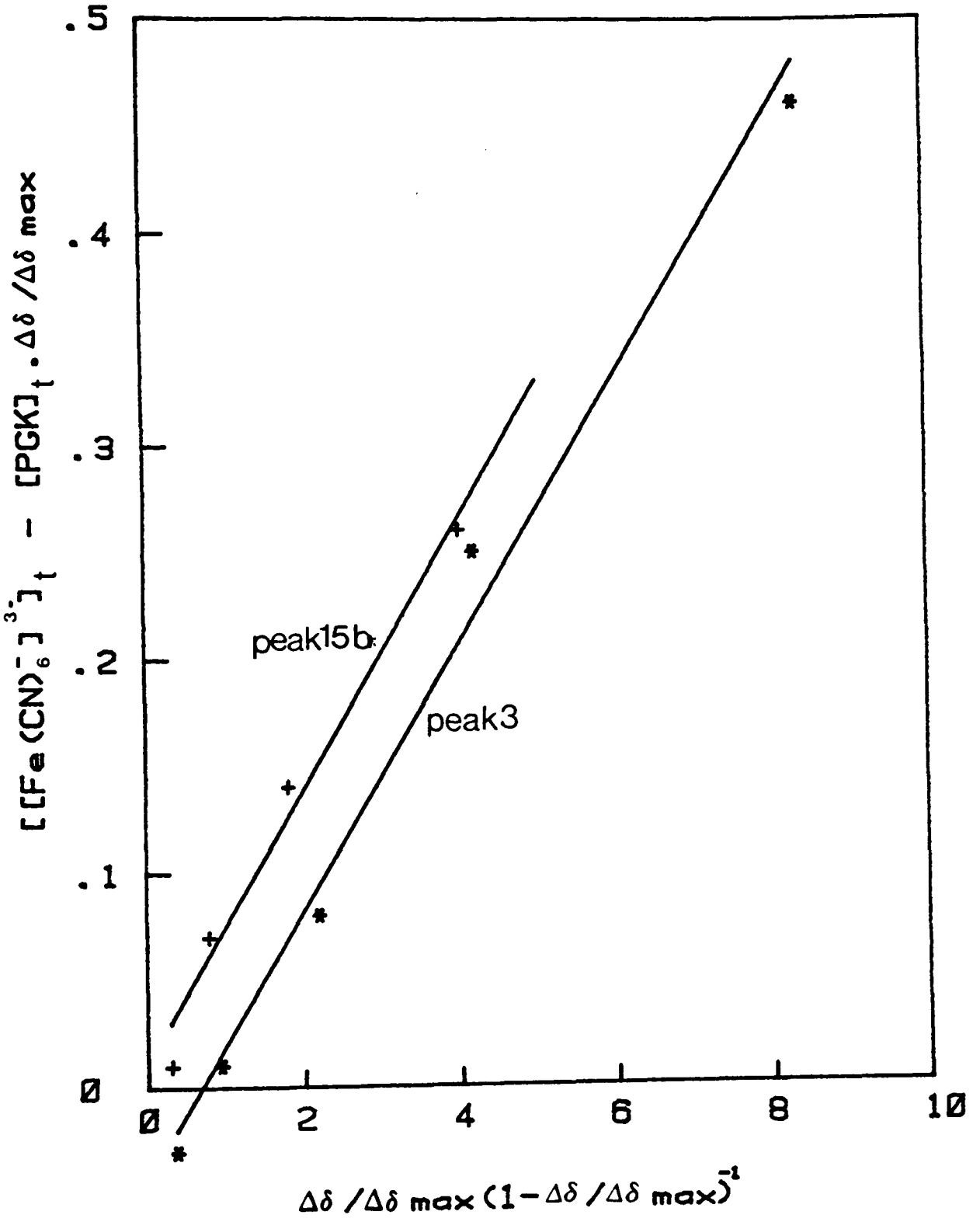

Figure 6.11 Evaluation of the dissociation constant of the primary complex of $[Fe(CN)_6]^{3-}$ and PGK.

The resulting x and y values are plotted in figure 6.11 and the slope evaluated. Thus the primary dissociation constant for $[Fe(CN)_6]^{3-}$ and PGK is calculated to be 63μM (I=100mM).

Returning to figure 6.9, peak 4 is seen to be moved first in one direction by $[Fe(CN)_6]^{3-}$ and then in the opposite direction by binding of the anion at the second site. Thus peak 4 is ideal for examining the strength of secondary binding. Extrapolation of the initial curve indicates that peak 4 is shifted a total of 0.08ppm upfield by the binding of $[Fe(CN)_6]^{3-}$ at the primary site and therefore this value is taken as the baseline for shifts caused by secondary binding. The x-value of this origin corresponds to the addition of one molar equivalent of $[Fe(CN)_6]^{3-}$ to the protein, i.e. a calculated ratio of 1.0 which is equivalent to an apparent ratio of 1.2. The curve is replotted in figure 6.12.

The dissociation constant is evaluated as before, the data from figure 6.12 being presented in table 6.6, and the subsequent x and y values being plotted in figure 6.13. Thus the dissociation constant for binding at the secondary anionic site is calculated as 1.0mM (I=100mM).

The dissociation constants calculated for $[Fe(CN)_6]^{3-}$ at the first and second sites are compared with those determined by Scopes' gel filtration study (1978b) in table 6.7. As expected, binding at the first site is strongest for the polyvalent triose phosphate, and for $[Fe(CN)_6]^{3-}$. Binding at a second site is at least as strong for the paramagnetic probe as it is for metal-nucleotide.

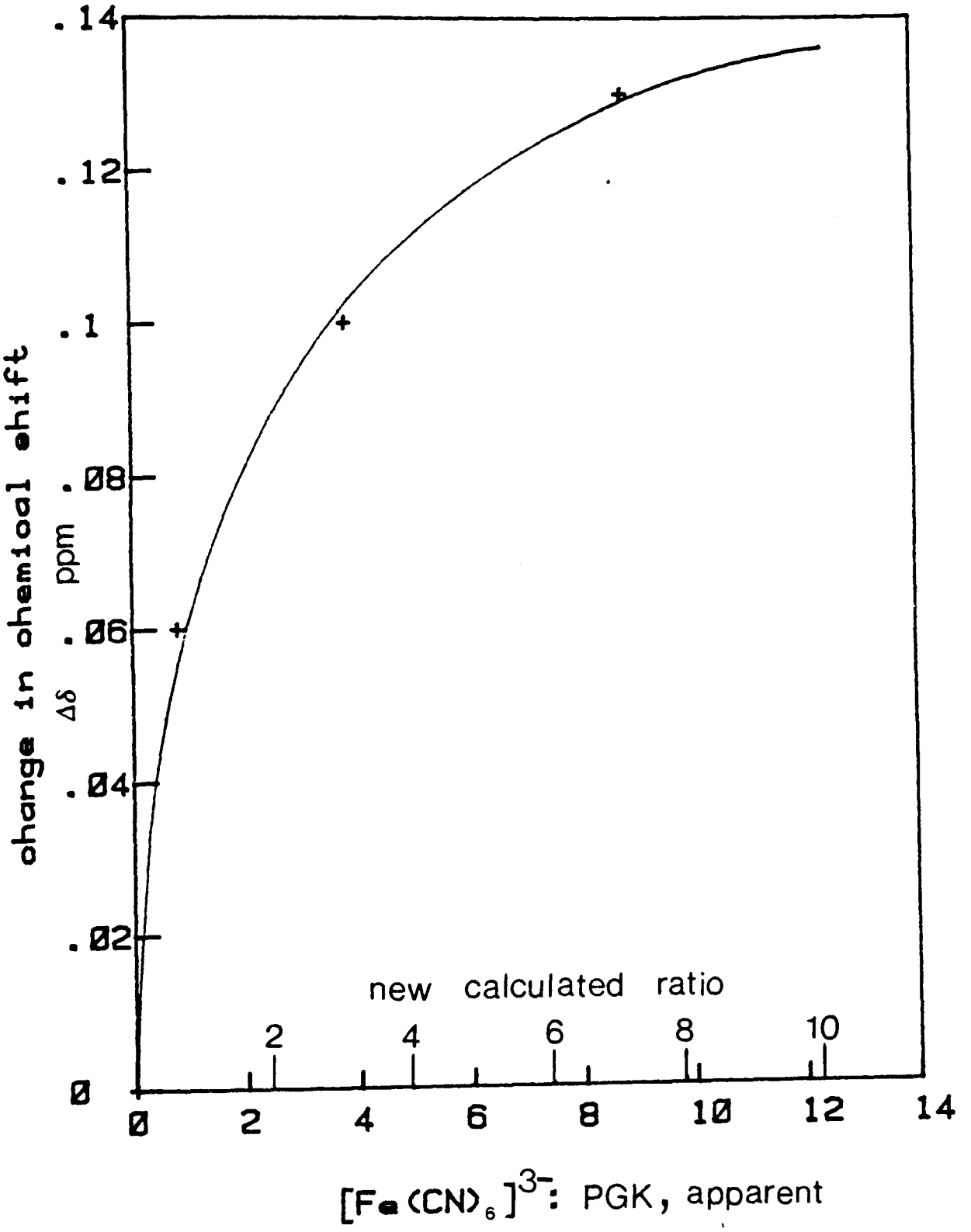

Figure 6.12 The change in chemical shift of peak 4 on the addition of $K_3Fe(CN)_6$. The origin represents the system after the addition of one equivalent of $[Fe(CN)_6]^{3-}$ to the enzyme (see figure 6.9).

Table 6.6 Evaluation of the secondary dissociation constant of $[Fe(CN)_6]^{3-}$ and PGK from the change in chemica shift of peak 4. It is assumed that the first equivalent of $[Fe(CN)_6]^{3-}$ is bound at the primary site and is not available for binding at the second. x and y are as for Table 6.5

$[Fe(CN)_6]^{3-}$:PGK	total volume 70mM $K_3Fe(CN)_6$ µl	total available $[[Fe(CN)_6]^{3-}]$ mM	[PGK] total mM	$\Delta d/\Delta\delta max$	x	y mM
1	13.33	1.284	1.284	0.500	1.00	0.64
2	20.00	2.522	1.261	0.650	1.86	1.70
3	26.67	3.716	1.239	0.729	2.69	2.81
4	33.33	4.869	1.217	0.789	3.74	3.91
5	40.00	5.983	1.197	0.836	5.10	4.98
6	46.67	7.059	1.177	0.864	6.35	6.04
7	53.33	8.099	1.157	0.893	8.35	7.07

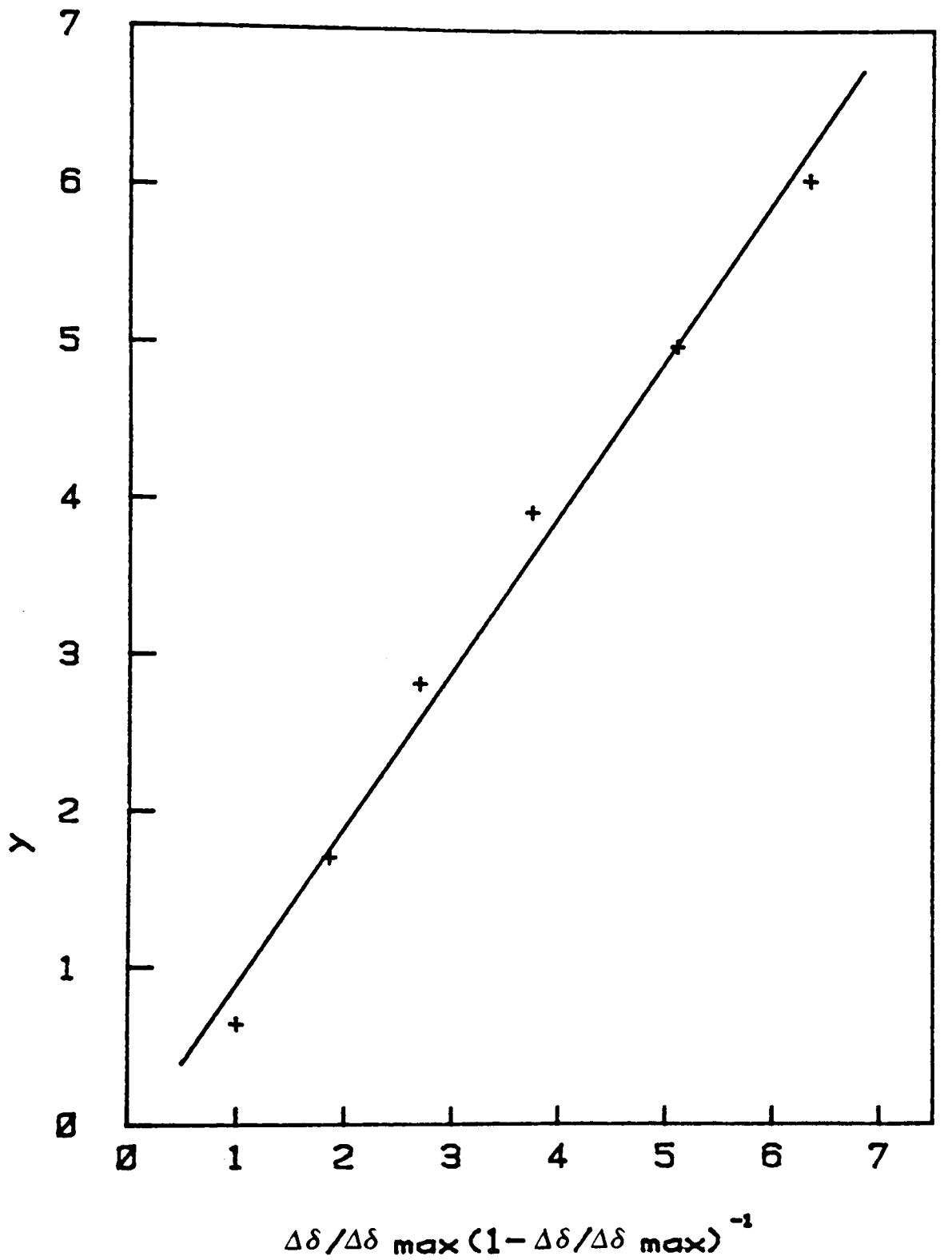

Figure 6.13 Evaluation of the dissociation constant of the secondary complex of $[Fe(CN)_6]^{3-}$ and $[PGK\text{-}[Fe(CN)_6]^{3-}]$.

$y = [[Fe(CN)_6]^{3-}]_t - [PGK]_t \Delta\delta/\Delta\delta max$.

1st site ligand	dissociation constant(mM)	2nd site ligand	dissociation constant(mM)
$[Fe(CN)_6]^{3-}$	0.06	$[Fe(CN)_6]^{3-}$	1.0
3-PG	0.03	MgADP	1.0
HPO_4^{2-}	1.1	MgATP	4.0
SO_4^{2-}	1.6		

Table 6.7 Comparison of the dissociation constant of $[Fe(CN)_6]^{3-}$ and yeast PGK, I=100mM, pH6.0 with those of various ligand, calculated by Scopes (1978b), I=150mM, pH7.5.

It is noted here that under Scopes' conditions, 75% 3-PG is calculated to be in the (4-) form. In the present work, at pH 6.0, 85% 3-PG is trivalent, and thus its binding to PGK is weakened. Indeed, evidence in the following section suggests that $[Fe(CN)_6]^{3-}$ replaces 3-PG from the active site.

In conclusion, it is seen that:

(i) from the effects on resonances 3,12,4 and 6, the area including histidines 62,167 and 170 is confirmed as the primary site of anion binding,

(ii) further effects at these resonances show that the second anionic site is also found in this region,

(iii) with an excess of $[Fe(CN)_6]^{3-}$, effects at resonances 2 and 11 reveal binding near the surface histidines 52,53 or 149 and effects at resonances 1 and 5 reveal binding at histidine 123,

(iv) evidence of continuing conformational changes on the addition of anion is provided by the numerous effects seen among the upfield aromatic and methyl resonances.

Once again, it is recalled that peak 7a is assigned (Scheffler and Cohn, 1986) to trp 308, a surface residue which is located near the nucleotide site, in the active groove of the protein. Thus, peak 7a is seen to be affected by binding of $[Fe(CN)_6]^{3-}$ in the active groove.

6.3.3 With $[Fe(CN)_6]^{3-}$, ATP and 3-PG

The third paramagnetic experiment examined the competition and interaction between $[Fe(CN)_6]^{3-}$ and substrate ligands. Equimolar amounts of $K_3Fe(CN)_6$, ATP and then 3-PG were added to a solution of 1.2mM PGK in 100mM sodium d_3-acetate. Finally, the concentration of $K_3Fe(CN)_6$ was increased to give a ten fold excess. The resolution enhanced 300MHz proton spectra are shown in figures 6.14 and 6.15 and the effects summarised in table 6.8.

On the addition of equimolar $[Fe(CN)_6]^{3-}$, evidence of binding at the active site is given by the shifts of resonances 3,4 and 6 in the same directions and by similar amounts as on the equimolar addition in the previous section, with the exception that the very slight upfield shift of peak 12 is not observed here. Also as before, conformational effects are indicated by shifts at upfield aromatic resonances 14a, 15b and 17. Effects in the aliphatic region at peaks 108 and 21 are the same as before, no effects are seen at peaks 31 and 35 and additional effects are seen at peaks 23 and 24.

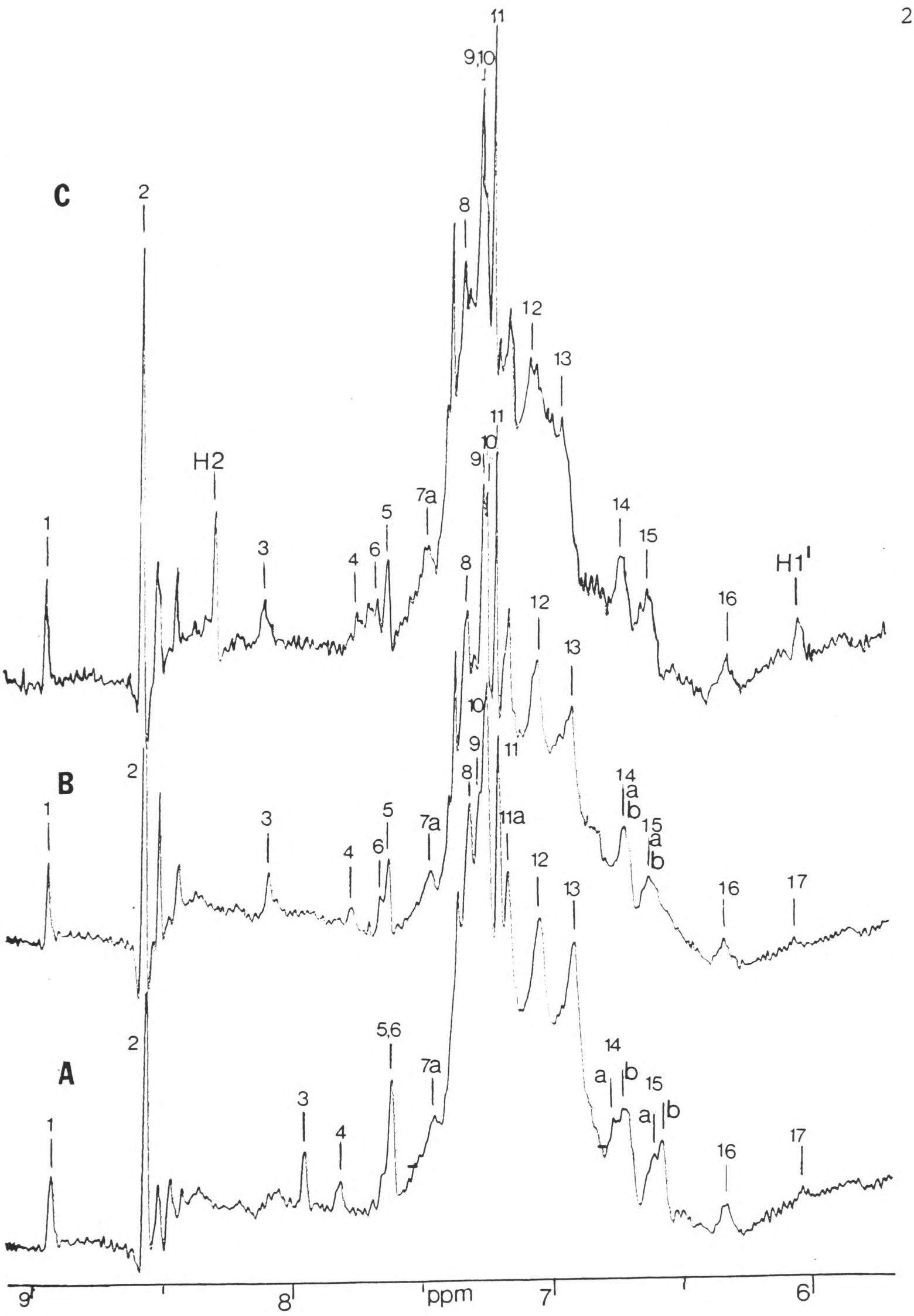

Figure 6.14 The aromatic region of the spectrum showing the effect of various anions. Resolution enhanced, 300MHz.

(a) 1.2mM PGK, 100mM sodium d_3-acetate, pH5.8.

(b) as (a) with 1:1$[Fe(CN)_6]^{3-}$:protein;

(c) as (b) with 1:1 ATP;

(d) as (c) with 1:13-PG;

(e) as (d) with 10:1$[Fe(CN)_6]^{3-}$ (total).

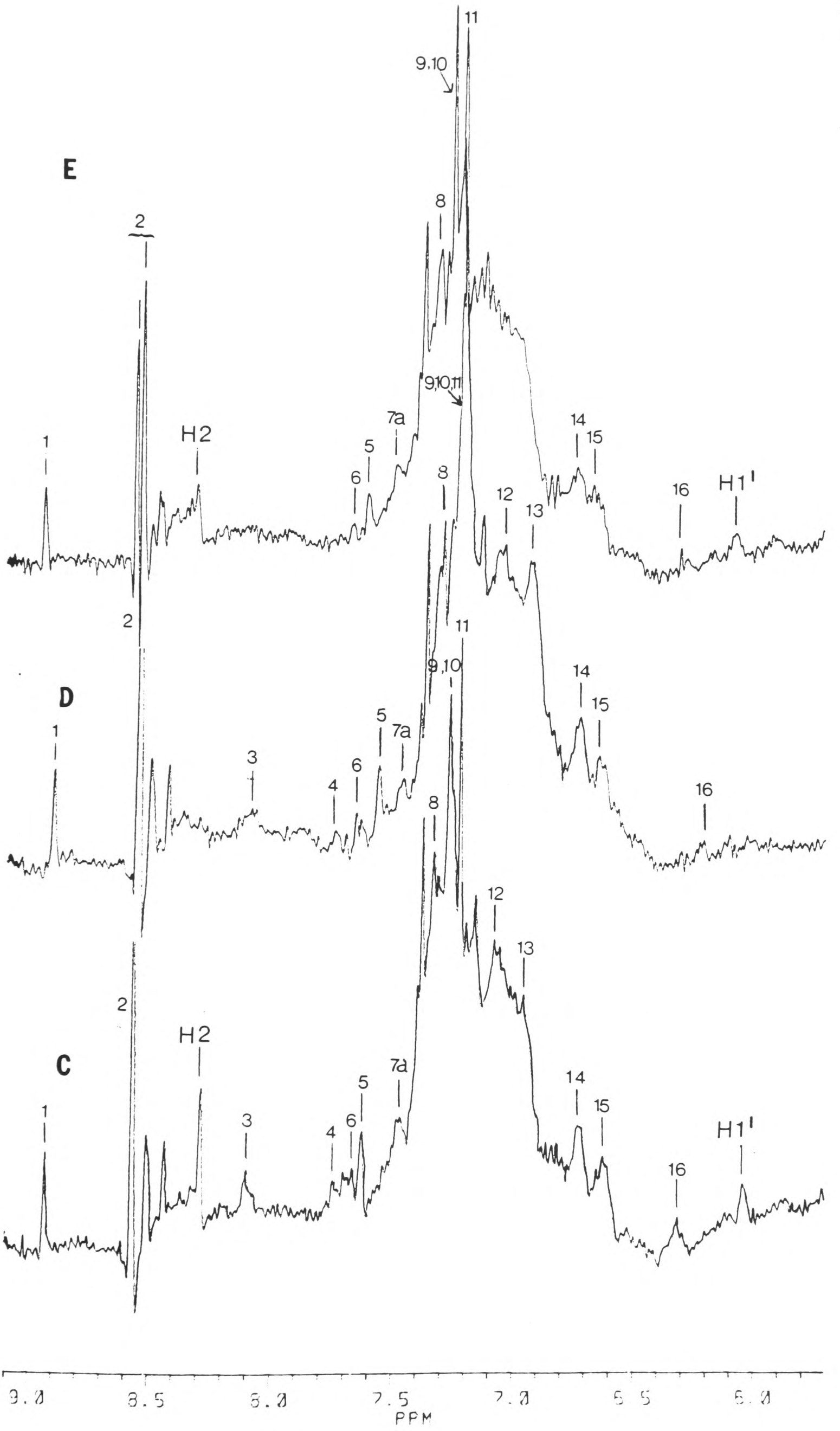
E
D
C
1
2
H2
6
5
7a
9,10
11
8
14
15
12
13
16
H1'
3
4
9,10,11
PPM
9.0
8.5
8.0
7.5
7.0
6.5
6.0

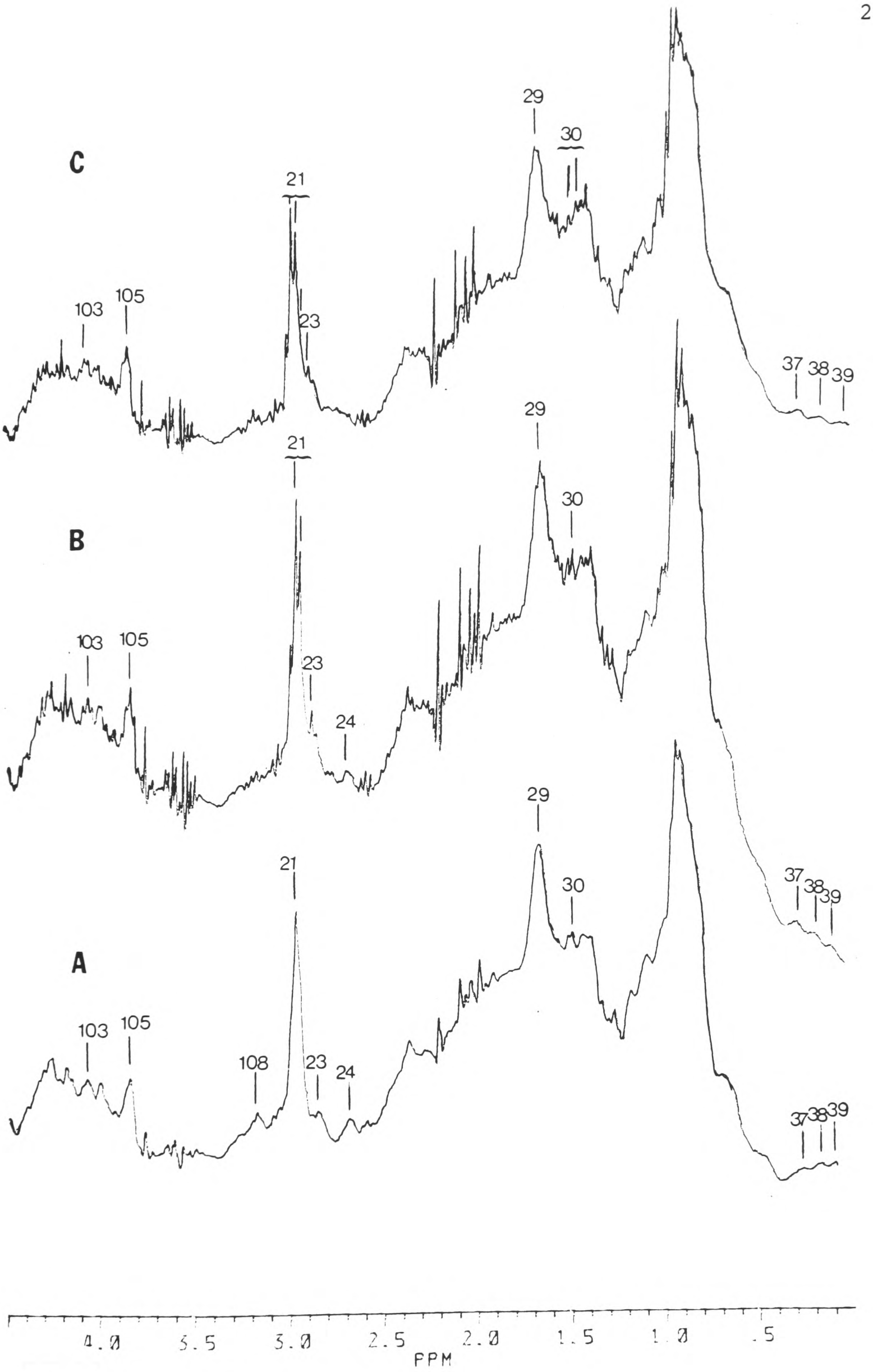

Figure 6.15 The aliphatic region as for figure 6.14

(a) blank; (b) 1:1$[Fe(CN)_6]^{3-}$; (c)1:1ATP;

(d) 1:1 3-PG; (e) 10:1$[Fe(CN)_6]^{3-}$.

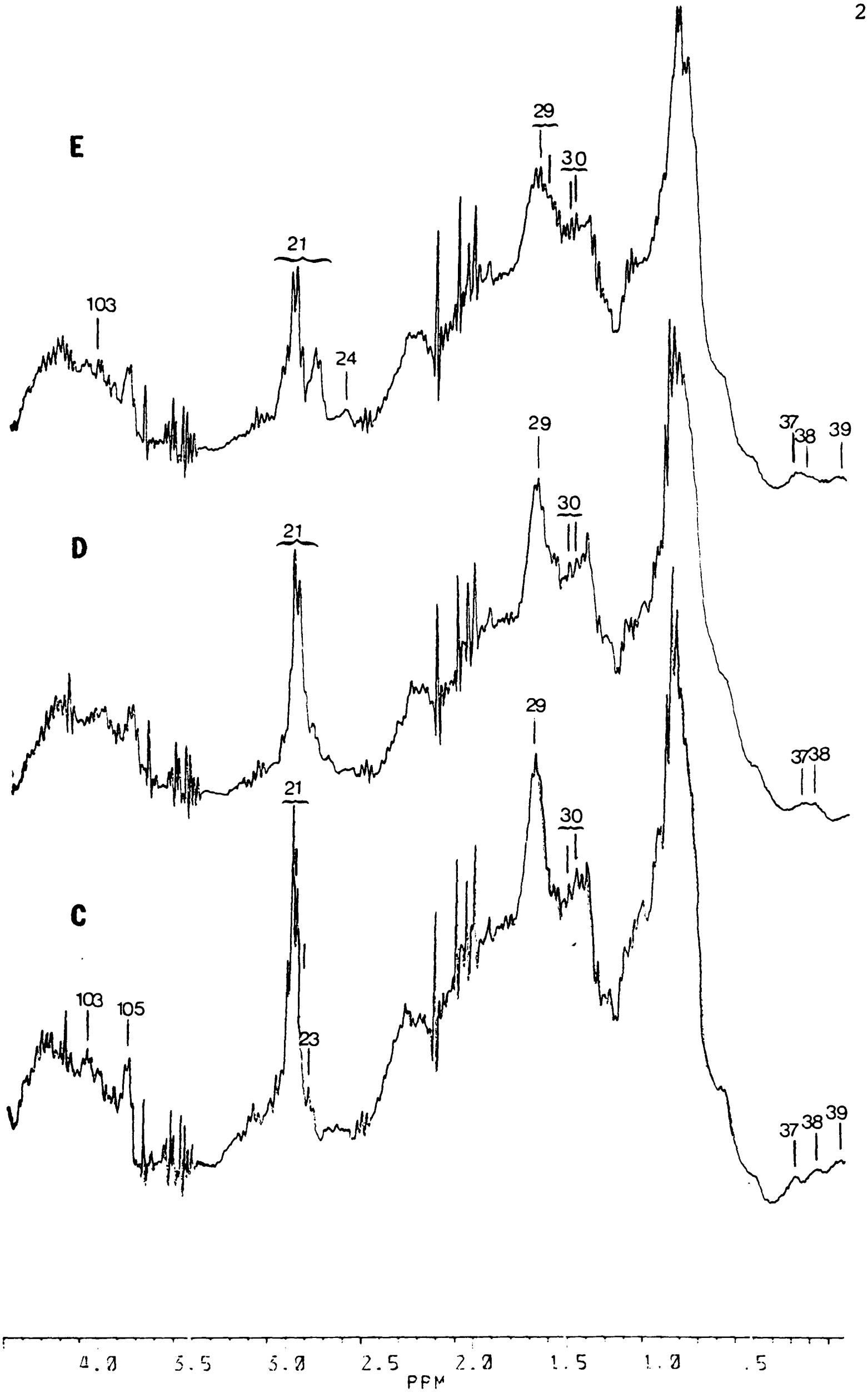
E
29
30
21
103
24
37
38
39
D
29
30
21
37
38
C
29
30
21
103
105
23
37
38
39
4.0
3.5
3.0
2.5
2.0
1.5
1.0
.5
PPM

AROMATIC RESONANCE

ADDITION		1	5		3	4	6	12		2	9	10	11		7a	8	11a	13		14a	b	15a	b	16	17	18		
(i) equimolar $[Fe(CN)_6]^{3-}$					+.13	-.05	+.02											x		-.02			+.03		+.03			
(ii) as (i) plus equim. ATP					+.13	-.07	+.02	x								x		+.03 x		-.02			+.03	-.03	+.03			
(iii) as (ii) plus equim. 3-PG		-.02	-.07		+.13 x	-.07 xx	+.02	x			+.03	+.03			x	x		+.03 x		-.02			+.03	-.15 xx	xxx			
(iv) as (iii) plus 10:1 $[Fe(CN)_6]^{3-}$		.00	-.03		xxx	xxx	+.02 xx	xxx		-.03	.00	-.01	+0.2		x	x		xxx		-.02	xx		+.03 xx	-.10 xx	xxx			

ALIPHATIC RESONANCE

ADDITION	100	101	102	103	104	105	108		21	22	23	24	25		26	27	28		29	30	31	32	33	34	35	36	37	38	39
(i) equimolar $[Fe(CN)_6]^{3-}$							xxx		-.02		+.03	x																	
(ii) as (i) plus equimolar ATP							xxx		-.02		+.03	xxx								-.05								-.02 x	-.04 x
(iii) as (ii) plus equim. 3-PG	xxx			xxx		x	xxx		-.02		+.03	xxx							x	-.05			x				-.02	-.02 x	-.06 x
(iv) as (iii) plus 10:1 $[Fe(CN)_6]^{3-}$	0			x			xx		-.13		+.03	0							-.05	-.05							0	-.02 x	-.04 x

NUCLEOTIDE RESONANCE

ADDITION		H8		H2		H1'	
(ii) equimolar ATP and $[Fe(CN)_6]^{3-}$		xxx		x		-.09 x	
(iii) as (ii) plus equim. 3-PG		xxx		xxx		xxx	
(iv) as (iii) plus 10:1 $[Fe(CN)_6]^{3-}$		xxx		+.02 xx		-.06 xx	

Table 6.8 The effect of various ligands on the 300MHz spectrum of yeast PGK; the effect of the interactions on the nucleotide spectrum.

On the addition of equimolar ATP there is no evidence that $[Fe(CN)_6]^{3-}$ is replaced. Active site resonances 3 and 6 remain shifted 0.13 and 0.02ppm downfield, while peak 4 shifts a further 0.02ppm downfield and peak 12 broadens slightly. The conformational effects seen at peaks 14a, 15b and 17 and effects at aliphatic peaks 108, 21 and 23 remain as before. Effects seen in the previous chapter to be characteristic of ATP binding are repeated here: peak 8 broadens, peak 13 shifts downfield, peaks 16 and 39 and a component of peak 30 shift upfield and peak 24 broadens out completely. An additional conformational effect is noted at peak 38.

Once again, the nucleotide peaks are strongly affected by the interaction. The H8 resonance is broadened out completely, the H2 resonance is broadened (but not shifted), and the H1' resonance is broadened and shifted upfield.

The addition of 3-PG to the sample gives little evidence of displacement of $[Fe(CN)_6]^{3-}$ from the active site. Apart from broadening at peaks 3 and 4, the four active site histidine residues remain as they were. There is evidence that substrate binds near surface histidines, as follows

(i) Peaks 1 and 5 shift upfield, implicating his123 in the interaction. This effect was noted in section 6.2 on the addition of excess 3-PG and is consistent with a partial deprotonation of the histidine by the binding phosphate group.

(ii) Peaks 9 and 10, associated with histidines 52, 53 and 149, are shifted downfield by 0.03ppm. These peaks were also previously affected, by the addition of excess 3-PG.

A conformational effect, characteristic of secondary 3-PG binding, is revealed by the large upfield shift of peak 16. Further conformational influence is seen at resonances 17,37 and 39. Other effects noted in the aliphatic region are the broadening of resonances 100, 103 and 105 in the "αCH region" between 4.5 and 3.8ppm.

Finally, it is remarked that the two nucleotide peaks H2 and H1' broaden out completely, but the reasons for this are not clear.

When the concentration of $[Fe(CN)_6]^{3-}$ is increased ten fold, broadening is seen throughout the spectrum. All of the active site histidines broaden considerably, three of them disappearing completely. The effects, seen on the addition of 3-PG, at the surface histidine resonances 1,5,9 and 10 are reversed, indicating that $[Fe(CN)_6]^{3-}$ competes with the triose phosphate at these secondary sites. Shifts are also seen at surface histidine peaks 2 and 11, which were affected by the excess $[Fe(CN)_6]^{3-}$ addition of the previous section and give evidence of secondary binding as does the downfield shift of the major components of peaks 21 and 29 and the broadening of peak 13.

Further evidence of the replacement of 3-PG from its secondary site is given by the partial reversal of the upfield shift of peak 16, the partial restoration of the sharpness of peaks 100, 103 and 105 and the return to their original positions of peaks 37 and 39. In addition, the nucleotide peaks reappear, only slightly broadened.

In conclusion, it is seen that

(i) equimolar ATP and $[Fe(CN)_6]^{3-}$ can bind to the protein simultaneously more or less independently;

(ii) 3-PG fails to replace $[Fe(CN)_6]^{3-}$ from the protein (at pH6.0) and instead binds at secondary sites on the surface of the protein, and

(iii) the further excess of $[Fe(CN)_6]^{3-}$ displaces 3-PG from these secondary sites as well.

6.3.4 With $[Cr(CN)_6]^{3-}$

In the fourth and final part of this investigation $K_3Cr(CN)_6$ was added to a 3.5mM solution of PGK, buffered at pH7.2 with 10mM Tris. The addition took the form of a titration with consecutive $[Cr(CN)_6]^{3-}$:protein ratios of 0.3, 0.6 and 1.0. The effects on the 300MHz spectrum are illustrated in figure 6.16 and summarised in table 6.9.

At a ratio of 0.3:1 $[Cr(CN)_6]^{3-}$ to enzyme, active site resonances 4 and 6 broaden out completely, and broadening is seen at upfield aromatic peaks 15b and 17. In the aliphatic region, peaks 100 and 101 of the αCH region, peaks 21 and 23 of the ε-lysine region and peaks 29 amd 30 broaden, while there is an upfield rearrangement in the methyl peak 34/35. As the level of $[Cr(CN)_6]^{3-}$ is increased, active site peaks 3 and 12 broaden, surface histidine peaks 9,10 and 11 broaden slightly and upfield aromatic peaks 15b and 17 broaden further. In the aliphatic region, peaks 100 and 101 broaden out completely, peak 21 broadens further and broadening is seen at peaks 25b and 27 and at upfield methyl peak 37. Peak 31 increases in intensity. These effects are categorised as follows.

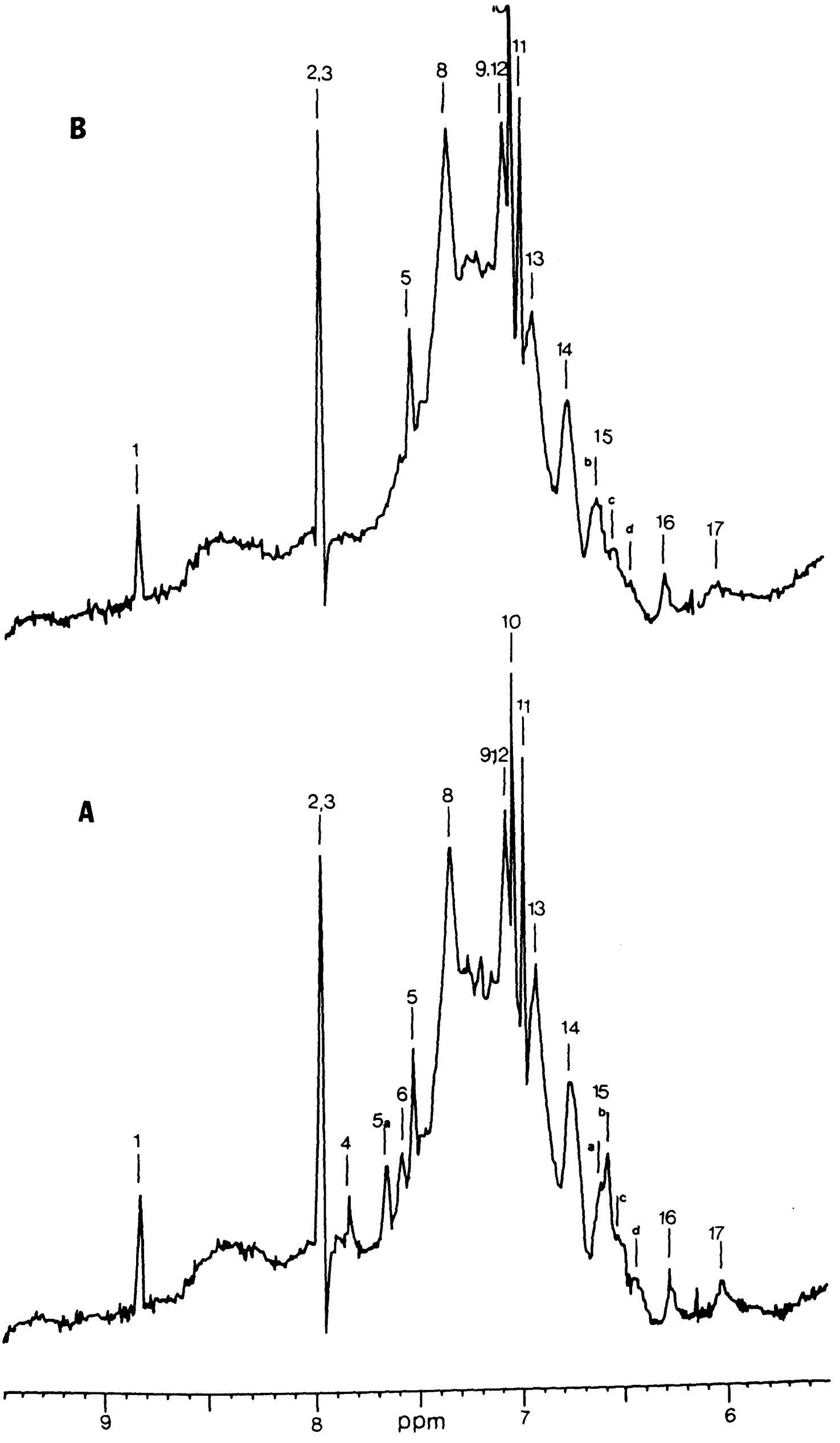

Figure 6.16 The effect of $[Cr(CN)_6]^{3-}$ on the aromatic region of the 300MHz, resolution enhanced spectrum of yeast PGK.

(A) 3.5mM PGK,

(B) as (A) plus 1.2mM$[Cr(CN)_6]^{3-}$.

Table 6.9 The effect of $[Cr(CN)_6]^{3-}$ on the 300MHz spectrum of yeast PGK.

AROMATIC RESONANCE

ADDITION		1	5		3	4	6	12		2	9	10	11		8	12	13		14a	15a	b	16	17					
0.3:1 $[Cr(CN)_6]^{3-}$:PGK						xxx	xxx														x		xx					
) 0.6:1 "						xxx	xxx														xx		xxx					
i) 1.0:1 "					xx	xxx	xxx	x			x	x	x								xx		xxx					

ALIPHATIC RESONANCE

ADDITION	100	101	102	103	104	105	108		21	23	24		25a	25b		26	27	28		29	30	31	32	33	34	35	36	37
0.3:1 $[Cr(CN)_6]^{3-}$:PGK	x	x							x	x										xx	x				x	+		
0.6:1 "	xxx	xxx							xx	x				x			x			xx	x	++			x	+		x
) 1.0:1 "	xxx	xxx							xx	x				xx			xx			xx	x	++			x	+		x

(i) The broadening of active site peak 4 and of upfield aliphatic peak 37 was observed on the addition of equimolar $K_3Co(CN)_6$, the diamagnetic blank, to the enzyme and is interpreted as a conformational effect, caused by binding of the anion at the active site.

(ii) The effects observed at the active site at peaks 3,6 and 12 and at peaks 15b,21,31 and 35 reflect those occasioned by an equimolar addition of the contact shift probe $[Fe(CN)_6]^{3-}$.

(iii) The effects at peaks 9,10 and 11(implicating histidines 52,53 and 149), at peak 27(linked to exposed methionine 267), and at peak 23 correspond to those observed previously at excess levels of $[Co(CN)_6]^{3-}$ and of $[Fe(CN)_6]^{3-}$. They are indicative of secondary binding.

(iv) The broadening of peaks 17,100,101,25b,29 and 30 does <u>not</u> correspond to previous observations and displays the longer range influence of the broadening reagent.

Thus it is seen that $[Cr(CN)_6]^{3-}$ binds principally at the active site, with the usual conformational effects, and is also dispersed over the surface of the protein.

6.4 Summary

The use of paramagnetic probes gives direct evidence of primary binding of anions at the active site in the inter-domain groove of yeast PGK, and of secondary binding near this site and also at various points dispersed over the surface of the protein. This is summarised in table 6.10 and illustrated by figure 6.17. These results are consistent with the location of a second site (Scopes, 1978b) in the groove of the protein, close to the active site. Anion interaction at this site does not inhibit the binding of 3-PG to the enzyme but rather increases the activity of the enzyme by encouraging the displacement of tightly bound product 1,3-P_2G.

The anion probe $[Fe(CN)_6]^{3-}$ is found to replace 3-PG from the protein, indicating that it binds more strongly at the active site (at pH6.0). It does not compete with ATP binding, indicating the independence of binding at the anionic nucleotide sites.

Table 6.10 Summary of PGK nmr resonances and the associated residues located by anion binding.

resonance	residue	anion effect
3,4,6,12	his62,167 and 170	primary and secondary sites
1,5	his123	
2,9,10,11	his52,53 and 149	secondary sites
27	met267	
14a; 15b,16,37	tyr193, hinge region; hydrophobic area	primary site - conformational effect
17,36,38	hydrophobic area, hinge region?	secondary site - conformational effect

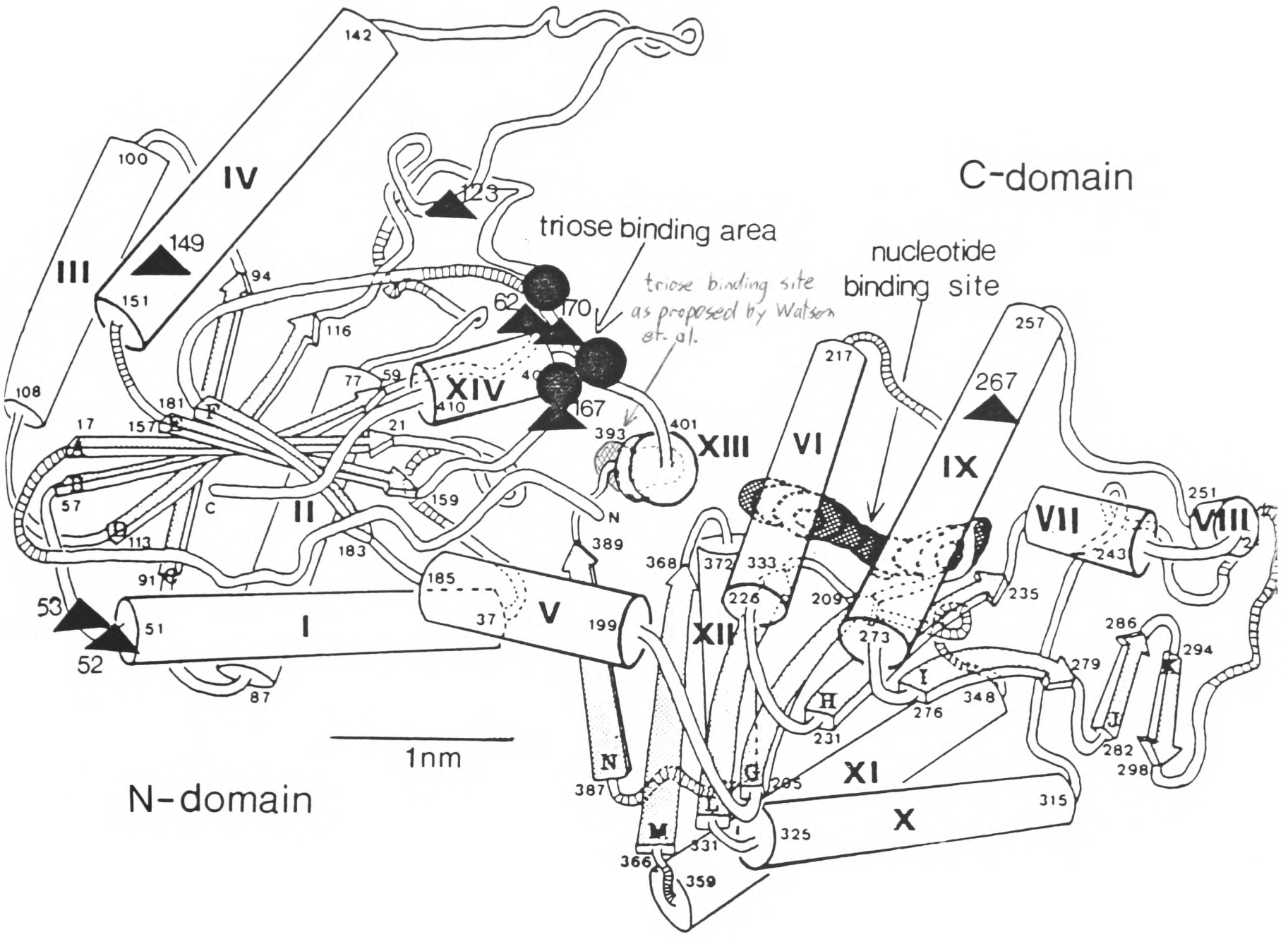

Figure 6.17 Scheme of the open form of yeast PGK, showing residues implicated in anion binding:

●, primary site;
▲, secondary site.

Chapter 6 References

Adams, S.R., Sparkes, M.J. and Dixon, H.B.F. (1983) Biochem.J. 213, 211-215.

Huang, Z-X. and Moore, G.R. (1983) J.Mag.Res. 52, 505-510.

Orr, G.A. and Knowles, J.R. (1974) Biochem.J., 141, 721-723.

Scheffler, J.E. and Cohn, M. (1986) Biochemistry, 25, 3788-3796.

Schierbeck, B. and Larsson-Raznikiewicz, M. (1979) Biochim.Biophys.Acta, 568, 195-204.

Scopes, R.K. (1978a) Eur.J.Biochem., 85, 503-516.

Scopes, R.K. (1978b) Eur.J.Biochem., 91, 119-129.

Tanswell, P. (1974) D.Phil. Thesis, University of Oxford, U.K.

Tanswell, P., Westhead, E.W. and Williams, R.J.P. (1976) Eur.J.Biochem., 63, 249-262.

Tompa, P., Hong, P.T., and Vas, M. (1986) Eur.J.Biochem., 154, 643-649.

Watson, H.C., Walker, N.P.C., Shaw, P.J., Bryant, T.N., Wendell, P.L., Fothergill, L.A., Perkins, R.E., Conroy, S.C., Dobson, M.J., Tuite, M.F., Kingsman, A.J. and Kingsman, S.M. (1982) EMBO J., 1, 12, 1635-40.

Wrobel, J.A. and Stinson, R.A. (1978) Eur.J.Biochem., 85, 345-350.

CHAPTER 7.

THE CONFORMATION OF THE TERNARY COMPLEX OF PGK

Chapter 7 Contents

7.1 INTRODUCTION

Various lines of evidence suggest that the (yeast) PGK molecule adopts a "closed" conformation (see figure 7.1) on binding both substrates. These are as follows.

The small angle X-ray scattering studies of Pickover et al. (1979) demonstrated that the binding of MgATP decreased the radius of gyration of the molecule more than binding of 3-PG, and that binding of both these substrates decreased the radius by more than the sum of the individual effects. This last effect was equated to a rotation of one lobe around another by about 10^{o} and was compared to the cleft closure found in hexokinases.

The ultracentrifugation investigation of the hydrodynamic properties of the enzyme by Roustan et al. (1980) indicated that binary complexing, to give enzyme-MgATP or enzyme-3PG complexes, does not induce a significant conformational change in the molecule but that it is induced by formation of the ternary complex, enzyme-ATP-3PG (with or without Mg^{2+}). Furthermore, it showed that this conformational change can also be induced simply by interaction with sulphate anions.

An X-ray investigation of crystals of horse muscle PGK (Rice and Blake, 1984) has revealed two non-interconvertible crystal forms, A and B. Crystals of form A are destroyed by the addition of 3-PG, whereas those of form B can be grown only in its presence. Moreover, nucleotides bound to form A can be removed by diffusion while in the 3-PG/MgATP crystal, the substrates are apparently unaccessible to solvent. These properties are consistent with forms A and B representing, respectively, open and closed forms of the enzyme.

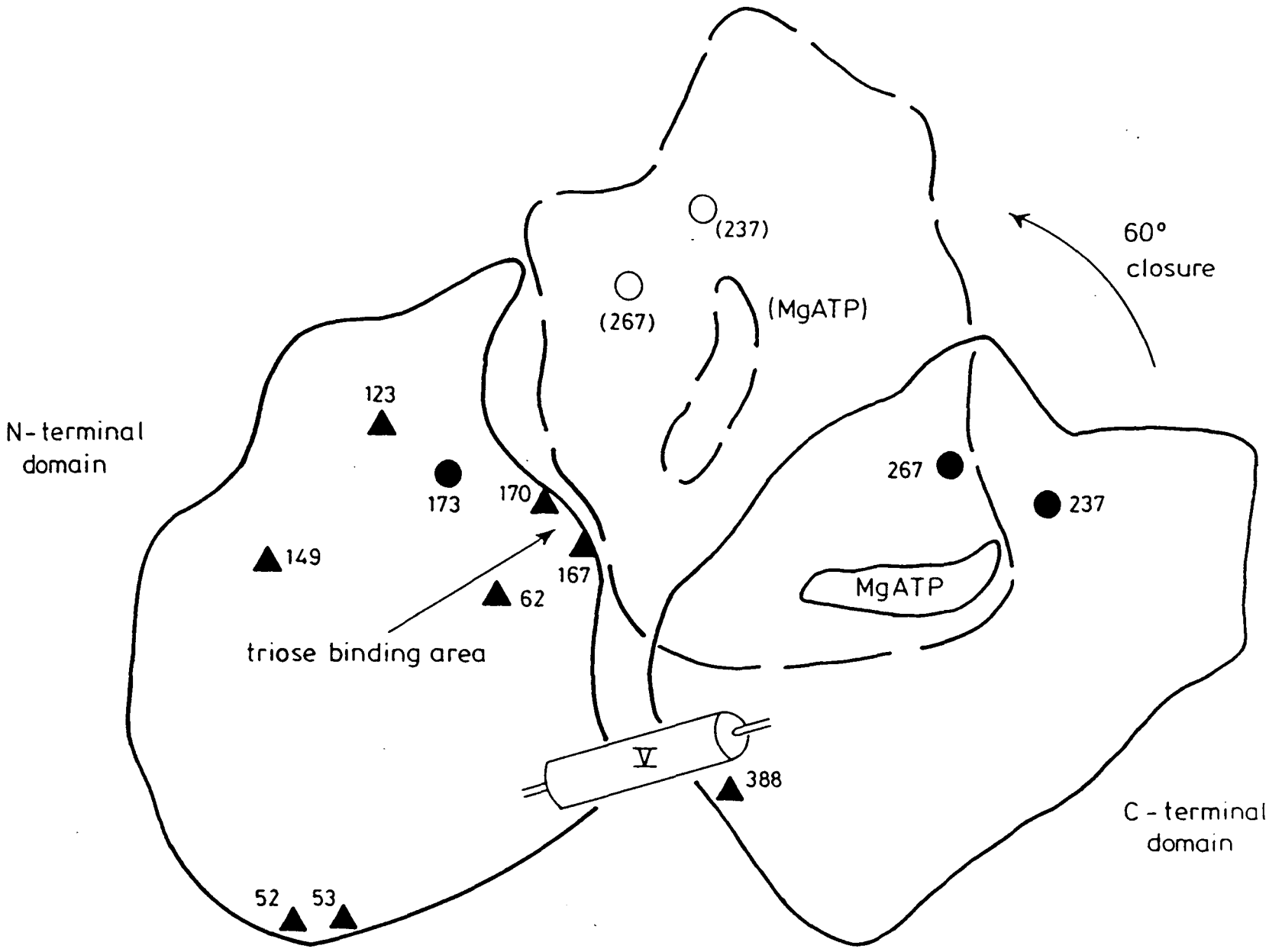

Figure 7.1 Outline of the yeast PGK molecule showing the open crystallographic form and a proposed closed form (broken line). Histidine residues (▲) and methionine residues (●) are indicated and the outlines of helix V and of bound nucleotide are included. (After Watson and Gamblin, 1985)

The nmr studies of Tanswell et al. (1976) showed that

(i) interaction with 3-PG affected the enzyme spectrum as much as interaction with nucleotide, both having effects among the upfield aromatic peaks;

(ii) the effect of binding both 3-PG and MgADP or MgATP was largely equivalent to the sum of the effects of binding the individual species;

(iii) the addition of 3-PG broadened the resonances of enzyme bound nucleotide but did not significantly perturb the enzyme-metal-nucleotide conformation, at least not in the inactive ADP, 3-PG system.

Thus the available evidence strongly suggests that some degree of closure of the molecule does occur but uncertainty remains over the extent of the closure and over the conditions required to bring it about. Unfortunately the two probable forms of the enzyme have not been crystallised.

The mechanism of this closure is now considered. Two theories are proposed which are by no means mutually exclusive. They are illustrated by figure 7.2, and are as follows.

(i) The lobes of the free enzyme are kept apart by electrostatic repulsion across the active groove. The positively charged face of the N-domain is opposed to the similarly charged residues (including lys213 and lys217) of the nucleotide site in the C-domain. The binding of either nucleotide and triose phosphate substrate tends to neutralise these charges and makes closure of the enzyme thermodynamically attractive.

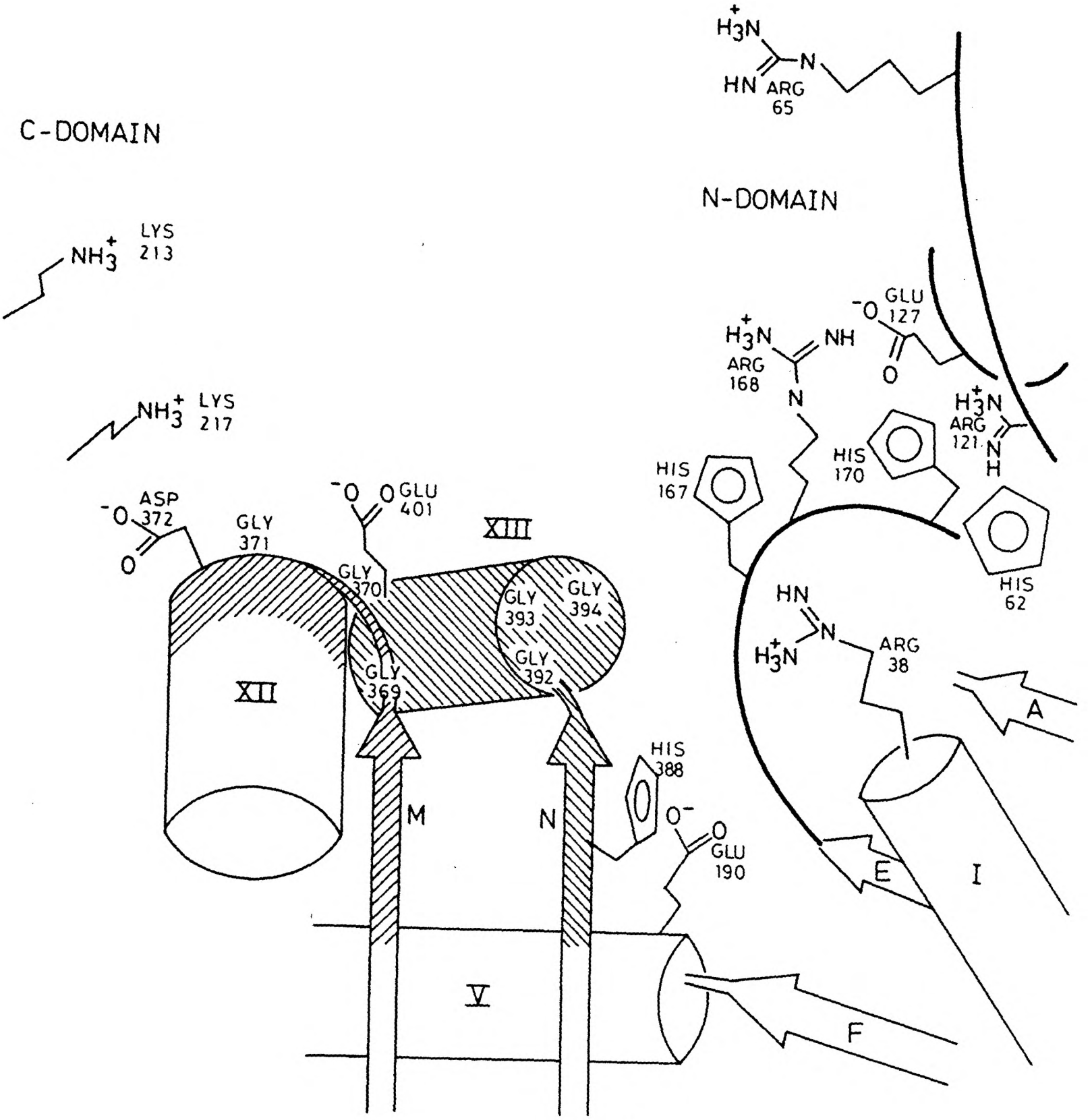

Figure 7.2 The yeast PGK molecule showing the positive face of the N-domain facing the nucleotide phosphate binding area of the C-domain, across the hinge region. The conserved areas are denoted by shading.

(ii) In the absence of regulatory anions a hydrogen bond, the "hinge hydrogen bond", exists between his388 and glu190 in the hinge region and is responsible for holding the enzyme in an open conformation. Interaction with anions weakens this bond and encourages closure of the enzyme.

It is remarked here that there is a very high degree of conservation in the β-sheet strands M and N, that they are both linked to the subsequent helices by a trio of glycine residues, and that helix XIII is completely conserved. Thus there is a link preserved between the hinge region of the protein and the phosphate chain of bound nucleotide, involving asp372, the peptide NH of gly371 and possibly glu401. Further evidence of this link is provided by the work of Hjelmgren et al. (1976) which shows that the binding of MgATP to the enzyme inhibits the nitration of an exposed tyrosine residue - a residue which is very possibly tyr193 of the hinge region.

This suggests a possible scheme of action of the enzyme as follows:

(i) the binding of nucleotide is communicated to β-sheet N and the his388-glu190 hydrogen bond becomes more exposed to competition;

(ii) anions, including 3-PG, bind preferentially at the active site in the groove of the protein;

(iii) excess anions, including 3-PG, interact with his388 and weaken the hydrogen bond, thereby acting in a regulatory role and allowing closure of the protein and thence phosphoryl transfer to take place.

Electrostatic energies are involved in all three stages.

It has already been noted (Tanswell et al., 1976; Roustan et al., 1980) that sulphate anions cause conformational changes in the enzyme that may well be consistent with closure of the molecule. Such influence may operate either through neutralisation of active groove repulsion or through interference with the hinge hydrogen bond. Activation of the enzyme reaction by sulphate (and other anions) may well be linked simply to removal of 1,3-P_2G as proposed by Scopes (1978b) and as supported by the evidence in the previous chapter of competition with triose phosphate.

The presence of a secondary regulatory anion binding site (Schierbeck and Larsson-Raźnikiewicz, 1979) may also reflect either interference with the hinge hydrogen bond or competition with 1,3-P_2G.

A mutant form of yeast PGK has recently been prepared (Wilson et al., 1985) which has his388 replaced by gln388 and thus (very probably) lacks the hinge hydrogen bond. Proposed sedimentation velocity work with this mutant should reveal whether it has assumed a closed conformation and kinetic investigation should then indicate if such a conformation leads to greater activity.The nmr work of the present study, see below, should reveal, at least, any similarities between the mutant conformation and the conformation of the binary and ternary complexes.

The previous two chapters have considered the interaction of nucleotide at its hydrophobic site in the C-terminal domain of yeast PGK and the electrostatic

interaction of anions including triose phosphate at the active site in the N-terminal domain. The local, direct effects of these interactions have been characterised by changes in the proton nmr spectrum of the enzyme and longer range, conformational effects have been indicated by shifts and broadenings in the upfield regions of both the aromatic and aliphatic parts of the spectrum.

In the present chapter, the effect of the binding of both the substrates on the conformation of the protein is examined and further attempts are made to induce and characterise a "closed" form of the protein. Finally, an investigation is made of the mutant form of PGK, which is thought to favour a more closed conformation.

7.2 THE TERNARY COMPLEX

The fully bound, inactive analogue complex PGK-MgAMPPN-3-PG was formed and the effects of the interaction on the 300MHz spectra of both the enzyme and the nucleotide were examined.

7.2.1 PGK with MgAMPPNP, 3-PG and Gd^{3+}

In the first experiment, enzyme sample and solutions to be added were buffered with Tris at pH6.5. The sample concentration of PGK was 0.5mM; 80mM solutions of nucleotide and triose phosphate were used, and the Gd^{3+} stock solution was 3.5mM $GdCl_3$. 2mM MgAMPPNP was added first to the enzyme solution, followed by a similar addition of 3-PG. Finally, 50μM Gd^{3+} and then 250μM Gd^{3+} was added. The effects observed in the nmr spectrum are summarised in table 7.1 and figure 7.3.

The addition of MgAMPPNP, in 4:1 excess, is found to have the following results.

(i) The adenine ring binds in its hydrophobic cleft of the C-domain. This is characterised by the shift of peak 8, (assigned by Scheffler and Cohn (1986) to trp 308) the upfield shift of a component of peak 30 and the effects of the nucleotide aromatic peaks, which are the complete broadening out of peak H8, the broadening and downfield shift of peak H2 and the broadening and upfield shift of peak H1'.

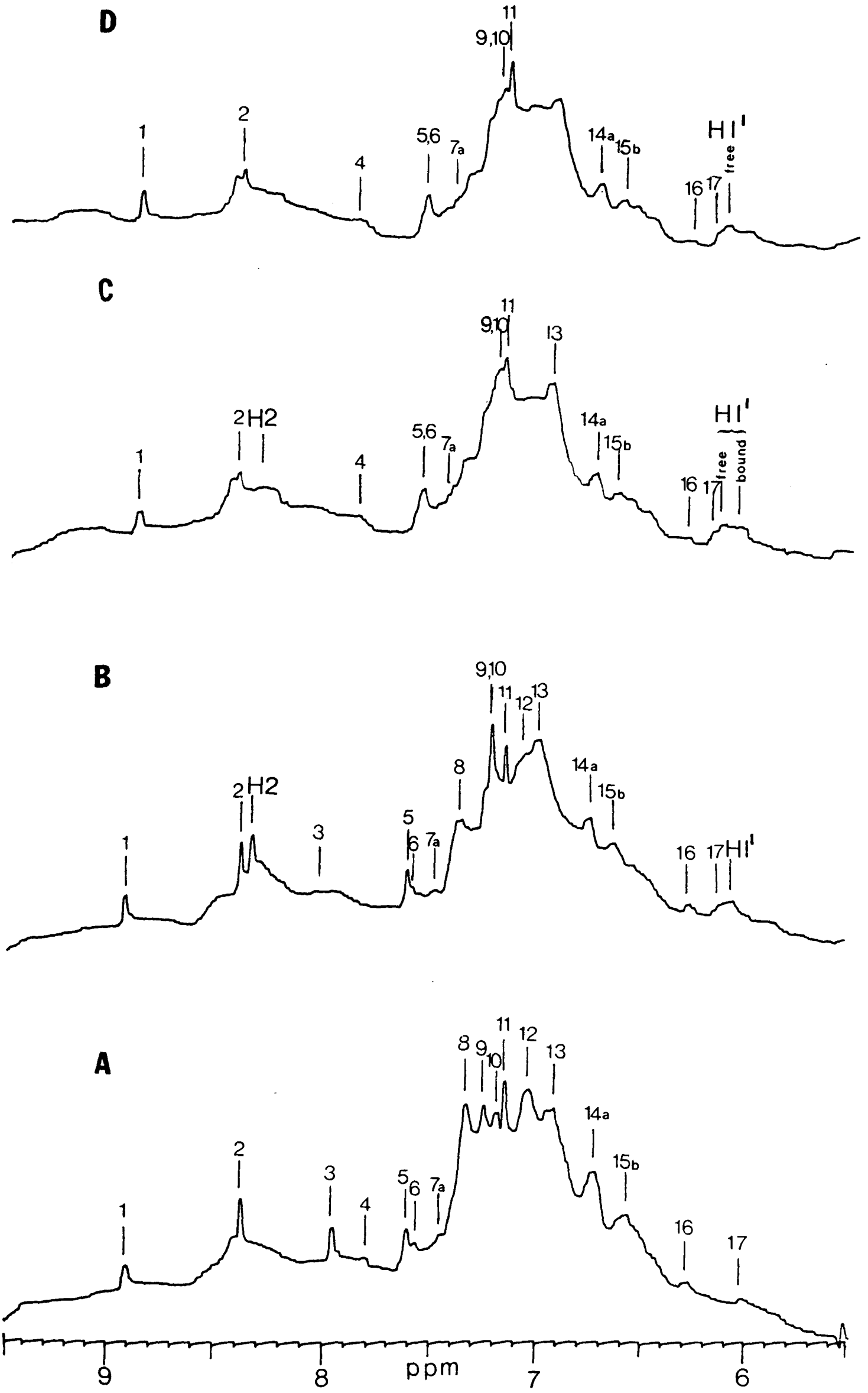

Figure 7.3 The effect of interaction with 3-PG, MgAMPPNP and Gd^{3+} on the 300MHz spectrum of yeast PGK. (A) 0.5mM yeast PGK; (B) as (A) with 2mM MgAMPPNP; (C) as (B) with 2mM 3-PG; (D) as (C) with 50μM $GdCl_3$.

AROMATIC RESONANCE

ADDITION	1	5		3	4	6	12		2	9	10	11		7a	8	13		14a	b	15a	b	16	17					
(i) 2mM MgAMPPNP	-.01	-.02		+.04 xx	xxx	+.02	+.05 xx		-.02	-.02	+.01	-.02		-.01	+.02 x	+.02					+.02	-.04	+.05					
(ii) 2mM 3-PG	-.05	-.07		+.08 xx	+.03 x		xxx		+.01	-.02	+.01	-.02			xxx	-.02		-.01			+.02	.00	+.05					
(iii) 50μM $GdCl_3$	-.05	-.07		xxx	+.03 x		xxx		+.01	-.02	+.01	-.02			xxx	xxx		-.01			+.02		+.05					
(iv) 250μM $GdCl_3$	-.05	-.07		xxx	+.03 xx		xxx		+.01	-.02	+.01	-.02			xxx	xxx		-.01			+.02		xxx					

ALIPHATIC RESONANCE

ADDITION	21	23	24		25b		26	27	28		29	30	31	32	33	34	35	36		37	38	39						
(i) 2mM MgAMPPNP		x	x		-.03		-.01					-.02										-.04						
(ii) 2mM 3-PG			xxx		-.03							-.04										-.04						
(iii) 50μM $GdCl_3$			xxx		-.03				x			-.04						xx				x						
(iv) 250μM $GdCl_3$			xxx		-.03				x			-.04						xx				x						

NUCLEOTIDE RESONANCE

ADDITION		H8		H2		H1'	
(i) 2mM MgAMPPNP		xxx		+.05 x		-.05 xx	
(ii) 2mM 3-PG		xxx		+.05 xx		.00 -.09 xx	
(iii) 50μM $GdCl_3$		xxx		+.05 xxx		.00 x xxx	
(iv) 150μM $GdCl_3$		xxx		xxx		.00 x xxx	

Table 7.1 Changes in the 300MHz spectra of enzyme and nucleotide on the addition of MgAMPPNP, 3-PG and Gd^{3+} to 0.5mM yeast PGK. (A horizontal line through a box signifies that a peak is unobservable)

(ii) The phosphate chain of the nucleotide interacts, probably indirectly, with the active anion site of the N-domain which results in the usual catalogue of effects at the active site peaks, and produces a large broadening and/or downfield shift of peak 4.

(iii) Conformational effects, characteristic of the addition of equimolar nucleotide, are the shifts of upfield aromatic peaks 15b, 16 and 17 and of upfield methyl peak 39. Also characteristic of equimolar nucleotide binding in the broadening of peak 24 and the upfield shift of peak 25b.

(iv) Excess nucleotide disperses over the surface of the enzyme and interacts at his123 (peaks 1 and 5) and at histidines 52, 53 and 149 (peaks 2, 9, 10 and 11).

On the addition of excess 3-PG, to form the ternary complex, the following is observed.

(i) Peak 3 is shifted further downfield, peak 4 reappears, only slightly broadened, 0.03ppm downfield of its original position, peak 6 is unobservable under peak 5, and peak 12 is completely broadened out. This suggests that 3-PG blocks the interaction of nucleotide at the primary anion site but does not replace it from the nucleotide site.

(ii) Peaks 1 and 5 shift further upfield, and peak 2 shifts downfield, revealing further effects of surface binding at his123 and at his52, 53 or 149 as the anion concentration is increased.

(iii) The effects noted at resonances 24 and 30, characteristic of nucleotide binding, increase.

(iv) The conformational effects, in the upfield regions of the spectrum, are largely unchanged but peak 16 is seen to revert to its original position.

(v) Most significantly, there is evidence of the intermediate and slow exchange kinetics of the nucleotide-protein interaction. Thus, of the enzyme resonances, peak 8 possibly associated with phe340 or trp308 and shifted downfield by interaction with the adenosine moiety, is now seen to broaden out completely. Of the nucleotide resonances, peaks H8 and H2 appear unaffected, but peak H1' splits, to give a comparatively sharp component at 6.15ppm, the chemical shift for free MgAMPPNP, and a broad peak 0.09ppm upfield at 6.06ppm. From the intensity of the two peaks, 65% of the nucleotide is calculated to be in the free form. This compares well with the value of 75% nucleotide in the free state calculated using Scopes' dissociation constant of 1mM, for MgATP at I=150mM.

The addition of Gd^{3+} results in the complete broadening of peak 3 of the active site but peak 4 persists (while in the absence of 3-PG it had not), indicating protection from nucleotide bound Gd^{3+} by bound triose phosphate. Peak 13 broadens out completely, an effect seen previously with MgADP/Gd^{3+}. Of the upfield resonances, peaks 17 and 36 broaden. The surface histidine residues are unaffected and thus there is no evidence of binding of Gd^{3+} on the surface of the protein.

Of the nucleotide peaks, the H2 resonance is broadened considerably as is the enzyme-bound H1' resonance. The free nucleotide H1' resonance, on the other hand, is unaffected. Thus, when 3-PG is bound at the primary anionic site, Gd^{3+} binds preferentially to nucleotide that is on the enzyme. This indicates some degree of cooperativity of binding of the metal ion, probably involving the carboxyl groups of enzyme residues asp372 and glu401 or possibly of bound 3-PG.

In contrast, in the absence of triose phosphate, that is with the binary complex PGK-MgAMPPNP, the cation was seen to bind preferentially to the free nucleotide. In this binary complex, it appears that the positively charged anion site competes with the Gd^{3+} ions for the phosphate group of the nucleotide.

7.2.2 With 3-PG and MgAMPPNP

In the second of these experiments the ternary complex is formed in the alternative order. 2mM 3-PG and then 4mM MgAMPPNP are added to a 0.8mM enzyme solution, the system being standardised throughout at pH 6.25 with Tris buffer. The effects on the 300MHz spectra are recorded in table 7.2 and in figure 7.4.

The effects of this addition of excess triose phosphate have already been detailed in the previous chapter. They include the effects of binding at the active site, on peaks 3,4,6 and 12; the conformational effects, on peaks 15b, 16 and perhaps 14a, and the secondary, surface binding effects at histidines 123,52,53 and 149, involving peaks 1,5,9,10 and 11.

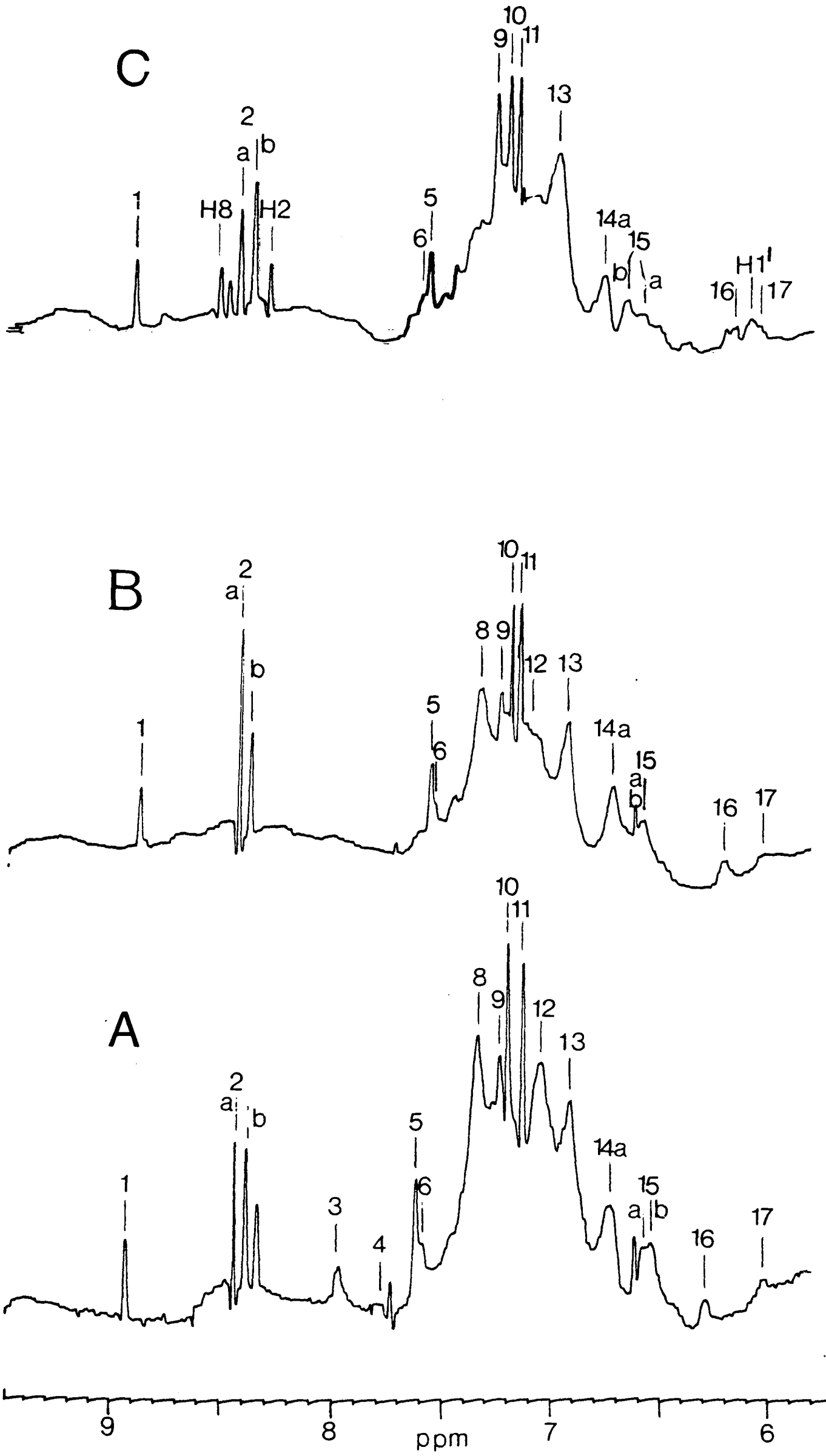

Figure 7.4 The effect of interaction with 3-PG and MgAMPPNP on the 300MHz spectrum of yeast PGK. (A) 0.8mM PGK; (B) with 2mM 3-PG; (C) with 4mM MgAMPPNP.

AROMATIC RESONANCE

ADDITION	1	5		3	4	6	12		2a,b	9	10	11		7a	8	13		14a	b		15a	b	16	17	18			
(i) 2mM 3-PG	-.05	-.05		-.07 xx	xxx	-.04	+.05 x			+.01	-.01	+.03			+.01			-.03				+.03	-.10					
(ii) 4mM MgAMPPNP	-.06	-.07		+.10 xxx	xxx	-.03	xxx		-.03	-.01	-.03	-.01			xxx	+.02		-.03				+.06	+.03	-.01	-.05			

ALIPHATIC RESONANCE

ADDITION	108		21	23	24		25b		26	27	28		29	30	31	32	33	34	35		38							
(i) 2mM 3-PG							x											x									
(ii) 4mM MgAMPPNP	xx				xxx		-.07		-.03					-.06							-.01							

NUCLEOTIDE RESONANCE

ADDITION		H8		H2		H1'	
to 4mM MgAMPPNP							
0.8mM PGK, 2mM, 3-PG		xxx		x		x x -.10	

Figure 7.2 The addition of 2mM 3-PG and then 4mM MgAMPPNP to a 0.8mM PGK- the effect on the 300MHz spectra of the enzyme and of the nucleotide.

The addition of excess nucleotide results in the following.

(i) Some of the effects at the active site intensify - peak 3 broadens and moves further downfield and peak 12 broadens out completely.

(ii) Peaks 1 and 5 shift further upfield and effects are seen at peaks 2,9,10 and 11, revealing further effects of surface binding at his123,52,53 and 149 as the anion concentation is increased.

(iii) Peak 24, a possible lysine peak, broadens out completely and both peak 26, tentatively assigned to methionine 237, and peak 25b shift upfield. A component of peak 30 shifts upfield. These have been characterised as effects of nucleotide binding.

(iv) Further conformational effects are seen in the upfield regions of the spectrum.

(v) Evidence of slow exchange is provided by the broadening of peak 8 and once again by the appearance of two distinct H1' peaks, for free and bound nucleotide, at 6.15 and 6.05ppm respectively. Although less than 20% of the nucleotide is calculated to be bound to the enzyme, the peaks are of nearly equal size - but the situation is confused by the presence of peak 17, which coincides with the bound nucleotide H1' resonance.

7.2.3 Conclusion

Most of the observable aromatic resonances, which tend to represent residues which are close to the surface, are

shifted or broadened by interaction with one of the substrates. So, as found by Tanswell et al. (1976), the effect of binding both substrates is largely equivalent to the sum of the effects of binding the substrates individually, and it is difficult to characterise the ternary conformation by a clear cut effect at a previously unaffected resonance.

Evidence of a more tight conformation of the molecule on the addition of the second molecule is, in fact, provided by the intensification of the effects of

(i) 3-PG at the active site, and of

(ii) nucleotide at peaks 24 and 30.

Evidence of slow exchange kinetics, as seen previously for the binary complex PGK-MgAMPPNP, is given by the splitting of nucleotide resonance H1' and by the broadening of enzyme peak 8, assigned to phe340 or trp308 of the nucleotide site. Furthermore, Gd^{3+} is seen to bind preferentially to enzyme bound nucleotide, provided the positive, anion binding site is occupied by triose phosphate.

7.3 WITH ADENOSINE 5'-TETRAPHOSPHATE

Adenosine 5'-tetraphosphate (A4P) was added to the enzyme in an attempt to bind one ligand to both the nucleotide site and the anion site simultaneously and so to induce a high degree of closure of the molecule, in a mimic of the ternary complex. This nucleotide is expected to be anchored by its adenine ring in the hydrophobic cleft of the C-domain site in such a way that its extended phosphate chain reaches across the groove of the protein and interacts with the face of the N-domain. The first and second pK_a (20^oC, I=100mM) values of A4P are 6.8 and 4.1 (Serjeant and Dempsey, 1979) and so at pH5.8 the terminal phosphate has an average of one negative charge, the same as the phosphate group of 3-PG.

The experiment took the form of a titration. A 35mM solution of A4P was used, together with a 2mM solution of $GdCl_3$ and a 0.8mM sample of yeast PGK. Both were buffered at pH5.8 with 100mM sodium d_3-acetate. A4P was added to the sample to levels of 0.5, 1.0 and 2.0mM. $GdCl_3$ was then added to 50 and 150μM levels. The effects of the interaction on the 500MHz spectrum are shown in figure 7.5 and summarised in table 7.3.

On the first addition of A4P, evidence that the nucleotide is bound at the hydrophobic cleft is given by the nucleotide signals. Characteristically, the H8 resonance is broadened out completely while the H2 and H1' peaks diverge (slightly). Typical of the effects of nucleotide triphosphate on the aromatic peaks of the enzyme are the

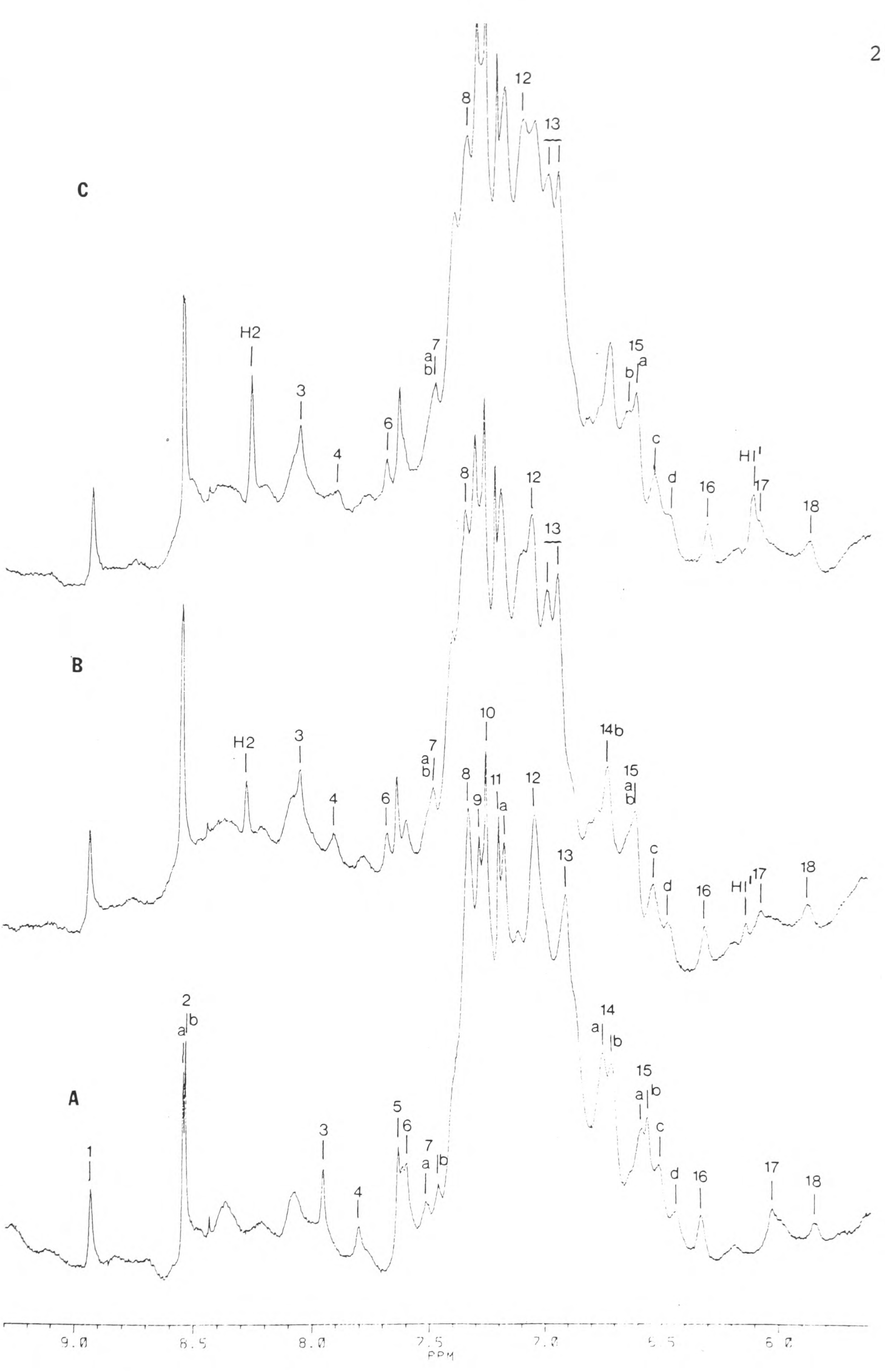

Figure 7.5 The effect of A4P and Gd^{3+} on the 500MHz spectrum of yeast PGK. pH5.8.

(A) 0.8mM PGK;

(B), (C) and (D) as (A) with 0.5, 1.0 and 2.0mM A4P;

(E) and (F) as (D) with 50 and 150μM Gd^{3+}.

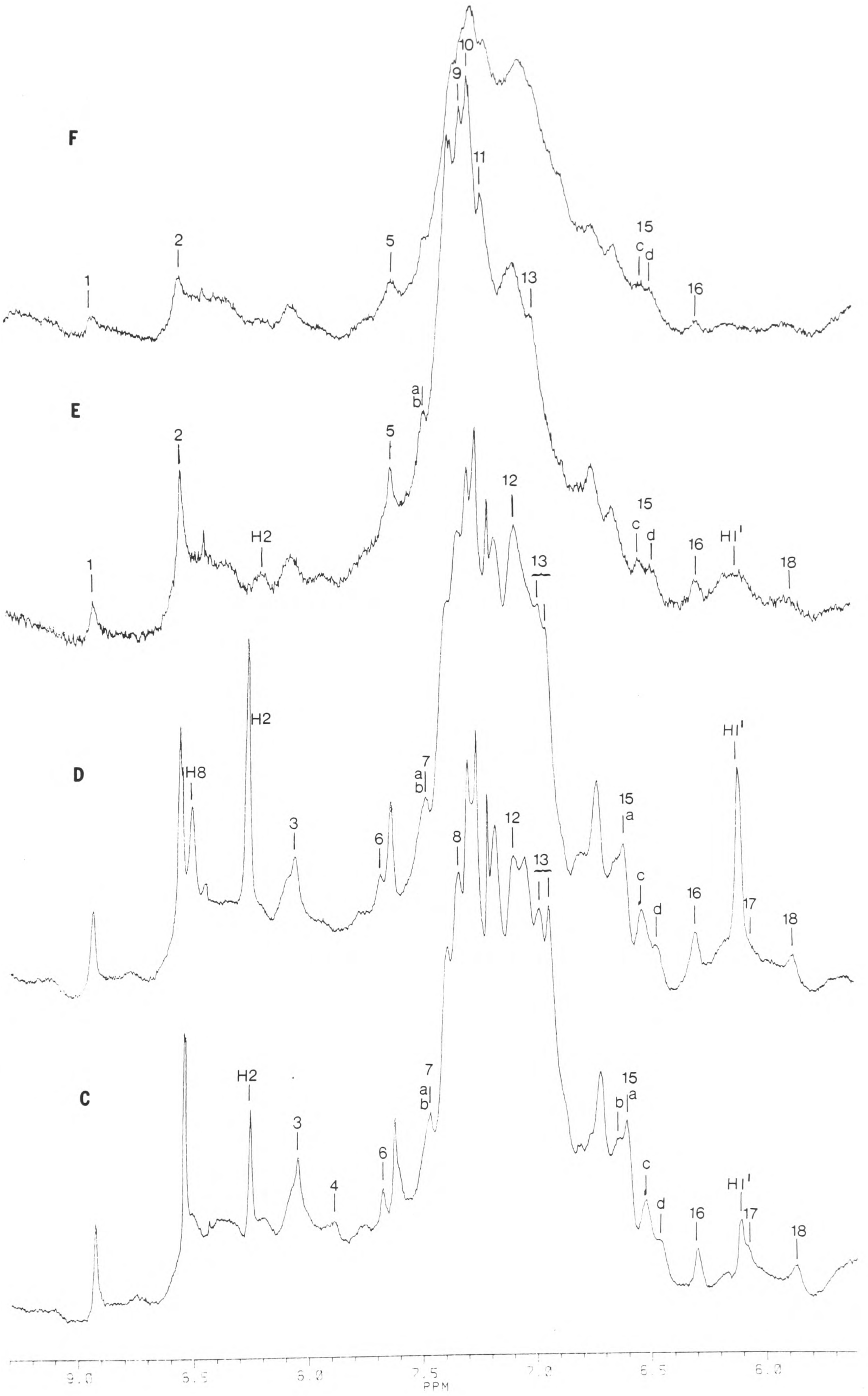
F
1
2
5
10
9
11
15
c
d
13
16
E
a
b
2
5
12
15
c
d
16
H1'
18
1
H2
13
D
H8
H2
7
a
b
3
6
8
12
13
15
a
c
d
16
17
18
H1'
C
H2
7
a
b
15
b
a
3
6
4
c
d
16
H1'
17
18
9.0
8.5
8.0
7.5
PPM
7.0
6.5
6.0

AROMATIC RESONANCE

ADDITION	1	5		3	4	6	12		2	9	10	11		7a	8	13		14a	b		15a	b	c	d	16	17	18	
(i) 0.5mM A4P				+.10 x	+.11 x	+.06	+.01							-.05	xx	+.04		xxx				+.04		+.01	-.05	+.02 x		
(ii) 1.0mM A4P				+.11 x	+.11 xx	+.08	+.03							-.05	xx	+.04		xxx				+.06	+.01	+.01	-.06	+.04 xx	+.02	
(iii) 2.0mM A4P				+.11 x	xxx	+.08 x	+.03							-.04	xxx	+.04		xxx				xxx	+.02	+.02	-.07	+.04 xx	+.01	
(iv) 50μM Gd^{3+}	x	x		xxx	xxx	xxx	xxx		x					-.04	xxx	+.04 xxx		xxx			xxx	xxx	+.02 xx	+.02 xx	-.07 x	xxx	+.01 xx	
(v) 150μM Gd^{3+}	xx	xx		xxx	xxx	xxx	xxx		xx	xx	xx	xx		xxx	xxx	+.04 xxx		xxx			xxx	xxx	+.02 xx	+.02 xx	-.07 x	xxx	xxx	

ALIPHATIC RESONANCE

ADDITION	21	23	24		25a	b		26	27	28		29	30	31	32	33	35	36		37	38	39						
(i) 0.5mM A4P			x		+								-.02		xx					-.08		-.08 x						
(ii) 1.0mM A4P			x		+								-.02		xx					-.08		-.08 x						
(iii) 2.0mM A4P		+.02	+.02 x		+	-.02		x	x				-.04		xx		+.02			-.08		-.06 x						
(iv) 50μM Gd^{3+}	xx	+.02	-.01 x		0	-.02 xx		xx	xx				-.04		xxx		xxx			-.06 x	x	-.06 x						
(v) 150μM Gd^{3+}	xx	+.02	-.01 x		0	-.02 xx		xxx	xxx				-.04	x	xxx	x	xxx			-.06 xx	xx	xxx						

NUCLEOTIDE RESONANCE

ADDITION		H8		H2		H1'	
(i) 0.5mM A4P		xxx		+.01 x		-.01 xx	
(ii) 1.0mM A4P		xxx		+.01 x		-.04 xx	
(iii) 2.0mM A4P		-.03 xx		+.01 x		-.04 x	
(iv) 50μM Gd^{3+}		xxx		+.01 xx		-.04 xx	
(v) 150μM Gd^{3+}		xxx		xxx		xxx	

Table 7.3 The effect of A4P and Gd^{3+} on the 500MHz spectrum of 0.8mM yeast PGK, and the effects of the interaction on the nucleotide spectrum.

broadening of peak 8, (Tryp308/Phe340) the shift of a component of peak 13, the complete broadening out of peak 14a, and various effects at peaks 15b, 16 and 17. Peak 7a, which was broadened by equimolar MgATP and was shifted very slightly upfield by MgAMPPNP, is here shifted 0.05ppm upfield. In the aliphatic region, all the effects are repeats of those seen with MgATP and its analogue MgAMPPNP, apart from the large upfield shift of peak 37. Thus there is ample evidence that A4P has bound at the nucleotide site.

The effects among the primary anion binding site resonances are very marked indeed and resemble those seen previously for the binding of triose phosphate, rather than of nucleotide. In particular peaks 3 and 4 both shift about 0.10ppm downfield.

In this way, all the spectral effects are accounted for by the effects of binding of the individual substrates and, notwithstanding the large upfield shifts of peaks 16 and 37, there is no evidence of a large, novel conformational change.

The nucleotide concentration is increased to 1.0mM, to give a slight excess over the enzyme, with the following results.

(i) Nucleotide resonance H1' shifts further upfield.

(ii) Shifts and broadenings at peaks 15b,16,17 and 18 give evidence of continuing conformational change in the protein.

(iii) Increased effects at peaks 3,4,6 and 12 reveal stronger binding at the primary anion site.

At the final nucleotide concentration of 2.0mM the following is observed.

(i) The preponderance of free nucleotide is marked by the reappearance of resonance H8, 0.03ppm upfield from its free position, and the sharpening up of the H2 and H1' peaks. The kinetics are fast exchange

(ii) Of the upfield aromatic peaks, resonance 15b broadens out completely and peaks 37 and 39 both move slightly downfield - evidence again of continuing conformational change.

(iii) Active site histidine peak 4 broadens out completely.

(iv) Peaks 25b and 30 move upfield which are typical effects of nucleotide triphosphate binding.

(v) Novel effects are seen at peaks 23 and 24 of the lysine ε-CH_2 region, which move downfield towards peak 21, and at methionine resonances, peaks 26 and 27, which broaden slightly.

Next, 50μM Gd^{3+} is added to the sample and the following observations made.

(i) The three A4P resonances broaden showing that Gd^{3+} binds to the nucleotide.

(ii) The broadening effect of this Gd^{3+} is immediately seen at the active site histidine resonances which all completely broaden out. This comprehensive broadening was not seen for GdATP.

(iii) Evidence of dispersal of Gd^{3+} over the surface of the protein is given by broadening of his123 resonances, peaks 1 and 5; by the broadening of lysine ε-CH_2 resonance, peak 21, and by the broadening of methionine resonances, peaks 26 and 27.

(iv) More generally, broadening is seen among the upfield resonances and in particular, peaks 35 and 15a broaden out completely. This last effect was seen on the addition of MgATP/Gd^{3+} to the protein.

Finally, the Gd^{3+} concentration is raised to 150μM with the following effects.

(i) The A4P resonances broaden out completely.

(ii) Broadening at peaks 1 and 5 and at peaks 2,9,10 and 11 implicates histidine residues 123,52,53 and 149 in the dispersal of Gd^{3+} over the surface of the protein. The complete broadening out of peak 27 indicates that exposed methionine residue 237 is involved as well.

(iii) Generally, most of the spectrum is broadened, including all the remaining upfield peaks. This reflects the excess of A4P over enzyme and the widespread dispersal of Gd^{3+}.

The T_2 relaxation study of PGK in the presence and absence of A4P is recorded in section 3.2 of chapter 4, the introductory chapter. The results re-affirm the present findings that the addition of roughly equimolar A4P has no effect on the surface residues, that is those of long relaxation time, that are selected for by the relaxation experiments. Thus surface histidine peaks 2,9,10 and 11 are unaffected, as is the lysine ε-CH_2 resonance 21 and exposed methionine peaks 27 and 28. The long relaxation time resonances of both even and odd multiplicity from 1.5 to 0.5ppm are also unaffected, apart from a slight rearrangement of methyl peak 34/35.

In summary, the binding of A4P mimics formation of the ternary complex (see table 7.4), showing the effects of both nucleotide and triose phosphate binding.

The A4P-PGK interaction shows fast exchange kinetics on the nmr time scale, as seen for the two nucleotide substrate complexes, but not for the MgAMPPNP complex.

7.4 MUTANT PGK

For this preliminary investigation, yeast PGK was prepared from the plasmid pMA27 (Wilson et al., 1985) in both a normal or "wild-type" form, and in the mutant form, with his388 replaced by gln388 (see figure 7.6). The nmr samples were prepared as before with about 0.5mM enzyme buffered at pH5.9 in deuterium oxide with 100mM sodium d_3-acetate. The aromatic regions of the 300MHz spectra are compared in figure 7.7, and the differences are detailed in table 7.4.

The spectrum of the "wild-type" plasmid-produced enzyme is identical to that of PGK obtained conventionally from yeast cytolysis. This confirms the validity of the preparation.

It is immediately remarked that in the mutant PGK spectrum, none of the histidine C2 or C4 resonances is missing. This result has, in fact, already been incorporated into the assignment of the nmr spectrum, in the introductory chapter, where it is concluded that the his388 C2 and C4 protons are not represented by, or at least not readily assigned to, peaks of the aromatic region. The following observations are also made.

(i) The active site histidine resonances, peaks 3, 4 and 6 are not affected. They pertain to the surface, albeit the inner surface, of the N-domain and even with a high degree of closure of the molecule, are not expected to be affected in the absence of substrate.

(ii) Similarly the resonances assigned to histidines 123, 52,53 and 149 of the outer surface of the N-domain are unaffected.

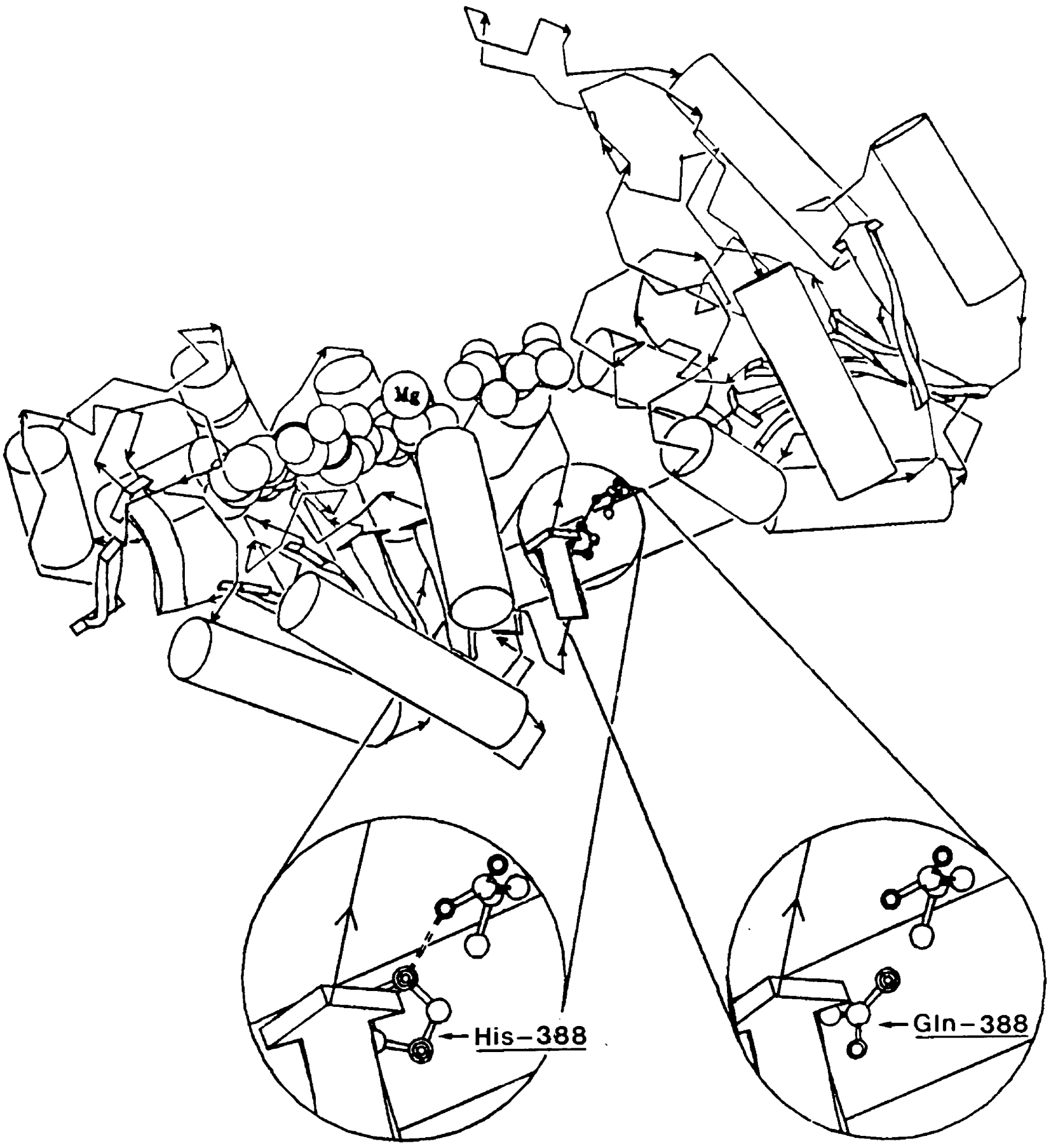

Figure 7.6 A schematic drawing of the yeast PGK molecule. α-helices are represented by cylinders, β-sheets by arrows and the remainder of the structure is represented by lines drawn between each α-carbon. The location of bound MgATP and 3-PG is indicated. The inset on the left shows the interaction between his388 and glu190 in the native enzyme. On the right is shown the situation after his388 has been replaced by gln388.

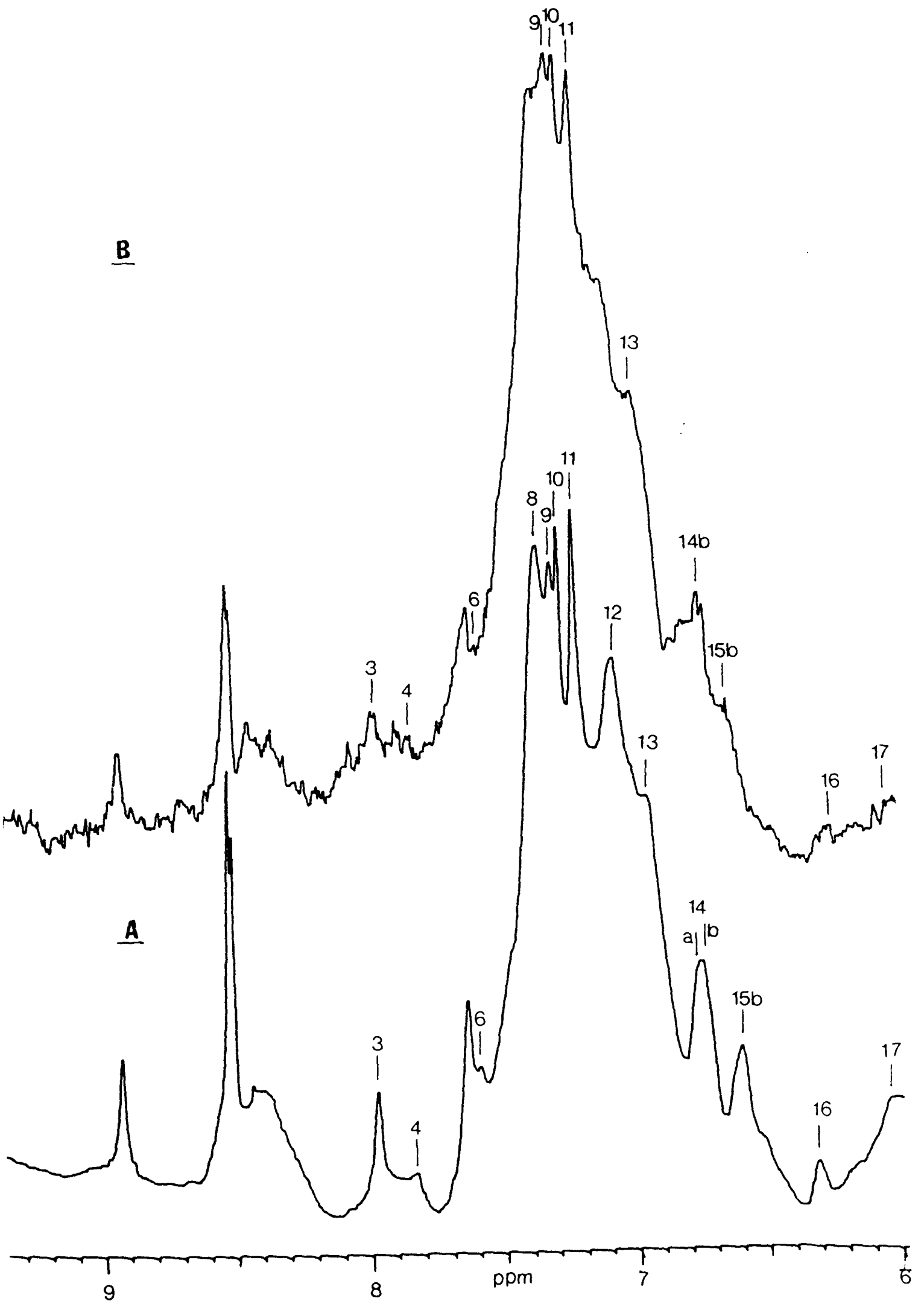

Figure 7.7 The aromatic region of the 300MHz spectrum of plasmid-produced yeast PGK, pH5.9: the effect of the his388-gln388 mutation; (A) wild-type, (B) mutant.

AROMATIC RESONANCE

ADDITION	1	5		3	4	6	12		2	9	10	11		7a	8	13		14a	b	15a	b				16	17		
MgATP				+.06 x	x	+.05	+.02							xxx	x	+.08		xxx			+.08				-.02	+.03		
3-PG				+.10 xx	xxx	-.03	+.05							+.01				- .01			+.03				-.02			
MgAMPPNP + 3-PG	-.05	-.07		+.08 xx	+.03 x	-	xxx		+.01	-.02	-.01	-.02			xxx	-.02		-.01			+.02				.00	+.05		
A4P				+.11 x	+.11 xx	+.08	+.03							-.05	xx	+.04		xxx			+.06				-.06	+.04 xx		
MUTATION							+.03 xxx								xxx	+.04		xxx			+.07				-.06	+.02		

ALIPHATIC RESONANCE

ADDITION	21	23	24		25a	b		26	27	28		29	30	31	32	33	34	35	36		37	38	39					
MgATP			xxx		+	-.02		-.01			,		-.04		x			x					-.04 -.10					
3-PG																			X									
MgAMPPNP + 3-PG			xxx			-.03							-.04										-.04					
A4P			x		+								-.02		xx						-.08		-.08 x					
MUTATION													-.07			xx			xx				-.05					

NUCLEOTIDE RESONANCE

ADDITION		H8		H2		H1'	
MgATP		xxx		+.02 xx		-.03 xx	
MgAMPPNP + 3-PG		xxx		+.05 xx		x -.09 xx	
A4P		xxx		+.01 x		-.04 xx	

Table 7.4(a) Summary and comparison of the effects on both enzyme and nucleotide spectra of the interaction of PGK with (i) MgATP, (ii) 3-PG, (iii) MgAMPPNP + 3-PG(excess) and (iv) A4P. (b) The differences between the 300MHz spectrum of mutant plasmid produced PGK and that of the wild type.

(iii) Apart from the broadening of peak 33, the differences in the spectrum that <u>are</u> seen are reminiscent of and frequently exceed the effects of substrate binding. They are as follows.

(a) Shifts at peaks 13,15b,16,17,30 and 39 and the broadening of peak 14a are nucleotide binding effects.

(b) Peak 36 broadens. This is a triose phosphate binding effect.

(c) Peak 8 broadens out completely and the entire bulk of peak 12, including the sharp component assigned to an active site histidine, is lost either due to a large downfield shift or to a broadening effect. These are effects previously associated only with formation of the ternary complex.

To continue the investigation of the mutant enzyme, 3mM MgAMPPNP is added to the sample. Evidence of interaction at the primary anion site is given by the upfield shifts of the two remaining active site histidine resonances, peaks 4 and 6. The addition of 30μM Gd^{3+} confirms this direct interaction by removing the two peaks. Under the conditions used, it is <u>not</u> possible to say whether there are any further changes in the spectrum, due to any further conformational change.

7.5 CONCLUSION

The investigation of mutant PGK showed that many of the effects of substrate binding on the nmr spectrum of yeast PGK are, in fact, evidence of the changing conformation of the protein, rather than of immediate interaction at the binding sites. The resonances involved include many of the upfield peaks which may well be associated with the highly aromatic hinge region. In the case of the mutant species such hinge residue resonances would, of course, be liable both to short range effects of the replacement of his388 and to any conformational changes.

The effects of the mutation on the conformation of the protein reveal very definite structural and functional relevance of the his388-glu190 hydrogen bond in particular and the (highly conserved) hinge region in general.

Chapter 7 References

Hjelmgren, T., Arvidsson, L. and Larsson-Raźnikiewicz, M. (1976) Biochim.Biophys.Acta, 445, 342-349.

Pickover, C.A., McKay, D.B., Engelman, D.M. and Steitz, T.A. (1979) J.Biol.Chem., 254, 11323-9.

Rice, D.W. and Blake, C.C.F. (1984) J.Mol.Biol. 175, 219-223.

Roustan, C., Fattoum, A., Jeanneau, R. and Pradel, L-A. (1980) Biochemistry, 19, 5168-5175.

Scheffler, J.E. and Cohn, M. (1986) Biochemistry, 25, 3788-3796.

Schierbeck, B. and Larsson-Raźnikiewicz, M. (1979) Biochim.Biophys.Acta, 568, 195-204.

Scopes, R.K. (1978b) Eur.J.Biochem., 91, 119-129.

Serjeant, E.P. and Dempsey, B. (1979) "Ionisation constants of organic acids in aqueous solutions" IUPAC Chemical Data Series no.23, Pergamon Press, Oxford.

Tanswell, P., Westhead, E.W. and Williams, R.J.P. (1976) Eur.J.Biochem., 63, 249-262.

Watson, H.C. and Gamblin, S.J. (1985) Proc.Int.Symp. Biomol.Struct.Interactions, Suppl. J. Biosci., 8, 499-506.

Wilson, C.B.A., Tuite, M.F., Dobson, M.J., Kingsman, S.M., Kingsman, A.J., Glover, L.A., Hardman, N., Watson, H.C. and Fothergill, L.A. (1985) Biochem.Soc.Trans., 604th meeting, 278-9.

CHAPTER 8.

THE PGK/SUBSTRATE INTERACTION-OVERALL CONCLUSION

Chapter 8 Contents

8.1 INTRODUCTION

This final chapter concerns the interaction of the enzyme PGK with it substrates. New ^{31}P nmr data are presented for several phosphate anions, in the absence and presence of PGK and comparison is made with the effects seen for the model phosphate/amine interactions of chapters 2 and 3 on both ^{1}H and ^{31}P nmr spectra.

Previous ^{31}P nmr studies of the interaction of PGK with its substrates have used yeast PGK (Rao et al., 1978) and halibut muscle PGK (Huskins et al., 1982). The following observations were made.

(i) In the presence of PGK, at pH7.0, the chemical shift of the 3-phosphate signal of 3-PG and 1,3-P_2G is shifted 2ppm downfield. The ATP, MgATP and ADP signals are unaffected and the MgADP signals are shifted about 1.5ppm upfield.

(ii) The 1,3-P_2G signals are independent of pH over the range pH5.9 to pH8.0.

(iii) While fast exchange kinetics were observed for the interactions of 3-PG and of MgATP with PGK, enzyme -bound and free 1,3-P_2G are in slow exchange, at pH7.0, 7.5°C and in the presence of 100mM buffer.

8.2 IONISATION CHARACTERISTICS OF SUBSTRATE ANIONS

The ionisation characteristics of 3-PG, ATP and PPP, in the absence and presence of enzyme, are examined here.

8.2.1 3-Phosphoglycerate

In the first titration, the initial sample contained 5mM 3-PG and 0.5mM EDTA, adjusted to pH9.5 with NaOD. The ^{31}P nmr spectrum was recorded and the pH lowered 0.5 units at a time, the chemical shift being recorded at each stage. The profile is shown in figure 8.1. It was analysed following the Henderson-Hasselbalch method. The gradient was near unity, indicating a simple, independent ionisation and the data fitted the analysis well, indicating that the maximum error is that of pH measurement. Thus the pK_a was determined to be 6.84±0.02 (I=60mM).

The sample in the second titration contained 0.9mM 3-PG, and 0.5mM EDTA, in the presence of 1.10mM enzyme. Using the value of 1.1μM for the dissociation constant at low ionic strength as determined by Scopes (1978b), it was calculated that over 95% of the nucleotide was bound to the enzyme. The pH titration was carried out as before and is also recorded in figure 8.1. At high pH, interaction with the enzyme moves the chemical shift 1.2ppm downfield. As the pH is lowered, the phosphate group remains deprotonated as the dianion. This indicates that the pK_a has been lowered to $\leqslant$pH4 by a strong electrostatic interaction of the substrate phosphate group with a positively charged site on the enzyme.

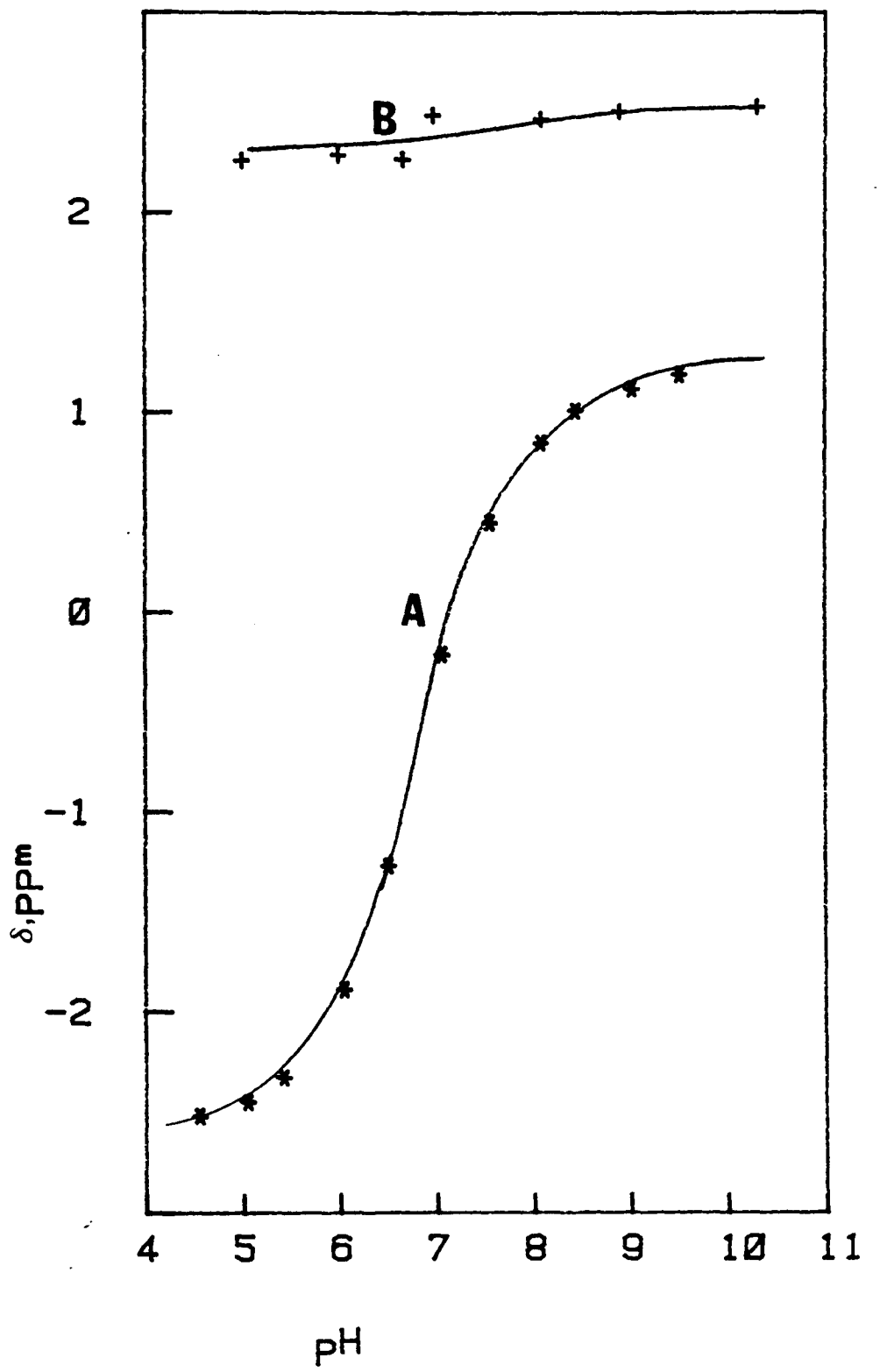

Figure 8.1 ^{31}P nmr of 3-PG pH dependence in the absence and presence of PGK.

(A) 5mM 3-PG.

(B) 0.9mM 3-PG, 1.1mM PGK.

8.2.2 ATP

A pH titration of ATP was carried out in the absence and presence of PGK. The samples contained 0.7mM nucleotide, 0.1mM EDTA and 80mM sodium d_3-acetate. For the titration in the presence of enzyme, the sample contained 1.0mM PGK and under these conditions, using Scopes' dissociation constant of 0.11mM, 80% ATP is calculated to be enzyme-bound. The movement of the γ-phosphate ^{31}P nmr resonance with pH is shown in figure 8.2, which includes, for comparison, the pH profile of ATP is the presence of excess trien, reported in chapter 3.

The profiles are subjected to Henderson-Hasselbalch analysis and the data fit well, so the maximum error is that of pH measurement, ±0.02pH units. The pK_a values are given below, and the ionic strength, $I=\frac{1}{2}cz^2$, for each pK_a is given in parenthesis.

free ATP	with PGK	with excess trien
6.95(90mM)	6.30(90mM)	4.54(270mM)

The effect of interaction with PGK is seen to be similar to, but much less than, that of interaction with trien.

8.2.3 Tripolyphosphate

The free PPP sample contained 5mM phosphate, 0.1mM EDTA and 100mM sodium d_3-acetate. The enzyme bound sample contained 1mM PPP and 1mM PGK, together with 0.1mM EDTA and

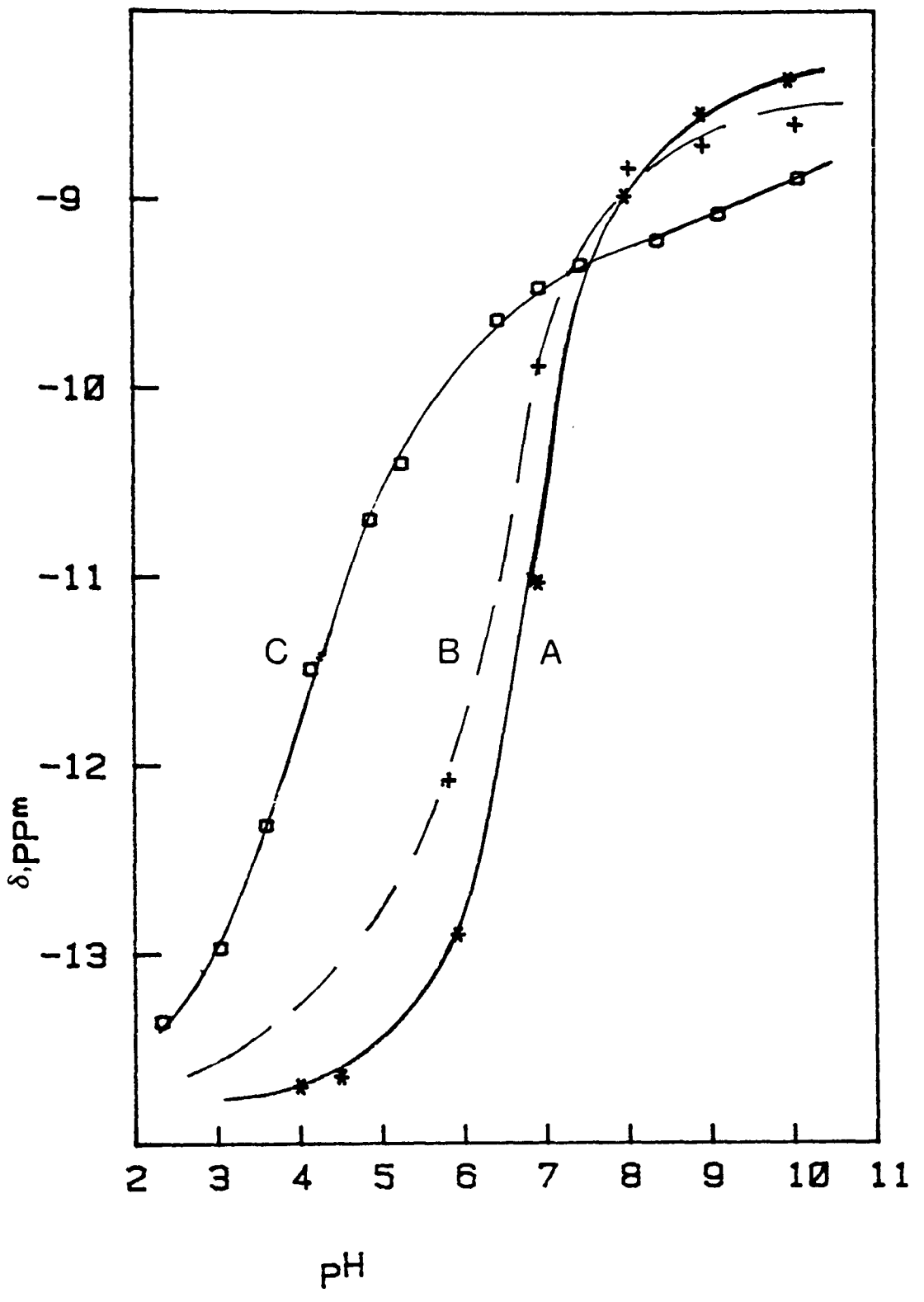

Figure 8.2 pH profile of ^{31}P nmr resonance of γ-phosphate of ATP.

(A) 0.7mM ATP;

(B) 0.7mM ATP with 1.1mM PGK, and

(C) 5.0mM ATP with 50mM trien.

100mM sodium d_3-acetate. The pH profiles are given in figure 8.3, together with that determined for PPP in the presence of excess trien (chapter 3).

The pK_a values (±0.02pH units) are calculated as before and are as follows.

free PPP	with PGK	with excess trien
8.22 (150mM)	7.77(110mM)	5.25(260mM)

As with ATP, the effect of PGK interaction is less than that of trien interaction.

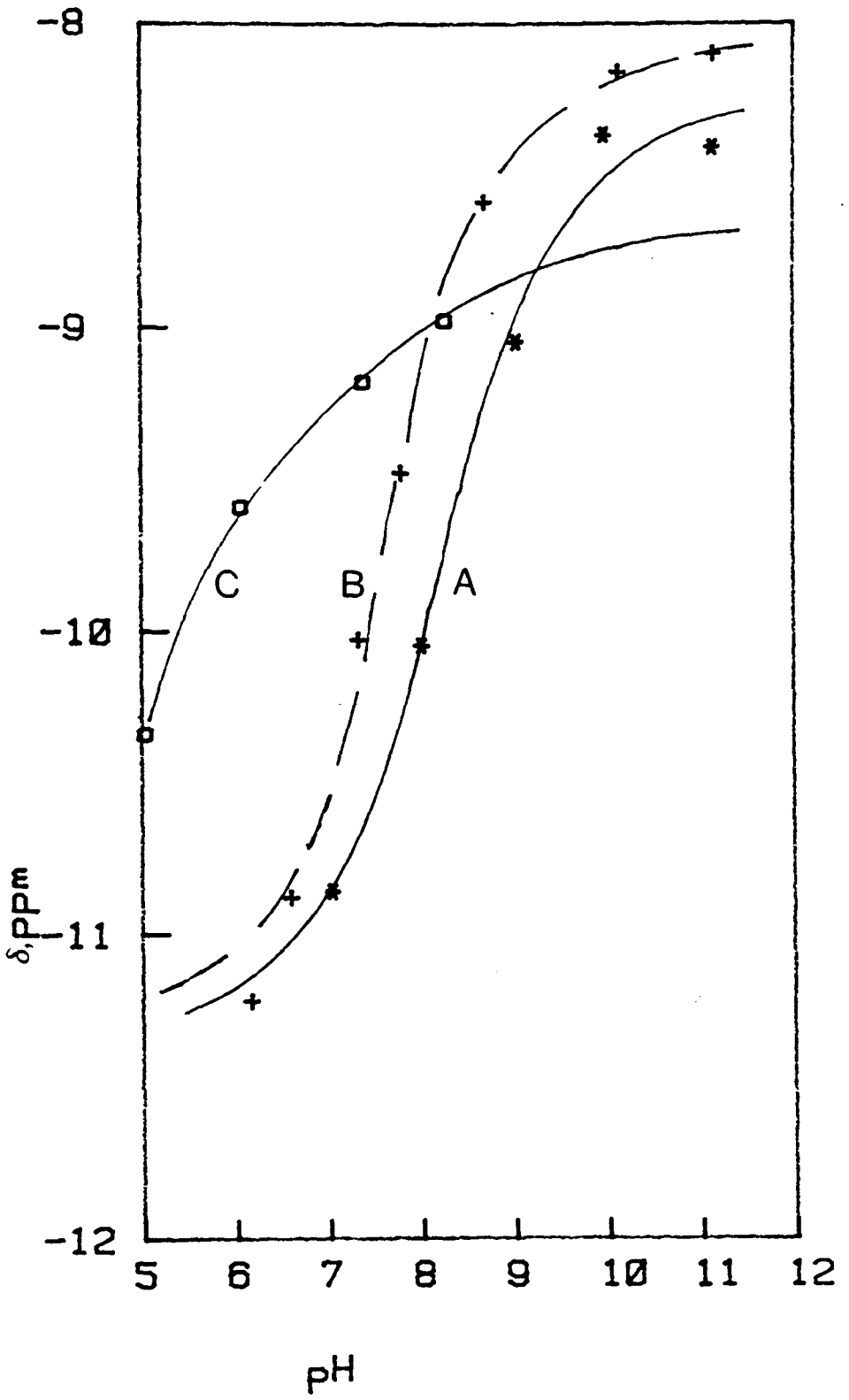

Figure 8.3 pH profile of ^{31}P nmr resonance of α-phosphate of PPP.

(A) 5.0mM PPP;

(B) 1.0mM PPP with 1.0mM PGK, and

(C) 5.0mM PPP with 50mM trien.

8.3 RELAXATION PROBE STUDIES

In this section the effect of the line broadening reagent Gd^{3+} on the ^{31}P nmr resonances of MgAMPPNP and 3-PG in the absence and presence of PGK is used to examine the nature of the enzyme-substrate interactions.

8.3.1 Nucleotide binding

The line-broadening effects of Gd^{3+} on the three ^{31}P nmr signals of MgAMPPNP were investigated in the absence and presence of enzyme. The sample for the first experiment contained nucleotide, $MgCl_2$ and HMPA all at 5mM, and was buffered at pH6.5 with 100mM HEPES. Three additions of Gd^{3+} were made, up to a concentration of 150μM, and the effect on the "relative linewidths" of the three phosphate signals is recorded in table 8.1. (The "relative linewidth" of a peak was calculated by dividing its half-height linewidth, in Hertz, by that of the internal standard, HMPA.) For comparison with the second titration the amount of Gd^{3+} calculated to give the same Gd^{3+}: nucleotide ratio when added to a 0.75mM nucleotide solution is shown. For the second titration, the solution used contained nucleotide, Mg^{2+} and line-width standard all at a concentrtion of 0.75mM, buffered as before, and 0.9mM PGK. Under these conditions, 75% of the enzyme is calculated to be enzyme bound. The effects of Gd^{3+} addition are again recorded in table 8.1. Both sets of results, the free enzyme results corrected to an equivalent 0.75mM nucleotide concentration, are displayed graphically in Figure 8.4.

Table 8.1 The effect of Gd^{3+} and PGK on the linewidth of MgAMPPNP

(A) Free nucleotide

$[Gd^{3+}]$,μM to 5mM nucleotide	equivalent $[Gd^{3+}]$,μM to 0.75mM nucleotide	linewidth, Hz, of HMPA	relative linewidths of phosphate peaks		
			α	β	γ
0	0	20.6	2.0	2.2	1.2
50	7.5	20.0	5.3	4.7	4.1
100	15	18.6	8.5	7.4	7.6
150	22.5	20.8	12.3	9.6	9.6

(B) 75% nucleotide bound to yeast PGK

$[Gd^{3+}]$,μM to 0.75mM nucleotide	linewidth, Hz, of HMPA	relative linewidths of phosphate peaks		
		α	β	γ
	19.2	3.4	6.9	2.5
	20.6	3.7	5.7	3.0
	17.7	5.3	9.1	4.7
	26.4	7.35	-	5.7

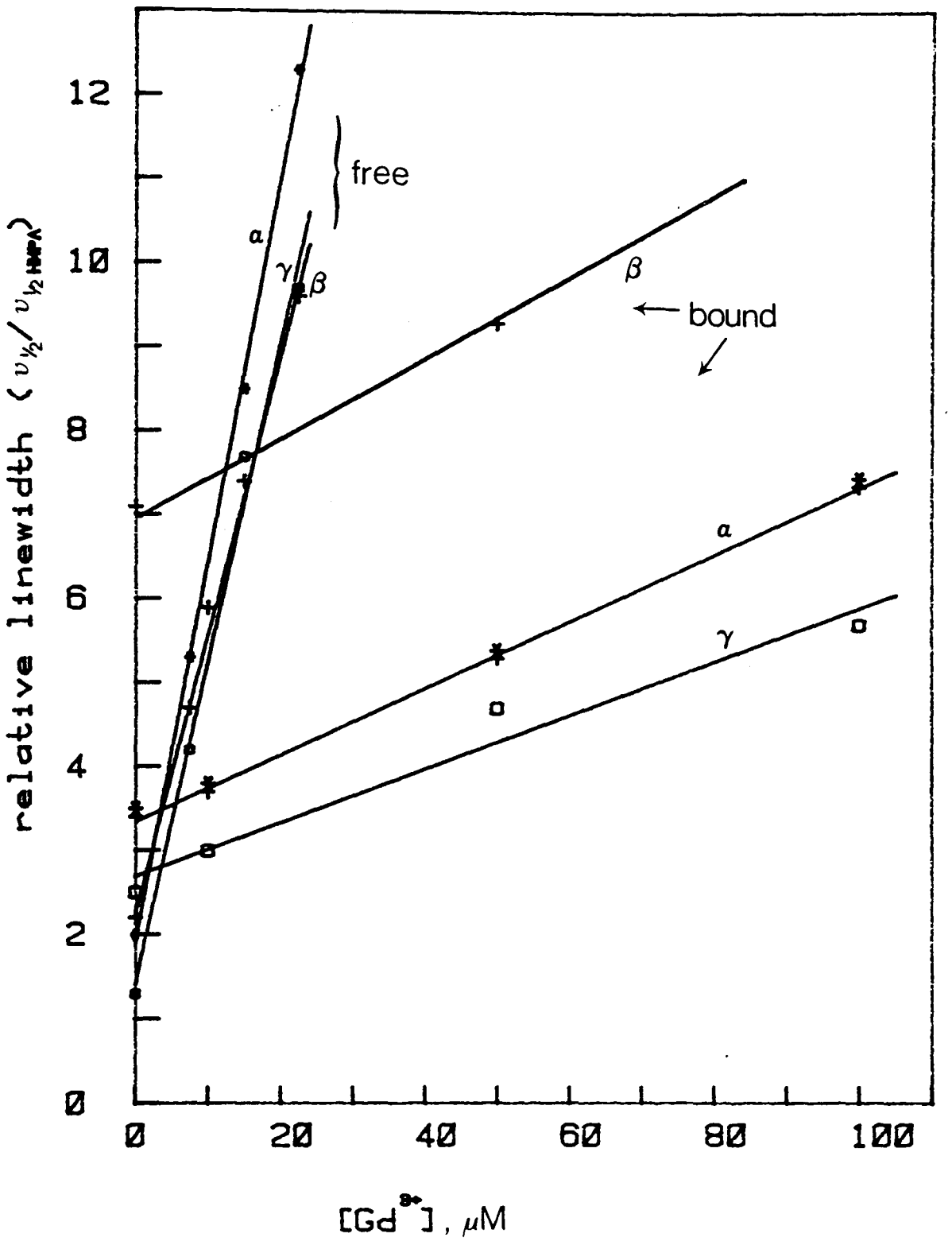

Figure 8.4 The effect of Gd^{3+} on the relative linewidths of the MgAMPPNP ^{31}P nmr spectrum.

0.75mM MgAMPPNP, pH6.5.

(*,+,□) α,β,γ phosphate signals of the free nucleotide;

(* , + , □) α,β,γ phosphate signals in the presence of PGK.

From these experiments it can be seen that, firstly, in the absence of Gd^{3+}, interaction with the enzyme broadens the nucleotide peaks, especially that of the β-phosphate, known to be coordinated to both lys217 and asp372. Secondly, the interaction of Gd^{3+} and nucleotide is considerably reduced, by a factor of some twenty-fold by the presence of enzyme. This would be consistent with a competing interaction between the bound nucleotide and the positive face of the triose binding site.

This latter conclusion agrees with the effect on the ^1H spectrum of MgAMPPNP observed in chapter 5, section 2.5. There it was seen that on the addition of $GdCl_3$ to a solution of 2.8mM MgAAMPPNP and 2mM PGK (67% nucleotide enzyme bound) the free nucleotide H2 and H1' resonances are observed to broaden, rather than the enzyme-bound resonances. Thus, as here, Gd^{3+} was found to bind preferentially to the free nucleotide. (No such distinction could be made for the MgADP and MgATP complexes which, because of fast exchange kinetics, display only one set of nucleotide resonances).

8.3.2 Triose phosphate binding

The first experiment is a blank. The effect of the additions of the line-broadening reagent Gd^{3+} in the presence and absence of AMPPNP on the linewidth of 3-PG was examined (table 8.2): the sample in this experiment was 0.5mM 3-PG buffered at pH6.5 with 100mM HEPES. On addition of Gd^{3+}, the triose phosphate signal, originally of relative linewidth 1.8, broadened and disappeared completely. On the addition

of 0.5mM AMPPNP the peak returned, sharper than before. As expected, the nucleotide has removed the Gd^{3+} (and any line broadening impurity) from the 3-PG.

In the second experiment, the sample was the same as before, but 0.75mM yeast PGK was present. Using Scopes' dissociation constant of 0.03mM, at I = 0.15M, this implies that over 90% of the triose phosphate is enzyme-bound. On the addition of 5μM Gd^{3+}, only slight broadening of the phosphate peak was observed. The metal ion fails to bind presumably because it has to compete with the positive charge of the triose binding site. On the addition of AMPPNP, the linewidth is seen to increase. Once again, the nucleotide binds the metal ion, but this time both substrates are enzyme-bound, and the nucleotide presumably positions the Gd^{3+} close to the triose phosphate.

Table 8.2 The effect of Gd^{3+} and nucleotide on the linewidth of 3-PG

Without PGK	relative linewidth
0.5mM 3-PG, pH6.5	1.8
+5μM Gd^{3+}	10
+0.5mM AMPPNP	1.0
With 0.75mM PGK (3-PG 90% bound)	
0.5mM 3-PG, pH6.5	1.0
+5μM Gd^{3+}	1.3
+0.5mM AMPPNP	2.1

(The relative linewidth of a signal is obtained by dividing its width (Hz) by the width of HMPA, the internal standard)

8.4 COMPARISON WITH PHOSPHATE/AMINE STUDIES

In the second and third chapters of this thesis it was obseved that phosphate/amine interaction could change the chemical shift of a signal either by direct influence or by changing the protonation state of the species concerned.

A summary of the changes caused by direct influence, that is not involving a change in protonation state, is given in table 3.7. A summary of the corresponding influence of PGK, noted previously in this chapter is as follows.

phosphate	change in ^{31}P nmr chemical shift ppm
$3\text{-}PG^{3-}$	+1.2
ATP^{4-}	-0.2
PPP^{5-}	+0.2

It is not possible to establish a pattern in these shifts on the basis of those recorded in chapter 3. The changes do not reflect the working of a single phenomenon.

The effect on chemical shift exerted via shifts in protonation equilibria, reported throughout chapter 3, is more readily categorised. Of the interaction of an amine and a phosphate, when both are susceptible to changes in protonation state, the amine tends to gain a proton while the phosphate tends to lose one, and thus they both tend to become more highly charged. The amine resonance(s) moves downfield and the pK_a is seen to <u>increase</u>. The phosphate

resonance also moves downfield as its pK_a is seen to <u>decrease</u>. The situation is illustrated as follows.

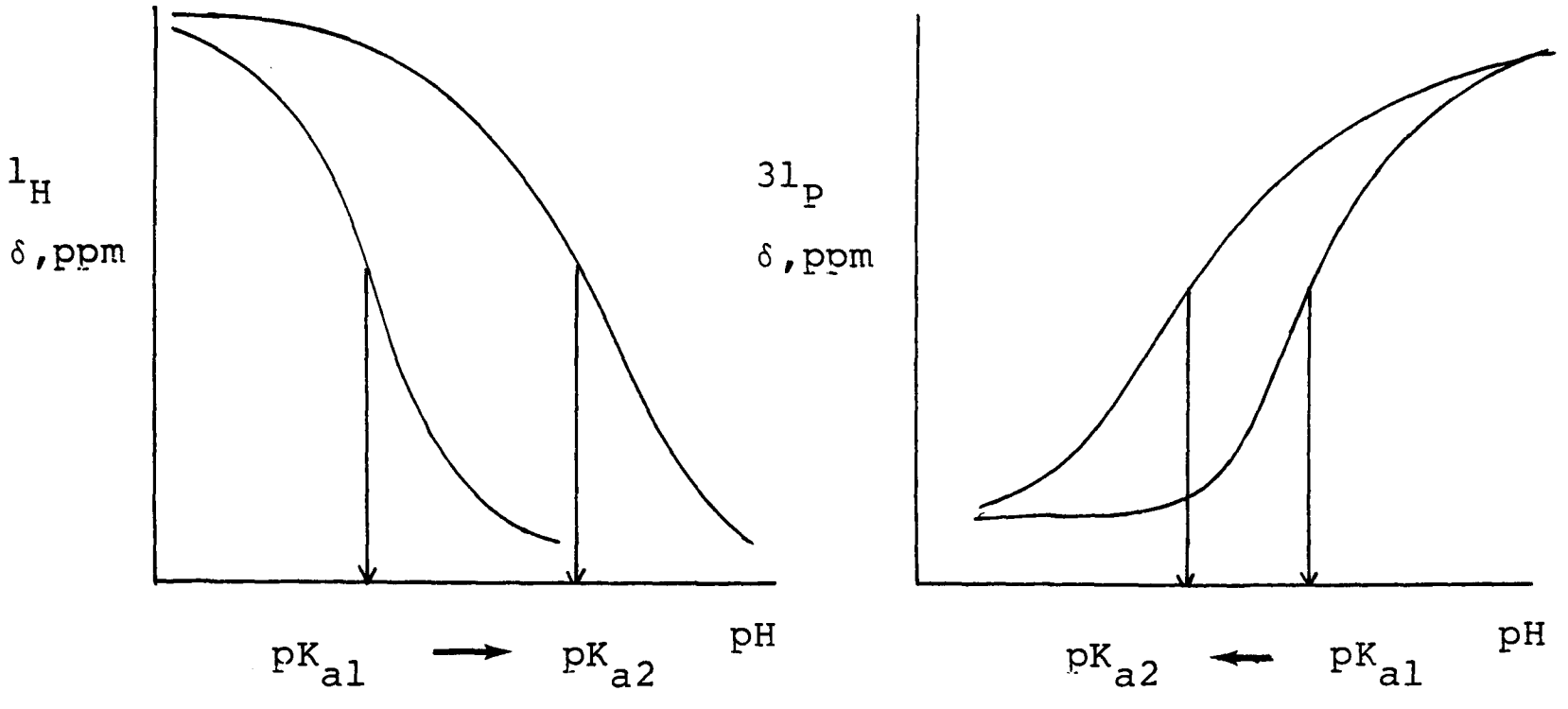

Various PGK/phosphate interactions have been investigated by monitoring the ^1H spectrum of the protein and the ^{31}P spectrum of the substrate anion. In the former case, several resonances have been confirmed as corresponding to C2 and C4 protons of deprotonated histidine residues. These are active site residues, located among basic residues (hence their deprotonated state) in the positively charged face of the N-domain, a known phosphate binding site. The influence of such interaction on these resonances is summarised as follows.

	proton type and resonance			
	C2	C4	C2	C2
phosphate	3	12	4	6
MgADP	+.01	-.03	x	x
MgATP	+.06	+.02	x	+.05
MgAMPPNP	+.02	+.02	+.01	+.07
A4P	+.11	+.03	+.11	+.08
3-PG	+.10	+.05	-	-.03
PPP	+.03	+.02	+.05	+.04

The following observations are made

(i) With the exception of the upfield shifts of peaks 12 and 6 caused by MgADP and 3-PG respectively, all the shifts are downfield and, therefore, consistent with a (limited) protonation of the histidine residue.

(ii) The largest shift is +0.11ppm. If this is solely due to protonation effects, it corresponds to about 10% protonation.

(iii) As might be expected, the effects of the interaction tend to be greater for the C2 resonance, located between the two NH groups, than for the C4 resonance, next to only one.

(iv) The nucleotides are thought to be anchored by their adenine rings to the C-domain and it follows that the longer phosphate chains can interact more readily with the N-domain site. Thus the largest shifts are seen with A4P and the smallest with MgADP.

(v) 3-PG and PPP bind directly to the N-domain site. Of the two, the influence of the substrate is the greater.

The influence of PGK on the pK_a of phosphate anions is reported in the second section of this chapter. A decrease in pK_a of about 0.6pH units was observed for ATP and for PPP, while enzyme-bound 3-PG appeared to be independent of pH over the range examined, indicating a drop in pK_a of $\geq$2.5pH units.

Thus both the ^{1}H and ^{31}P nmr data are fully consistent with the established characteristic movement of protons from the phosphate anion to the amine cation.

8.5 OVERALL CONCLUSIONS AND PROSPECTS FOR FURTHER WORK

In the present work, the effect of the interaction of phosphates and amines on ^{1}H and ^{31}P nmr spectra has been characterised. Changes in chemical shift and particularly, in pK_a values, have been recorded and transfer of a proton from the phosphate to the amine has been shown to describe the interaction. Strengths of association have been determined for various species in various charge states and comparison of lgK_b with charge product has underlined the importance of spatial distribution of charge.

Several resonances of the ^{1}H nmr spectrum of yeast PGK have been assigned

(i) to individual histidines;

(ii) to groups of histidines,

and, tentatively,

(iii) to individual methionines, and

(iv) to the inter-domain hinge region.

Spectral effects relating to the binding of both triose phosphate and nucleotide molecules have been identified, as have those relating to formation of the ternary complex. Comparisons have been made with the established phosphate/amine effects.

The scope of the nmr investigation is seriously hampered by the size of the protein. It has been shown to be possible to split the molecule (Adams et al., 1985) but the solubility of the resulting N-domain is prohibitively low. More promising for future work is the use of site specific mutagenesis to produce PGK with key residues replaced and

thus to further assign the nmr spectrum and to investigate the relevance of these residues in terms of the activity of the enzyme.

Solid state nmr spectroscopy may characterise the "open" crystal structure of PGK as defined by X-ray analysis, as opposed to the dynamic equilibrium observed in solution.

In these ways the structural basis of the action of PGK and in particular of the hinge region may be investigated further and the general mechanism of enzyme domain movement more fully understood.

Chapter 8 References

Adams, B., Burgess, R.J., and Pain, R.H. (1985)
Eur.J.Biochem., 152, 715-720.

Huskins, K.R., Bernard, S.A. and Dahlquist, F.W. (1982)
Biochemistry, 21, 4180-8.

Nageswara Rao, B.D., Cohn, M. and Scopes, R.K. (1978)
J.Biol.Chem., 253, 22, 8056-60.

Scopes, R.K. (1978b) Eur.J.Biochem., 91, 119-129.

Appendix I. lgK_b correction for incompletely formed complexes.

The calculation was done using the following microprogram. Various lines of the program are referred to in the subsequent explanation.

BASIC MICROPROGRAM for CALCULATION of lgK_b

```
10  PRINT "INPUT INITIAL VALUE OF X"
20 INPUT X
30 LET W = X
40 Z = 55 + EXP ((3-X)*2.303)
50 Y = (Z - SQR(Z*Z - 1000))*0.1
60 V = W - (0.434 * LOG(Y))
70 IF ABS(V-X) < 0.005 THEN GOTO 100
80 LET X = V
90 GOTO 40
100 PRINT "THE FINAL VALUE OF Y IS";Y
110 PRINT "THE FINAL VALUE OF X IS"; X
120 PRINT "DO YOU WANT TO PUT IN ANOTHER VALUE"
130 INPUT F$
140 IF F$ = "Y" THEN GOTO 10
150 END
```

Interaction of amine (A) and phosphate (P) to form the complex (AP) is expressed as follows.

$$A + P = AP; \quad K_b = \frac{[AP]}{[A][P]}$$

For initial concentrations of 5mM amine and 50mM phosphate, equilibrium concentrations are as follows.

$$\underset{(5-C)}{A} + \underset{(50-C)}{P} \rightleftharpoons \underset{(C)}{AP}; \quad K_b = \frac{C}{(5-C)(50-C)}\ mM; \qquad (1)$$

where C is the equilibrium concentration (mM) of complex. For a given value of $\lg K_b$, X; strength of association is expressed by

$$K_b = 10^x\ M^{-1}$$

$$\rightleftharpoons \quad K_b = 10^x\ 10^{-3} mM^{-1}$$

$$\rightleftharpoons \quad K_b = 10^{x-3}\ mM^{-1}$$

(1) now implies that $\frac{C}{(5-C)(50-C)} = 10^{x-3}$

$$\rightleftharpoons \quad C.10^{3-x} = C^2 - 55C + 250$$

$$\rightleftharpoons \quad C^2 - (55 + 10^{3-x}).\ C + 250 = 0 \qquad (2)$$

Let $z = 55 + 10^{3-x}$

The program uses natural logarithms with the notation "EXP x" for e^x, so z is expressed as follows.

$$z = 55 + e^{(2.303(3-x))} \qquad \text{(line 40)}$$

The quadratic formula is now applied to solve (2):

$$C = \frac{z \pm (z^2-1{,}000)^{\frac{1}{2}}}{2}$$

Of the +/- option, only the latter is found to yield a meaningful value for C, less than 5, so

$$C = \frac{z - (z^2 - 1{,}000)^{\frac{1}{2}}}{2}$$

The concentration of complex expressed as a proportion of the total amine concentration (5mM) is given by $Y = \frac{C}{5}$.

$$Y = \frac{z - (z^2 - 1{,}000)^{\frac{1}{2}}}{10} \qquad \text{(line 50)}$$

This value of Y is used to calculate a new value of $\lg K_b$, V.

$$\frac{K_{b\ new}}{K_{b\ old}} = \frac{100\%}{\%\ bound}$$

$$\Rightarrow \quad \frac{10^V}{10^X} = \frac{1}{Y}$$

$$\Rightarrow \quad V = X - \lg Y.$$

With natural logarithms this is expressed

$$V = X - 0.434\ \ln Y \qquad \text{(line 60)}$$

This new value of $\lg K_b$ is then fed back into the process to give a new value of Y etc.

$$X = V \qquad \text{(line 80)}$$

The process is repeated until the difference in successive values for $\lg K_b$ is less than 0.005 units,

i.e. $|V-X| < 0.005$ (line 70)

This gives the final estimate of $\lg K_b(X)$ and of extent of association (Y).

Appendix II. K_d calculation from change in chemical shift

The equilibrium concentrations for a 1:1 ligand/enzyme interaction are as follows:

enzyme + ligand ⇌ complex

$([enzyme]_t - [complex])$ $([ligand]_t - [complex])$ $[complex]$

where $[enzyme]_t$ is the initial or total concentration of enzyme. It is assumed that

$\Delta\delta/\Delta\delta max = [complex]/[enzyme]_t$

where $\Delta\delta$ is the change in chemical shift and $\Delta\delta max$ is the maximum change.

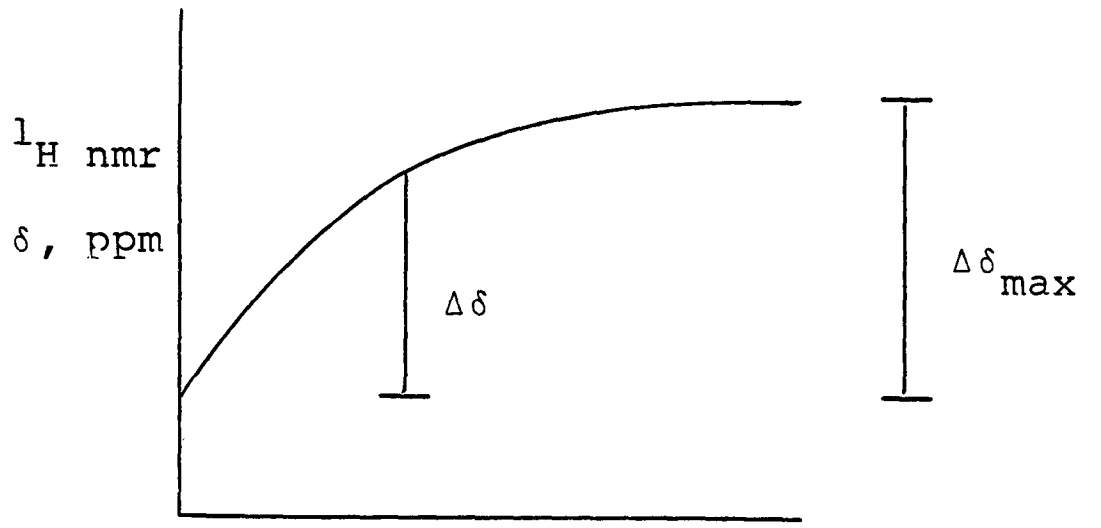

The dissociation constant is given by

$$K_d = \frac{\{[enzyme]_t - [complex]\}\{[ligand]_t - [complex]\}}{[complex]}$$

$$\rightleftharpoons K_d = \frac{\{[\text{enzyme}]_t - [\text{enzyme}]_t \Delta\delta/\Delta\delta\text{max}\}\{[\text{ligand}]_t - [\text{enzyme}]_t \Delta\delta/\Delta\delta\text{max}\}}{[\text{enzyme}]_t \ \Delta\delta/\Delta\delta\text{max}}$$

$$\rightleftharpoons K_d = \frac{(1-\Delta\delta/\Delta\delta\text{max})\{[\text{ligand}]_t - [\text{enzyme}]_t \Delta\delta/\Delta\delta\text{max}\}}{\Delta\delta/\Delta\delta\text{max}}$$

$$\rightleftharpoons K_d = \{[\text{ligand}]_t - [\text{enzyme}]_t \Delta\delta/\Delta\delta\text{max}\} \div \Delta\delta/\Delta\delta\text{max}(1-\Delta\delta/\Delta\delta\text{max})^{-1}$$

i.e. a graph of $\{[\text{ligand}]_t - [\text{enzyme}]_t \Delta\delta/\Delta\delta\text{max}\}$

versus $\Delta\delta/\Delta\delta\text{max}(1-\Delta\delta/\Delta\delta\text{max})^{-1}$

has slope of K_d.